Universidad Autónoma de Madrid
Facultad de Ciencias
Departamento de Biología Molecular

Notch signalling in zebrafish heart and fin regeneration

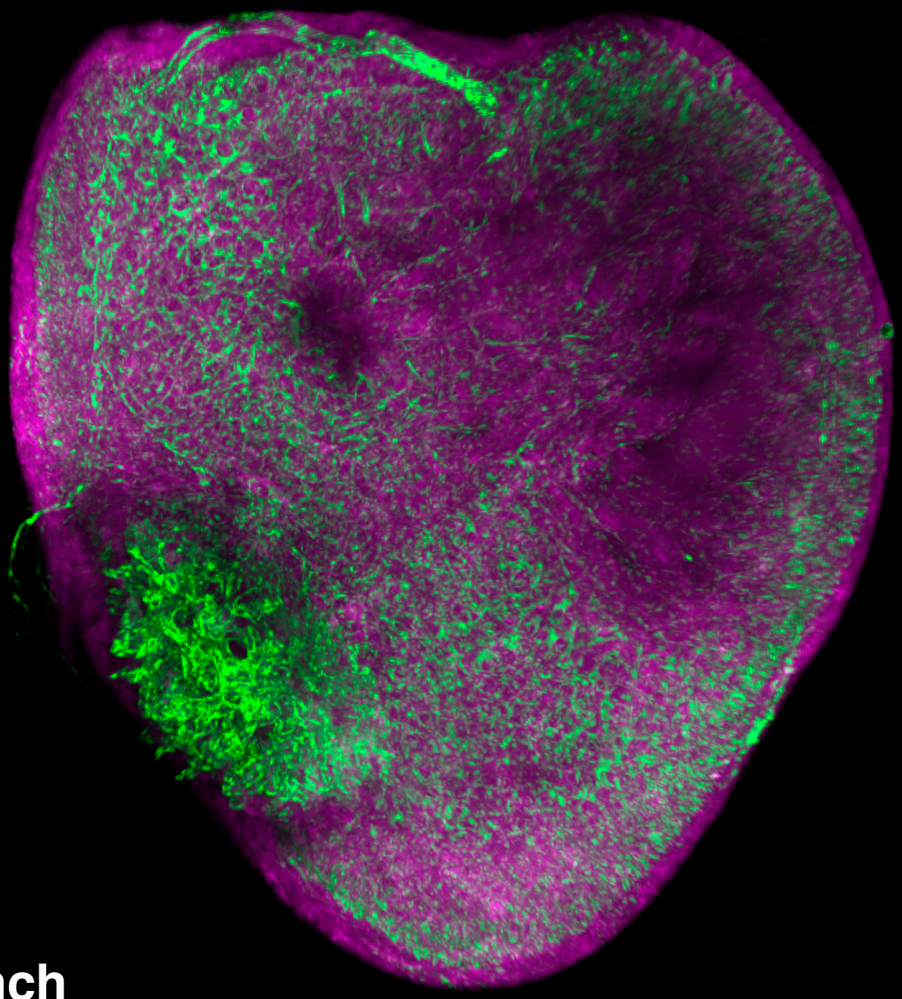

Juliane Münch

Madrid 2015

Universidad Autónoma de Madrid
Facultad de Ciencias
Departamento de Biología Molecular

Doctoral thesis

Notch signalling in zebrafish heart and fin regeneration

Juliane Münch

graduated in Biology

Director: Dr. José Luis de la Pompa Mínguez
Tutor: Dr. Cristina Grande
Centro Nacional de Investigaciones Cardiovasculares (CNIC)
Madrid 2015

To my parents, my grandparents, to Nele and Marco.

The noblest pleasure is the joy of understanding.

Leonardo da Vinci

This work was performed in Dr. José Luis de la Pompa's laboratory at the Centro Nacional de Investigaciones Cardiovasculares (CNIC) in Madrid.

This study was funded from grants of the Spanish Ministry of Economy and Competitiveness (MINECO) [SAF2010-17555 and SAF2013-45543-R]; Red Temática de Investigación Cooperativa en Enfermedades Cardiovasculares (RECAVA) [RD06/0014/0038 and RD12/0042/0005]; Red de Terapia Celular (TERCEL) [RD06/0010/1013 and RD12/0019/0003] and by a European Union grant [EU FP7-ITN 215761] (NotchIT) to José Luis de la Pompa.

Juliane Münch holds a PhD fellowship linked to grant FP7-ITN 215761 (NotchIT).

Acknowledgements

“I am not the same having seen the moon shine on the other side of the world.”

Mary Anne Radmacher

The CNIC is a great place for carrying out a PhD thesis, not only because of its excellent facilities and resources but especially because of the people working there, from -3 to the 4th floor.

First of all I want to thank José Luis for giving me the opportunity to come to Spain, to work with zebrafish and to develop my project in the lab. Thank you for your trust in me and my work, for giving me experimental freedom and for sending me to so many meetings. Thank you also for bringing together so many great people and scientists that made the last 6 years unforgettable. People from DLP group made the lab a very special place to work and Madrid my second home. I am grateful to everybody sharing experiences, buffers, protocols, reagents, pipets etc.

Quiero darle las gracias a Belén por su ayuda con tantos protocolos e indicaciones. Gracias a Bea mi compañera de poyata, por su compañía en el labo y por dejarme invadir su sitio cuando hacia falta. Gracias a Sara, mi otra compañera de poyata por su ayuda con los genotipos pero también por nuestros conversaciones sobre animales y manualidades. Gracias a Vane no solo por ayudarme con las Maxis de vez en cuando pero sobre todo por su compañía en tantas salidas y cañas y por sus historias curiosas que nos contaba durante las comidas. Thanks to Patri for her help in the lab, for her humour and her funny imitations that made me laugh so many times. Grazie Lao, por tu humor tan especial, por tener un corazón tan grande, por no ser resentido y por compartir los reactivos conmigo.

Has sido un placer enorme pasar todo este tiempo de la tesis al lado de Gaetano D'Amato, un grande ricercatore. Creo que compartimos casi todo lo posible durante este periodo. Gracias Gaetano por tu ayuda con los protocolos, por tu compañía hasta muy tarde en el labo, por tu cariño y por tu confianza y respeto en mi y mi trabajo. Gracias por ser mi amigo. Disfruté muchos viajes, fiestas, comidas y lab meetings contigo.

I especially want to thank Dimitris, my current zebrafish colleague. I could share with him so many problems, concerns and uncertainties that I had during the last years. Thank you Dimitris for helping me to worry less about small things and to increase the faith in myself. Thanks for helping me out in the lab, whenever it was needed, even at the weekend. I learned so many things from you and I am sure I will still learn much more. I appreciate you a lot and I am happy of having you on my site during my PhD. Είσαι ο καλύτερος.

Gracias a Tania por ayudarme en el labo, con la tesis, el paper y siempre cuando tenia cualquier duda. πολλές ευχαριστίες Tania por tu tiempo, por escucharme, por proveernos con galletas en la zona postdoc y por ser mi amiga.

Muchas gracias a Paula y Marcos por presentar todos los viernes en el lab meeting, por compartir bufferes, por siempre ofrecer su ayuda para cualquier cosa y por su compañía en el labo. Sois un muy buen fichaje para el labo. Lo mismo digo de Rebeca y Ale, los más jóvenes. Rebeca muchas veces me hizo compañía en el labo hasta muy tarde. Quiero darle las gracias a Abel, por su ayuda con los ratones y también por siempre intentar de ayudar aún más para facilitar el trabajo. Thanks to Donal, the great mind in the lab for the numerous discussions, comments and questions in the seminars and for the beers in JJ.

Quiero dar las gracias también a la gente que ya se fue del labo y quien me recibió tan bien aquí en Madrid. Muchísimas gracias a Álvaro, mi primero compañero de los peces del labo. A el le debo el estar aquí en Madrid. Me enseño casi todas las técnicas auqui en el labo y sin el esté trabajo no hubiera sido posible. El me ayudó de hacerme investigadora de peces. Gracias Álvaro por ser tan buena y divertida persona. He disfrutado el tiempo contigo en el labo y también en los congresos. Te aprecio un montón.

Quiero darle las gracias a Ana por su ayuda enorme con los peces en el laboratorio siempre cuando era necesario. Gracias Ana por tu compañía en labo, por escucharme y por ser mi amiga.

Gracias a Luis, que me enseñó tantas cosas en Photoshop pero sobre todo por tantas conversaciones divertidas durante las comidas y en algunas cañas. Gracias a Guille por su ayuda con muchos protocolos, por facilitarme un montón mi incorporación en el labo al principio y por convertir la 3N en un sitio menos serio. Gracias a Mauro por nuestras conversaciones sobre experimentos, ciencia y de cosas fuera del labo y por su compañía en varios meetings de TERCEL. Gracias a Meritxel por ser una persona tan especial y por ver las cosas de manera diferente. Gracias a Gonzalo por compartir mi fascinación por el buceo. Gracias Jesús por interesarte tanto por mi proyecto de la regeneración de la aleta y por tu ayuda con las in situs. Gracias a Eva por su compañía en el labo.

I want to thank former and current people from 3N for sharing reagents, for their company and making the 3N such a nice place to work. I am especially grateful to Nadia and her group for sharing zebrafish issues and reagents with us and for the numerous

discussions we had. Thanks to Juanma and Hector for discussions, Maria for protocols and advises and Laura for her company in the postdoc area. Also thanks to several former and current lab members from Miguel Manzanares group. Especially to Susana, Teresa and Sergio for their help with scientific questions but also for their company in activities outside the lab. I enjoyed the time with you a lot. Thanks to Claudio for sharing technical experience. I want to thank people from Rui's lab, for sharing reagents, for discussions and for their company in the lab until midnight and at the weekends. I want to thank Tania, my other postdoc area neighbour for her help with the Spanish and Briane with the English language. Thanks also to Dorota and Esther, for sharing problems and concerns during the PhD. Thank you Esther for showing me how to operate neonates but especially for your help during the last weeks with the preparation and organization of this work. Thanks also to the Torres' group, especially to Alberto and Irene for some discussions, advice and reagents. I am further very grateful to Teresa, Mary, Beatriz, Almudena, Marta and Angel, who made many things around the research much easier. Thanks to Sandra, especially for her great help on my first day at the CNIC but also for organizing all my trips.

Gracias Vero por nuestros discusiones de ciencia, por tu compañía y la música en la área de las lupas 3N y gracias por escuchar mis preocupaciones. Me alegro que ahora trabajes con el pez cebra en la ciencia. Gracias a Marina, mi compañera de master y de los peces. Hemos pasado casi todo el largo tiempo de la tesis juntas. Fue un placer compartir alegría, problemas, intereses y peces contigo y nunca se me van a olvidar los zebrafish meetings contigo. Mil gracias a Melisa, mi compi de master, de tesis y de piso. Gracias por enseñarme el mundo de los enhancers, por escuchar mis problemas, por animarme, por compartir novedades y por ser mi amiga. Estoy contenta de haberte conocido y de que hemos pasado todos estos años de la tesis juntas.

Also outside of the 3N many people helped and made this work possible. I want to thank people from the fish room, John, Antonio and Eva for taking excellently care of our fish. Of cause a great thanks to Edu, for his professionalism, his concern about the fish but also for his countless jokes and his interest in the German culture. I want to thank the microscopy team, Elvira, Vero and Antonio, for teaching me how to use so many microscopes, for their helpfulness and for making the microscopy room such a likable place to work. Thanks to people of the Genomic and Bioinformatic Facility, Manuel, Carlos, Alberto and Sergio, who helped me with the RNAseq. Thanks to Rosin and her

team for their beautiful histological stainings. Thank you Simon, for reading and correcting the papers, which helped me a lot to improve my writing.

I am grateful to my UAM-tutor, Cristina Grande, for her patience and encouraging words during the last month and for always being flexible when I needed her signature.

I also want to thank Dr. Heiner Grandel, who showed me how to work and investigate with zebrafish but also how fascinating research is, preparing me well for my PhD thesis.

Gracias a Pilar, Carmen y Joaquín por cuidarme y darme una casa en Alicante durante todos estos años.

Ich möchte meiner Familie danken, für die es nicht immer leicht war, dass ich soweit weg gewesen bin. Ich danke meiner Mutti und meinem Vati für ihre Unterstützung während meines Studiums, als Vorrausetzung für diese Doktorarbeit. Vielen Dank Mutti für dein großes Verständnis und dein Vertrauen in mich. Dank Holger für die vielen Nachtfahrten zum Flughafen und die jährlichen Besuche in Madrid. Vielen Dank Vati und Angelika für eure Begeisterung die ihr in guten Momenten mit mir teilt und die schönen gemeinsamen Erlebnisse in Spanien. Vielen Dank Opa, dass du immer an mich glaubst. Besonders dankbar bin ich meiner Oma, die immer Vertrauen in mich hatte, für ihr großes Interesse an meiner Arbeit und für ihre vielen aufmunternden und verständnisvollen Worte.

Gracias Marco, por apoyarme tanto todo este tiempo, por creer en mi, por escucharme, por entenderme, por animarme y por acompañarme al CNIC los fines de semana. Gracias por ayudarme a desconectar del trabajo tantas veces cuando hacia falta. Sin ti yo no habría logrado todo esto.

Summary

Zebrafish have the capacity to regenerate several organs. More than a decade ago Raya *et al.* (PNAS, 2003) reported Notch pathway genes to be expressed in the regenerating zebrafish fin and heart. Further investigation was needed to understand the function of this pathway during the regeneration of these two organs.

On the first part of this thesis we studied the role of Notch signalling during fin regeneration. Fin regeneration proceeds through the formation of a blastema, a group of dedifferentiated, highly proliferating cells that will differentiate in the proximal region of the fin regenerate and replace the lost tissue. Notch signalling was activated just when the blastema was formed and remained active throughout the regeneration process. Chemical inhibition and morpholino-induced knockdown of Notch signalling interfered with blastema proliferation and regenerative outgrowth. Further, Notch pathway overactivation resulted in increased proliferation and expansion of the blastema. This was characterized by augmented expression of blastema markers (*msxb*, *msxe*) and of the proliferation regulator *aldh1a2*, indicating an increased amount of undifferentiated cells within the regenerate. Moreover Notch over activation caused an expansion of early osteoblasts differentiation genes (*runx2*, *tcf7),* but an impaired expression pattern of later osteoblast markers (osx), suggesting that Notch signalling interferes with osteoblast differentiation in the regenerating fin. Altogether we showed that Notch signalling maintains blastema cells in a plastic, undifferentiated and proliferative state, which is an essential requirement for fin regeneration.

The second part of this thesis focused on the role of Notch signalling during heart regeneration. We used the cryoinjury technique to induce a cardiac damage that results in massive cell death, inflammatory cell infiltration, fibrotic tissue deposition and removal. Finally cardiomyocyte dedifferentiation and proliferation allow cardiac muscle renewal. We detected Notch signalling gene expression in endocardial cells after cryoinjury and studied the endocardium more in detail, as little was known about endocardial function and behaviour upon cardiac injury in zebrafish. 3D-whole mount imaging of injured hearts revealed that GFP-labelled endocardial cells in *ET33-mi60A* transgenic fish become rapidly activated and highly proliferative at 3 days post cryoinjury (dpci). The endocardium then expands and organizes in the injury site at 9 dpci into a complex and cellular-dense structure. Gain- and loss-of-function experiments revealed that Notch is not only required for the organization of the endocardium, but also for cardiomyocyte proliferation. RNA-seq analysis showed that Notch signalling inhibition affects endocardial gene expression and genes related to extracellular matrix remodelling and inflammation. Moreover we observed that Notch is required to attenuate inflammatory cell infiltration. These results demonstrate that the endocardium plays a novel structural and signalling role during heart regeneration, a process in which endocardial Notch signalling is crucial.

El pez cebra tiene la capacidad de regenerar varios órganos, incluidos el corazón y las aletas. Hace más de una década Raya *et al*. (PNAS, 2003) describieron que varios genes de la vía de señalización de Notch se expresan durante la regeneración de la aleta y del corazón. Sin embargo, no se conocían los detalles acerca del funcionamiento de esta vía durante la regeneración de ambos órganos.

Esta tesis se ha centrado en estudiar el papel que la vía de señalización Notch tiene en la regeneración de la aleta y del corazón. La regeneración de la aleta requiere la formación de un blastema, una estructura primordial cuyas células están indiferenciadas, son altamente proliferativas y tienen la capacidad de diferenciarse siguiendo un patrón próximo-distal para reemplazar el tejido perdido.

En la primera parte de este trabajo, se llevaron a cabo estudios sobre la ganancia y pérdida de función que indicaron el papel de Notch en el mantenimiento y proliferación de las células del blastema. Esta vía de señalización se activa tras la formación del blastema y permanece activa durante todo el proceso de regeneración. Su inhibición, inducida farmacológicamente o mediante la inyección de morfolinos, interfiere en la proliferación y crecimiento del blastema regenerativo de la aleta. Además, la sobreactivación de la vía de Notch produce un aumento de la proliferación y tamaño del blastema, caracterizado por la expresión aumentada de los marcadores de blastema (*msxb*, *msxe*) y del regulador de la proliferación *aldh1a2*. Esto indica un aumento del número de células indiferenciadas en la zona en regeneración. Por otro lado, el análisis de marcadores de diferenciación de osteoblastos tras la sobreactivación de la vía de Notch indica una expansión del patrón de genes de diferenciación temprana (*runx2*, *tcf7*) y una reducción de los marcadores tardíos de osteoblastos (osx). Todo ello sugiere que la manipulación de la vía de señalización de Notch interfiere en la diferenciación de osteoblastos durante la regeneración de la aleta. Por tanto, se demuestra que la función de Notch es mantener las células del blastema en un estado indiferenciado y proliferativo, lo cual supone un requisito indispensable para la regeneración de la aleta.

La segunda parte de esta tesis se ha centrado en el papel de la vía de señalización de Notch en la regeneración del corazón. Se empleó la técnica de criolesión para producir un daño cardíaco y desencadenar los procesos de muerte celular masiva, infiltración de células inflamatorias y deposición de tejido fibrótico. La posterior eliminación de este tejido y, finalmente, la desdiferenciación y proliferación de cardiomiocitos permiten la regeneración del músculo cardíaco en un proceso que dura unos 90 días. Observamos que los elementos de la vía de señalización de Notch se expresan en células endocárdicas y decidimos estudiar la respuesta del endocardio tras una lesión cardiaca. La captura de imágenes en 3D del corazón completo lesionado reveló que las células endocárdicas marcadas con GFP en peces transgénicos *ET33-mi60A* se activan rápidamente

y proliferan notablemente a los 3 días de la criolesión (ddl). El endocardio se expande y se organiza en el lugar de la lesión a los 9 ddl. Experimentos de ganancia y pérdida de función de Notch revelaron que esta vía es necesaria en la organización del endocardio y en la proliferación de los cardiomiocitos. El análisis de secuenciación de ARN en la región adyacente a la lesión mostró que la inhibición de Notch afecta a la expresión de algunos genes del endocardio y de otros genes relacionados con la remodelación de la matriz extracelular e implicados en procesos inflamatorios. Además, observamos que Notch es necesario para reducir la infiltración de células inflamatorias. Todos estos resultados demuestran el papel estructural y de señalización del endocardio durante la regeneración del corazón y la crucial importancia de la vía de señalización de Notch en este proceso.

Index of contents

Index of figures, tables and videos

Tables

Supplementary data are provided in the digital format of the thesis.

Supplementary Table 1: RNAseq data RO vs. DMSO

Videos

Movie 1: IMARIS volume rendering of the apex of a *ET33-mi60a* (green); *Tg(myl7:mdsred)*(magenta) cryoinjured transgenic heart at 24 hpci.

Movie 2: IMARIS volume rendering of the apex of a *ET33-1A* (green); *Tg(myl7:mdsred)*(magenta) cryoinjured transgenic heart at 24 hpci.

Movie 3: IMARIS volume rendering of the apex of a *ET33-mi60a* (green); *Tg(myl7:mdsred)*(magenta) cryoinjured transgenic heart at 3 dpci.

Movie 4: IMARIS volume rendering of a whole mount *ET33-mi60a* (green); *Tg(myl7:mdsred)* (magenta) cryoinjured transgenic heart at 24 hpci.

Movie 5: IMARIS volume rendering of a whole mount *ET33-mi60a* (green); *Tg(myl7:mdsred)* (magenta) cryoinjured transgenic heart at 36 hpci.

Movie 6: IMARIS volume rendering of a whole mount *ET33-mi60a* (green); *Tg(myl7:mdsred)* (magenta) cryoinjured transgenic heart at 3 dpci.

Movie 7: IMARIS volume rendering of a whole mount *ET33-mi60a* (green); *Tg(myl7:mdsred)* (magenta) cryoinjured transgenic heart at 9 dpci.

Movie 8: IMARIS volume rendering of a whole mount *ET33-mi60a* (green); *Tg(myl7:mdsred)* (magenta) cryoinjured transgenic heart at 1 mpci.

Movie 9: IMARIS volume rendering of a whole mount *ET33-mi60a* (green); *Tg(myl7:mdsred)* (magenta) cryoinjured transgenic heart at 3 mpci.

Abbreviations

acta1a	alpha skeletal actin
AFOG	acid fuchsin orange G staining
aldh1a2	aldehyde dehydrogenase 1 family, member A2
ankrd1a	ankyrin repeat domain 1a
aqp1	aquaporin 1
arg2	arginase2
AVC	atrioventricular canal
bmp	bone morphogenic protein
BrdU	bromodeoxyuridine
BSA	bovine serum albumin
cldn5b	claudin5b
col	collagen
cts	cathepsins
cxcl12	C-X-C motif chemokine 12
DAPT	(N-[N-(3,5-Difluorophenacetyl)-L-alanyl]-S-phenylglycine t-butyl ester
DMSO	dimethyl sulfoxide
dpa	days post amputation
dpci	days post cryoinjury
dpi	days post injury
dpt	day post MO-transfection
ECM	extracellular matrix
egr1	early growth response factor 1
EMT	epithelial to mesenchymal transition
FGF	fibroblast growth factor
GATA 4	GATA binding protein 4
GFP	green fluorescent protein
GO	gene ontology
H&E	hematoxylin *and* eosin *stain*
hand2	heart- and neural crest derivatives-expressed protein 2
has1	hyaluronan synthase 1
heg	heart of glass
hpf	hours post fertilization
hyal2	hyaluronidase-2
id1	inhibitor of DNA binding 1
IGF	insulin-like growth factor
IHC	immunohistochemistry
IP	intraperitoneal injection
is	injury site
ISH	*in situ* hybridisation

jag1b	jagged1b
klf	krüppel-like transcription factor
lfng	lunatic fringe
mf20	myosin heavy chain II
mmp9	matrix-metalloprotease 9
MO	antisense morpholino oligomer
mRFP	membrane bound red fluorescent protein
msx	muscle segment homeobox
myl7	myosin light chain 7
mylk3	cardiac specific myosin light chain kinase 3
nkx2.5	homeobox protein NK-2 homolog E
osn	osteocalcin
osx	osterix
p-smad	phospho-smad
PCNA	proliferating cell nuclear antigen
pde7a	phosphodiesterase 7a
ptgs2b	prostaglandin-endoperoxide synthase 2b
qPCR	quantitative real-time PCR
RA	retinoic acid
rbpjk	recombination signal binding protein for immunoglobulin kappa J region
RNA-seq	RNA sequencing
RO	RO4929097
runx2	runt-related transcription factor 2
sgpl1	sphingosine-1-phosphate lyase 1
shh	sonic hedgehog
tbx	T-box protein
tcap	titin-cap
tcf	T-cell-specific transcription factor
Tg(UAS:NICD)	Tg(hsp70l:Gal4)^{kca4} ; Tg(UAS:myc-Notch1a-intra)^{kca3}
Tgfβ	transforming growth factor beta

Introduction

1. Regeneration - different mechanisms and experimental models

Regeneration describes the replacement of a lost or damaged tissue, which includes the structural and functional restoration of the organ (Gemberling, Bailey et al., 2013). A wide range of model organisms all along the phylogenetic tree is used for regeneration studies. One of the first organisms where regeneration was described is the freshwater polyp *Hydra* (S.G. Lenhoff, 1986). Hydra is able to regenerate new polyps from only small parts of the body (Bode & Bode, 1980). Whole body regeneration is also intensively studied in the planarian *Schmidtea mediterranea* (Reddien & Sanchez Alvarado, 2004), which holds a more complex body organization than *Hydra*. A subset of vertebrates also serves as a model to study complex tissue regeneration. They include the zebrafish (*Danio rerio*), the clawed frog (*Xenopus leavis*), the newt (*Notophthalmus viridescens*), and the axolotl (*Ambystoma mexicanuma*) (Poss, 2010). Whereas in *Xenopus,* tail regeneration is stage-restricted (Beck, Christen et al., 2003), salamanders retain their regenerative capacity throughout lifetime (Roy & Gatien, 2008). Numerous studies have reported their remarkable capacity to regenerate an amputated tail or limb, including complex tissues such as the spinal cord, notochord, nerves and muscles (Brockes & Kumar, 2005, Simon & Tanaka, 2013). Further investigations also revealed a high cardiac regenerative potential in the newt (Mercer, Odelberg et al., 2013, Witman, Heigwer et al., 2013). Also in mammals regeneration occurs but is restricted to certain organs (e.g. blood, skeletal muscle, liver, pancreas, digit tip) and ages (Poss, 2010). This holds true for heart regeneration (Porrello, Mahmoud et al., 2011) which has been reported for neonatal mice (see below).

In the process of regeneration the production of new cells that replace lost tissue is achieved through diverse mechanisms, which are neither organ nor species specific. Regeneration can proceed through resident pluripotent or tissues specific stem cells (Fig. 1A). Stem cells have the capacity to self renew and differentiate into a certain cell type (Weissman, Anderson et al., 2001). *Hydra* exhibits three multipotent stem cell types contributing to the regeneration of different tissues (Bosch, 2007). However in planarians, one pluripotent stem cell type called neoblasts, represent the main source for tissue regeneration. Neoblasts are proliferating cells, characterized by *smedwi-1* expression (Reddien, Oviedo et al., 2005) and give rise to all adult cell types (Reddien, 2013). More specific stem cells have been described in the context of muscle regeneration in vertebrates. In the axolotl, $Pax7^{+}$ muscle satellite cells contribute to new skeletal muscle (Sandoval-Guzman, Wang et al., 2014). In mammals, there similarly exist $Pax7^{+}$ satellite cells, which are activated upon injury and contribute to skeletal muscle repair (Abou-Khalil & Brack, 2010).

However many tissues lack those stem cells and regeneration often proceeds through epimorphic regeneration meaning that differentiated, highly functional cells return to a more primitive or undifferentiated state (Fig. 1B). This includes the diminution of specific cellular functions and gene expression patterns and is often accompanied by the reexpression of embryonic genes (Poss, 2010). This process allows cells to reach a state that permits cell division for producing new cells and compensating for tissue loss. Recent studies in the newt have described this mechanism during skeletal muscle regeneration. Differentiated muscle fibres undergo fragmentation, allowing their cell proliferation and the contribution to new skeletal muscle (Sandoval-Guzman et al., 2014). Moreover this study showed that despite the phylogenetic proximity of the two species, axolotl and newt, skeletal muscle regeneration involves different mechanisms (Sandoval-Guzman et al., 2014). Also zebrafish heart and fin regeneration proceed through dedifferentiation as will be discussed in more detail later in the text.

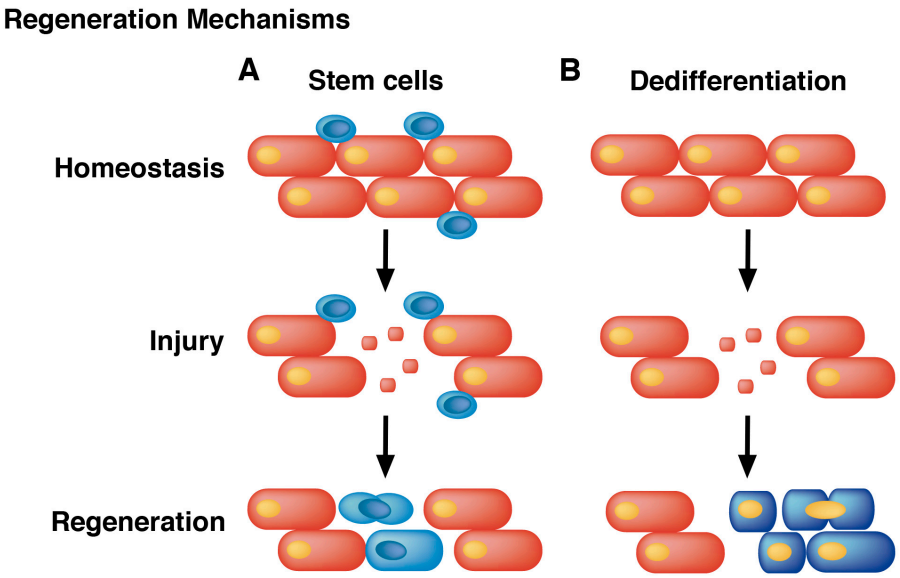

Figure 1: Mechanisms of Regeneration
A: Regeneration through resident stem cells: Injury-induced cell death triggers the activation of resident stem cells (blue). They proliferate and differentiate to replace lost tissue. **B**: Epimorphic regeneration proceeds through dedifferentiation of adjacent cells (blue) induced by injury signals. Dedifferentiated cells proliferate and redifferentiate to replace lost tissue.

Dedifferentiation of cells can include the change of cellular fate, meaning transdifferentiation. This is the conversion from one cell type to another, which directly occurs from a differentiated cell type into another or via an undifferentiated intermediate state (Shen, Burke et al., 2004). Recent studies described transdifferentiation in the mouse pancreas, where after almost complete β-cell ablation, new β-cells derived from α-cells (Thorel, Nepote et al., 2010).

2. The zebrafish – a prestigious regeneration model

Due to its short generation time and its transparency during embryonic development the zebrafish represents the perfect model to study developmental processes. Moreover during the last 20 years the adult zebrafish has gained immense on attention due to its extensive regenerative capacity. The zebrafish is an excellent model to study various mechanisms of regeneration as it regenerates many organs and tissues. These include parts of the nervous systems. The brain exhibits several neurogenic niches (Grandel, Kaslin et al., 2006) and radial glia-type progenitor cells proliferate and generate new neurons following a traumatic stab lesion (Kroehne, Freudenreich et al., 2011). Motor neurons also regenerate after spinal cord lesion (Reimer, Sorensen et al., 2008). Further, sensory organs can regenerate, shown by the successful replacement of hair cells within the zebrafish lateral line (Lush & Piotrowski, 2014). Injured retinas lead to the dedifferentiation of Müller glia cells to regenerate the lost tissue (Fausett & Goldman, 2006). Also, in the adult zebrafish chemical, genetic and surgical ablation of pancreatic cells induce high proliferation and regeneration of pancreatic tissue (Moss, Koustubhan et al., 2009, Ninov, Hesselson et al., 2013). More recent studies reported the existence of self-renewing nephron stem/progenitors cells that enable zebrafish kidney regeneration (Diep, Ma et al., 2011).

3. Fin regeneration

3.1. The process of fin regeneration

The zebrafish regenerates all its fins. For regeneration studies scientists mainly used the caudal fin because it is the biggest and easy accessible for amputation. The zebrafish caudal fin consists of 16 to 18 segmented bony fin rays (lepidotrichia) separated by soft interray tissue (Fig. 2A). Two concave hemirays built up each fin ray and enclose blood vessels, nerve fibres, fibroblasts, and melanocytes (Fig. 2B) (Tal TL, 2010). Osteoblasts line the hemiray and secret bone matrix (Knopf F, 2011). A multi-layered epidermis covers the fin rays and interray tissue (Tal TL, 2010).

During fin regeneration three different phases can be distinguished: wound healing, blastema formation and regenerative outgrowth (Akimenko, Johnson et al., 1995, Poss, Keating et al., 2003). Rapidly after fin amputation (12 hours post amputation (hpa)) adjacent epidermal cells migrate to cover the wound in a multi-layered fashion (Fig. 2C). Next (18- 24 hpa) the basal epidermal layer, composed of cuboidal cells forms (Poss et al., 2003). This layer provides crucial signals for fin regeneration and intercellular signalling occurs between the basal epidermal layer and underlying blastema cells (see below). Proliferating cells in the stump, migrate distally and form a blastema, a heterogeneous pool of dedifferentiated cells, distal to each fin ray until 2 dpa (Fig. 2A- C) (Knopf,

Hammond et al., 2011, Nechiporuk & Keating, 2002, Poleo G, 2001, Santos-Ruiz, Santamaria et al., 2002). Blastema cells are characterized by the expression of muscle segment homeobox-family members *msxb* and *msxe*, which label undifferentiated/progenitor-like cells in a variety of regenerating tissues (Akimenko et al., 1995, Nechiporuk & Keating, 2002, Yoshinari, Ishida et al., 2009).

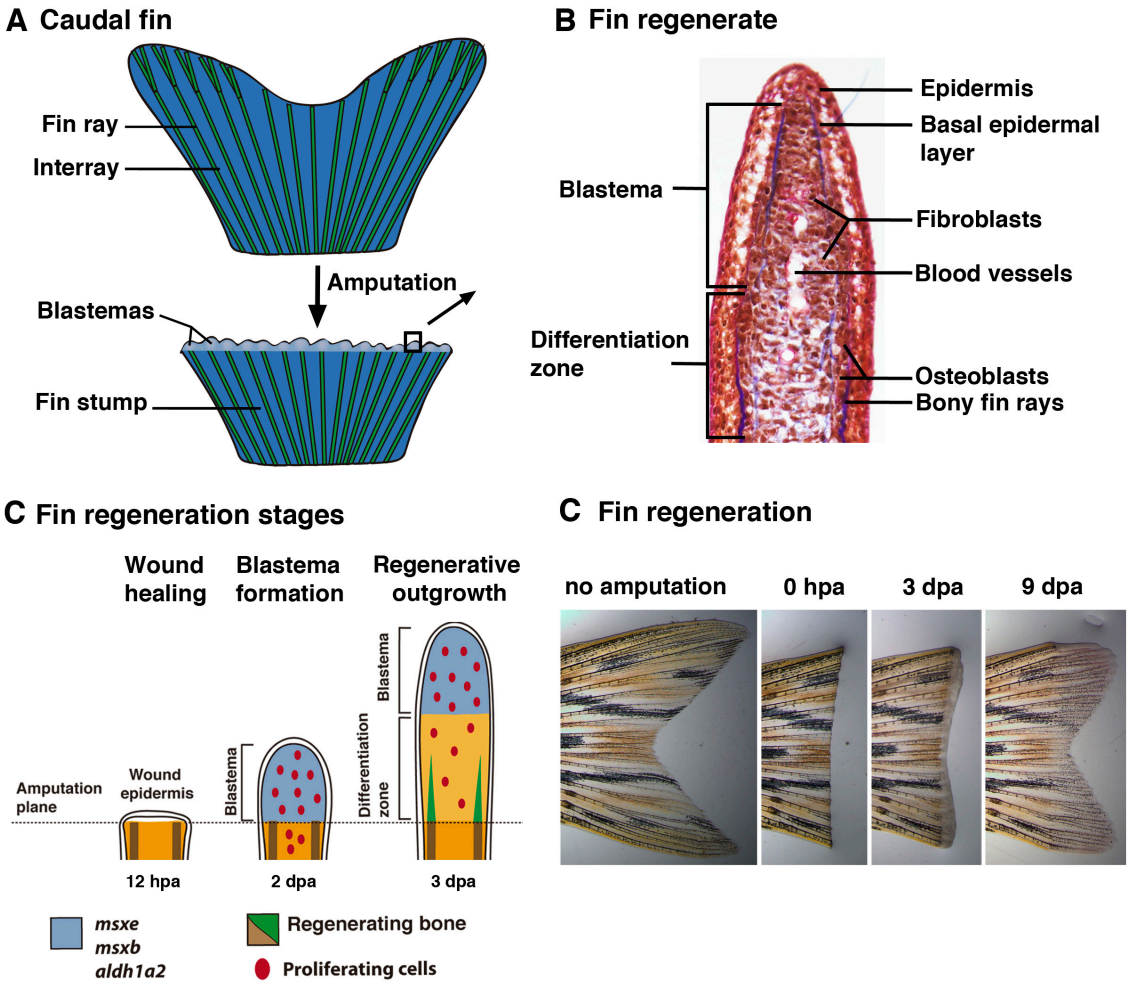

Figure 2: Fin regeneration
A: The zebrafish caudal fin ray exhibits bony rays and soft interray tissue. Following amputation a blastema forms distal to each fin ray. **B**: H&E stained fin section showing the morphology of the fin regenerate at 3 dpa. The blastema is located distally and differentiated cells more proximal. The fin contains fibroblasts, blood vessels and osteoblasts. A multi-layered epidermis and the underlying basal wound epidermis surround the regenerate. **C**: Stages of fin regeneration. The wound is closed by a multi-layered the epidermis (12 hpa). Cells within the fin stump proliferate and migrate distally to form the blastema (2 dpa). At 3 dpa cells in the proximal region of the regenerate redifferentiate to built up new bone whereas in the distal region the highly proliferating blastema remains. **D**: Whole mount time-lapse images before amputation and during regeneration.

This blastema is maintained throughout regeneration in the distal region of the fin (Fig. 1C). The most distal region of the blastema is characterized by a few non-proliferating cells, whereas in the more proximal central region, the blastema consists of highly proliferating cells (Nechiporuk & Keating, 2002, Santos-Ruiz et al., 2002). These include dedifferentiated osteoblasts, indicated by the expression of osteogenic markers (*runt-related transcription factor 2, runx2*), which are mostly aligned with the epidermis (Knopf et al., 2011, Sousa, Afonso et al., 2011). However, during regenerative outgrowth (from 3 dpa, Fig. 2B, C, D) cells become more differentiated along the distal proximal axis, indicated by *osterix* (*osx*; intermediate) and *osteocalcin* (*osn*; differentiated) expression (Knopf F, 2011). Fin regeneration is completed within around 14 days, representing a fast model to study regeneration (Poss et al., 2003).

More recently the fin has been used to study the response to bone crush injury. Genes involved in wound healing like *adenovirus E1A enhancer-binding protein* (*pea3*) and *lymphoid enhancer-binding factor 1* (*lef1*) are rapidly upregulated upon a crush injury, which similarly occurs in fin amputation. Blastema markers are expressed but delayed and likewise genes involved in skeletogenesis (*osx*, *osn*) (Geurtzen, Knopf et al., 2014, Sousa, Valerio et al., 2012). These studies revealed that bone healing and regeneration proceed through similar mechanisms.

3.2. Signalling pathways involved in fin regeneration

The multi-layered wound epidermis in the regenerating fin is characterized by a specific proximal-distal gene expression pattern that includes components of the Hedgehog, fibroblast growth factor (FGF), wingless/ int gene family (Wnt) and insulin-like growth factor (IGF) signalling pathways. These signals are required for fin regeneration by regulating either blastema cell proliferation or regenerative outgrowth (Wehner & Weidinger, 2015). Cell communication also occurs from blastema to epidermal cells, as has been demonstrated for IGF signalling. The ligand *igf2b* is expressed in blastema cells and activate IGF signalling in adjacent apical epithelial cells (Fig. 3A). This intercellular signalling is crucial for correct epidermal gene expression as well as blastema cell proliferation (Chablais & Jazwinska, 2010). An important signalling factor throughout the regeneration process is retinoic acid (RA). The RA-synthesizing enzyme aldehyde dehydrogenase 1a2 (aldh1a2/ raldh2) is expressed early on (at 6 hpa) in the fin stump, where RA induces the cell cycle entry of mesenchymal cells in the fin stump (Blum & Begemann, 2012). The blockage of RA synthesis at this stage prevents the formation of a blastema. Further *aldh1a2* is expressed in proliferating blastema cells, where it is required for maintenance and survival of blastema cells. Finally Blum *et al*. describe a complex regulatory network, where RA negatively regulates noncanonical Wnt signalling, however favours *fgf20* and *wnt10b* expression (Blum & Begemann, 2012). The activation of both, *fgf20* and *wnt10b* is required for the formation of the

blastema (Stoick-Cooper, Weidinger et al., 2007, Whitehead, Makino et al., 2005). Wnt signalling has been intensively studied in fin regeneration and holds a very complex role, integrating several signalling pathways (Stewart, Gomez et al., 2014, Stoick-Cooper et al., 2007, Wehner, Cizelsky et al., 2014). Various Wnt ligands are expressed in the epidermis or the distal blastema (Fig. 3A) and Wnt signalling inhibition blocks blastema cell proliferation (Stoick-Cooper et al., 2007). However, Wnt signalling does not regulate cell proliferation in a cell autonomous manner, as pathway activation was reported in the most distal non-proliferating cells. There, it directly regulates the expression of *aldh1a2*, which maintains cell proliferation in the adjacent more proximal zone. Further, Wnt signalling also orchestrates the activation of FGF, Activin, IGF and the bone morphogenic protein (BMP) pathways. Beside in the distal non-proliferating cells, Wnt is activated in osteoblast progenitors and actiniotrichia forming cells (Fig. 3A), where it regulates bone maturation (Stewart et al., 2014, Wehner et al., 2014).

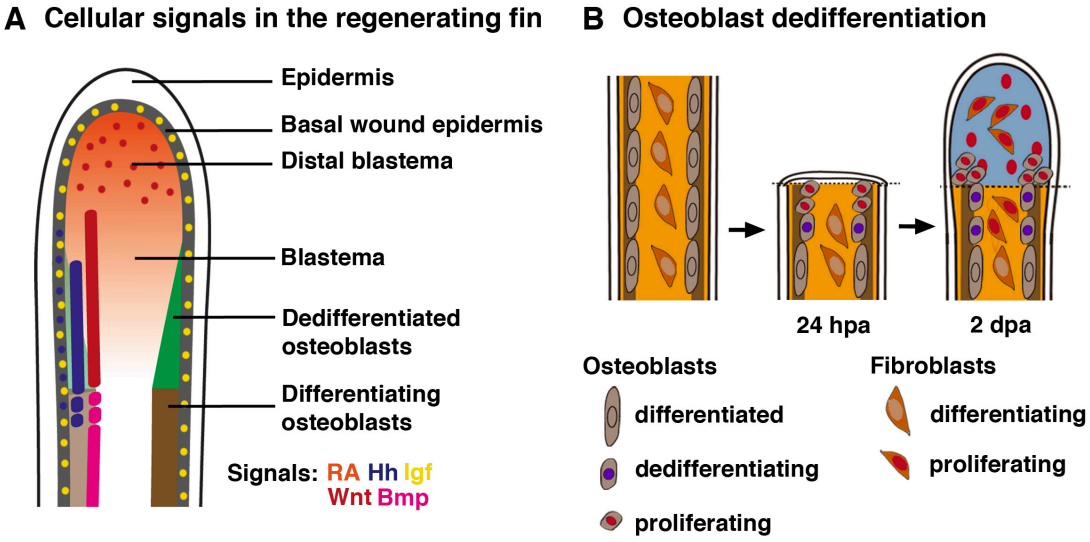

Figure 3: Molecular signals and the dedifferentiation of osteoblasts in the regenerating fin
A: Fin regenerate at 3 dpa. Retinoic acid (RA) acts in the blastema but less in the proximal regenerate. Wnt pathway activation takes place in the distal blastema and in dedifferentiated osteoblasts. Activated Hedgehog (Hh) signalling can be found in the epidermis and underlying osteoblasts whereas BMP expression is restricted to the proximal region of differentiated osteoblasts. IGF signalling is activated in the basal wound epidermis. **B**: Differentiated osteoblasts line the bony fin ray and secrete bone matrix. After amputation osteoblasts in the fin stump dedifferentiate and start to proliferate. They migrate distally and proliferate. Osteoblasts are mainly located adjacent to the epidermis in the fin regenerate. Fibroblasts also proliferate within the fin blastema.

BMP signalling acts in more proximal osteoblasts and promotes its differentiation (Fig 3A) (Smith, Avaron et al., 2006). One regulator of BMP is Hedgehog signalling (Hh) that equally promotes bone formation (Quint, Smith et al., 2002). Also Notch signalling pathway elements have been

shown to be expressed by *in situ* hybridisation (Raya, Koth et al., 2003) and in a microarray based gene profiling (Schebesta M, 2006). However the function of Notch on fin regeneration had not been described at the beginning of this PhD thesis project.

3.3. Growth control during fin regeneration

Fin regeneration proceeds independently of the level of amputation within the fin and fin outgrowth terminates when the former fin length is achieved (Akimenko, Mari-Beffa et al., 2003). Several studies have addressed the question how regenerative growth is controlled during fin regeneration (Kujawski, Lin et al., 2014, Mateus, Lourenco et al., 2015, Stoick-Cooper et al., 2007). The non-canonical Wnt ligand *wnt5b* is expressed in the epidermis of the regenerating fin and just underneath in the distal most blastema (Stoick-Cooper et al., 2007). It restricts the expression of genes, such as *shh*, that is involved in osteoblast differentiation, in more proximal epidermal cells (Lee Y, 2009). The fact that *wnt5b* overexpression completely inhibits regeneration and that regeneration is accelerated in *wnt5b*-mutant fish, led to the assumption that non-canonical Wnt signalling controls fin outgrowth (Stoick-Cooper et al., 2007). Moreover, a recent study showed that Calcineurin signalling is crucial for growth control in uninjured and regenerating fins. Thus pharmacological Calcineurin inhibition led to an increase in blastema size and unproportional growth of proximal structures during fin regeneration (Kujawski et al., 2014). Finally, the Hippo pathway, which controls growth in various organ systems (Halder & Johnson, 2011), is required for blastema proliferation and fin outgrowth. Mateus *et al*. propose that tension changes induced by variations in cellular density within the blastema, regulate Hippo pathway activation and thus fin growth (Mateus et al., 2015).

3.4. Lineage restriction in the regenerating fin

The zebrafish fin is a complex structure, consisting of diverse tissues such as bone, nerves, blood vessels and fibroblasts. For a long time the blastema had been assumed to be a homogeneous pool of stem cell-like progenitor cells that can give rise to different tissue types within the fin. Numerous lineage-tracing studies however demonstrated that cells are lineage restricted in the fin. By transposon based clonal analysis Tu *et al.* identified nine distinct lineages, including epidermis, osteoblasts, vascular endothelium, dermal fibroblasts and others. The authors did not observe any transdifferentiation within these lineages, suggesting that cells retain their fate during fin regeneration (Tu S, 2011). Further, lineage restriction and dedifferentiation have been extensively studied in osteoblasts, which line the bony fin ray and secrete bone matrix (Knopf et al., 2011, Sousa et al., 2011). Early upon fin amputation (24 hpa) osteoblasts in the fin stump, dedifferentiate, detach from the bony fin ray and migrate distally to contribute to the blastema (Fig. 3B). These

osteoblasts strongly proliferate, align to the epidermis and redifferentiate in the proximal region during regenerative outgrowth (Fig. 3B) (Knopf et al., 2011). Recent reports pointed out that RA is crucial to regulate this dedifferentiation programme. This includes, first the upregulation of the retinoic acid-metabolizing cytochrome 26b1 (cyp26b1) in the stump to allow osteoblast dedifferentiation and second, the maintenance of a proximal distal gradient of RA within the regenerate that prevents redifferentiation of osteoblasts in the distal region (Blum & Begemann, 2015). Although lineage-tracing studies satisfactorily demonstrate that new osteoblasts derive from dedifferentiated osteoblasts of the fin stump, genetic ablation of all osteoblasts within the fin does not interfere with fin regeneration, including bone reconstitution. The authors of this study propose that *de novo* osteoblast can arise during fin regeneration (Singh, Holdway et al., 2012).

4. Heart regeneration

4.1. The zebrafish heart

Zebrafish possess a two-chambered heart, consisting of atrium, ventricle and bulbus arteriosus (outflow tract) (Fig. 4A). Similar to the mammalian heart, the zebrafish ventricle exhibits three cardiac layers: an outer layer or epicardium which surrounds the heart, an internal layer, the endocardium a specialized endothelium that delineates the myocardium, the muscle tissue that provides the contractile force of the heart (Fig. 4A´). The ventricular myocardium consists of a thin outer layer of primordial muscle, the cortical compact myocardium and the inner trabecular myocardium (Gupta & Poss, 2012). In contrast to mammals, where trabeculae are a transient developmental structure that disappear through the process of compaction (Sedmera, Pexieder et al., 2000), in the fish heart trabecular myocardium constitutes the mayor part of the heart throughout lifetime (Hu, Yost et al., 2001). The cortical myocardium is innervated and vascularized (Fig. 4A´) (Hu et al., 2001, Mahmoud, O'Meara et al., 2015). However, oxygen supply of the trabeculated myocardium is assured by diffusion through the endocardial layer (Hu et al., 2001).

4.2. Heart injury models in zebrafish

Initial studies on zebrafish heart regeneration consisted of the resection of about 20% of the ventricular apex (Fig. 4B). This injury causes the rapid formation of a blood clot, which closes the wound, prevents further bleeding and ensures the survival of the fish (Jopling, Sleep et al., 2010, Poss, Wilson et al., 2002). The rapid activation and migration of epicardial cells lead to the coverage of the injured cardiac muscle (Lepilina, Coon et al., 2006) and regeneration is

predominantly achieved through the replacement of lost myocardium by cortical cardiomyocytes (Gupta, Gemberling et al., 2013, Gupta & Poss, 2012).

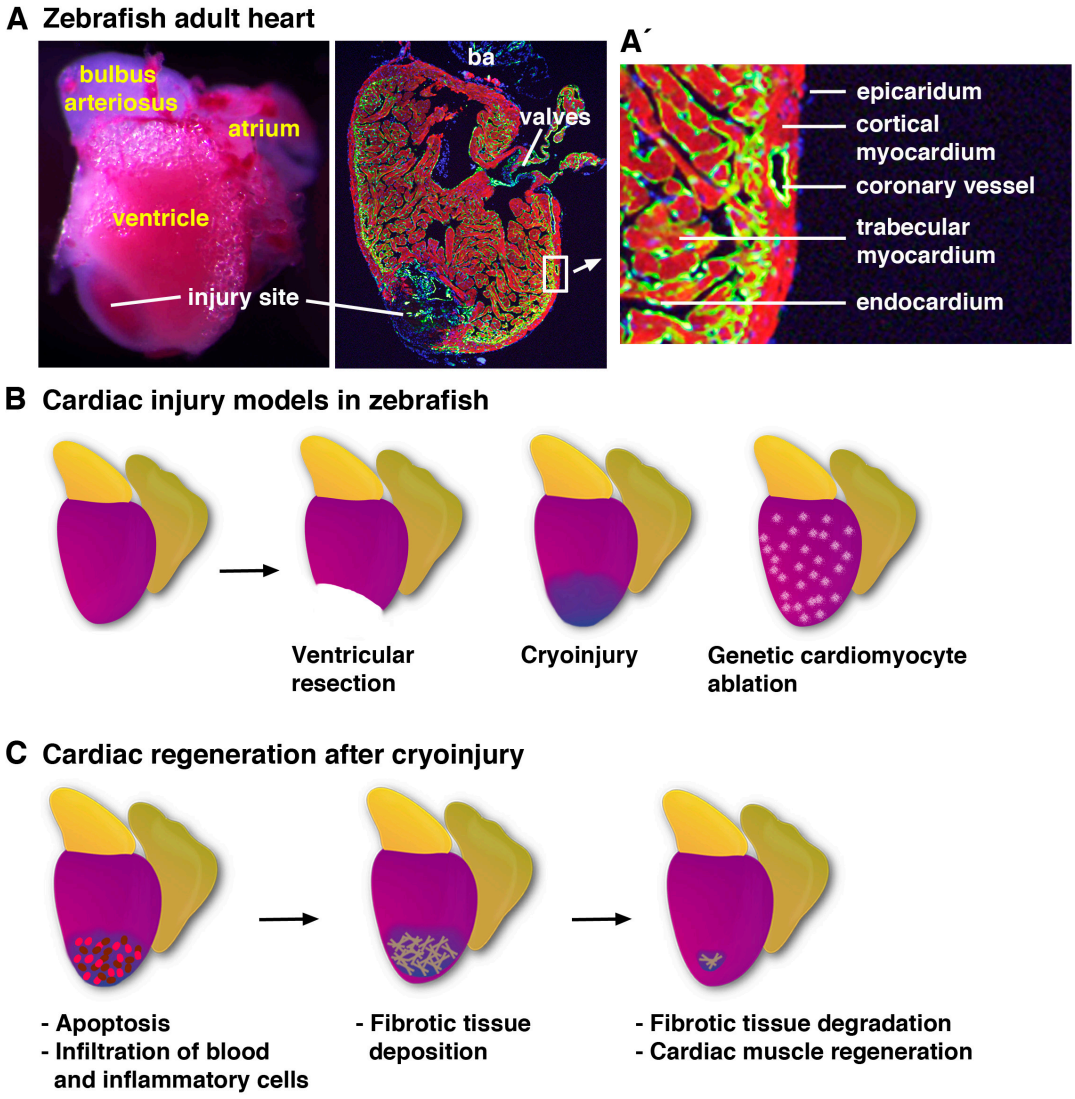

Figure 4: Cardiac injury in zebrafish

A: Whole mount view and immune stained section of a cryoinjured zebrafish heart. The ventricle consists of trabeculated and cortical myocardium (red), which is line by the endocardium (green). The Epicardium surrounds the ventricle. Coronary vessels are present within the cortical myocardium. **B**: Different models to study cardiac regeneration in the zebrafish. Whereas 20% of the ventricle is removed after resection, after cryoinjury the damaged tissue remains. In a third model cardiomyocytes are specifically ablated whereas the other tissues remain intact. **C**: Cardiac regeneration. After cryoinjury blood and inflammatory cells infiltrate the injury site and fibrotic tissue is deposited. Cardiac muscle regeneration proceeds with the progressive degradation of fibrotic tissue and the substitution of the lost muscle by regenerated one.

A more recent, second regeneration model that was used in this thesis is the cryoinjury model (Fig. 4B) (Chablais & Jazwinska, 2012a, Gonzalez-Rosa, Martin et al., 2011, Schnabel, Wu et al., 2011). In this model, cardiac damage is caused by the contact with a cold copper probe that induces apoptosis in cells of the three cardiac layers: myocardium, endocardium and epicardium. As a consequence, blood and inflammatory cells infiltrate this area of dying cells and the tissue is cleared of cells debris (Fig. 4C). With time, a collagenous and fibrous scar is deposited (Fig. 4C). These events are very similar to observations after cardiac injury in mammals (see below). However in fish the fibrotic tissue is almost removed at 90 dpci (Fig. 4C) and at 130 dpci, the lost muscle is completely restored (Chablais & Jazwinska, 2012a, Gonzalez-Rosa et al., 2011, Schnabel et al., 2011). Cardiac muscle regeneration may occur through trabecular and cortical cardiomyocytes; a region of thickened compact myocardium indicates the site of injury (Gonzalez-Rosa, Guzman-Martinez et al., 2014).

A third approach is to genetically ablate over 60% of cardiomyocytes (Fig. 4B). This cardiac injury results in a reduced stress tolerance in fish. However, dedifferentiated cardiomyocytes replace lost cardiac muscle within a few days and the heart recovers form and function (Wang, Panakova et al., 2011).

4.3. Cardiac tissue activation during regeneration

Cardiac injury rapidly induces an organ wide response, which is restricted to the injury site with time (3 dpa) (Fang, Gupta et al., 2013, Kikuchi, Holdway et al., 2011b). This includes the rapid activation of the epicardium, which induces expression of embryonic genes such *fgf17b*, *aldh1a2*, *tcf21* and the gene encoding for T-Box Protein 18 (*tbx18*) (Fig. 5A). Epicardial cells all over the ventricle highly proliferate and migrate towards the injury to close the injury site (Fig. 5A) (Kikuchi, Gupta et al., 2011a, Lepilina et al., 2006). A subset of epicardial cells undergoes epithelial to mesenchymal transition (EMT) and contributes to the formation of new blood vessels within the injury site (Kim, Wu et al., 2010, Lepilina et al., 2006). Also myofibroblasts and perivascular cells arise from epicardial cells in the regenerating heart (Fig. 5A) (Gonzalez-Rosa, Peralta et al., 2012, Kikuchi et al., 2011a). The epicardium provides important signals for cardiomyocyte proliferation and migration allowing regeneration to proceed. Extracellular matrix molecules (ECM) like fibronectins (*fn1a*, *fn1b*) are strongly expressed in epicardial cells and required for cardiac regeneration (Wang, Karra et al., 2013). This is consistent with observations in the regenerating newt heart (Mercer et al., 2013) suggesting that epicardial ECM molecule secretion is a fundamental, evolutionally conserved mechanism for cardiac regeneration. Further, the epicardial production of the cytokine C-X-C motif chemokine 12a (cxcl12a) is crucial for the migration of cardiomyocytes that express the associated receptor cxcr4 (Itou, Oishi et al., 2012).

Finally, recent genetic ablation studies of epicardial cells underlined the high regenerative potential and its high implication in cardiac repair. Epicardial cells fully recover after genetic ablation receiving Hedgehog signals from the bulbus arterious during this process (Wang, Cao et al., 2015).

An early organ wide response arises also in the endocardium. Endocardial cells up-regulate *aldh1a2* and *heg* expression all over the ventricle, which is restricted to the injury site in later stages. Endocardial cell activation upon ventricular resection includes proliferation and morphological and gene expression changes (Fig. 5B), indicated by GFP expression driven by promoters of heart- and neural crest derivatives-expressed protein 2 *(hand2)*, GATA binding protein 5 (*gata5)* and fetal liver kinase *(flk1/kdrl)*. Further, endocardial RA production is required for cardiomyocyte proliferation (Kikuchi et al., 2011b).

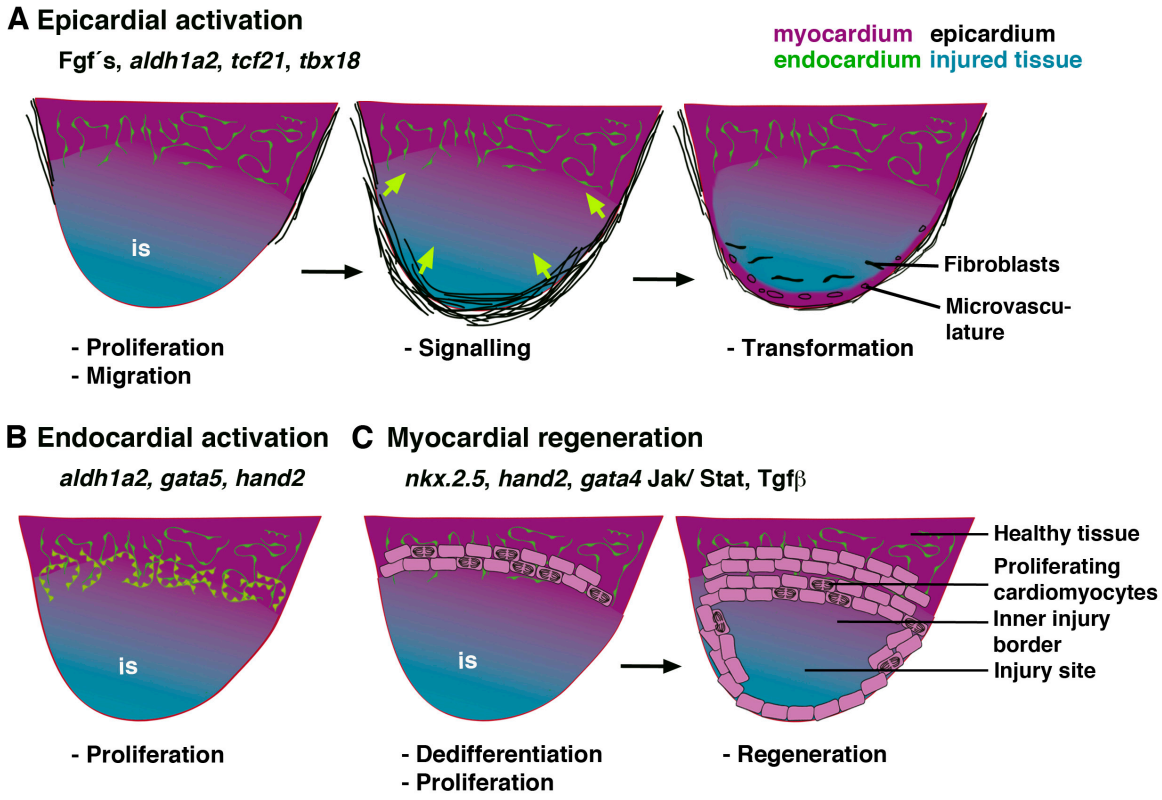

Figure 5: Tissue activation upon cardiac injury
A: Epicardial activation: Upon injury epicardial cells become activated, changing morphology and expressing embryonic genes, proliferate and migrate to and cover the injury site (is). The epicardium provides signals to adjacent tissues. Epicardial cells undergo EMT and can give rise to microvessels and fibroblasts within the injury site (is). **B**: The endocardium becomes activated and proliferates. **C**: Myocardial regeneration: Cardiomyocytes adjacent to the injury site dedifferentiate by reexpressing embryonic genes and proliferate. These dedifferentiated cardiomyocytes contribute to replace lost cardiac muscle.

The myocardium has captured most of the attention in regeneration studies. Cardiac muscle loss in zebrafish results in the re-expression of embryonic genes in cardiomyocytes adjacent to the injury. These include *hand2*, *tbx20*, *tbx5*, *gata4* and the homeobox protein NK-2 homolog E (*nkx2.5*) (Fig. 5C). This, together with the disassembly of sarcomeric structures, suggests the dedifferentiation of cardiomyocytes adjacent to the injury site. These dedifferentiated cardiomyocytes proliferate and restore the lost cardiac muscle (Jopling et al., 2010, Kikuchi, Holdway et al., 2010, Lepilina et al., 2006, Poss et al., 2002) (Fig. 5C). Lineage tracing studies nicely demonstrated that cardiomyocytes of regenerated ventricles derive from existing cardiomyocytes (Jopling et al., 2010, Kikuchi et al., 2010),confirming that cardiac regeneration proceeds through dedifferentiation and redifferentiation in the adult zebrafish. Additionally, regeneration studies in the embryonic heart demonstrated that transdifferentiation of atrial cardiomyocytes into ventricular cardiomyocytes could also be achieved (Zhang, Han et al., 2013).

Additional studies have shown how injury-related signals modulate regenerative processes. Fang *et al.* demonstrated that cytokines, such as interleukin 11a (il11a), produced by the endocardium activate the janus kinase/signal transducer and activator of transcription (Jak/Stat3) pathway in injury-adjacent cardiomyocytes. The inhibition of this pathway in cardiomyocytes interferes with proliferation and heart regeneration (Fang et al., 2013). A multifunctional role for transforming growth factor beta (TGFβ) signalling was reported in cryoinjured hearts: The TGFβ receptor activin A receptor type II-like kinase 5b (*alk5b*/ *tgfbr1b*) and its ligands are expressed in cells within the injury site and adjacent cardiomyocytes. Chemically inhibition studies revealed the implication of TGFβ in scar depostion, tissue remodelling and cardiomyocyte proliferation (Chablais & Jazwinska, 2012b).

4.4. Cardiac injury in mammals

In contrast to fish, the adult mammalian heart fails to regenerate after a cardiac injury due to the permanent deposition of massive fibrotic tissue and the inability of the heart to replace lost cardiac muscle with new cardiomyocytes.

The occlusion of a coronary artery results in myocardial infarction. This ischemic injury, caused by insufficient blood supply, induces massive cell death, affecting all tissues of the cardiac ventricle. Shortly after, blood and inflammatory cells penetrate this region (Frangogiannis, 2008). Thus, a transient fibrin clot is deposited and leukocytes remove cell debris. This is named inflammatory phase and is characterized by high protease activity that degrades the homeostatic cardiac matrix, allowing injured tissue remodelling (Dobaczewski, Gonzalez-Quesada et al., 2010). Next, fibroblasts populate this area and produce a stable fibrotic matrix by secreting ECM

molecules such as collagen and hyaluronan. Crosslinking of collagen fibres increases the stability of the scar that gives mechanical support to the injured heart and prevents cardiac rupture (Lopez, Gonzalez et al., 2010, Whittaker, Boughner et al., 1991). However, with time this rigid structure interferes with the regular heartbeat.

Historically the adult mammalian heart has been described as a post-mitotic organ. However more recent studies addressed adult cardiomyocyte proliferation by different techniques and found a limited number of proliferating cardiomyocytes and progenitor-like cardiac stem cells, although results are somehow conflicting (Senyo, Lee et al., 2014). In the adult homeostatic heart, cardiomyocyte turnover is very low reaching a frequency of 1.3-4% per year. Although cardiomyocyte proliferation increases upon myocardial infarction, is does not reach sufficient level to replace lost cardiac muscle (Malliaras, Zhang et al., 2013). However, individual cardiomyocytes in adult hearts undergo hypertrophy to compensate ventricular wall stress after myocardial infarction (Frey & Olson, 2003). This includes the activation of embryonic genes simultaneously to an increase in sarcomeric proteins (Nicol, Frey et al., 2001). These cardiomyocytes do not divide but increase in size, which prevents full recovery of cardiac function (Frey & Olson, 2003).

Although regenerative potential is low in adult mammalian hearts, recent reports demonstrate a high reparative capacity of the heart shortly after birth (Porrello & Olson, 2014). The mouse neonate heart fully recovers after an injury, occurring between birth and postnatal day 7 (P7). Cardiomyocytes show sarcomere disassembly, proliferate and replace lost cardiac muscle (Porrello et al., 2011), which in some aspects is reminiscent to zebrafish and newt heart regeneration. We chose to study adult cardiac regeneration in zebrafish using the cryoinjury model, as it reproduces quite faithfully the situation in the human heart after a myocardial infarction and the knowledge gained with our studies will help us to understand why regeneration fails in the mammalian heart after injury.

5. Notch signalling

5.1. The Notch signalling pathway

The conserved Notch signalling pathway mediates cell-to-cell communication via ligand receptor interactions to determine cell fate decisions and to regulate processes such as proliferation, apoptosis, cell differentiation and tissue patterning (Artavanis-Tsakonas, Rand et al., 1999, Bolos, Grego-Bessa et al., 2007).

Notch receptors are single-pass transmembrane proteins with three evolutionary conserved domains (Fig. 6). The large extracellular domain (NECD) contains 11-36 tandem epidermal growth

factor (EGF)-like repeats, three Lin/Notch repeats and one heterodimerization domain. The transmembrane domain spans the membrane and connects both the intracellular domain (NICD) and NECD. NICD contains a RAM23 domain, 6 ankyrin repeat domains, two nuclear localization signals (NLS) and a terminal PEST domain (Kopan & Ilagan, 2009). The Notch receptor is translated as a single protein, and cleaved by a furin-convertase at the Golgi apparatus (Fig. 6). This first cleavage (S1) allows the formation of the heterodimer, where NICD and NECD are hold by covalent interactions (Logeat, Bessia et al., 1998). The receptor can be further modified by the addition of O-fucose glycans by a glycosyl-transferase (Fig. 6). Three different transferases have been described: Manic fringe, Radical fringe and Lunatic fringe. This modifications favour the interaction with Delta ligands instead of the interaction with Jagged (Panin, Papayannopoulos et al., 1997). Notch ligands (Delta or Jagged) similarly exhibit an EGF-like repeats containing extracellular domain together with a Delta, Serrate, lin12 (DSL) domain, that serves for ubiquitylation (Kopan & Ilagan, 2009). Upon Notch receptor and ligand interaction in two adjacent cells, the ligand is ubiquitylated by an E3 ubiquitin ligase (mind bomb) and endocytosed in signalling cells (Fig. 6). (Itoh, Kim et al., 2003).

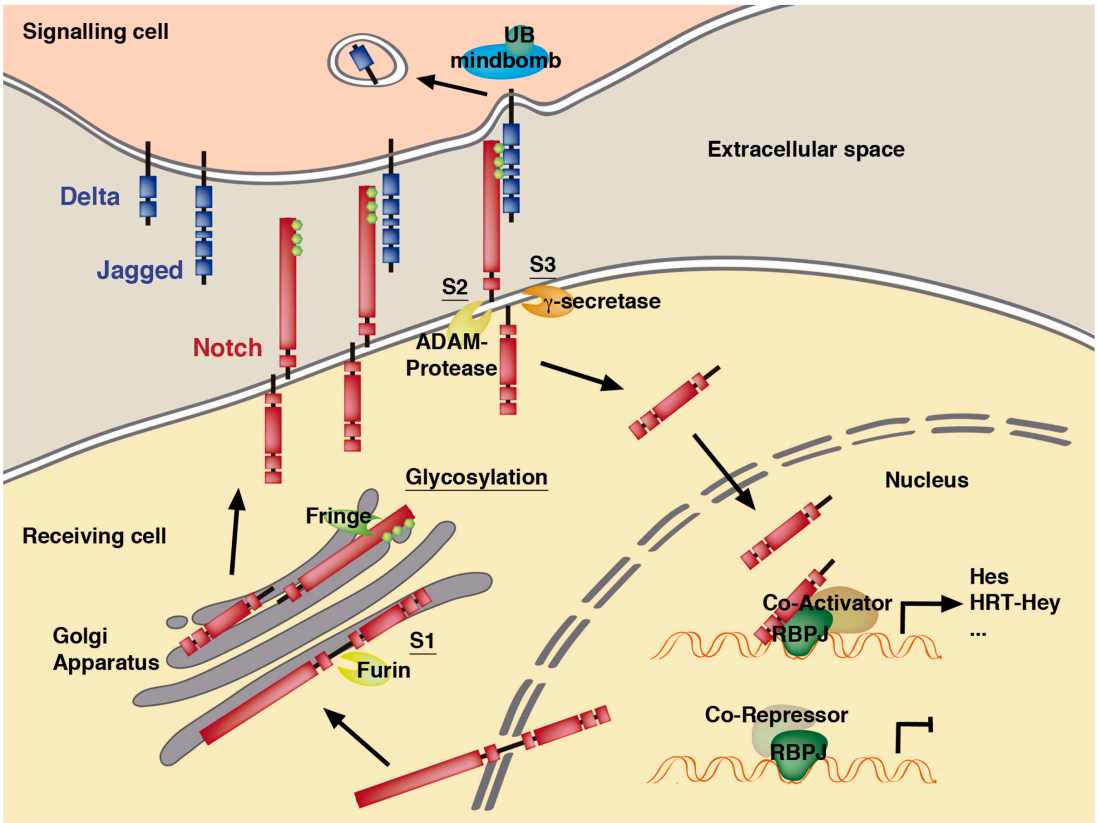

Figure 6: The Notch signalling pathway
A: The Notch receptor is cleaved by Furin at the Golgi apparatus (S1). Next, the receptor can be glycosylated by Fringe glycosyltransferases. When located to the membrane, the Notch receptor acts with a ligand (Delta/ Jagged) of an adjacent signalling cell. Receptor ligand interaction allows the second cleavage by ADAM-proteases (S2) at the membrane. The extracellular domain is released and Mindbomb in the signalling cells mediates the ubiquitinylation of the ligand-receptor complex. The intracellular domain of the Notch receptor is further cleaved at the membrane by a g-secretase (S3) and released to move to the nucleus. There it prevents the adhesion of a Co-repressors complex to RBPJ but favours the recruitment of a set of Co-activators to induce the expression of Hes/ HRT-Hey family genes.

At the same time, in the receiving cell ADAM metalloproteases cleave the receptor (S2) (Parks, Klueg et al., 2000). This is followed by a third cleavage (S3) induced by a γ-segretase/presenelin that liberates the NICD into the cytoplasm (Fig. 6) (Okochi, Steiner et al., 2002). The DSL domain allows the translocation of NICD to the nucleus where it binds to the transcription factor recombination signal binding protein for immunoglobulin kappa J region (RBPJ), also termed Suppressor of Hairless (Su(H)) (Jarriault, Brou et al., 1995). This complex delocates co-repressors bound to RBPJ/Su(H) and recruits transcriptional co-activators to regulate Notch target gene expression, including encoding basic-helix-loop-helix (bHLH) repressor transcription factors of the Hes and Hey (HESR) families (Iso, Kedes et al., 2003) (Fig. 6).

Zebrafish exhibit four Notch receptors: notch1a, notch1b, notch2 and notch3 (Bierkamp & Campos-Ortega, 1993, Kortschak, Tamme et al., 2001, Westin & Lardelli, 1997). There are five Delta ligands deltaA, deltaB, deltaC deltaD and delta-like 4 (dll4) (Dornseifer, Takke et al., 1997, Haddon, Smithers et al., 1998), and three Jagged ligands, jagged1a, jagged1b and jagged2 (Lorent, Yeo et al., 2004).

5.2. Notch signalling in organ regeneration

Numerous studies have demonstrated the implication of the Notch pathway in the regeneration of different organs in vertebrates and invertebrates. This goes in line with the evolutionary conserved role for Notch signalling in regulating stem cell maintenance and/or differentiation. In the sea urchin (*Lytechinus variegatus*) Notch signalling activity is required for tube feed and spine regeneration, which proceeds though the activation of multipotent progenitors (Reinardy, Emerson et al., 2015). Further, Notch receptors are expressed during *Xenopus* tail regeneration in the regenerating spinal cord and ectopic activation of the pathway promotes regeneration of spinal cord and notochord even in the refractory period when regeneration normally fails (Beck et al., 2003). In the newt telencephalon Notch holds a cell specific role regulating neural precursor fate after cholinergic neuron ablation (Kirkham, Hameed et al., 2014). In the zebrafish nervous system

the function of Notch is context dependent. In the brain, neurogenic niches contain proliferating radial glia cells with strong Notch receptor expressions (de Oliveira-Carlos, Ganz et al., 2013), suggesting the its requirement for progenitor cell maintenance. However in the regenerating spinal cord Notch negatively regulates neurogenesis. Notch activation decreases progenitor proliferation and pharmacological Notch inhibition increases it (Dias, Yang et al., 2012). Upon hair cell ablation in the zebrafish lateral line, Notch similarly controls cell proliferation and Notch signalling attenuation results in excessive hair cell regeneration (Ma, Rubel et al., 2008). Notch pathway activation in the regenerating retina occurs in dedifferentiating Müller glia cells and defines this progenitor cell population, acting in a regulatory feedback loop with heparin-binding epidermal-like growth factor (Hb-Egf) (Wan, Ramachandran et al., 2012, Yurco & Cameron, 2007).

5.3. The role of Notch signalling in cardiovascular development, disease and repair

Notch signalling is crucial for various step of heart development. Early on, Notch signalling activation occurs in second heart field progenitors and is required outflow tract development (High, Jain et al., 2009, Jain, Engleka et al., 2011). Studies in mice showed the implication of endocardial Notch signalling during chamber morphogenesis, regulating cardiomyocyte proliferation in a non-cell autonomous manner. In this context endocardial Notch activation mediates *Ephrinb2* expression and Neuregulin and Bmp signalling (Grego-Bessa, Luna-Zurita et al., 2007). During valve morphogenesis, Notch signalling in the atrioventricular canal (AVC) endocardium is involved in mediating epithelial-to mesenchymal transition in the interplay with BMP2 signalling (Luna-Zurita, Prados et al., 2010, Timmerman, Grego-Bessa et al., 2004). Also in zebrafish Notch pathway genes are strongly expressed in the AVC (Del Monte, Grego-Bessa et al., 2007) and *notch1b* expression in this region depends on blood flow-mediated *klf2a* expression (Vermot, Forouhar et al., 2009). Moreover, Notch signalling regulates the differentiation and patterning of the endocardium in the ventricle and AVC region (Beis, Bartman et al., 2005, Timmerman et al., 2004).

Numerous studies have shown the implication of the Notch signalling pathway in cardiovascular diseases. As endocardial Notch signalling is required during heart development (Del Monte et al., 2007, Grego-Bessa et al., 2007, Luna-Zurita et al., 2010), several diseases are attributed to the lack of Notch signalling components during embryonic development. Mutations in the mind bomb E3 ubiquitin protein ligase 1 (Mib1), which ubiquitylates Notch ligands, results in left ventricular non-compaction (LVNC) due to reduced Notch signalling activation during chamber development (Luxan, Casanova et al., 2013). Further, patients with heterozygous mutations in NOTCH1 exhibit bicuspid aortic valves with severe calcification. In this context the reduction of NOTCH signalling activation induced an early developmental defect but also favours

the expression of RUNX2, an early osteoblast marker, which is implicated in valve calcification (Garg, Muth et al., 2005).

The crucial role of Notch signalling during heart development further has let to numerous studies, investigating the implication of Notch signalling in the adult heart upon cardiac injury, however with controversial results. Whereas during development Notch signalling is activated in the endocardium (Del Monte et al., 2007), studies in the prenatal mammalian heart reported the presence of the activated form of Notch1 (NICD) in cardiomyocytes upon myocardial infarction (Gude, Emmanuel et al., 2008), in immature cardiomyocytes (Collesi, Zentilin et al., 2008) or c-kit^{+} cardiac stem cells (Urbanek, Cabral-da-Silva et al., 2010). However, the number of cardiomyocytes exhibiting NICD declines with age (Collesi et al., 2008). Notch signalling activation in the heart increases the number of cardiac stem cells and their proliferation in the neonatal and stressed adult heart (Collesi et al., 2008, Nemir, Metrich et al., 2014) and protects from apoptosis after myocardial infarction (Yu & Song, 2014). Further, Kratsios *et al* showed that ectopic Notch pathway activation in adult cardiomyocytes results in increased cardiomyocyte proliferation, hyperplasia and impaired differentiation and that the delivery of a pseudoligand Notch1 enhances cell survival and angiogenesis upon myocardial infarction (Kratsios, Catela et al., 2010). Additionally Notch activation reduces myofibroblast proliferation upon pressure overload (Nemir et al., 2014). Finally, recent studies have shown that in neonates the reduction of cardiomyocyte proliferation coincides with decreased Notch signalling activation and that upon myocardial infarction in the adult heart Notch target gene expression fails due to epigenetic modifications (Felician, Collesi et al., 2014).

Objectives

The correct activation of the Notch signalling pathway is crucial during development, disease and regeneration of many organ systems, as Notch mediated cell fate decisions result in proliferation, apoptosis, cell differentiation and tissue patterning (Artavanis-Tsakonas et al., 1999, Bolos et al., 2007). To better understand the mechanisms on how Notch signalling can mediate tissue regeneration, the objective of this thesis was to study the role of Notch signalling during the regeneration of two different organs in the adult zebrafish: the fin and the heart.

Objectives:

1. Determine the role of Notch signalling in fin regeneration

- Examination of Notch signalling elements during fin regeneration
- Study the consequences of Notch inhibition on fin regeneration
- Analyse phenotypic changes on Notch signalling gain-of-function on fin regeneration

2. Determine the role of Notch signalling in heart regeneration

- Examination of Notch signalling gene expression during heart regeneration upon cryoinjury
- Characterization of the endocardium during heart regeneration
- Phenotypic analysis of heart regeneration in Notch gain- and loss-of function models
- Analyse global gene expression changes in the regenerating heart upon Notch signalling inhibition and study the spatio-temporal expression of selected genes

Materials and Methods

1. Zebrafish husbandry and transgenic lines

Zebrafish were raised under standard conditions at 28ºC (Kimmel, Ballard et al., 1995). Experiments were performed with 6 to 16-month-old adults if not indicated otherwise. Zebrafish lines, used during this thesis, are listed in Table 1.

Table 1: Wild-type and transgenic fish lines

Name	Acronym	Reference	Description
AB	wild-type		wild-type fish
Tg*(hsp70l:Gal4)*^{kca4};Tg*(UAS:myc-Notch1a-intra)*^{kca3}	*Tg(UAS:NICD)*	(Scheer, Groth et al., 2001)	heat shock-inducible NICD-overexpression
ET(krt4:EGFP)$^{sqet33\text{-}mi60A}$	*ET33-mi60A*	(Poon, Liebling et al., 2010)	endocardial/ lfng enhancer trap line
ET(krt4:EGFP)$^{sqet33\text{-}1A}$	*ET33-1A*	(Poon et al., 2010)	GFP expression in endocardial cells
Tg(myl7:GFP)	*Tg(myl7:GFP)*	generated by A. Raya, Barcelona, Spain	GFP expression in cardiomyocytes
Tg(fli1a:GFP)y1	*Tg(fli:GFP)*	(Lawson & Weinstein, 2002)	GFP expression in endocardial/ endothelial cells
Tg(myl7:mRFP)	*Tg(myl7:mRFP)*	(Rohr, Otten et al., 2008)	membrane bound RFP expression in cardiomyocytes

2. Interventions

2.1. Anaesthesia

Prior to fin amputations, cardiac injury, substance injection and live imaging of the regeneration fin adult fish were anesthetized with trichaine methane sulphonate at a concentration of 0.04 % in fish water.

2.2. Fin amputation and fin ray injury

Fin amputation was performed as described (Akimenko et al., 1995). The anesthetized fish were placed on a plastic dish and half of the caudal fin was removed with a scalpel. The fish was returned to fish water immediately and maintained at 28ºC during regeneration. For fin ray injury experiments the fish were similarly anesthetised and up to three fin rays were fractured with forceps.

2.3. Heart cryoinjury

The cryoinjury was performed following the published protocol (Gonzalez-Rosa & Mercader, 2012). The anesthetized fish were placed on a wet sponge under a stereomicroscope. To open the cardiac cavity an incision on the chest was made using an iridectomy scissors. Pressing on the belly provoked the appearance of the heart, which was dried with a piece of filter paper. Subsequently the heart was touched with a liquid nitrogen cooled probe for ten seconds. Immediately the fish was returned to the fish tank.

2.4. Treatment with chemical substances

During this thesis fish were treated with different chemical substances: DAPT (N-[N-(3,5-Difluorophenacetyl)-L-alanyl]-S-phenylglycine t-butyl ester, Sigma), RO4929097 (S1575, selleckchem.co) and Bromodeoxyuridine (5-bromo-2'-deoxyuridine, BrdU). DAPT and RO were dissolved in dimethyl sulfoxide (DMSO) and kept as stock solution (RO 50mM). DMSO was applied to a control experimental group in the equivalent concentration. Chemical substances were added to fish water or intraperitoneally injected (Table 2). To minimize the required amount of substances, fish were maintained in smaller containers, meaning in a 500 ml glass beaker (with BrdU for 30 min) or in a 800 ml plastic box (with RO or DMSO for 3 days). Embryos were kept in 100 ml petri dishes during the treatment with RO or DMSO. For intraperitoneally injections fish were anesthetized and placed on a humid sponge. 30 ml of PBS with RO, DMSO or BrdU were injected intraperitoneally (IP) some millimetres rostral to the anal fins. Fish were immediately returned to the tanks after injection.

Table 2: Chemical substances

Substance	Way of application	Concentration
DAPT	in fish water	50 μM
RO	in fish water	10 μM/ 15 μM
RO	IP injection	600 μM
BrdU	in fish water	10 mM
BrdU	IP injection	2.5 mg/ ml

2.5. Heat shock application

Heat shocks of 38ºC in a serial way (Table 3) were applied automatically using the immersion thermostat LAUDA E300, placed in a mouse cage, which was connected to the fish water system allowing fresh water supply.

Table 3: Heat shock protocols

Experiment	Time	Series
fin regeneration	10 hours	60 min at 38ºC; 90 min at 28ºC
fin regeneration	12 hours	60 min at 38ºC; 90 min at 28ºC
fin regeneration	3- 5 days	60 min at 38ºC; 180 min at 28ºC
heart regeneration	2- 6 days	40 min at 38ºC; 450 min at 28ºC
heart regeneration	90 days	60 min at 38ºC; 1500 min at 28ºC

2.6. Morpholino transfection

Morpholino antisense oligomer (MO) experiments were performed following the published protocol (Thummel, Bai et al., 2006). After two days of fin regeneration fish were anesthetised and placed on an agarose-filled petri dish. MO solution was injected into the blastema distal to each fin ray of the dorsal half of the fin. Next, fish were returned to a petri dish containing fish water and trichaine. The fin was electroporated with an Electro Square Porator ECM 830, BTX (Harvard Apparatus) following this protocol: 5 series of 3 pulses of 15V every 30 sec. The fish was subsequently returned to the tank.

2.7. Live imaging of the regenerating fin

For time lapse imaging of the regenerating fin, fish were anesthetised and placed on a petri dish. Pictures were taken on a Leica Stereo scope MZFLIII connected to an Olympus camera DP71. Fish were then immediately returned to the fish tank. Image analysis is described below.

3. Histology and tissue staining

For heart dissection fish were anaesthetized with trichaine (0.16%) and sacrificed by surgically removing the head with dissection scissors. Fins were obtained from sacrificed fish or living animals after anaesthesia. Hearts, fins and embryos were fixed overnight in 4% PFA for histology and histological staining or in 2% PFA for direct imaging of endogenous fluorescence.

3.1 Tissue processing

Following fixation fins, hearts and embryos were washed twice with PBST (PBS + 0.1% Tween 20). Fins were kept in 5 mM EDTA for 24 h at 4ºC to decalcify the tissue. For paraffin embedding tissues were dehydrated via EtOH series (10 min 50% EtOH; 10 min 70% EtOH; 10 min 80% EtOH; 10 min 90% EtOH; 10 min 95% EtOH; 2x10 min 100% EtOH) and then kept in xylene for 2x 10 min. Tissues were then transferred to paraffin at 65ºC and maintained there for at least 4

hours (2x 30 min; 3x 60 min) before mounting. Paraffin blocks were sections at 7 mm. Haematoxylin and eosin staining (H&E) and Acid fuchsin orange G-staining (AFOG) were performed following standard protocols (Kikuchi et al., 2011b).

For whole mount *in situ* hybridisation (WISH) fins and embryos were washed twice with PBST for 10 min and dehydrated with MetOH (10 min 50% MetOH; 10 min 100% MetOH) and stored in 100% MetOH at – 80ºC.

3.2. Immunohistochemistry

For histological stainings paraffin sections were incubated for 2x 10min in xylene to remove the paraffin and subsequently rehydrated passing through an EtOH series (2x 5min 100% EtOH; 90% EtOH; 70% EtOH; 50% EtOH; 30% EtOH 2 min each) and washed in water. For antigen retrieval, sections were heated for 15 min in 5 mM citrate buffer. To block endogenous peroxidases slides were incubated in 6% H_2O_2 in water for 20 min. Next, for permeabilization tissues were washed with PBSTx (PBS + 0.03% Triton X) followed by PBS washes. Slides were than incubated for at least 2 hours in blocking solution (goat serum, bovine serum albumin (BSA), Mg^{2+}, Tween 20). For signal amplification using the biotin-streptavidin system (see below) tissue sections were additionally blocked using the Biotin-Streptavidin blocking kit (Vector).

Table 4: Primary antibodies

Protein	Brand	Concentration	Amplification
aldh1a2	GeneTex	1:400	TSA
BrdU	BD	1:30	-
c-myc	Santa Cruz Biotechnology	1:100	Biotin/ Streptavidin
collagen type I	SP1.D8, DSHB	1:100	TSA
Delta-4	Santa Cruz Biotechnology	1:100	TSA
GFP	Living colours (rabbit)	1:100	-
GFP	Living colours (mouse)	1:100	-
GFP	AVES (chicken)	1:500	-
mef2	Santa Cruz Biotechnology	1:100	-
Mf20	DSHB	1:100	-
osterix/ sp7	Abcam	1:100	-
PCNA	Santa Cruz Biotechnology	1:100	-
V-CAM	Santa Cruz Biotechnology	1:100	TSA

The primary antibody (Table 4) was added to the slides in blocking solution and incubated overnight at 4ºC. On the second day the slides were washed with PBST (3x 10 min) and the

secondary antibody was added in 5% BSA solution. Incubation time was one hour. Slides were washed with PBST afterwards. Amplification of the antibody signal was achieved either through amplification with a secondary antibodies coupled to horseradish peroxidase (1:100, Dako Cytomation) and tyramides coupled to Cy3 (TSA, 1:100, Perkin Elmer) or by using a secondary biotin-conjugated antibody (Invitrogen) that react with a streptavidin-coupled fluorescent protein. For this, slides were incubated 45 min with streptavidin-Cy3 substrate (Vector) and washed subsequently in PBS. For tyramide amplification the substrate was added 1:100 to the amplification buffer and slides were incubated for 3.5 min. Successive washes with PBST removed the TSA solution. As a final step sections were incubated with DAPI for 10 min, washed at 3x 10 min with PBST and mounted with fluoromount.

3.3. Riboprobe synthesis

A fragment of cDNA, prepared from heart or embryonic RNA (see below), was amplified by Taq polymerase PCR, using gene specific, exon spanning, primers (Table 5). The PCR product was extracted from an agarose gel and ligation into a pGEM®T easy vector was performed in an overnight reaction following the pGEM®-T Easy Vector Systems Protocol.

Table 5: Primers of generated probes

Gene	Forward	Reverse
col11a1b	TCCCGGTGTCGTATCCCTC	AGCCTGGTGTTTTCTTCACTC
col12a1a	CTGCTGCGCTCTTGACTCT	GTCCGAGCTGTACTGAACCAC
col12a1b	TGAGTCCAGAACAGGCCCTA	CAATCATTTCAGATCGCACAC
ctssb.1	GATGAAAATGCCCTCAAGCAG	AAGATAAGACGCACTTGGAT
egr1	CATTGTATTATTCTTGAGCAGG	TAGAAGCCATAAACAGTCAC
has1	TTCTTTGACTGTGTCTCCTGCAT	TGGCCTCCCTGTAAATCGT
heg	TTGCTCTTATTGTCACCTGCT	GAACATCACTTCATCAGCTCC
her6	CATCATTGCCGCACCA	TGTGTTTAGGGCAGCGGTCAT
her9	CGTTCCGCATCTAAT CCTAA	GGCCATCATCTGTCCCATACA
id1	CACTATCGACAACTCAACAAGCC	ACGTCACGCTTGTCATGTCCA
myc-b	TTTACCACGGCTACGGCACT	CGGATTCGCTGTCACTACTG
mylk3	GAGCCCACACATGTCCAGA	CTGTTGTTTCCATCCCCAT
serpine1	GTT TGCTGAAGCCGTCCAGT	TCCACGCCATCCTTAGACAC
tnfrsf9a	TACGGAAAACTCAGAGTCCA	TTTGAGTATTCTCTCCCCAA
vegfc	AACAGAGCTTCAACAGGGACA	GAGTTGCAAAACATTTCATGGC

The plasmid was transformed into Dh5-Alpha bacteria. Colonies were tested by PCR reactions using gene specific primers and the primer of the T7 promoter to estimate the direction of PCR

product insertion into the plasmid. Bacteria were grown to increase the amount of plasmid and DNA was isolated using the Quiagen Plasmid Maxi Kit.

An enzymatic digestion of 10 mg of the plasmid pGEM®T easy was performed overnight and the linearized plasmid was purified. The equal volume of phenol was added and centrifuged for 5 min. The same volume of chloroform was added to the supernatant and centrifuged again for 5 min. For precipitation of the plasmid acetic acid, 100% EtOH and glycogen was added and the sample was stored at -80ºC for at least 30 min. After centrifugation the precipitated DNA was washed with 70% EtOH and suspended in water. We used 1 mg linearized plasmid for RNA transcription with either T7 or Sp6 polymerase for 2 h. RNA probes were then purified with the illustra AutoSeq G-50 Kit and stored at -80ºC.

3.4. *In situ* hybridisation on sections (ISH)

Sections were deparaffinized by two washes with xylene (10 min) and subsequently rehydrated via EtOH series (2x 5 min 100% EtOH; 90% EtOH; 70% EtOH; 50% EtOH; 30% EtOH 5 min each) and washed with PBS. Sections were then fixed with 4% PFA for 20 min. After two short washes with PBS, sections were treated with proteinase K (10 mg/ml) for 15 min at 37ºC, washed with PBS and refixed with 4% PFA for 5 min. After PBS-washes, slides were incubated for 15 min in HCL and washed again with PBS. This was followed by incubation with triethanolamine/ acetic anhydrite solution for 10 min. Following washes with PBS and water; slides were covered with hybridisation buffer in a humid chamber at 65ºC for at least two hours. Afterwards hybridisation buffer containing the riboprobe (Table 5, 6) was added to each slide and incubated overnight. During the second day slides were incubated with posthybridisation buffer I and II at 65ºC. After 3 washes with maleic buffer (MABT) slides were incubated for two hours in blocking solution containing blocking reagent (ROCHE) and FBS. The anti-DIG antibody coupled to alkaline phosphatase was diluted 1:2000 in blocking solution and slides were incubated overnight. After 3 hours of washes with MABT to completely remove the antibody, slides were washed 3x 10 min with AP-Buffer. Then, the signal was developed with BM-purple. To stop the staining reaction sections were washed twice with PBS, fixed with 4% PFA for 15 min and washed again with PBS. Slides were dehydrated through EtOH series (2 min 30% EtOH, 2 min 50% EtOH, 2 min 70% EtOH, 2 min 90% EtOH, 2x 5% 100% EtOH) and than incubated for 2x 7 min in xylene before they were mounted with Entellan® (Merk Millipore). More details can be found in (Kanzler, Kuschert et al., 1998).

Table 6: Previously published riboprobes

Gene	Reference
aldh1a2	(Grandel, Lun et al., 2002)
atf3	(Chen, Huang et al., 2012)
bmp10	(Laux, Young et al., 2013)
cdh5	(Larson, Wadman et al., 2004)
hand2	(Yelon, Ticho et al., 2000)
her15	(Shankaran, Sieger et al., 2007)
jagged1b	(Zuniga E, 2010)
klf2a	(Vermot et al., 2009)
klf2b	(Vermot et al., 2009)
klf6	(Veldman, Bemben et al., 2010)
l-plastin	(Yoshinari et al., 2009)
lunatic fringe	(Prince, Holley et al., 2001)
mmp9	(Wong, Rehn et al., 2012)
msxb	(Akimenko et al., 1995)
msxe	(Akimenko et al., 1995)
nfatc1a	(Wong et al., 2012)
nkx2.5	(Chen & Fishman, 1996)
notch1b	(Westin & Lardelli, 1997)
notch2	(Westin & Lardelli, 1997)
notch3	(Westin & Lardelli, 1997)
tcf7	(Li, Felber et al., 2009)

For double fluorescent *in situ* hybridization after proteinase K and PFA treatment, slides were incubated for 10 min in an acetylation solution followed by PBS washes. Than endogenous peroxidases were blocked using a 3% hydrogen peroxide solution. Hybridization and post-hybridization washes were performed following the previously described in ISH protocol. We used anti-digoxigenin-POD and anti-fluorescein-POD antibodies (Roche) to detect dig- or fluorescein labelled probes. For signal amplification tyramides coupled to Cy3 or fluorescein (TSA, 1:100, Perkin Elmer) were utilized.

ISH combined with immunohistochemistry was performed as described (Gonzalez-Rosa et al., 2012). Tissue sections were incubated in immunohistoblock solution for 1 h (see above) and than incubated with the primary antibody overnight at 4ºC. Following washes with PBS, slides were incubated for 1h with a secondary biotin-conjugated antibody. Next we used the ABC-Kit (Vector) to amplify the signal. The straining reaction was performed using the DAB Substrate Kit (Vector).

3.5. Whole mount *in situ* hybridisation

Whole mount *in situ* hybridisation (WISH) for fins and embryos was performed following the same protocol (Poss, Shen et al., 2000). Fins stored in 100% MetOH were rehydrated through MethOH/ PBST series (5 min 75% MetOH, 5 min 50% MetOH, 5 min 25% MetOH) followed by several washes with PBST. The tissue was next digested with proteinase K (fins 20 mg/ml 20 min; embryos 10 mg/ml: 2 dpf 15 min; 3 dpf 20 min), washed with PBST and refixed with 4% PFA for 20 min. After several washes with PBST fins were incubated in hybridization solution at 65ºC. After two hours this was replaced by hybridization solution containing a riboprobe and left overnight at 65ºC. During the second day, fins were washed with saline sodium citrate + 0.1% Tween 20 (SCCT) (3x 20 min 50% SCCT 2mM/ 50%Formamide; 2x 20 min SCCT 2mM; 3x 30 min 0.2 mM SCCT). After 4 washes of PBST fins were incubated in blocking solution containing blocking reagent (Roche) and FBS. Incubation with the anti-DIG antibody coupled to alkaline phosphatase proceeded overnight in blocking solution. During the third day of ISH, fins were washed in PBST for at least 3 hours followed by 3x 5 min incubation in AP-buffer. The staining was revealed with BM-purple. To stop the developing process fins were washed in PBS, fixed with 4% PFA overnight and washed in PBST again.

3.7. Alizarin red staining

For whole-mount alizarin-red staining, fixed fins were rehydrated through a decreasing MetOH series, bleached by 30 min in 0.8% KOH, 0.6% H_2O_2. Subsequently, fins were washed twice with water and washed for 20 min in a saturated alizarin-red solution containing 1% KOH, followed by several washes with water and transferred to glycerol.

4. Imaging

4.1 Microscopy and confocal imaging

Images of stained whole fins or embryos were obtained on a Leica Stereo scope MZFLIII connected to an Olympus camera DP71. Photographs of stained sections were taken using an Olympus BX51 fluorescent microscope fitted with a Nikon DP71 camera and CellA controller software. Further, immune-stained sections were imaged using a confocal microscope (Leica TCE 2500 SP-E, NIKON A1R).

4.2 Whole mount confocal imaging

For whole mount 3-dimentional (3D) imaging, hearts were fixed in 2% PFA overnight. Following 3 washes in PBS, hearts were incubated in CUBIC I (Susaki, Tainaka et al., 2014) at 37ºC overnight. Using a Leica TCE 2500 SP-E confocal microscope, we scanned the apical halve of the ventricle or up to 1 mm of the whole hearts. Z-stacks were taken every 7 μm for imaging with a 10x objective and every 3 μm for imaging with the 20x objective.

4.3 Image analysis

ImageJ64 was used to measure the size of fin regenerates from the amputation plane to the distal tip of each fin ray or just of the seven dorsal and ventral rays of both fin halves for MO transfection analysis. The value for the ventral half of each fin served as an internal control. Mean fin length was calculated for each animal. Outgrowth size after MO-transfection was calculated from the formula $(dL_{t2}-dL_{t1})/(vL_{t2}-vL_{t1})$, where dL is the mean length of the dorsal regenerate, vL the mean length of the ventral regenerate, t1 is the day of MO-transfection, and t2 two days later.

Fin width, excluding the epidermal layer, was measured on H&E-stained sections with ImageJ64. For cell number analysis we counted $DAPI^+$ and $PCNA^+$, GFP^+ or $BrdU^+$ cells within the regenerated tissue using Adobe Photoshop CS5.1. and calculated the total amount of labelled cells per $DAPI^+$ nuclei. To analyse osx-stained fin sections, we used ImageJ64 to measure both the osx^+ proximal fin region and the osx^- distal region. We estimated the proportion of both regions within the whole regenerated fin. Statistical significance was calculated by Student t-test. The length of the calcified bone was measured accordingly.

BrdU-incorporation in injured hearts was analysed by counting $mef2^+$ cardiomyocytes flanking the injury site and $mef2^+$ cardiomyocytes that exhibit BrdU-labelling. We analysed 7- 8 hearts and 4- 8 sections per heart. Accordingly, endocardial cell proliferation was estimated using 3- 4 hearts per time point and condition and analysing 4- 6 sections per heart. To estimate cardiomyocyte density, the number of $mef2^+$ cardiomyocytes adjacent to the injury site was divided by their area. Statistical significance was calculated with Student's t-test.

The amount of fibrotic tissues on AFOG-stained heart sections was measured as followed: the size of the injury site was related to the size of the ventricle, measured on at least four sections of four different levels of one heart with ImageJ64 and averaged. This allows estimating the size of the injured region in three dimensions. The amount of fibrin was calculated by relating the area indicating fibrin deposition (red) with the size of the injury site. Graphs represent the mean +/- standard deviation.

For 3D volume rendering and volume quantification, we used IMARIS x64 software, with manual selection of the injury site (myl7:mRFP$^-$). A mask of this area was used to select the GFP$^+$ endocardium within the injury site, and the volumes of both were calculated and compared (Fig. 7). Graphs represent values of individual hearts and means ±standard deviation. Statistical significance was calculated with Student's t-test. Filopodia like protrusions at the outer front of the injury-induced endocardium (Fig. 35C) were quantified on 3-5 optical sections per heart and 4 hearts per condition. For each section filopodia numbers were related to the length of the outer endocardial front, analysed by using IMARIS x64 software. The graph represents mean values of individual hearts and means ±standard deviation. Statistical significance was calculated with Student's t-test.

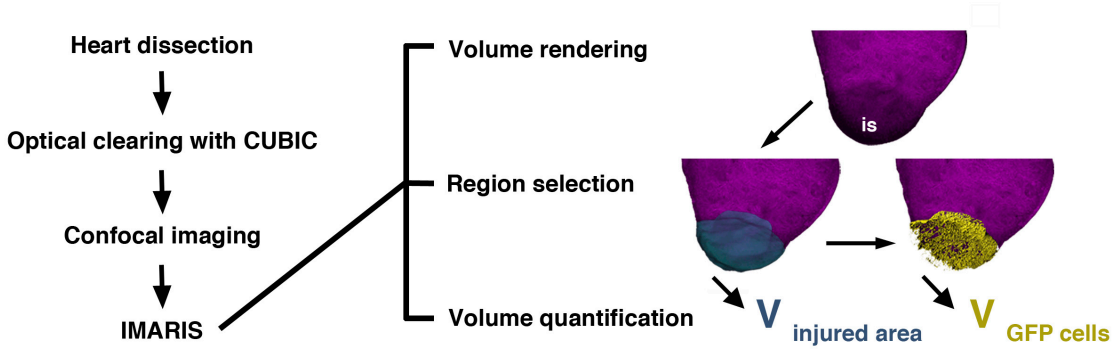

Figure 7: Workflow scheme for 3D imaging and volume quantification
Procedure for 3D imaging and volume quantification with IMARIS software. The volume of the ventricular region lacking mRFP$^+$ cardiomyocytes was determined (blue, $V_{injured\ area}$); this was used as a mask to label GFP$^+$ cells in this region (yellow) and determine their volume ($V_{GFP\ cells}$).

5. Gene expression analysis

5.1. RNA extraction and cDNA preparation

RNA extraction of fins, heart or embryonic tissues was obtained by using the Direct-zol™ RNA MiniPrep (Zymo Research) or by manual extraction using TRizol (Invitrogen). For this, the tissue was homogenized in TRizol by pipetting (fins, embryos) or by using the tissue TissueLyser II (Quiagen) to break the tissue (heart). cDNA was synthesized with SuperScript III First Strand (Invitrogen) with 1 µg RNA per reaction.

5.2. Quantitative RT-PCR

For gene expression analysis of regenerating fins, three fins were pooled for one sample and qPCR was performed of 4-5 samples. Power SYBR Green Master Mix (Applied Biosystems) was

used for quantitative RT-PCR (qPCR) with the ABI PRISM 7900HT FAST Real-Time PCR System. Gene expression levels were normalized to *elf1a*- or *rspm*- expression levels. Further, three hearts were pooled in one sample and data represented in this work result from 4-6 samples.

Table 7: qPCR primer sequences

Gene	forward	reverse
aldh1a2	GGGGGAAGCTACTGTTCAAAT	TCCAGAGACTCCAGGGTAGC
atf3	ACCACCTTAATGTTGTTACG	CTGACAAATTCAGACCTTCC
cathepsin B, a	GCACGACTGCCATACACAAG	GGCTGAGATCACACACAGGA
collagen11a1a	AAAGGGTAAATCAGGTCCAA	CAAGTTTTCCCTTCTCTCCT
collagen12a1b	TGTGTCTGATAATGGCAAAACAC	GCTGGTGGTGGGATCATAAA
copeb/ klf6	AAGCACACTGGTGCAAAGC	CAGGTGGTCCGACCTAGAGA
ctssb.1	CCAGATTCACTGGATTGGAGA	CCAACAAGAACCACAAGCAC
deltaC	CGCAGAAACCTCTGACCAGT	CAGTCCTCACTGATAGCGAGTC
deltaD	GTTCACCAACCCCATTCCTT	TGTGCAGCGCTTCAATAATC
elf1a	CAGCTGATCGTTGGAGTCAA	TGTATGCGCTGACTTCCTTG
has1	TTGACTGTGTCTCCTGCATCA	TGGTTGTACCAGGATTCGAGA
heg	TTGGAGGTTTCAACTGCAATAA	GCAATGACCACAATCAACAGA
her15	TCGCTCTGCTCAGAAACA	ACCACTGGCTTTCGAAT
her4.1	CAGAGAAACTCTACTGACAAACAAGC	GCTGCTGTTGATTCGCTCT
her6	GGCTTCGGAACACAGAAAGT	TGACCCAAGCTTTCGTTGA
hyal2	TTTGTCTACAGCCGCCCTAC	CAATGGTGGACACCAGATCA
jag1b	ACATGCGAGTGTCAAGAAGGT	CATGGGTTACTTTCACAATCGTT
lfng	TCTGTTGAGGAGGACCCATC	GCACCAAGGAGTGTCTGGAT
mmp9	TGCTCTCCCAGCTGTCATC	CCACTGTAAACCCAGAACTGTCT
msxb	GGTCAAACTCTTCATCTTTCACATC	TCTTGTGCTTGCGTAAGGTG
msxe	GAGCGGAGCACATGGGTA	CCGGTTGGTTTTGTGTTTTC
myc-b	TGTTTCCCTTTCCACTGAC	CTTCATCATCTTCGTCATCG
mylk3	AAGTTGAGTCGACACTGCTGAT	ACAATGCGATGGTCGAATG
notch1a	TGTGAATGCACCCCAGGT	GACGCACACTCGTTGATGTC
notch1b	GGGCACCTGCGTACAGAA	CAAATTCCTGCCGACCTG
rpsm	GATGGCGGACACTCAGAAC	CCAATCCAACGTTTCTGTGA
serpine1	GTCTATTCCAAGGTTCTCCAT	CTGAAAATGTCTCCAAGACC
sgpl1	CCATTATTATGAAGAATCCGAAAGA	CATCGATCGGTCAGGAATG
tcap	GGGACGATCAATGTCTCAGG	CGTCCATAAAGTCTTTGACTCATATTT
thbs2b	AGGAGACGCCTGCTCTGTT	GGCAGTTGTCTCGCTCATTC
tnfrsf9a	AACTGGACTCCTTCAGGAAAAA	TCTTTTCACCAAGCGGTTTC

Gene expression were similarly related to *elf1a*- or *rpsm*-levels and than compared to gene activation in either no cryoinjury samples (wild-type genes expression analysis), in DMSO treated heart samples (in RO-treatment experiments) or *Tg(hsp70l:Gal4)*^{kca4} only or *Tg(UAS:myc-*

Notch1a-intra)^{kca3} only heart samples (Notch over-activation experiments). Primer sequences can be found in Table 7.

5. 3. RNA sequencing analysis

For RNA sequencing (RNAseq) analysis we used three pools of three apexes from either RO- or DMSO treated fish. The Genomics Unit at CNIC, SPAIN performed library production and sequencing. We used a standard TruSeq RNA Sample Preparation Kit v2 (Illumina, San Diego, CA) to prepare cDNA libraries. These were sequenced in a Genome Analyzer IIx Illumina sequencer using a 75bp single end elongation protocol. Sequenced reads were QC and pre-processed using cutadapt v1.6 (Martin, 2011) to remove adaptor contaminants. Resulting reads were aligned and gene expression quantified using RSEM v1.2.3 (Li & Dewey, 2011) over zebrafish reference genome Zv9_75. As differentially expressed we considered genes with altered expression levels with an adjusted $P<0.05$. RNAseq data were analysed using Ingenuity Pathway Analysis Software.

Results

I. The role of Notch signalling during fin regeneration

1. Notch signalling components are expressed in the blastema

To study the role of Notch signalling during fin regeneration we first examined the expression of a subset of Notch-related genes in the fin and performed quantitative real-time PCR (qPCR) and *in situ* hybridisation (ISH).

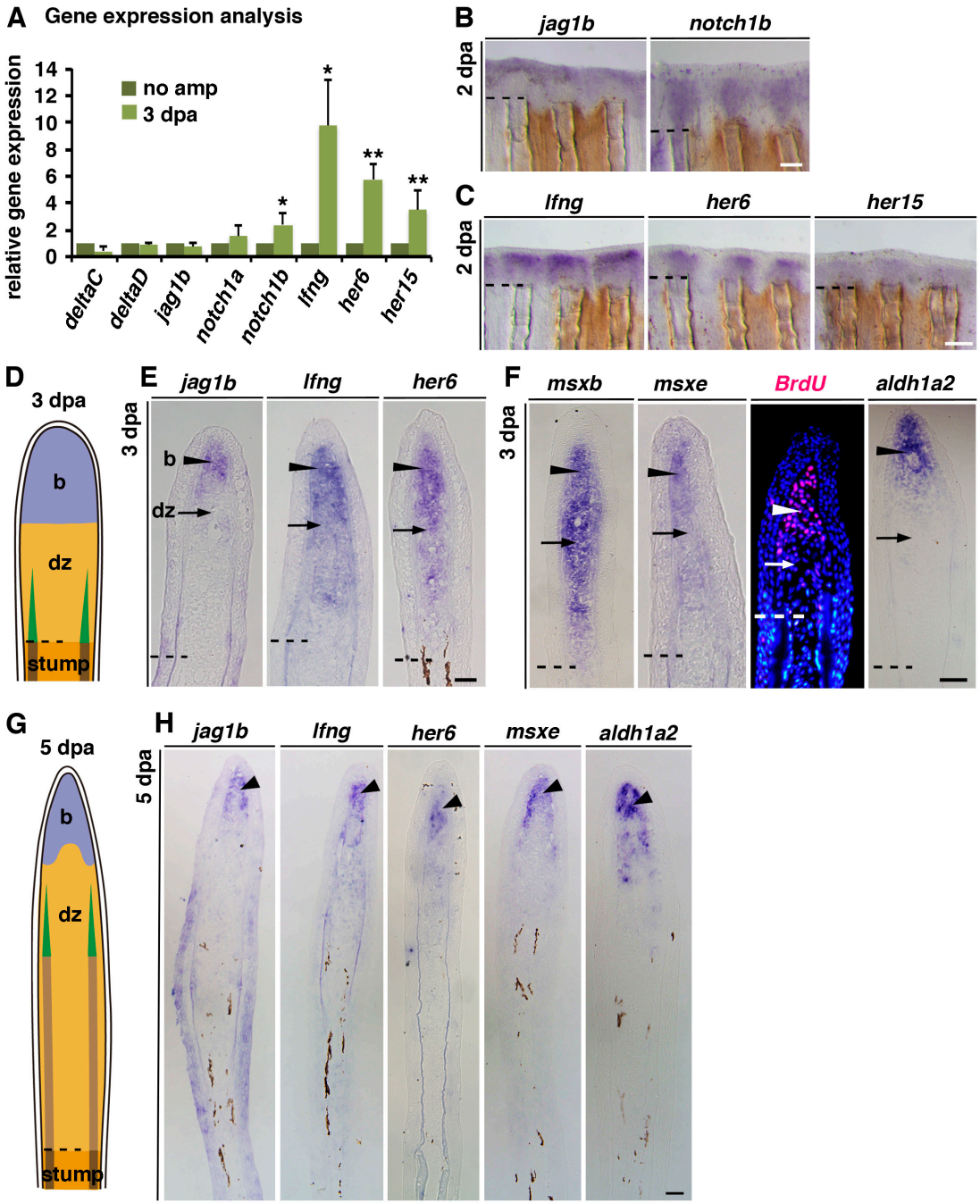

Figure 8: Notch signalling components are expressed in blastema cells.
A: RNA transcription levels, obtained by qPCR, of Notch signalling components in regenerating fins (3 dpa) comparing with no injured fin tissue (0 dpa). **B**: Whole mount *in situ* hybridization (WISH), indicating *jag1b* and *notch1b* expression in the fin blastema at 2 dpa. **C**: WISH of fins (2 dpa) against *lfng*, *her6* and *her15*, showing expression in the blastema. **D**: Scheme indicating the distally located blastema (b) and the proximal differentiation zone (dz) with differentiating osteoblasts (green) at 3 dpa. **E**: ISH on fin sections (3 dpa) showing strong *jag1b*, *lfng* and *her6* expression in the blastema (b, arrowhead) but reduced or no expression in the differentiation zone (dz, arrow). **F**: ISH on fin sections (3 dpa) indicating strong *msxb*, *msxe* and *aldh1a2* expression in the blastema (arrow head) but less or no expression in the dz (arrow). Immunohistochemistry (IHC) shows BrdU incorporation in the blastema region (white arrowhead) but not more proximal (white arrow). **G**: Scheme representing the different regions of the fin regenerate at 5 dpa: blastema (b) and differentiation zone (dz) with differentiating osteoblasts (green), more proximal: differentiated tissue. **H**: ISH on fin sections (5 dpa) showing *jag1b*, *lfng*, *her6*, *msxb* and *aldh1a2* expression only in the very distal region of the fin (arrowhead). (*P< 0.05, **P< 0.01; scale bars: B, C: 100 μm; E, F, H: 10μm. Dashed lines indicate the amputation plane.)

We compared regenerating (3 dpa) and non-injured fin tissue and detected elevated expression levels of genes encoding for the receptor *notch1b*, the glycosyltransferase *lunatic fringe* (*lfng*) and the two Notch target genes *her6* and *her15* (Fig. 8A). However we failed to detect significant changes in mRNA levels of the ligands *deltaC*, *deltaD*, *jag1b* and the receptor *notch1a* (Fig. 8A). Next, we performed ISH on whole fins at 2 dpa, the time when the blastema has formed. Although qPCR did not reveal increased levels of *jag1b*, ISH indicated *jag1b* expression upon fin amputation (Fig. 8B) Similarly *notch1b*, *lfng*, *her6* and *her15* were expressed in the regenerating fin, distal to the amputation plane (Fig. 8B, C). To better localize Notch pathway activation in the regenerating fin we performed ISH on fin sections at 3 dpa and compared Notch target gene with *msxb* and *msxe* expression, two markers for blastema cells (Nechiporuk & Keating, 2002) in the distal region of the fin (Fig. 8D-F). Notch pathway components expression was absent in the fin epidermis, however we detected strong expression of *jag1b*, *lfng* and *her6* in the very distal region of the blastema (Fig. 8E). Expression was weaker (*lfng*, *her6*) or absent (*jag1b*) in the more proximal region, where differentiation had already started (Fig. 8D, E). This pattern resembles *msxe* expression in the fin regenerate (Fig. 8F) and partially coincides with *msxb*, which showed strong expression throughout the entire blastema in our experiments (Fig. 8F). Notch signalling activation in the distal area also coincides with proliferating cells ($BrdU^+$) and *aldh1a2* expression (Fig. 8F), a regulator for blastema cell proliferation (Blum N, 2012). This suggests an implication for Notch signalling in proliferating blastema cells.

We next examined Notch pathway activation at later stages of fin regeneration (5 dpa), when proximal cells have already differentiated but the distal region still exhibits dedifferentiated blastema cells (Fig. 8G, H). In line with our previous observations, we detected *jag1b*, *lfng* and

her6 expression in the blastema region similar to *msxe* and *aldh1a2* expression (Fig. 8H), suggesting that Notch activation may be required in the blastema throughout the fin regeneration process. Altogether we conclude that Notch signalling pathway elements are expressed in the early blastema as soon as it is formed (2 dpa) and remains expressed throughout regenerative outgrowth.

2. Notch signalling activation coincides with proliferating blastema cells

To examine whether Notch activation was related to proliferation, we used the *ET33-mi60A* enhancer trap line, which expresses GFP upstream of *lfng* (Poon et al., 2010), allowing us to track lfng-mediated Notch signalling during fin regeneration. *ET33-mi60A* transgenic fish showed weak GFP expression within the caudal fin tissue, presumably in cells adjacent to the fin rays (Fig. 9A). In contrast, during fin regeneration (3 dpa) GFP expression strongly increased (Fig. 9A). Time-lapse analysis revealed, that wound closure and epidermis establishment (1 dpa) proceeded without GFP expressing cells (Fig. 9B). However during blastema formation (2 dpa), we detected high GFP expression in blastema cells that increased at 3 dpa (Fig. 9B). Combined immunohistochemistry against GFP and *her6* ISH confirmed that GFP expression in *ET33-mi60A* fish coincided with Notch activation, and was stronger in the distal region but weaker in the proximal regenerate (Fig. 9C). We next analysed if GFP is upregulated not only during fin regeneration but also after bone injury. For this aim we fractured fin rays with a forceps and examined GFP expression in the injured bone at different time points. GFP fluorescence intensity was low in uninjured tissue and completely absent directly after injury (0 hpi), indicating cell loss in this area (Fig. 9D). Bright field images showed the injured bony fin ray, which lacks GFP fluorescence at 24 hours post injury (hpi) (Fig. 9D). At 2 dpi however GFP was strongly upregulated in the injured tissue and GFP intensity was higher in a region with more severe bone fractures (Fig. 9D), suggesting the implication of Notch signalling in bone regeneration.

Notch signalling is involved in cell fate decisions and in directing proliferation in various contexts (Liu, Sato et al., 2010). To address if Notch signalling may be implicated in blastema cell proliferation we examined whether GFP expression coincides with the presence of the proliferating cell nuclear antigen (PCNA), a cell cycle mediator, at different stages of fin regeneration. By immunohistochemistry against GFP and PCNA we observed co-localization of both molecules in all stages examined and quantified GFP^+ and $PCNA^+$ cells in the fin regenerate (Fig. 10A- E). This analysis revealed a similar size of these two populations at 2 and 3 dpa (Fig. 10D), which represent the portion of blastema cells in the whole regenerate. At 2 dpa, 51% (±7%) of cells expressed GFP and were located beneath the epidermis (Fig. 10A, D). Moreover 79% (±14%) of these cells expressed PCNA (Fig. 10E). A similar correlation was evident at 3 dpa (Fig. 10B), with GFP-expressing cells constituting 51% (±9%) of total blastema cells (Fig. 10D); however, by this stage GFP-expressing cells were concentrated in the distal region and more proximal GFP-expressing

cells were located close to the epidermis. These regions containing GFP-expressing cells coincided with PCNA expression domains (Fig. 10B), and 78% (±7%) of GFP$^+$ cells co-expressed PCNA (Fig. 10E).

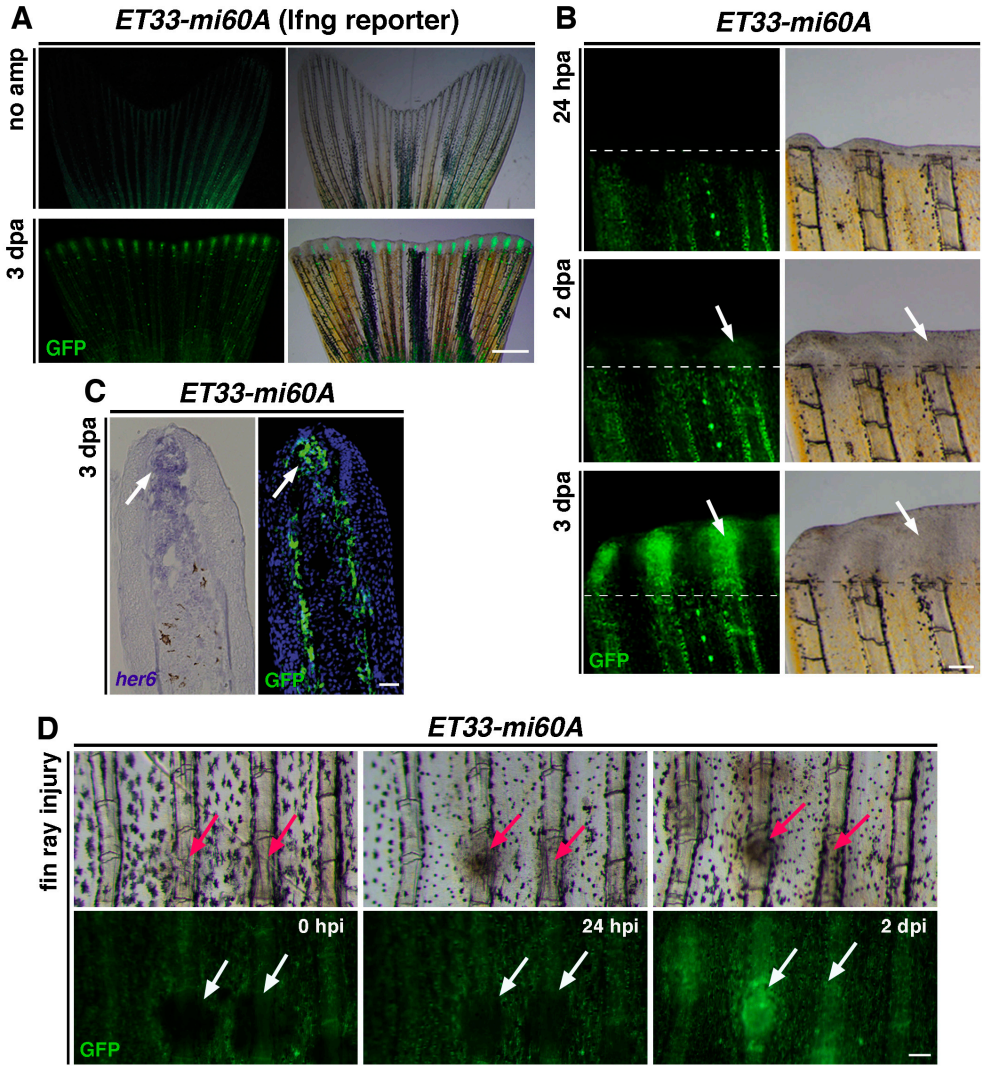

Figure 9: GFP is expressed in the blastema in *ET33-mi60A* transgenic fish.
A: GFP expression in the enhancer trap line *ET33-mi60* is weak in non-amputated fins but strong in the fin regenerate at 3 dpa. **B**: Time-course of *ET33-mi60A* regenerating fins. No GFP expression is seen in the wound epidermis at 1 dpa. GFP expression starts at 2 dpa within the blastema (arrows). GFP expression is strong within the blastema at 3 dpa (arrows). **C**: *her6* ISH and GFP IHC on a fin section at 3 dpa reveals GFP expression in cells in which Notch is activated (arrows). **D**: Whole mount time-lapse images after bone fracture in the caudal fin in *ET33-mi60A* fins. Bright field images showed injured radials. Strong GFP expression is apparent at 2 days post injury (dpi) but not earlier (24 hpci). (Scale bars: A: 1 mm; B, D: 100 µm; C: 10 µm. Dashed lines indicate the amputation plane.)

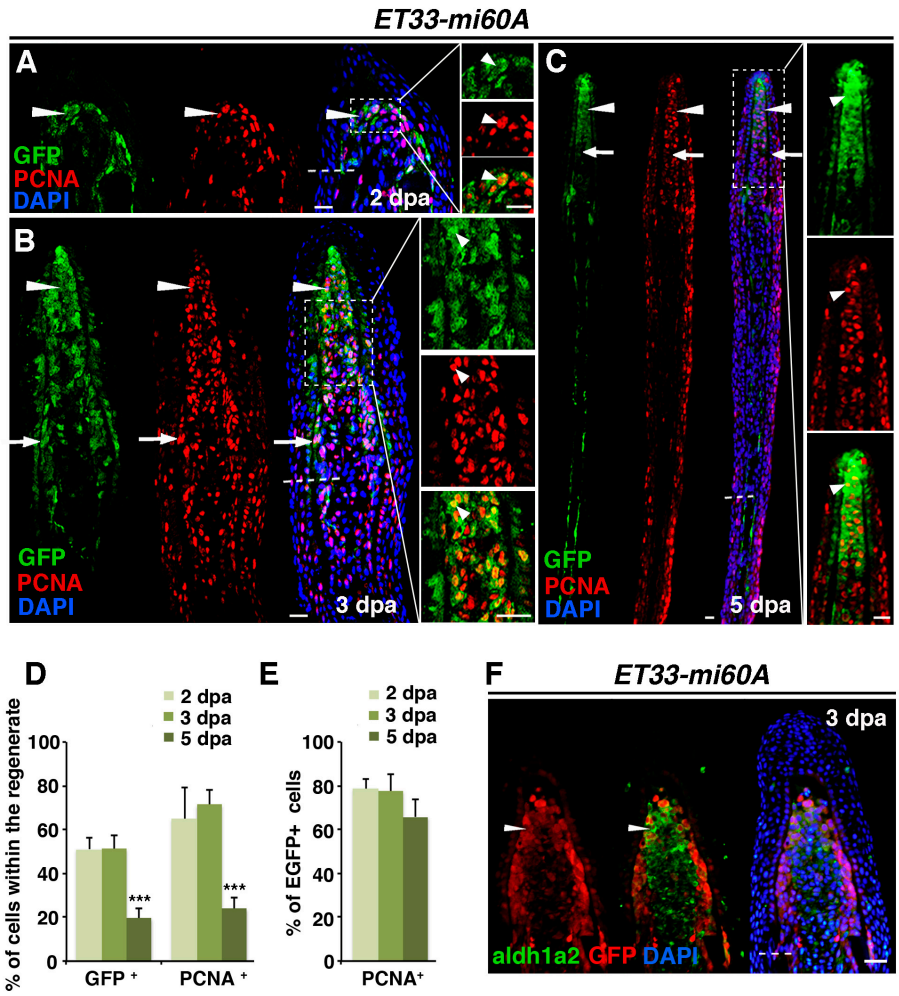

Figure 10: Lfng-mediated Notch signalling in proliferating blastema cells
A-C: Confocal microscopy images of double IHC for GFP and PCNA. The boxed area is shown at higher magnification in the panels on the right. GFP is expressed during blastema formation (2 dpa) in cells co-expressing PCNA (A, arrowheads). At 3 dpa, GFP expression is strong in all blastema cells (B, arrowheads), and is mosaic in proximal regions (B, arrows). Most cells are co-labelled with PCNA (B, arrowheads). At 5 dpa, GFP expression is strong in the blastema (C, arrowheads) but weak in the proximal region (C, arrows). Most cells in the GFP$^+$ area express PCNA (B, arrowheads). **D**: The bar chart represents the percentages of GFP$^+$ and PCNA$^+$ cells within the regenerate at 2, 3 and 5 dpa. The amount of both GFP$^+$ and PCNA$^+$ cells decreases at 5 dpa. **E**: Bart chart representing the percentage of GFP$^+$ cells that are labelled for PCNA at 2, 3 and 5 dpa. **F**: IHC against GFP and aldh1a2 on fin sections (3 dpa) indicating expression of GFP and aldh1a2 in blastema cells (arrowhead) (***P< 0.005; scale bars: 10 μm. Dashed lines indicate the amputation plane.)

At 5 dpa, when regeneration had resulted in a progressive differentiation of proximal tissue, we observed a marked decrease in the number of GFP- and PCNA-expressing cells within the whole fin regenerate compared with earlier stages (Fig. 10A-D). However the proportion of proliferating GFP-expressing cells remained high (66% ±5) (Fig. 10E). These double-labelled cells were mostly restricted to the distal region of the regenerate (Fig. 10C), consistent with our previous observation

of Notch signalling activation in the distal region (Fig. 8H). This indicates that Notch is active in proliferating blastema cells. We supported this observation by double immunohistochemistry in *ET33-mi60A* fins and detected aldh1a2, the blastema cell proliferation regulator (Blum N, 2012), in GFP^+ cells at 3 dpa (Fig. 10F).

3. Notch signalling inhibition impairs fin regeneration

To examine if fin regeneration requires Notch signalling activation we sought to inhibit Notch signalling during fin regeneration. For this aim we initially used the g-segretase inhibitor DAPT (N-[N-(3,5-difluorophenacetyl)-L-alanyl]-S-phenylglycine t-butyl ester). This inhibitor prevents the 2nd cleavage of the intracellular domain of the Notch receptor (NICD) at the membrane and thus the translocation of NICD to the nucleus and the activation of Notch target genes. DAPT successfully blocks Notch signalling activation in zebrafish embryos (Geling, Steiner et al., 2002). However to guarantee sufficient Notch downregulation DAPT needs to be used in a high concentration (100 mM for embryos) (Geling et al., 2002). To restrict the amount of DAPT, we performed experiments on juvenile fish (1 month) that can be hold in a smaller volume of fish water. At this stage most adult characteristics have been acquired, including complete squamation, and a bony ray-containing fin substitutes the larval fin fold (Fig. 11A). We examined the effect of Notch signalling inhibition on fin regeneration by measuring the regenerative outgrowth of the fin at 3 dpa. DAPT treatment reduced regenerative outgrowth in juvenile fish whereas DMSO apparently had no effect (Fig. 11A, B).

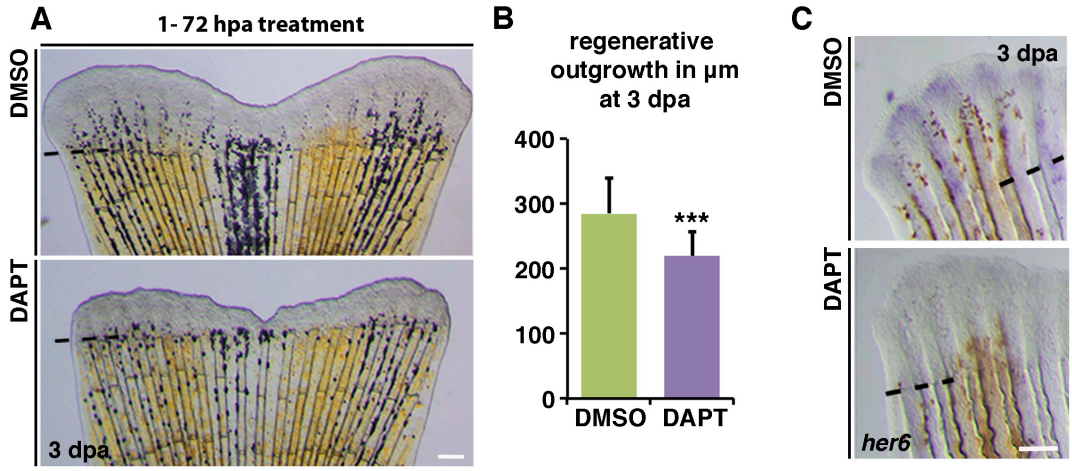

Figure 11: DAPT treatment inhibits fin regeneration.
A, B: Juvenile fish were treated with DAPT or DMSO as a control 1- 72 hpa. DAPT treatment leads to reduced regenerative outgrowth (B). **C**: WISH of fins, showing less *her6* expression after DAPT-treatment at 3 dpa. (***P< 0.005; scale bars: 100 µm. Dashed lines indicate the amputation plane.)

ISH against the Notch target *her6* on regenerated fins confirmed the inhibitory function of DAPT on Notch signalling activation (Fig. 11C). However, we sought to investigate if Notch signalling inhibition also interferes with fin regeneration in adult fish. This prompted us to test another γ-segretase inhibitor that can be used in lower concentration. This would eventually reduce the costs of treatment and diminish side effects caused by the drug itself or by DMSO at high concentration.

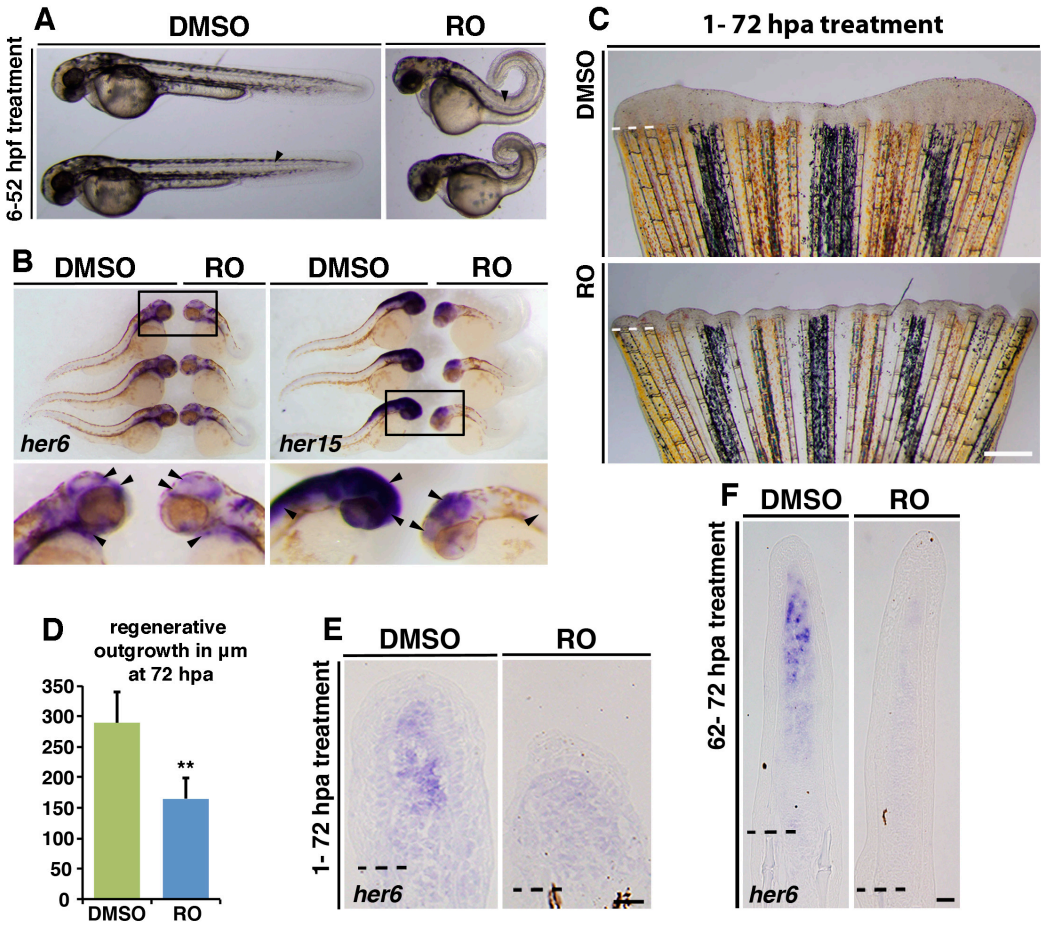

Figure 12: RO4929097 treatment decreases Notch signalling activation in zebrafish embryos and regenerating fins.
A: Embryos treated with DMSO or RO (10 µM) from 6- 52 hpf. RO-treated embryos exhibit a looped tail (arrowhead). **B**: WISH of DMSO- or RO-treated embryos showing that RO-treatment decreases the expression of *her6* and *her15* in the embryo, especially in the brain (arrowheads). **C**, **D**: Fish were treated with DMSO or 10 µM RO4929097 for 3 days starting at 1 hpa. Fin regeneration is blocked by RO treatment. Mean length of fin regenerates is represented in the bar chart (n= 5). **E**, **F**: ISH of *her6* showing Notch activity in regenerating fins with DMSO treatment from 62 to 72 hpa (or 1- 72 hpa) but not in RO-treated fins. (**P< 0.01; Scale bars: C: 1 mm; E, F: 10 µm. Dashed lines indicate the amputation plane.)

The γ-segretase inhibitor RO4929097 (RO,2,2-dimethyl-N-(S)-6-oxo-6,7-dihydro-5H-dibenzo[b,d]azepin-7-yl)-N'-(2,2,3,3,3-pentafluoro -propyl)-malonamide]), decreases Notch signalling activation in human carcinoma cells lines (Huynh, Poliseno et al., 2011) and is successfully used in preclinical studies (Luistro, He et al., 2009). This led us to test the functionality of RO initially on zebrafish embryos. We applied RO (10 mM) to embryos from 6 to 52 hpf and examined their phenotype during development. Notch signalling inhibition during vertebrate development results in a curved tail phenotype, as can be seen in mind bomb (mib) mutants (Zhang, Li et al., 2007), due to Notch signalling implication in somitogenesis (Lewis, Hanisch et al., 2009). Similarly, RO-treatment caused a looped tail in zebrafish embryos whereas DMSO- treated embryos appeared to be normal (Fig. 12A). To examine the effects of RO treatment on Notch target gene expression we performed ISH on whole embryos. We observed that RO decreased both, *her6* and *her15* expression throughout the embryo (Fig. 12B) and especially in the nervous system (Fig. 12B). We next applied RO to fish water for 1- 72 hpa to test its effect on adult fin regeneration. Wound closure and the blastema formation proceeded normally upon RO-treatment (Fig. 12C). However RO-induced Notch inhibition completely interfered with regenerative outgrowth (Fig. 12C, D), which supports our previous observation using DAPT. We confirmed diminished Notch signalling activation by ISH against *her6*, whose mRNA levels were reduced after long (1- 72 hpa, Fig. 12E) and also after short RO-treatment (62- 72 hpa, Fig. 12F). In contrast the expression of *msxe*, *msxb* and *aldh1a2* was unaffected by sustained RO-treatment (1- 72 hpa, Fig. 13A- C), indicating the presence of blastema cells. As we observed Notch signalling activation in proliferating cells (Fig. 10) we wondered if regeneration fails due to a blockade of proliferation upon Notch signalling inhibition. Blastema cells proliferate strongly at 2 and 3 dpa (Nechiporuk & Keating, 2002). We examined BrdU incorporation in the blastema at 72 hpa (10 hours RO- treatment, Fig. 13D, E) and at 110 hpa (12 h RO-treatment, Fig. 13 F, G). In both studies RO-treatment reduced BrdU incorporation in blastema cells (Fig. 13D- G). This suggests that Notch signalling activation is required for blastema proliferation at early stages when regenerative outgrowth starts (72 hpa) but also later when fin outgrowth proceeds (110 hpa).

Our gene expression analysis suggested that Notch in blastema cells proceeds through the interaction of the receptor notch1b and the ligand jag1b, involving also lfng activation. To proof the specific requirement of these three proteins we used specific antisense morpholinos (MO), which have been shown to successfully down regulate RNA splicing or translation and MOs are effective in regenerating fins (Thummel R, 2006).

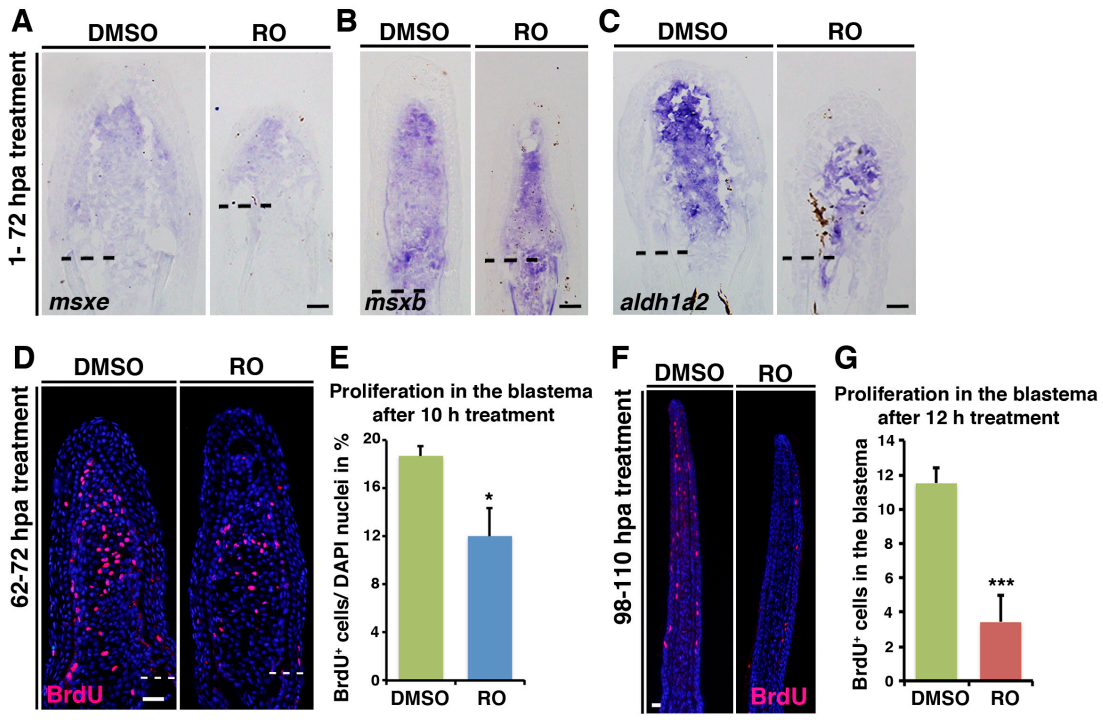

Figure 13: Notch signalling inhibition decreases blastema cell proliferation.
A- C: ISH on fin sections after DMSO- or RO-treatment (1- 72hpa) showing no differences in the expression of *msxe*, *msxb* and *aldh1a2*. **D**, **E**: BrdU- stained fin sections and quantification of BrdU$^+$ cells within the mesenchyme of RO-treated fins (n= 5) and DMSO-treated fins (n= 6, 62- 72 hpa treatment). **F**, **G**: BrdU- stained fin sections and quantification of BrdU$^+$ cells within the mesenchyme of RO-treated fins and DMSO-treated fins (98– 110 hpa treatment). (*P< 0.05; ***P< 0.005; scale bars: 10 μm. Dashed lines indicate the amputation plane.)

In addition to specific MOs against *notch1b*, *jag1b* (Lorent et al., 2004) and *lfng* (Nikolaou et al., 2009) we utilized a MO against *rbpjκ* (Sieger, Tautz et al., 2003), a transcription factor that, through its binding to the intracellular domain of Notch (NICD) regulates Notch target gene activation (Jarriault et al., 1995). This would globally reduce Notch target gene expression. Following the published protocol (Thummel R, 2006) we injected and electroporated either an unspecific control MO or MOs targeting *jag1b*, *notch1b*, *lfng* or *rbpjk* into the dorsal half of the regenerating fin at 2 dpa. We then compared the regenerative outgrowth of MO-transfected and non-transfected half of the fin at two days post MO-transfection (2 dpt/ 4 dpa). Control-MO transfection had minor effects on the regenerative outgrowth (Fig. 14A). In contrast, MOs targeting *notch1b*, *jag1b, lfng* or *rbpjκ*, decreased regeneration compared with the non-electroporated ventral portion by around 20 to 40% (Fig. 14B-F). To further test if this is due to a reduction in cell proliferation we examined BrdU-incorporation in blastema cells at 24 h post transfection with the *notch1b* targeting MO as this showed the strongest response on fin regeneration. We observed less blastema cell proliferation in MO-transfected fin halves comparing to non-transfected regenerates (Fig. 14G, H). This shows that the specific knock down of Notch pathway elements resembles the

effects of global γ-segretase inhibitor-induced Notch blockage: reduced blastema cell proliferation leading to impaired fin regeneration.

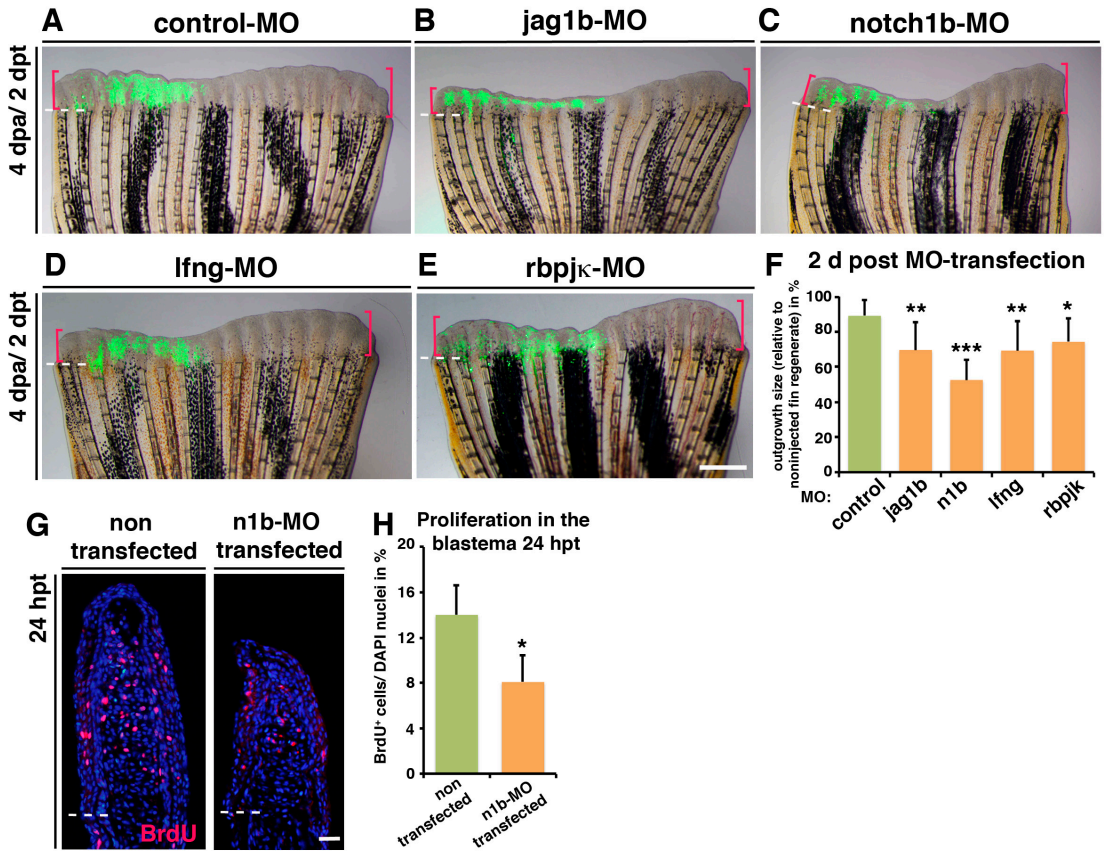

Figure 14: Transfection of morpholinos against Notch signalling components impairs fin regeneration.
A- E: Fins microinjected in the dorsal half with fluorescein-labelled morpholinos (MO, green) and electroporated at 2 days post-transfection (dpt): control (A; n= 9), jag1b (B; n= 12), notch1b (C; n= 9), lfng (D; n= 12) or rbpjκ (E; n= 6). The ventral half serves as an internal control. Pink brackets mark maximal regenerative outgrowth at 2 dpt. **F**: Mean outgrowth size of the dorsal (MO-electroporated) half of the fin relative to the ventral half at 4 dpa/2 dpt. **G**, **H**: BrdU-stained fin sections and quantification of $BrdU^+$ cells within the mesenchyme. The bar chart represents the mean percentage of $DAPI^+$ blastema cells in fin sections incorporating BrdU at 3 dpa/ 24 hpt (n= 3). Proliferation is reduced in notch1b-MO-transfected fin halves. (*P<0.05, **P<0.01 and ***P<0.005; scale bars: E: 1 mm; G: 10 µm. Dashed lines indicate the amputation plane.)

4. Notch signalling gain of function leads to blastema cell expansion and inhibits regenerative outgrowth

To gain further insight into the function of Notch signalling during fin regeneration we took advantage of the double transgenic line *Tg(hsp70l:Gal4);Tg(UAS:myc-notch1a-intra)*, abbreviated here as *Tg(UAS:NICD)* to induce the over activation of the Notch pathway during fin regeneration.

Heat-shock promoter activation in this line triggers Gal4 expression, which, by binding to the UAS promoter sequence, activates NICD expression (Scheer et al., 2001). This allowed us to control the timing of Notch activation. To analyse the phenotypic effect of sustained Notch signalling overactivation we applied heat shocks to control and transgenic *Tg(UAS:NICD)* fish and examined fin regeneration at different time points. Wound closure and the formation of the epidermis proceeded normally, examined at 1 dpa in transgenic and control animals (Fig. 15A). The blastema was properly formed by 3 dpa although we noticed a light swelling of the blastema in *Tg(UAS:NICD)* animals. At 5 dpa regenerative outgrowth had started in control fins and newly formed bony fin rays were present distal to the amputation plane (Fig. 15A). Transgenic fish showed reduced regenerative outgrowth and exhibited very little bony tissue (Fig. 15A, B) at 5 dpa. Instead, an enlarged, swollen blastema was apparent distal to the amputation plane. We confirmed this by measuring the width of the blastema on haematoxylin-eosin-stained (H&E) fin sections (Fig. 15C, D), which was expanded in transgenic fins and gave the sections a pear-shaped appearance. This relatively late phenotype (at 5 dpa) is consistent with our finding that Notch is active throughout the blastema early during regeneration, but distally restricted in later stages.

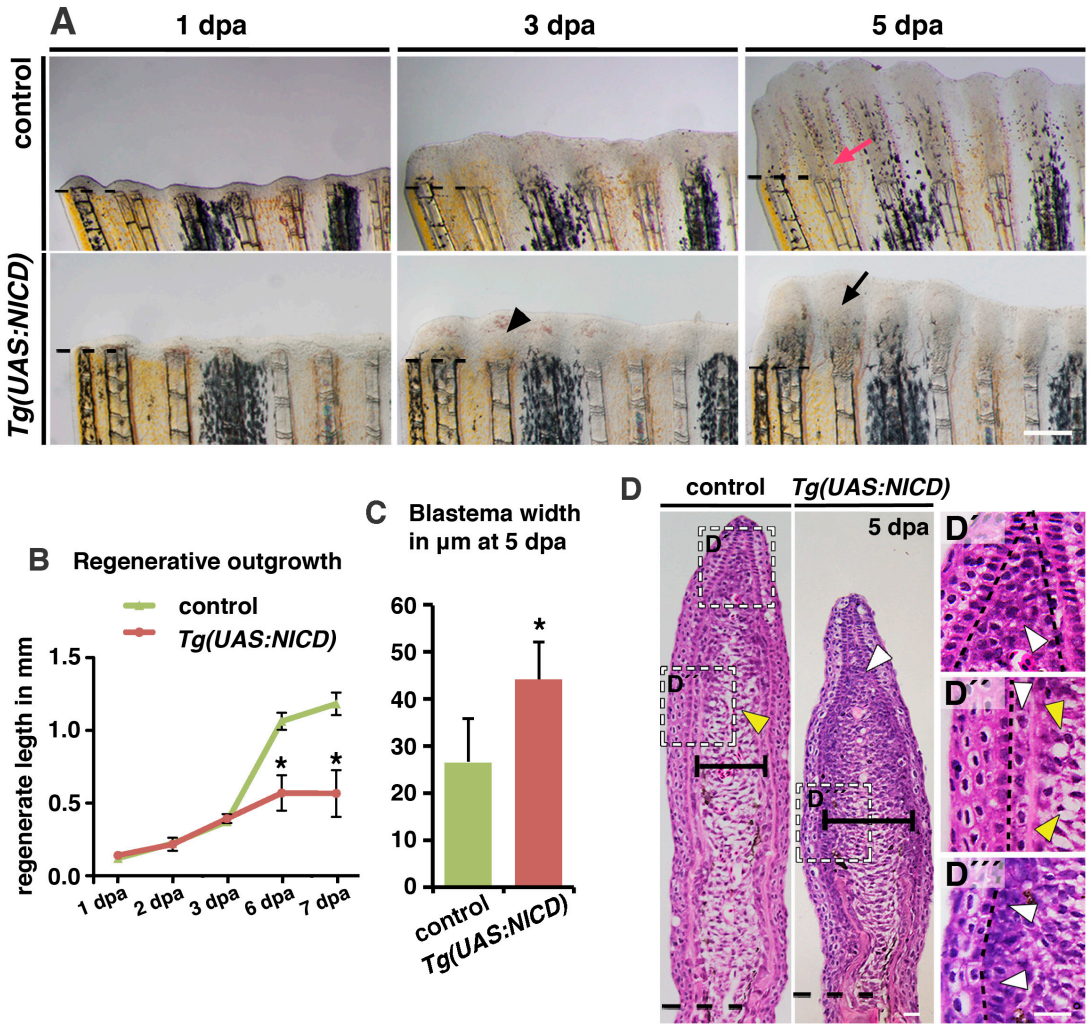

Figure 15: Notch gain of function leads to impaired fin regeneration but blastema expansion.
A: Control and *Tg(hsp70l:Gal4);Tg(UAS:myc-notch1a-intra)* fish, referred to as *Tg(UAS:NICD)*, were heat-shocked throughout the regeneration period. Live images of control and *Tg(UAS:NICD)* fins at 1, 3 and 5 dpa. No phenotypic differences were observed at 1 and 3 dpa between control and *Tg(UAS:NICD)*. Regenerative outgrowth and bone formation (red arrow) progress in 5 dpa control fish but is blocked in *Tg(UAS:NICD)* fish. The blastema is swollen proximal to each fin radial (arrow). **B**: Mean length of the regenerate at 1, 2, 3, 6 and 7 dpa: regenerative outgrowth is significantly reduced in *Tg(UAS:NICD)* fish at 6 and 7 dpa. **C**: Bar char representing the width of the blastema that is bigger in *Tg(UAS:NICD)* fins comparing to the control. **D**: Haematoxylin and Eosin stained fin sections (5 dpa): the blastema of regenerated *Tg(UAS:NICD)* fins is broader than control blastema (horizontal bars). Higher magnification views of control fins reveal densely packed distal blastema cells (D´, arrowhead), the looser organization in the central proximal region (yellow arrowhead) and the strict alignment in the periphery (D´´, arrowhead). In *Tg(UAS:NICD)* fins, cells are densely packed and disorganized in both blastema regions (D´´´, arrowheads). This structure is similar to the blastema (D´). (***P<0.005; scale bars: A: 200 µm, D: 10 µm. Dashed lines indicate the amputation plane.)

We next examined the morphology and organization of the cells within the regenerate on H&E stained fin sections in control and transgenic fish. Blastema cells in regenerating wild-type fins were densely packed lacking any orientation, whereas more proximal central cells were loosely organized (Fig. 15D, D´, D´´). Lateral cells were aligned with the epidermis (Fig. 15D, D´´) and have been identified as re-differentiating osteoblasts (Knopf et al., 2011). This cellular organization was altered in *Tg(UAS:NICD)* fin sections (Fig. 15D). Densely packed and disorganized cells were observed both in the distal and in the more proximal regenerate. Furthermore, instead of an alignment of prospective osteoblasts we found a dense accumulation of disorganized cells in the equivalent region close to the epidermis (Fig. 15D´, D´´´). Thus, our observations indicate that cellular organization differs in the regions within the fin regenerate and may represent the differentiation state of the cells as the distal region exhibits differentiated blastema cells whereas more proximal cells have redifferentiated already. Thus Notch overactivation impairs fin regenerating but expands the region with densely packed, disorganized cells.

To localize ectopic Notch activation in *Tg(UAS:NICD)* transgenic fish we performed immunohistochemistry against a myc-taq, which is coupled to the NICD transgene (Scheer et al., 2001). We detected myc-NICD-expression in the stump and the blastema of the regenerating fin in *Tg(UAS:NICD)* transgenic fish but not in control animals. We localized myc-NICD-expressing cells in the centre of the blastema and aligned to the epidermis, however rarely in the epidermis (Fig. 16A). This demonstrates that this system, *Tg(hsp70l:Gal4);Tg(UAS:myc-notch1a-intra),* allows the overactivation of the pathway in a region where we had observed Notch activation

before. We investigated if heat shocks thus lead to increased Notch signalling activation by ISH and qPCR. mRNA levels of the Notch targets *her6* and *her15* strongly augmented at 72 hpa upon 10 h heat shock application (Fig. 16B), indicating a direct regulation of *her6* and *her15* gene expression by NICD. Concomitantly, ISH revealed stronger expression and a proximal expansion of *her6* and *her15* expression domains after heat shock application for 4 days (Fig. 16C) or 12 hours (Fig. 16D).

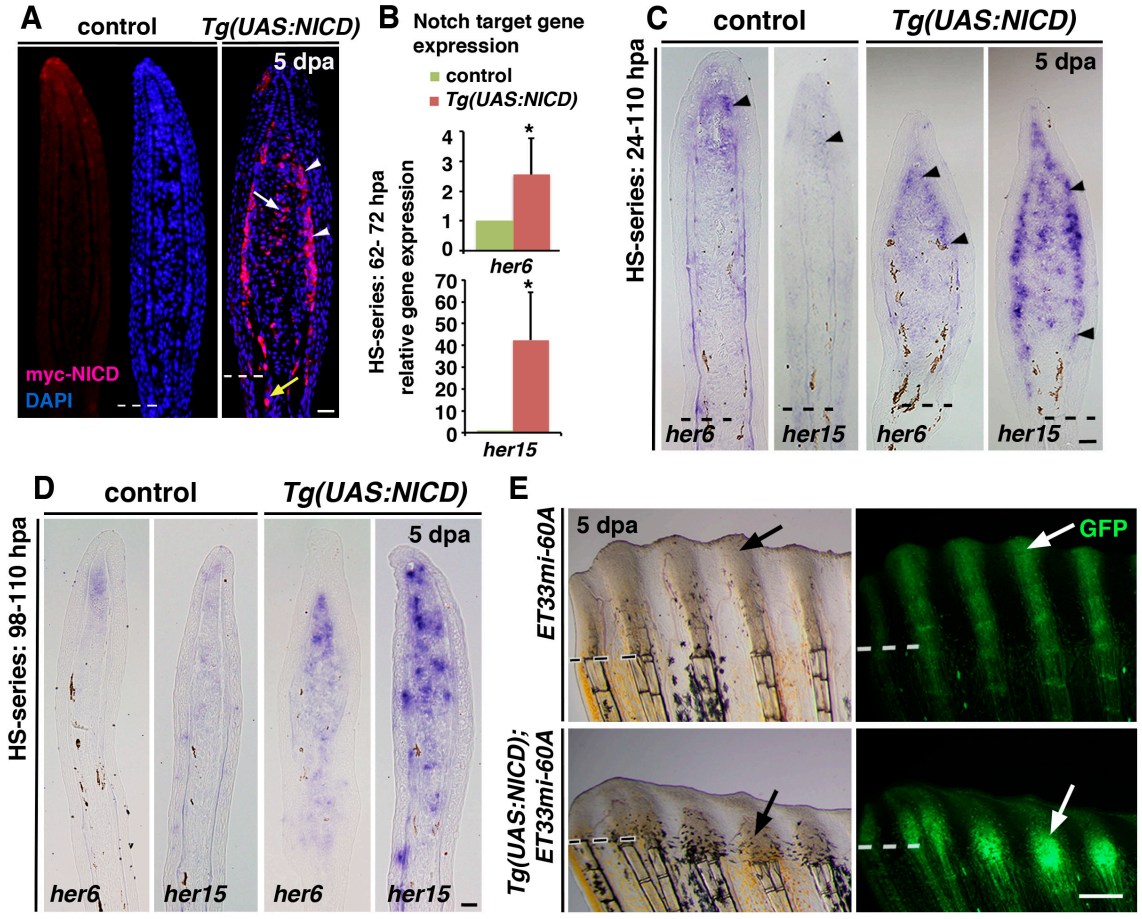

Figure 16: Heat shock-induced Notch overactivation in blastema cells of *Tg(UAS:NICD)* transgenic fish

A: IHC against the myc-tag on the NICD transgene (myc-NICD) in 5 dpa *Tg(UAS:NICD)* and control fin sections. No expression of myc was found in control fins. myc-NICD is mosaic in the blastema, in two or three cell layers beneath the epidermis (arrowheads) and in intraray blastema cells of *Tg(UAS:NICD)* fins (arrow). **B**: qPCR analysis of Notch target gene expression after a 10- hour heat-shock series (62- 72 hpa). **C**, **D**: ISH against Notch targets at 5 dpa. *her6* and *her15* transcription expands into the proximal blastema region in *Tg(UAS:NICD)* fins (arrowheads) after long (24- 110 hpa) and short (98- 110 hpa) heat shock induction. **E**: *Tg(UAS:NICD)* fish were crossed with *ET33-mi60A* fish and *Tg(UAS:NICD);ET33-mi60A* fish were exposed to a series of heat shocks during 5 days of regeneration. GFP expression is increased in *Tg(UAS:NICD);ET33-mi60A* fish at 5 dpa compared with *ET33-mi60A* fish. *P<0.05. Scale bars: 10 µm. Dashed lines indicate the amputation plane.)

We next crossed *Tg(UAS:NICD)* with *ET33-mi60a* transgenic fish and examined if Notch overactivation increases GFP expression in these fish during fin regeneration. Consistent with previous observations we detected swollen blastemas with high GFP fluorescence in transgenic comparing to control fins. However if this is due to the increased expression of GFP in the blastema or the increase in number of blastema cells is not clear.

As previous results indicated that Notch might be implicated in blastema cell proliferation, we investigated the effect of Notch over activation on blastema cell proliferation. To detect if Notch signalling directly regulates cell proliferation we examined BrdU-incorporation in blastema cells at 72 hpa after a short period of heat shocks (62- 72 hpa). Indeed Notch signalling overactivation significantly increased the number of blastema cells that incorporated BrdU and proximally expanded the proliferating blastema at this time point (Fig. 17A, B). As blastema proliferation is associated to *msxb* expression (Nechiporuk & Keating, 2002) and regulated by retinoic acid (RA) (Blum N, 2012) we examined blastema gene expression by qPCR and ISH at different time points in transgenic and control regenerating fins. Notch overactivation slightly but significantly increased *msxb*, *msxe* and *aldh1a2* expression in regenerating fins at 3 dpa (Fig. 17C) and 5 dpa (*msxb*, *msxe*, Fig. 17D) when applying short heart shock series (10h /12 h). After Notch signalling overactivation for a longer period (0- 5 dpa) we detected a stronger signal and a prominent expansion of *msxb*, *msxe* and *aldh1a2* expression into the proximal region of the fin regenerate in transgenic fish whereas blastema gene expression was restricted to the distal region in control animals at 5 dpa (Fig. 17E). Gene expression appeared especially strong in the lateral region (Fig. 17E) and is reminiscent to myc-NICD expression (Fig. 16A) and the distribution of dense disorganized blastema cells (Fig. 15D) in *Tg(UAS:NICD)* transgenic regenerating fins. Moreover double immunohistochemistry revealed that the expansion of aldh1a2^{+} expression into proximal regions in *Tg(UAS:NICD)* fins predominantly occurs in PCNA^{+} proliferating cells, whereas in wild-type fins both proteins are restricted to cells in the distal region at 5 dpa (Fig. 17F). Altogether we found that Notch overactivation leads to an expansion of the blastema cell pool, indicated by blastema gene expression and by increased cell proliferation.

5. Notch signalling overactivation prevents bone regeneration

Next we examined if Notch induced blastema cell expansion interferes with the differentiation of cells and the formation of new bone in the regenerating fin. For this aim we performed alizarin red staining, to label calcified structures in control and *Tg(UAS:NICD)* fish at 5 dpa after a long series of heat shocks. At 5 dpa control fins showed regular new regenerated fin rays proximal to each stump, which represented 58% ± 9% of the whole regenerate (Fig. 18A, B). Transgenic animals however exhibited minor calcified tissue distal to the amputation plane (27%± 5% of the whole regenerate, Fig. 18A, B), indicating that bone formation failed in these animals.

Bone regeneration in the fin precedes via the dedifferentiation, proliferation and redifferentiation of osteoblasts that secret bone matrix to reconstitute the lost fin radials (Knopf F, 2011). We further examined the expression of genes involved in osteoblast differentiation. The *T-Cell-Specific Transcription Factor* (*tcf7)* is expressed in early osteoblasts in the developing zebrafish jaw (Li et al., 2009). In control fish we observed strong *tcf7* expression in the basal epidermis of the distal region but also in cells aligned with the epidermis (Fig. 18C, D, arrowheads) suggesting that these cells are de-differentiated or early differentiating osteoblasts.

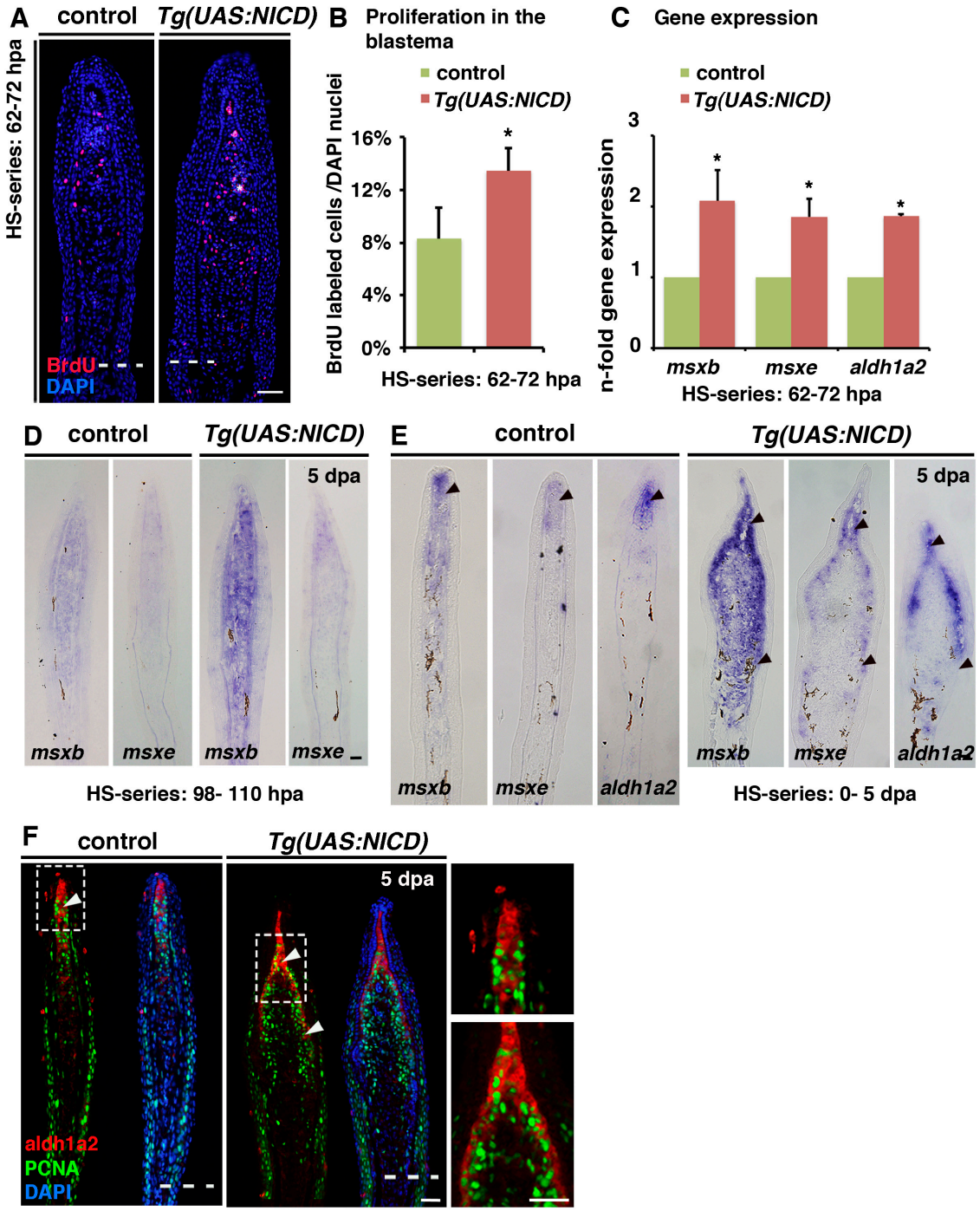

Figure 17: Notch gain of function increases proliferation and is accompanied by an expansion of distal blastema marker expression into proximal regions.
A, **B**: BrdU-stained fin sections after a 10-hour heat-shock series (62- 72 hpa) and quantification of the percentage of BrdU-labelled DAPI nuclei in the blastema: more cells incorporate BrdU in *Tg(UAS:NICD)* fins than in the control (asterisk indicates autofluorescent blood vessels). **C**: qPCR analysis after a 10-hour heat-shock series (62-72 hpa): *msxb*, *msxe* and *aldh1a2* transcripts are increased in *Tg(UAS:NICD)* fins. **D**: ISH for *msxb* and *msxe* at 5 dpa after a short heat shock series (98- 110 hpa). Expression is increased in *Tg(UAS:NICD)* fins. **E**: ISH for *msxb*, *msxe* and *aldh1a2* at 5 dpa after a long heat shock series (0- 5 dpa). Arrowheads delimit expression of *msxb*, *msxe* and *aldh1a2*, which is expanded in *Tg(UAS:NICD)* fins. **F**: IHC of PCNA and aldh1a2 on 5 dpa fin sections. Double labelled cells are restricted to the distal region of the control fin (arrowhead) but are expanded proximally in *Tg(UAS:NICD)* fins at 5dpa (arrowheads). (*P<0.05. Scale bars: 10 µm. Dashed lines indicate the amputation plane.)

However *tcf7* gene expression was absent in the proximal region, where differentiated osteoblasts are located. In contrast, *Tg(UAS:NICD)* fins showed a proximal expansion of *tcf7* expression (Fig. 18C, D). We also detected the *runx2*, a marker for dedifferentiated osteoblasts, restricted to a few cells within the blastema in control fish but expanded to the proximal region in transgenic animals. This indicates the presence of de-differentiated and early differentiating osteoblasts throughout the fin regenerate in *Tg(UAS:NICD)* fins at 5 dpa. To determine if the progression of osteoblast differentiation was blocked in transgenic fins, we examined the expression of osterix (osx), an intermediate-differentiation marker for osteoblasts (Knopf et al., 2011, Singh et al., 2012, Sousa et al., 2011). In the 5 dpa control fin, osx was expressed in cells aligned with the epidermis, within the stump and proximal to the amputation plane, but not in the distal region of the regenerate (Fig. 18F). In contrast, *Tg(UAS:NICD)* fins contained only a few osx-positive cells close to the amputation plane (Fig. 18F). We next measured the length of the distal domain of the fin regenerate that lacks osx^+ cells in control and transgenic fins at 5 dpa after a long-term heat shock protocol. In control fish, the osx-negative undifferentiated distal blastema region constituted 23% (±7%) of the regenerating fin (Fig. 18F, G). In contrast, in *Tg(UAS:NICD)* fish up to 47% (±14%) of the fin regenerate lacked osx expressing cells (Fig. 18F, G) and locally coincided mostly with the presence of myc-NICD expression (Fig. 18F). This suggests that ectopic Notch activation in the regenerating fin does not only trigger expansion of dedifferentiated blastema cells but also prevents the progression through an intermediate state of osteoblast differentiation.

We next examined how Notch overactivation affects gene expression of different signalling pathways involved in skeletogenesis. Hedgehog signalling (Hh) together with BMP is implicated in osteoblast proliferation and promotes bone deposition (Quint et al., 2002, Smith et al., 2006). As expected, both genes, *sonic hedgehog* (*shh*) and *bmp2b*, were similarly expressed in control fins at 5 dpa: in osteoblasts lining the epidermis (Fig. 19A, B). Transgenic fish also expressed *shh* and *bmp2b*, however the region, that lacks gene expression was dramatically expanded to the proximal

regenerate (Fig. 19A, B). This observation goes in line with the assumption that Notch overactivation impairs bone regeneration. As Notch overactivation restricted fin outgrowth, we wondered if this might be related to the activation of noncanonical Wnt signalling, which controls regenerative outgrowth (Stoick-Cooper et al., 2007). Indeed we found that *wnt5b*-expression was dramatically expanded into the proximal region in *Tg(UAS:NICD)* fins, but restricted to the basal epidermis and underlying blastema cells in control fish at 5 dpa (Fig. 19C).

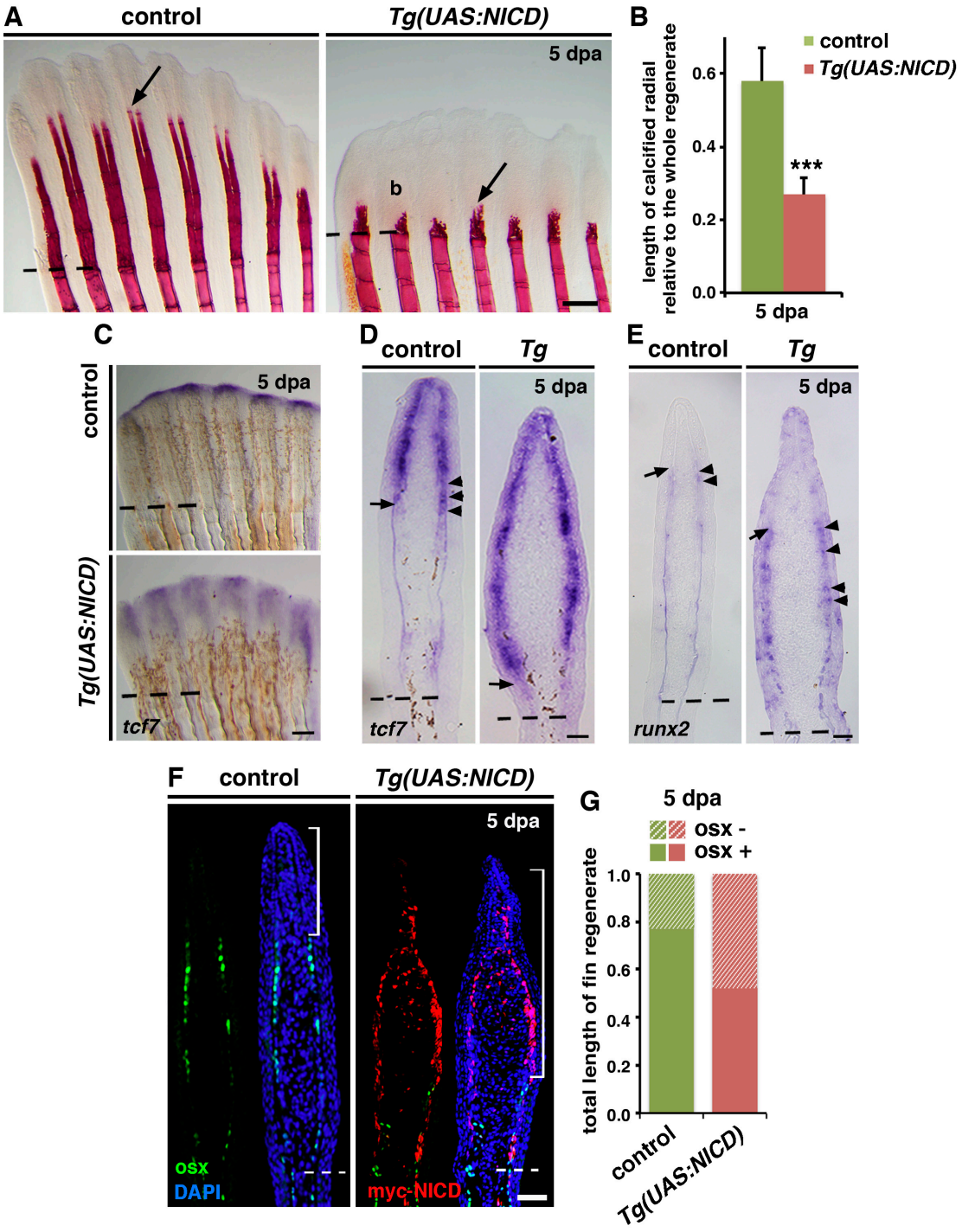

Figure 18: Notch signalling inhibits osteoblast differentiation and prevents bone regeneration.
A: Alizarin red staining of fins at 5 dpa reveals calcified bony rays in a control fin regenerate (arrow). Fin rays are poorly formed in *Tg(UAS:NICD)* fins, whereas the blastema (b) is expanded (arrow). **B**: Length of regenerated calcified radials of *Tg(UAS:NICD)* fins, relative to control fins. **C, D**: WISH and ISH on sections at 5 dpa. Control fins express *tcf7* in peripheral cells (osteoblasts, arrowheads) in the distal region (limited by the arrow), whereas transcription is expanded proximally in *Tg(UAS:NICD)* fins (arrow). **E**: ISH on fin sections showing *runx2* expression in osteoblasts (arrowheads). *Runx2* expression is restricted (arrow) in control fins. This distal *runx2*$^-$ region is expanded in *Tg(UAS:NICD)* fins whereas *runx2* expression reaches more proximal (arrowheads). **F**: IHC for osx and myc-NICD. In control fins, osx$^+$ cells (green) are present in the proximal fin region but scarce in the distal region (bracket). osx$^+$ cells are less numerous in regenerating *Tg(UAS:NICD)* fins and more proximally limited. The region of high myc-NICD expression does not contain osx$^+$ cells (bracket). **G**: Relative length of the proximal region of the fin regenerate, which contains osx$^+$ cells, and the distal region (brackets), which does not (osx$^-$). The distal, osx$^-$ region is larger in *Tg(UAS:NICD)* fins than in control fins. (***P<0.001, ***P<0.005. Scale bars: A: 200 µm; C, D: 10 µm. Dashed lines indicate the amputation plane.)

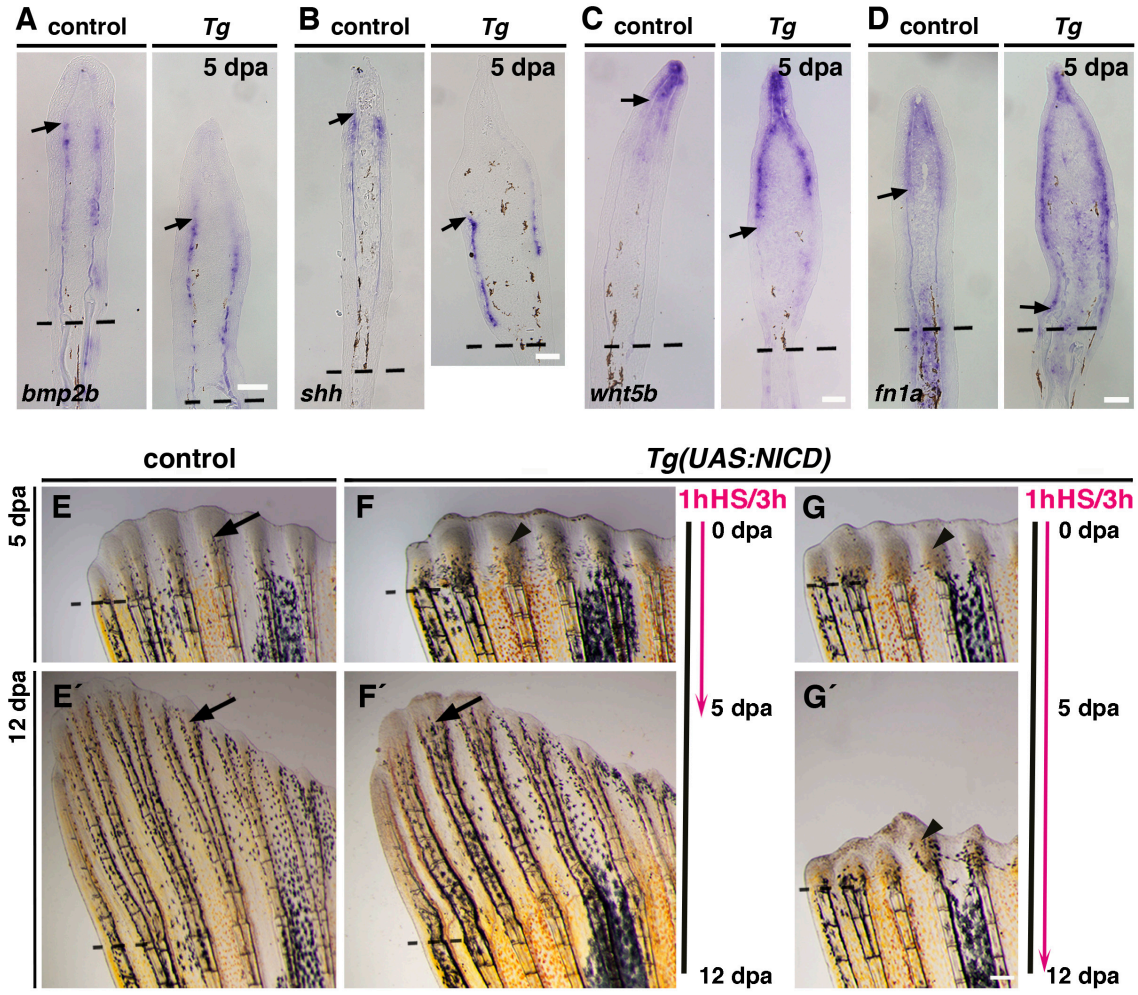

Figure 19: NICD-induction affects *bmp*, *shh* and *wnt* expression and induces reversible blastema expansion.
A, B: ISH for *bmp2b* and *shh* shows that the *bmp2b*$^{-}$/ shh^{-} region (arrowhead) is expanded in *Tg(UAS:NICD)* fins. **C**: ISH on fin sections indicates expanded expression of distal *wnt5b* in *Tg(UAS:NICD)* fins. **D**: ISH, showing that epidermal expression of *fibronectin 1a* (*fn1a*) is proximally expanded (arrow) in *Tg(UAS:NICD)* fins. **E**: Heat shock cycles were applied over 5 days of regeneration (E-F') or 12 days (G, G'). Black line: time of regeneration. Pink line: time of heat-shock treatment (1h of heat-shock every 3 hours during 5 or 12 days). Arrows: regenerating radials. Arrowheads: expanded blastemas. Regeneration is inhibited in *Tg(UAS:NICD)* (F, G) fins but not in control fins (E). Regeneration reverts to normal when heat-shock treatment is stopped (E', F', arrows) but the blastema remains close to the amputation plane (arrowhead) when heat shock continued up to 12 days (G'). (Scale bars: A- D: 10 μm; G 100μm. Dashed lines mark the amputation plane.)

This suggests, that Notch induced noncanonical Wnt signalling overactivation may restrict regenerative outgrowth in this setting. As cellular processes within the blastema highly depend on signals from the epidermis (Wehner & Weidinger, 2015) and vice versa, we examined the expression of *fibronectin1a*, which is expressed specifically in the epidermis surrounding the blastema (Yoshinari et al., 2009). We observed a similar expansion of this epidermal marker in *Tg(UAS:NICD)* regenerates compared to control fins (Fig. 19D), indicating that Notch overactivation, mainly in the blastema (Fig. 16A), also indirectly affects gene expression in the epidermis.

To investigate if blastema expansion is a reversible effect we exposed *Tg(UAS:NICD)* fish to a long-term heat-shock series over 12 dpa (Fig. 19E), while wild-type and another group of *Tg(UAS:NICD)* fish were heat-shocked for the first 5 dpa and subsequently maintained at 28°C until 12 dpa (Fig. 19F, G). As before, control fish showed no fin regeneration defect upon heat-shock treatment (Fig. 19E), whereas regeneration was impaired in *Tg(UAS:NICD)* fish at 5 dpa (Fig. 19F, G). However, when heat-shock treatment was halted at 5 dpa in transgenic fish, fins recovered the regeneration seen in control fish (Fig. 19F´). In contrast, when heat-shock treatment was continued up to 12 dpa, the blastema retained the altered form (Fig. 19 G´). This suggests that Notch signalling may be transiently activated in blastema cells during fin regeneration.

II. The role of Notch signalling during heart regeneration

1. Characterization of the endocardium

1.1. Notch signalling pathway elements are expressed upon cryoinjury

The expression of Notch signalling pathway components in the regenerating heart has been previously reported after ventricular resection (Raya et al., 2003). During this thesis, we carried out zebrafish heart regeneration studies by using the cryoinjury model (Gonzalez-Rosa & Mercader, 2012). Thus we performed ISH and immunohistochemistry against a selection of Notch signalling pathway components on heart sections after sham injury and at 3 and 7 days post cryoinjury (dpci). The zebrafish adult heart exhibits low- level expression of *notch1b* upon a sham injury, presumably in endocardial cells (Fig. 20A). Further we detected a few cells expressing *notch2* and *notch3* in the region of the cortical myocardium, suggesting that these cells are associated to coronary vessels (Fig. 20A). We did not detect dll4 protein in sham injured ventricles and hardly *lfng* transcripts (Fig. 20A). Next, we examined gene expression at 3 dpci and detected dll4 in cells within the injury site (is), indicated by the lack of $mf20^{+}$ cardiomyocytes. Dll4 was also present in cells lining injury-adjacent cardiomyocytes, suggesting that these are endocardial cells (Fig. 20B). Similarly we observed strong expression of the receptor-gene *notch1b* in cells surrounding injury-adjacent cardiomyocytes but also within the injury site at the inner injury border (Fig. 20B). Further *notch2*, *notch3* and *lfng* were strongly upregulated in cells at the inner injury border (Fig. 20B). At later stages the expression of dll4, *notch1b*, *notch2* and *notch3* was more evident in cells, within the injury site (Fig. 20C) and *notch1b* showed the strongest expression of the three receptors. The Notch signalling pathway typically regulates genes encoding basic-helix-loop-helix (bHLH) transcription factors of the Hes and Hey (HESR) families (Iso et al., 2003). We analysed the activation of a subset of Her genes upon cryoinjury by ISH. *Her6* was expressed presumably in endocardial cells, lining myocardial trabecules at 3 dpci (Fig. 21A). Further we detected *her9* expression in cells within the injury site at the inner injury border (3 dpci) but also later in the epicardial region (7 dpci, Fig. 21B). *Her4* expression was evident in cells lining injury adjacent cardiomyocytes however just in a minor population at 3 and 7 dpci (Fig. 21C). This shows that various Notch target genes are activated upon cryoinjury. However none of the Her genes examined, completely resembles the strong expression of *notch1b* at the injury site, suggesting that Notch signalling may activate further genes in this context. To confirm the localization of Notch pathway gene expression we performed immunohistochemistry of dll4 on heart sections of *ET33-1a* transgenic fish, an enhancer trap line that expresses GFP in endocardial cells (Poon et al., 2010). We detected dll4 in GFP-expressing cells, indicating Notch ligand expression by the endocardium in the cryoinjured regenerating heart (Fig. 21A). Further, double fluorescent *in situ* hybridisation

for *notch1b* and *aldh1a2*, encoding the RA-producing enzyme and being expressed in the endocardium (Kikuchi et al., 2011b) showed co-localization (Fig. 21B). This suggests that endocardial cells also express the receptor of the pathway and that Notch signalling activation occurs through endocardial cell- to- cell communication.

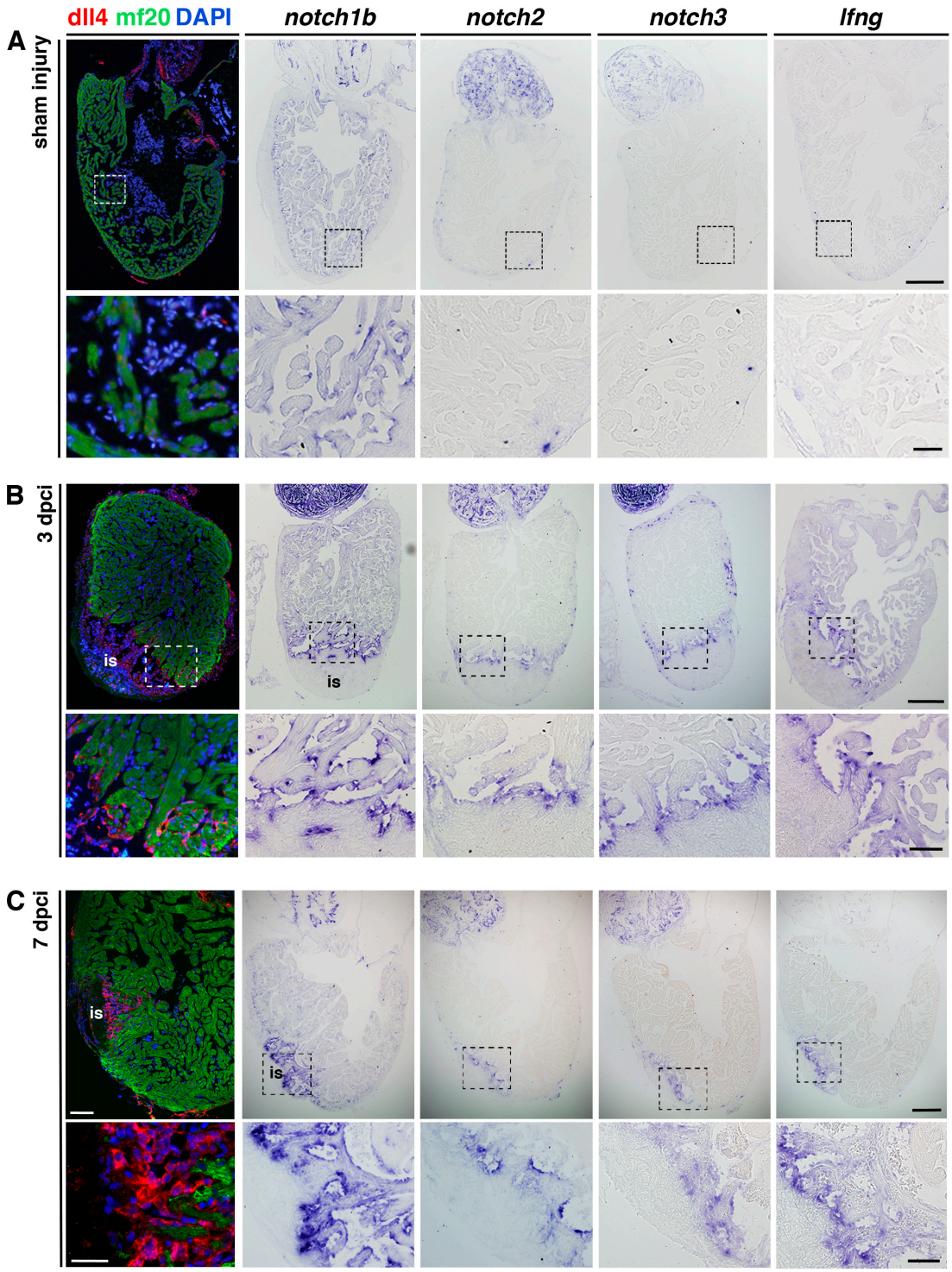

Figure 20: Notch signalling pathway elements are expressed upon cryoinjury.
A: Immunohistochemistry of dll4 and mf20 and ISH of *notch1b*, *notch2*, *notch3* and *lfng* in sham injured hearts. Weak *notch1b* expression is present in presumably endocardial cells in the ventricle. *Notch2* and *notch3* expression is apparent in cells adjacent to coronary vessels. Dll4 is not expressed in the ventricle and *lfng* very weakly. **B, C**: Immunohistochemistry of dll4 and mf20 and ISH of *notch1b*, *notch2*, *notch3* and *lfng* in regenerating hearts, showing expression adjacent to and within the injury site (is, 3 dpci, 7 dpci). Boxed areas are shown at higher magnification in the lower rows. (Scale bars A-C: 200 μm, magnified views: 50 μm).

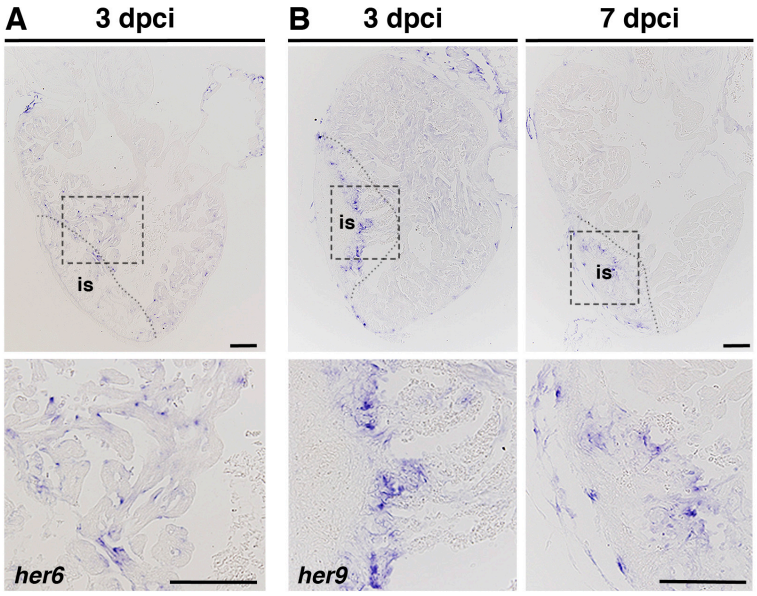

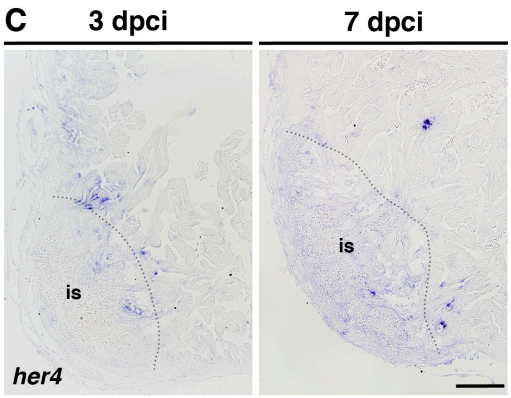

Figure 21: Notch signalling target genes are expressed upon cryoinjury.
A: ISH of *her6* showing expression in endocardial cells throughout the ventricle. **B**: ISH of *her9* showing expression in cells within the injury site (is) at 3 and 7 dpci. **C**: ISH on heart sections showing low numbers of *her4* expressing cells at 3 and 7 dpci. (Scale bars: 200 μm, magnified views: 100 μm).

1.2. Embryonic gene expression in the endocardium upon cryoinjury

Activation of cells during regeneration is, in many cases, associated to the reexpression of developmental genes (Poss, 2010). We sought to examine the presence of other developmental

gene transcripts, besides Notch, in the endocardium upon cryoinjury. ISH for *kinase insert domain receptor-like* (*kdrl*/ *flk1*/*vgfr4*), which is expressed in the developing endocardium and endothelium (Wong et al., 2012), indicated gene expression in endocardial cells within the injury site but also in the remote region (Fig. 22C). In contrast the expression of *cadherin5* (*cdh5*/ *ve-cadherin)* was dramatically increased in cells within the injury site, but weaker in the remote zone (Fig. 22C).

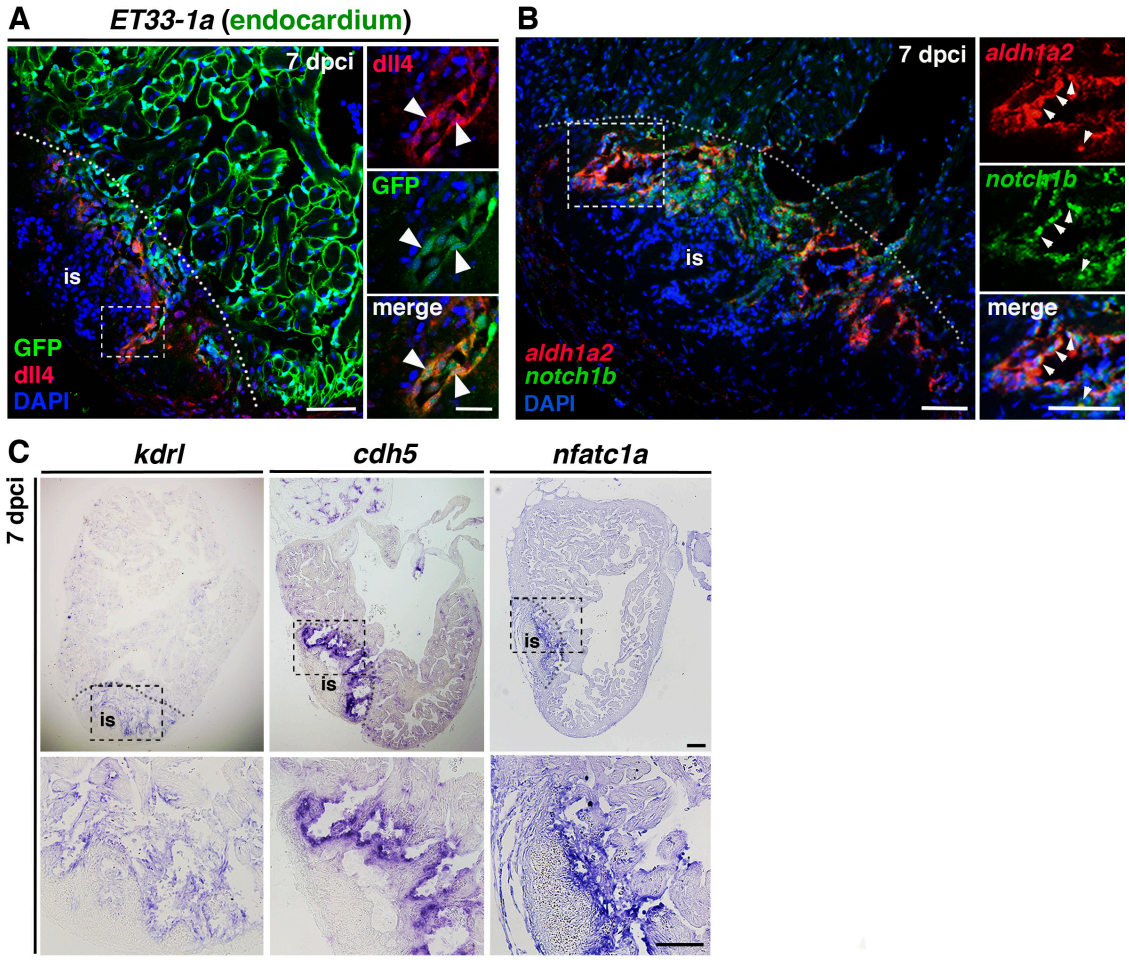

Figure 22: Notch signalling pathway elements are expressed in the endocardium, which activates embryonic genes.
A: Immunohistochemistry of GFP and dll4 on *ET33-1a* transgenic heart sections (7 dpci). The confocal image shows dll4-expression in GFP^{+} endocardial cells (white arrowheads) inside the injury site (delineated by the dotted line). The boxed area is shown at higher magnification in the panels on the right. **B**: Double fluorescence ISH against *notch1b* and *aldh1a2*, demonstrating co-expression of these genes (arrowheads) in the injury site (is) at 7 dpci. **C**: ISH against *kdrl*, *cdh5* and *nfatc1a* at 7 dpci, showing strong endocardial expression within the injury site (is). (Scale bars A, B, C: 200 µm, magnified views: 50 µm).

Cdh5 is a cell adhesion protein, expressed in endothelial cells (Lampugnani, Resnati et al., 1992) but also in the developing endocardium (Wong et al., 2012) and is required for the integrity of

cellular junctions and permeability control of the endothelial layer (Lampugnani et al., 1992). Further we examined the expression of one homolog of Nfatc1 (*nfatc1a*), a gene, specifically expressed in the endocardium during mouse and fish heart development (de la Pompa, Timmerman et al., 1998, Wong et al., 2012). We found weak expression in endocardial cells throughout the ventricle but augmented gene activation at the inner injury border at 7 dpci (Fig. 22C). Gene expression analysis thus revealed the upregulation of embryonic genes upon cryoinjury, indicating the activation of endocardial cells within the injury site.

1.3. Endocardial cells reside within the injured tissue after cryoinjury

Apart from the regenerating fin, *ET33-mi60A* transgenic fish also express GFP in endocardial cells of the embryonic heart (Poon et al., 2010), which prompted us to examine endocardial GFP expression in the adult injured ventricle. Whole mount examination of injured *ET33-mi60a* hearts revealed GFP expression throughout the ventricle (Fig. 23A). Surprisingly we detected high levels of GFP-fluorescence within the cryoinjury site, located at the apex of the heart, indicating the presence of endocardial cells in this region (Fig. 23A). Immunohistochemistry on heart sections confirmed the presence of GFP^+ endocardial cells in the injury site that lacks myosin heavy chain II $(mf20)^+$ cardiomyocytes (Fig. 23B). The fact that GFP-mRNA could be detected by ISH in those cells (Fig. 23B) and that these cells expressed the endothelial erythroblast-transformation-specific (ETS) transcription factor (ERG) (Fig. 23C), suggested that GFP^+ cells in this region retain their endocardial/ endothelial characteristics after injury. Double immunohistochemistry for GFP and dll4 also indicated the presence of Notch gene activation in these endocardial cells within the injury site (Fig. 23D).

Having this tool we sought to analyse more in detail the morphology and the behaviour of endocardial cells adjacent and within the injury site. The examination of histological sections provides limited information on tissue morphology. With the intention to study spatial distribution and behaviour of injury–activated endocardial cells we developed a protocol for 3D-confocal imaging of injured ventricles. We used two cardiac enhancer trap reporter lines: *ET33-mi60a* and *ET33-1a*, which express GFP in endocardial cells (Poon et al., 2010). We crossed both lines with a myocardial reporter fish, *myl7:mRFP*, expressing membrane-bound RFP in cardiomyocytes (Rohr et al., 2008). Hearts were optically cleared by incubation in CUBIC (Susaki et al., 2014) to improve the detection of endogenous fluorescence signal. Imaging of injured hearts at 24 hpci revealed a notable lack of myocardial cells after cryoinjury, indicated by a strong reduction of mRFP fluorescent signal (Fig. 24A, B; Movie 1, 2).

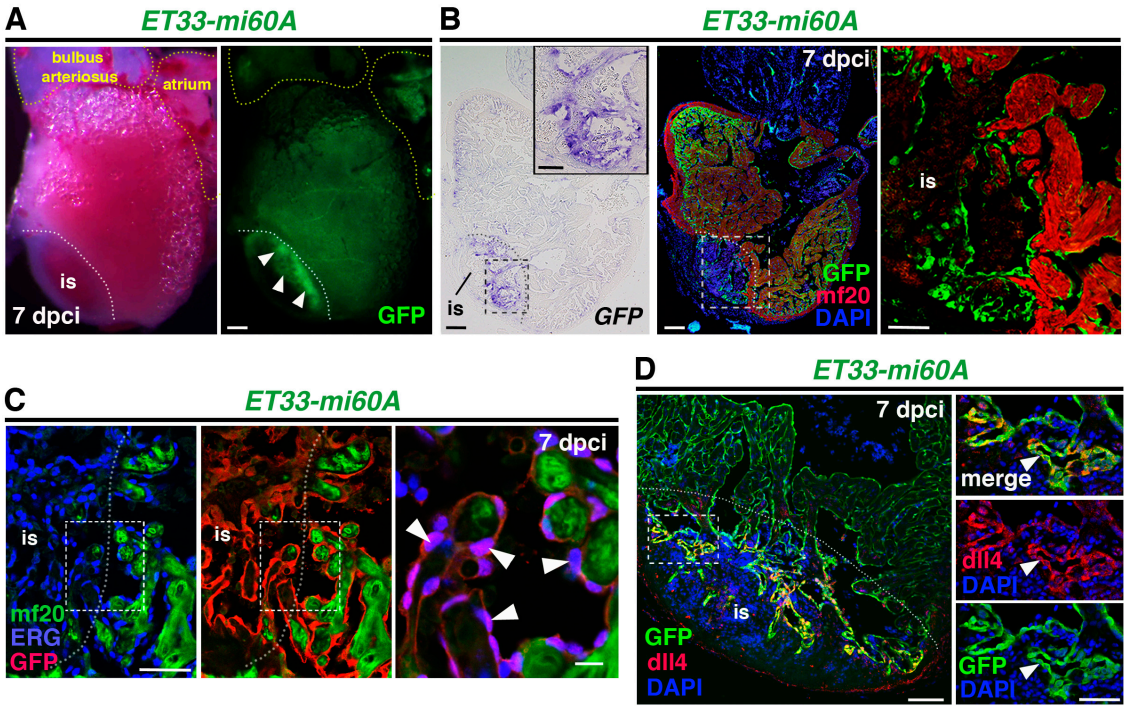

Figure 23: Endocardial cells in the injury site express GFP in *ET33-mi60A* transgenic hearts.
A, B: Bright-field and green-filter views of a whole-mount *ET33-mi60a* transgenic heart at 7 dpci and consecutive sections showing ISH against GFP (B) and immunohistochemistry against GFP (green) and mf20 (red) (magnified view on the panel top right). GFP is expressed throughout the ventricle but more strongly in the injury site (is, arrowheads in A). **C**: Immunohistochemistry against ERG, GFP and mf20 on sections of *ET33-mi60a* transgenic hearts (7 dpci) identifies GFP^+ cells inside and lining the injury site (is) as endocardial/endothelial cells (white arrowheads). **D**: Immunohistochemistry on a *ET33-mi60a* transgenic heart section (7 dpci) against GFP and dll4, demonstrating that GFP expression coincides with dll4 expression (white arrowheads) inside the is. (Scale bars A, B: 200 µm, D: 100 µm, C: 50 µm magnified views: A: 50 µm; B: 5 µm).

Also GFP fluorescence intensity was dramatically decreased in the injury site, indicating the loss of endocardial cells. However we detected spared GFP-labelled cells using both reporter lines (Fig. 23A, B; Movie 1, 2), indicating the presence of survivor endocardial cell within the region lacking $mRFP^+$ cardiomyocytes. We proceeded to 3D-image injured apexes at 3 dpci. Similarly, a clear lack of $mRFP^+$ cardiomyocytes indicated the injury site (Fig. 24C). However, we observed a massive amount of GFP^+ endocardial cells within this region (Fig. 24C; Movie 3).

Examination of optical sections revealed regions of different endocardial cell density (Fig. 24D). In undamaged tissue, scattered elongated endocardial cells surrounded cardiomyocyte clusters; in contrast, the cardiomyocyte-depleted injury site contained more rounded GFP^+ cells. The border of the injury site was characterized by invading cardiomyocytes, consistent with published reports (Chablais et al., 2011, Schnabel et al., 2011). Cardiomyocytes were surrounded

by a dense network of endocardial cells (Fig. 24D). Our 3D-analysis thus revealed that spared endocardial cells survive the cryoinjury, round up and are densely packed within the injury site and surrounding injury adjacent cardiomyocytes at 3 dpci.

1.4. Endocardial cells progressively increase within the injury site and form an organized structure

To analyse the timely progression of the endocardium in the injury site we performed a whole-mount 3D confocal imaging time course of *ET33-mi60A;myl7:mRFP* transgenic hearts (Fig. 25A).

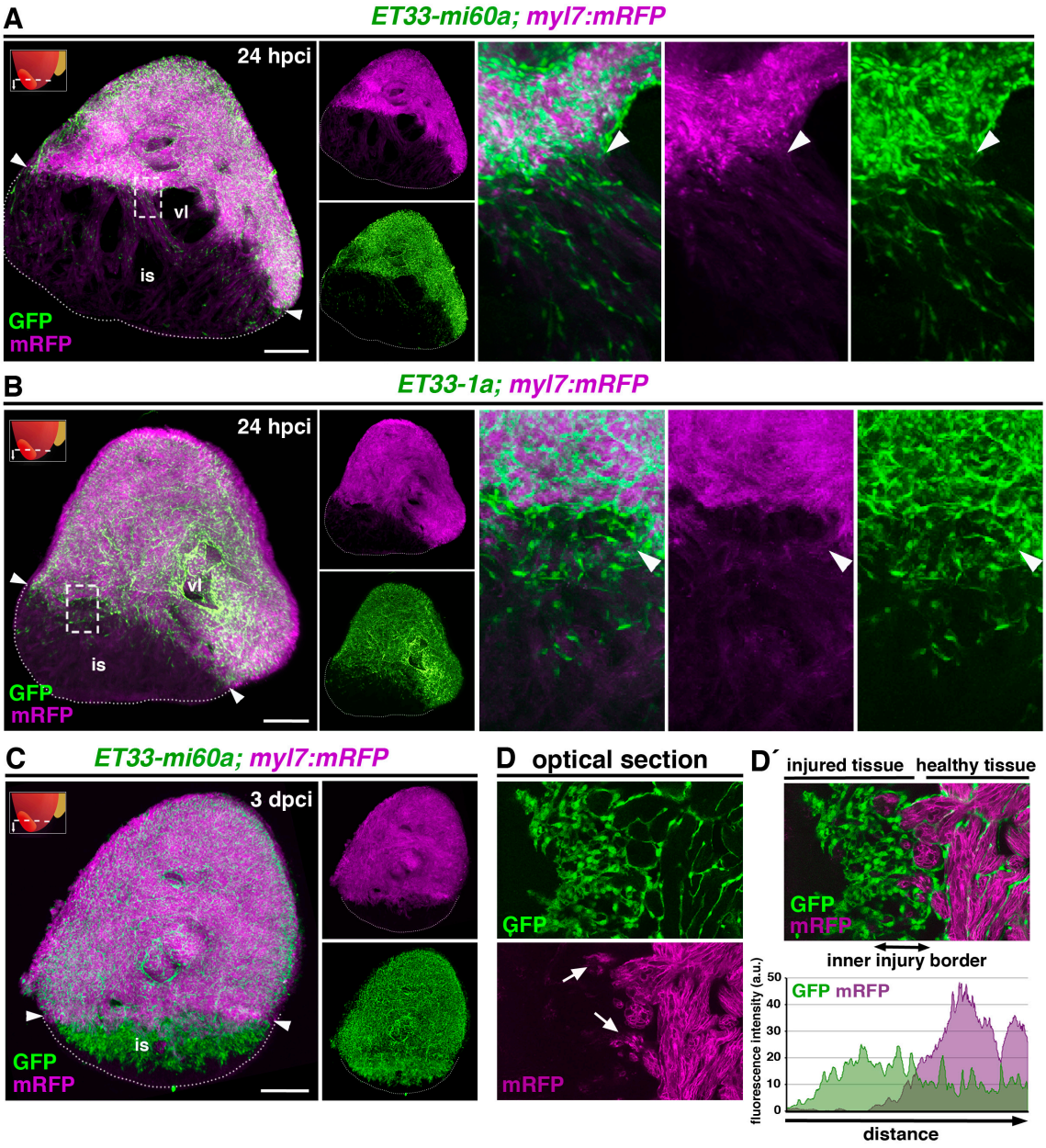

Figure 24: Endocardial cells reside within injury site.
A, B: Volume rendering of the apical injured half of the ventricle of a *ET33-mi60A;myl7mRFP* (A) or *ET33-1a;myl7mRFP* (B) heart (24 hpci); endocardium is labelled green and the myocardium magenta. The injury site is characterized by weak magenta fluorescence (indicated by white arrowheads). The dotted line demarcates the injured tissue. Spared GFP-labelled endocardial cells are present in the injury site. The boxed area is magnified in the panels on the right. **C, D**: Volume rendering of the apical injured half of the ventricle of *ET33-mi60A;myl7mRFP* heart (3 dpci) and an amplified optical section (D, D´), showing massive accumulation of endocardial cells within the injured tissue (delimited by white arrowheads in D) compared with healthy tissue. The dotted line in D demarcates the injured tissue. The inner injury border is characterized by protruding finger-like cardiomyocyte clusters (white arrows) surrounded by a dense endocardial network (D, D´). The healthy myocardium is enclosed by less dense but well-connected endocardial cells (D, D´). The graph shows the mean fluorescence intensity profile for panel D´, indicating high and constant green fluorescent intensity in the injured tissue that drops with increasing mRFP intensity at the inner injury border with the healthy tissue. (is, injury site; vl, ventricular lumen, small upper left panels in A, B, C indicate the confocal scanned region. Scale bars: A, B, C: 100 μm).

To estimate endocardial cell abundance, we used IMARIS software to 3D-reconstruct confocal images and performed volume quantification of the injury site, identified by its lack of $mRFP^+$ cardiomyocytes. Similarly, we quantified the volume of GFP^+ cells within the same region (Fig. 7, see Material and Methods). Putting these values in relation allowed us to estimate the relative volume that occupied GFP^+ endocardial cells within the injury site at different time points (Fig. 25A, C). Consistent with our previous observation GFP^+ cells were present but rare in the injury site at 24 hpci, occupying 3.5% ± 2.1% of the injured volume (Fig. 25A, C; Movie 4). By 36 hpci, the amount of GFP^+ cells slightly, but significantly increased (8.5% ± 3.8%; Fig. 25A, C; Movie 5). At 3 dpci most hearts exhibited a higher amount of GFP^+ cells (15.5% ± 8.9%; Fig. 25A, C). The high between-heart variability suggests that the increase in endocardial cell content initiates around 3 dpci. At 9 dpci, however GFP^+ cells occupied a much larger proportion within the injured tissue (47.1% ± 13.7%), suggesting a huge expansion of the endocardium between these time points (Fig. 25A, C; Movie 6). Also the morphology of the endocardium changed from 3 dpci to 9 dpci (Fig. 25A, compare Movie 5 and 6). Until three months post cryoinjury (mpci) the relative volume of GFP^+ cells still increased, albeit more gradually (Fig. 25A, C; Movie 6, 7). Also, over this timespan the total size of the injury site decreased (Fig. 25D) and the tissue was covered by compact myocardium (Fig. 25A, 1 mpci, 3 mpci) consistent with published data (Chablais, Veit et al., 2011), indicating that cardiomyocytes had already begun to replace lost cardiac muscle.

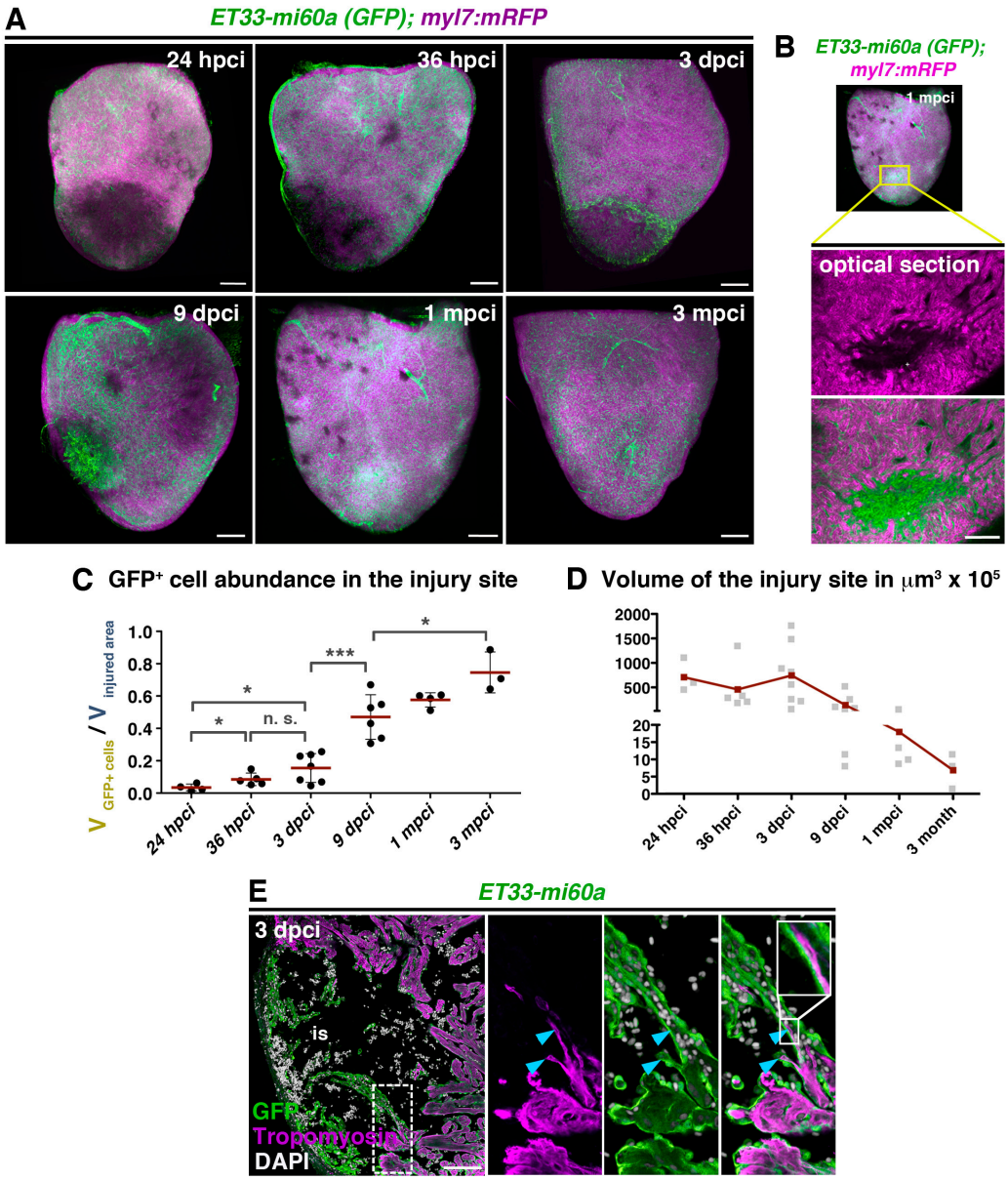

Figure 25: The endocardium expands within the injury site.
A: Volume rendering of injured ventricles of *ET33-mi60A; myl7mRFP* hearts, with endocardium labelled green and myocardium magenta, at 24 hpci, 36 hpci, 3 dpci, 9 dpci, 1 mpci, and 3 mpci. The injury site is characterized by weak magenta fluorescence. **B**: Amplified optical section from the centre of the heart in A (1 mpci). The endocardium completely fills the cardiomyocyte-free region. **C**: Scatter plot showing the relative volume occupied by GFP^+ cells in the injury site over time (red line= mean, SD, * $P< 0.05$; ** $P<0.01$, *** $P<0.005$). **D**: Scatter plot showing the evolution of injury-site volume after cryoinjury in *ET33-mi60a; myl7:mRFP* transgenic hearts, quantified with IMARIS. **E**: Immunohistochemistry for GFP and tropomyosin on heart sections of *ET33-mi60A* fish at 3 dpci, showing endocardial cells in close contact with myocardial protrusions at the inner injury border (blue arrowheads). The boxed area is magnified in the right hand panels. (Scale bars: A: 200 μm; E: 70 μm)

The analysis of optical sections of these hearts (1 mpci) revealed that regions lacking cardiomyocytes were filled with an organized network of endocardial cells (Fig. 25B). These data

suggest that endocardial cell expansion in the injury site precedes the migration of cardiomyocytes and that the endocardial structure may serve as a scaffold for cardiomyocyte repopulation of the injury site. Supporting this idea, immunohistochemistry against GFP and tropomyosin on tissue sections revealed that myocardial cell protrusions, a characteristic of migrating cardiomyocytes (Tian, Liu et al., 2015), were in close contact with the dense endocardial cell network (Fig. 25E).

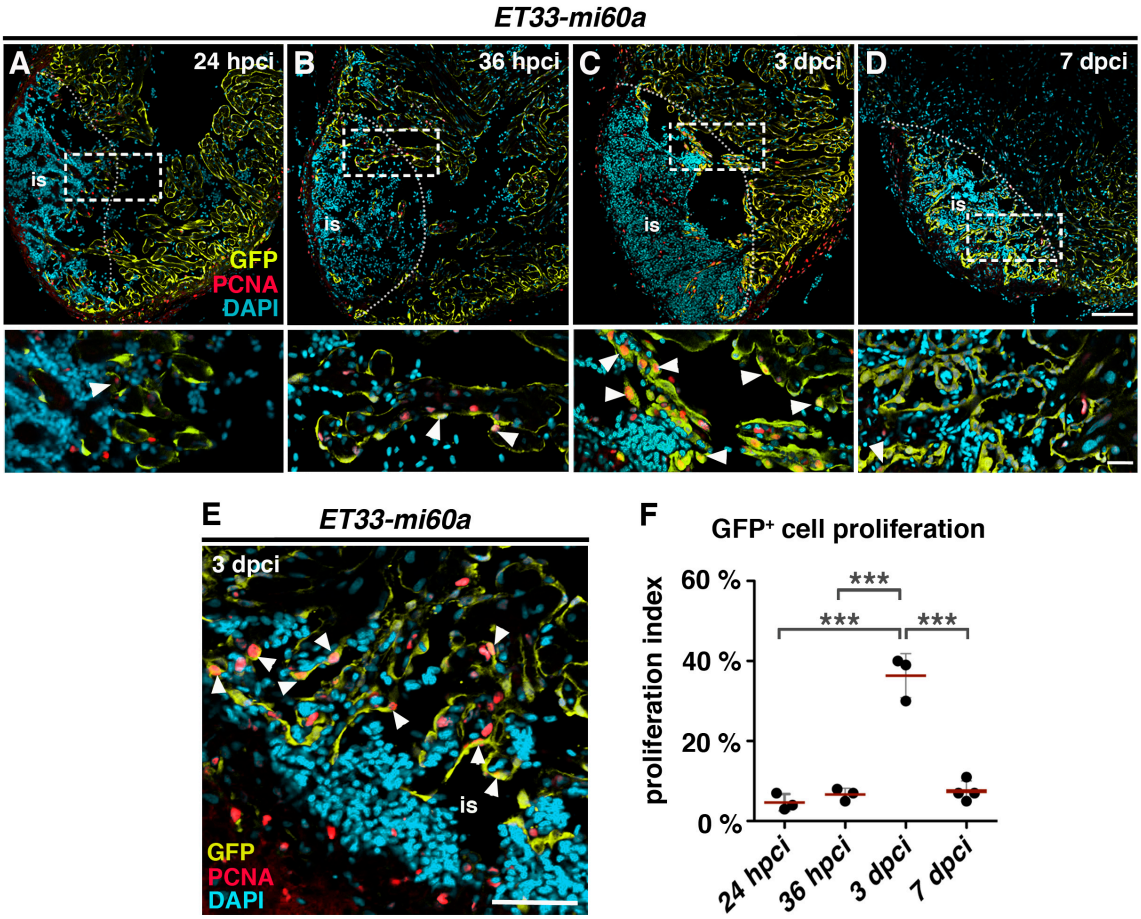

Figure 26: The endocardium strongly proliferates in the injury site
A-D: Immunohistochemistry against GFP and PCNA on heart sections of *ET33mi-60A* fish at 24 hpci, 36 hpci, 3 dpci and 7 dpci, showing massive PCNA-labelled endocardial nuclei at the inner injury border at 3 dpci, but not at other time points. Boxed areas are magnified in the panels below. **E**: Immunohistochemistry against GFP and PCNA on sections of *ET33-mi60a* transgenic hearts (3 dpci), showing high abundance of PCNA-expressing endocardial cells within the injury site (is) (white arrowheads). **F**: Scatter plot showing the percentage of $PCNA^{+}$/ GFP^{+} cells of GFP^{+} cells within and up to 50 µm adjacent to the injury site. (red line= mean, SD, *** $P<0.005$, Scale bars: 100 µm; amplified views: 20 µm).

To investigate whether the expansion of the endocardium derives from cell proliferation we performed immunohistochemistry against GFP and the proliferating cell nuclear antigen (PCNA) of heart sections of *ET33-mi60A* transgenic fish. At 24 hpci we observed PCNA-stained nuclei

within the injury site but very rarely in GFP$^+$ endocardial cells (Fig. 26A, F). The number of PCNA-stained endocardial cells remained low by 36 hpci (Fig. 26B, F). However at 3 dpci we detected a massive proliferative response of GFP$^+$ cells at the inner injury border and the rest of the injury site (Fig. 26C, E, F) in *ET33-mi60A* transgenic hearts indicated by PCNA staining. This is consistent with previous reports about endocardial/endothelial proliferation in fli:GFP$^+$ cells (Gonzalez-Rosa et al., 2011, Schnabel et al., 2011). At 7 dpci PCNA$^+$ /GFP$^+$ doubly-positive cells were almost absent within the injury site (Fig. 26D, F).

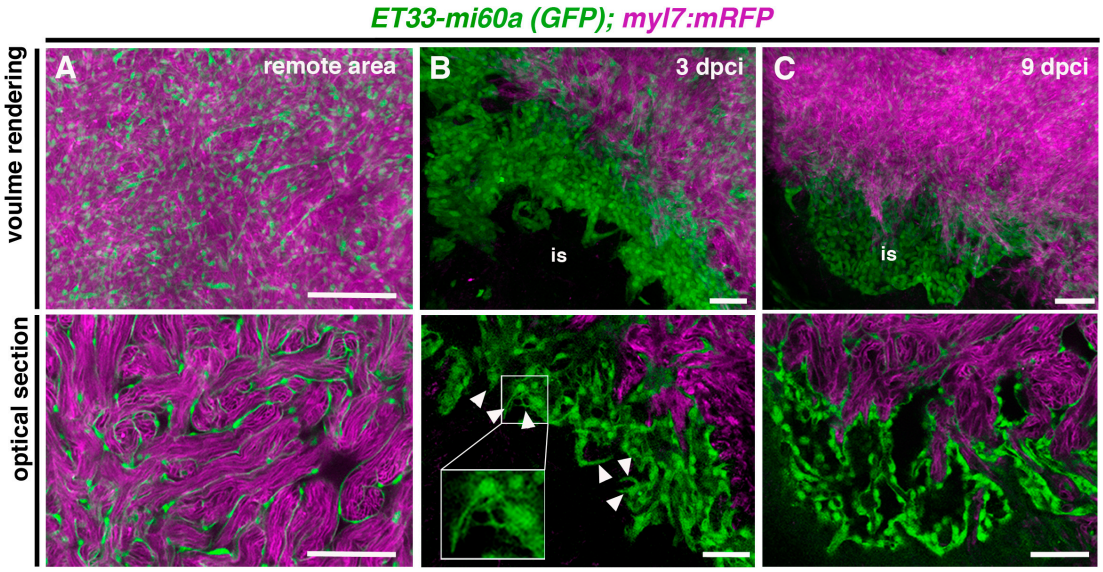

Figure 27: The endocardium organizes when regeneration proceeds.
A: Volume rendering and corresponding optical sections of a region of noninjured tissue in an *ET33mi-60A; myl7mRFP* heart. **B, C**: Volume rendering and corresponding optical sections of a part of the injury site from *ET33mi-60A; myl7mRFP* hearts at 3 dpci and 9 dpci. The endocardium is less organized, multi-layered and exhibits filopodia-like protrusions at 3 dpci. At 9 dpci the endocardium is organized and single-layered, without filopodia-like protrusions. (Scale bars: 80 μm)

To analyse endocardial cell morphology more in detail we performed 3D- imaging of the injured and remote region at higher magnification. Endocardial cells in the undamaged area of the heart surrounded clusters of cardiomyocytes and showed an elongated morphology (Fig. 27A) in contrast to the dense endocardial mesh in the injury site at 3 dpci (Fig. 24D, 27B). We observed a high abundance of filopodia-like protrusions at the outer front of the endocardial structure (Fig. 27B, arrowheads), suggesting that endocardial cells also migrate within the injured tissue at early stages. At 9 dpci GFP$^+$ cells remain at high density, however seemed to be organized (Fig. 27C). Only occasionally we detected filopodia-like endocardial cell protrusions and GFP$^+$ cells appeared as a single-cell layer, forming a homogenous GFP$^+$ endocardial structure within the injury site (Fig.

25A, 27C). Altogether these results indicate that endocardial cells heavily accumulate and expand within the injury site through proliferation at 3 dpci and presumably migration. These cells than organize and form an endocardial structure that occupies most of the injury site.

1.5. Endocardial cells surround inflammatory aggregates and are associated to collagen deposition

Beside the lack of cardiomyocytes the injury site displays densely packed nuclei with intense DAPI stain (Fig. 28A), a characteristic of apoptotic nuclei (Kulkarni & McCulloch, 1994). Previous studies demonstrated infiltration of the injury site by erythrocytes and leukocytes (Schnabel et al., 2011). Moreover endocardial cells in *ET33-mi60A* transgenic fish enclose cell clusters, including nuclei with high DAPI intensity at 3 dpci (Fig. 28A). We propose that these may be macrophages, removing cell debris from apoptotic cardiomyocytes. To prove this, we performed ISH against *l-plastin* a marker for macrophages in zebrafish (Herbomel, Thisse et al., 1999) in combination with immunohistochemistry against GFP in *ET33-mi60A* transgenic fish. We observed that single *l-plastin*$^{+}$ macrophages were attached to GFP^{+} endocardial cells (Fig. 28B, black arrowheads). Also we found aggregates of *l-plastin* expressing cells (red arrowheads) and cells with erythrocyte morphology (yellow asterisks) surrounded by a dense network of endocardial cells (Fig. 28B). The shape of these aggregates resample that of trabeculae, which are myocardial ridges overlaid by endocardial cells (Fig. 28B). This suggests that in an injured region in which cardiomyocytes die by apoptosis and their debris is removed by *l-plastin*$^{+}$ macrophages, spared endocardial cells remain, hold the injured tissue in place and may effect leukocyte adhesion and infiltration.

Moreover we detected the vascular cell adhesion molecule-1 (vcam1) expressed by GFP^{+} endocardial cells within the injury site in *ET33-1A* transgenic hearts (Fig. 28C). This adhesion molecule is induced by inflammatory cytokines and involved in leukocyte adhesion to endothelial cells (Wong & Dorovini-Zis, 1995). We also examined the spatial expression of *cathepsin Sb1* (*ctssb.1*), a protease-encoding gene that is rapidly activated upon cardiac injury in fish (Sleep, Boue et al., 2010) and mammals (Shalia, Mashru et al., 2012) in response to inflammatory signals (Cheng, Shi et al., 2012). Cathepsin S is expressed by cardiomyocytes, fibroblasts and macrophages within the infarct region and implicated in the regulation of ECM remodelling (Chen, Wang et al., 2013, Cheng et al., 2012). In the injured fish heart expression of *ctssb.1* is restricted to an area devoid of endocardial cells (Fig. 28D), suggesting that the presence of activated endocardial cells restricts the severity of tissue damage in the region bordering the undamaged tissue.

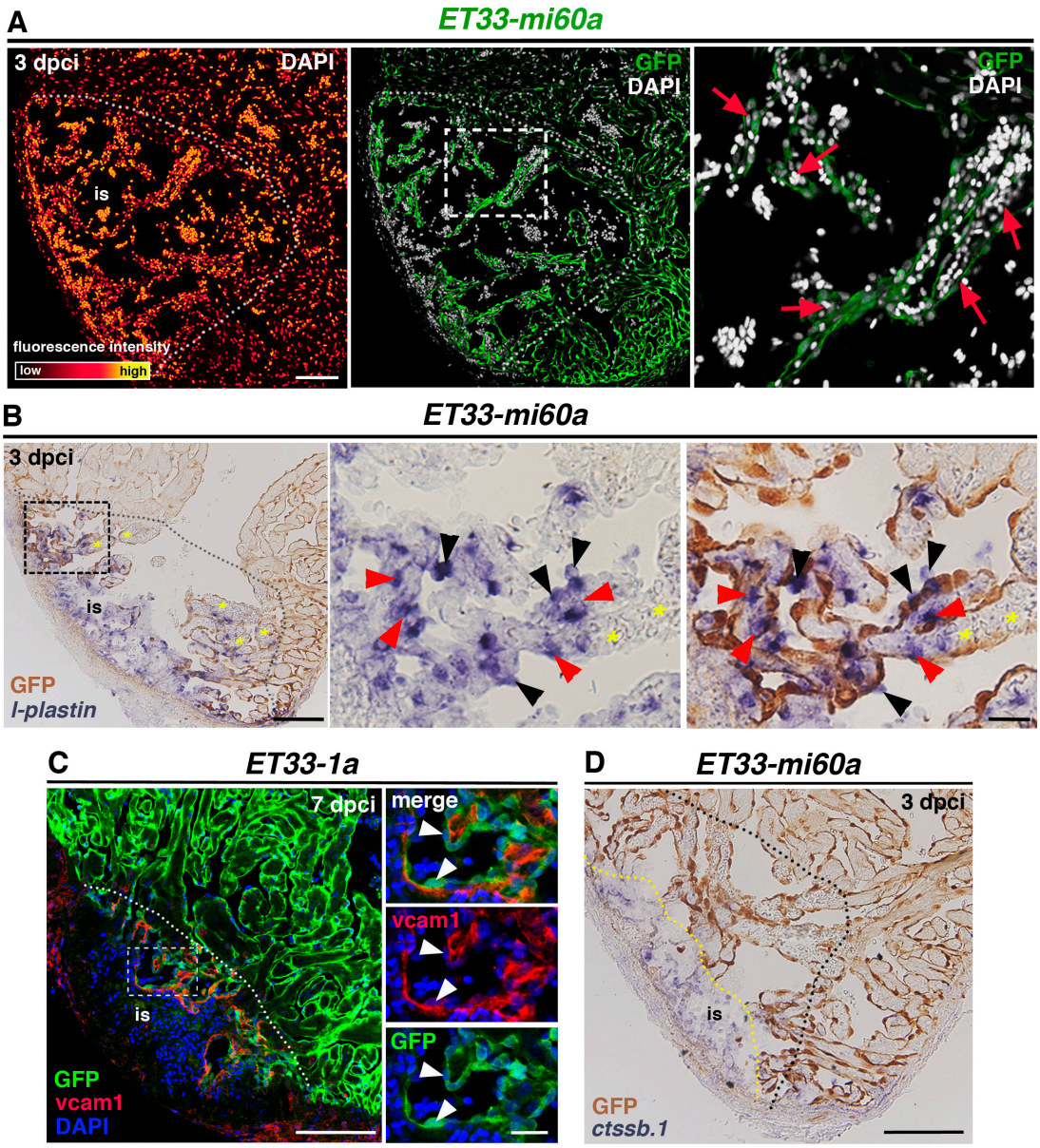

Figure 28: The endocardium surrounds inflammatory aggregates
A: Immunohistochemistry of GFP and DAPI on heart sections of *ET33-mi60A* fish at 3 dpci. The left panel shows strong pseudocoloured DAPI intensity within the injury site. GFP^+ cells surround cells with high DAPI intensity (red arrows in magnified view). **B**: *In situ* hybridization (ISH) against *l-plastin* combined with immunohistochemistry against GFP in *ET33-mi60A* transgenic hearts at 3 dpci. *l-plastin*$^+$ macrophages are enclosed by GFP^+ endocardial cells (red arrowheads) and attached to the endocardial layer (black arrowheads). Endocardial cells also enclose erythrocytes (yellow asterisks) and maintain the shape of trabecules. Boxed areas are magnified in the panels on the right; dotted lines delineate the injury site. **C:** Immunhistochemistry of vcam1 and GFP on *ET33-1A* transgenic fish show vcam1 expression in the endocardium in the injury site. **D**: ISH against *ctssb.1* combined with immunohistochemistry against GFP in *ET33-mi60A* transgenic hearts. *ctssb.1* is expressed in a region devoid of GFP^+ endocardial cells (delineated by the yellow dotted line) (Scale bars: 100 µm, magnified view 20 µm).

During the reparative phase cardiac tissue loss due to an ischemic injury is compensated by fibrotic tissue deposition in mammalian (Dobaczewski et al., 2010) and also in the zebrafish heart (Chablais & Jazwinska, 2012a, Gonzalez-Rosa et al., 2011, Schnabel et al., 2011). Strong collagen deposition is present after cryoinjury in the zebrafish heart at the inner injury border with a distribution reminiscent to endocardial morphology in this region (Fig. 29A, (Gonzalez-Rosa et al., 2011)). To test the possible association of collagen deposition with endocardial cells we performed immunohistochemistry against collagen 1 (col1) in cryoinjured *ET33-mi60a* transgenic hearts at 7 dpci. GFP^+ cells expressed or were associated to collagen1-expressing cells (Fig. 29B) and col1 follows the pattern of GFP^+ cells at the inner injury border (Fig. 29C). This suggests the involvement of the endocardium in the deposition of collagen at the inner injury border.

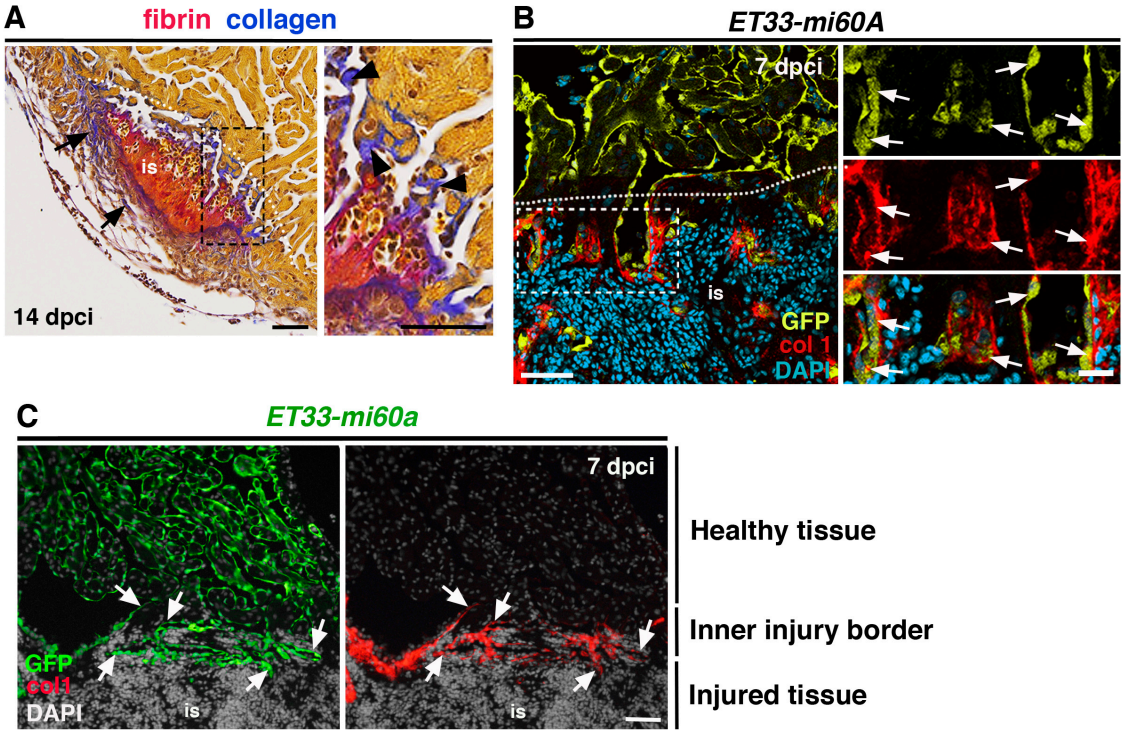

Figure 29: The endocardium is associated to fibrotic tissue.
A: Magnified view of the injury site (is) of an AFOG-stained heart section at 14 dpci. Collagen depositions (blue) are present in the outer, epicardial region of the injury site (arrows) and in the inner region (magnification of boxed area, arrowheads). **B**: Immunohistochemistry against collagen 1 (col1) and GFP on sections from *ET33-mi60a* transgenic hearts (7 dpci), showing that GFP^+ cells express col1 or are associated with $col1^+$ cells (arrows) in the injury site (is). Boxed areas are magnified in the right hand panels. **C**: Immunohistochemistry against GFP and col1 on sections of *ET33-mi60a* transgenic hearts (7 dpci), showing similar distribution of endocardial cells and col1 at the inner injury border (white arrowheads). (Dotted lines delineate the injury site, (is) Scale bars: A: 100 µm; B: l50 µm; C: 50 µm; magnified view B: 50 µm).

Taken together we observed that after cryoinjury spared endocardial cells remain in a region that lacks cardiomyocytes. They rapidly increase in number and preserve the outline of myocardial

trabeculae. However they enclose erythrocytes and leukocytes, which remove cell debris from apoptotic cardiomyocytes, and separate the injury site from undamaged tissue. In later stages (7 dpci) the organized endocardial structure serves as a scaffold for rapid and organized collagen deposition at the inner injury border and may facilitate cardiomyocyte entry.

2. Phenotypic analysis of Notch signalling modulation

2.1. Notch signalling is required for regeneration, cardiomyocyte proliferation but not endocardial cell proliferation

To study the function of Notch signalling during heart regeneration we preceded to perform functional experiments modulating Notch signalling activation. As described earlier, treatment with the γ-secretase inhibitor RO reduces Notch signalling activation in the regenerating fin and during embryonic development (Fig. 12). To attenuate Notch signalling in the regenerating heart we injected 30 µl of RO or DMSO-solution intraperitoneally.

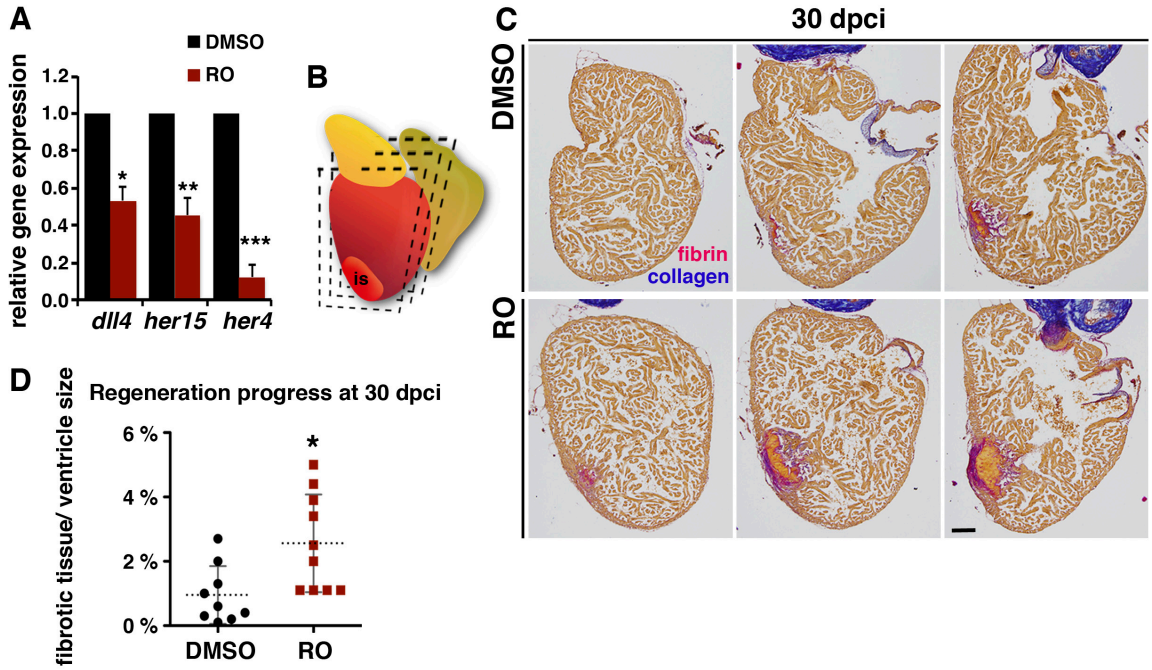

Figure 30: Notch signalling inhibition impairs heart regeneration
A: Relative gene expression (qPCR) of the Notch target genes *dll4*, *her15*, and *her4*, showing reduced expression after RO treatment. **B**: Scheme for analysis of AFOG–stained sections. The amount of fibrotic tissue was analysed in sections taken from different levels of the heart (injury site, is). **C**: Representative AFOG-stained sections from three levels of the same heart of a fish treated with DMSO or RO for 30 dpci. Cardiac muscle: brown; fibrin: pink/ orange; collagen: blue. **D**: Scatter plot showing the amount of fibrotic tissue relative to the ventricle size of hearts from fish treated with DMSO (n= 9) or RO (n=10) (discontinuous line = mean, **P*<0.05; ***P*<0.01; ***P< 0.005; scale bar: 100 µm).

Reduced mRNA levels of *dll4*, *her15* and *her6* indicated the downregulation of the pathway (Fig. 30A). To study the requirement for Notch activation during heart regeneration we treated fish for 30 dpci with RO or DMSO. The progress of regeneration was analysed by measuring the size of injured, fibrotic tissue (collagen fibrils and fibrin deposits) on acid-fuchsin-orange-G (AFOG)-stained serial sections of the ventricle (Fig. 30B). This analysis showed more fibrotic tissue in hearts after treatment with RO than with DMSO (Fig. 30C, D), indicating that long-term (30 dpci) Notch-inhibition impaired heart regeneration.

Notch signalling activation in stem- or progenitor cells regulates proliferation and/ or differentiation in various organ systems (Artavanis-Tsakonas et al., 1999). Thus, reduced cellular proliferation may be a possible cause of failing regeneration upon Notch signalling inhibition. During heart development endocardial Notch signalling also holds a non-cell autonomous role, regulating proliferation of adjacent cardiomyocytes (Grego-Bessa et al., 2007). This prompted us to analyse cellular proliferation in the endocardium but also myocardium following Notch signalling inhibition. We quantified BrdU incorporation by GFP^+ endocardial cells within and adjacent (50 μm) to the injury site in *E33-1A* transgenic fish at 3 dpci, however did not observe significant differences in endocardial cell proliferation upon Notch signalling inhibition (Fig. 31A, B). Next, we analysed cellular proliferation of $mef2^+$ cardiomyocytes in a 100 μm-wide region adjacent to the injury site at 7 dpci after two pulses of BrdU (5, 6 dpci). This is where the highest cardiomyocyte proliferation was reported (Bednarek, Gonzalez-Rosa et al., 2015, Sallin, de Preux Charles et al., 2014). The analysis revealed reduced BrdU- incorporation in cardiomyocytes in RO-treated hearts (Fig. 30C, D), suggesting that Notch signalling inhibition interferes with cardiomyocyte proliferation impairing heart regeneration.

2.2. Notch overactivation increases cardiomyocyte proliferation but impairs regeneration

To follow up these results we sought to perform complementary gain-of-function experiments using *Tg(hsp70l:Gal4);Tg(UAS:myc-notch1a-intra)* transgenic fish [here abbreviated as *Tg(UAS:NICD)*]. The functionality of the system in the heart was confirmed by the marked increase in transcript levels of the Notch targets *her4* and *her15* upon heat shock in *Tg(UAS:NICD)* hearts and immunohistochemistry against myc-NICD (Fig. 32A, B). We crossed *Tg(UAS:NICD)* transgenic fish with the myocardial reporter fish Tg(*myl7:GFP)* and applied heat shocks over 90 days. At this stage, zebrafish hearts exhibit little fibrotic tissue and the region lacking cardiomyocytes is minor, whereas at 130 dpci, regeneration is complete (Gonzalez-Rosa et al., 2011). Consistently, at 90 dpci the region, lacking cardiomyocytes, indicated by low GFP expression, was very small in control *Tg(myl7:GFP)* hearts (Fig. 32C). In contrast, the site of low GFP-expression in *Tg(UAS:NICD);Tg(myl7:GFP)* fish is still large (Fig. 32C), indicating impaired

cardiac regeneration. To confirm these results we analysed fibrotic tissue deposition on AFOG-stained sections at 33 dpci and 90 dpci.

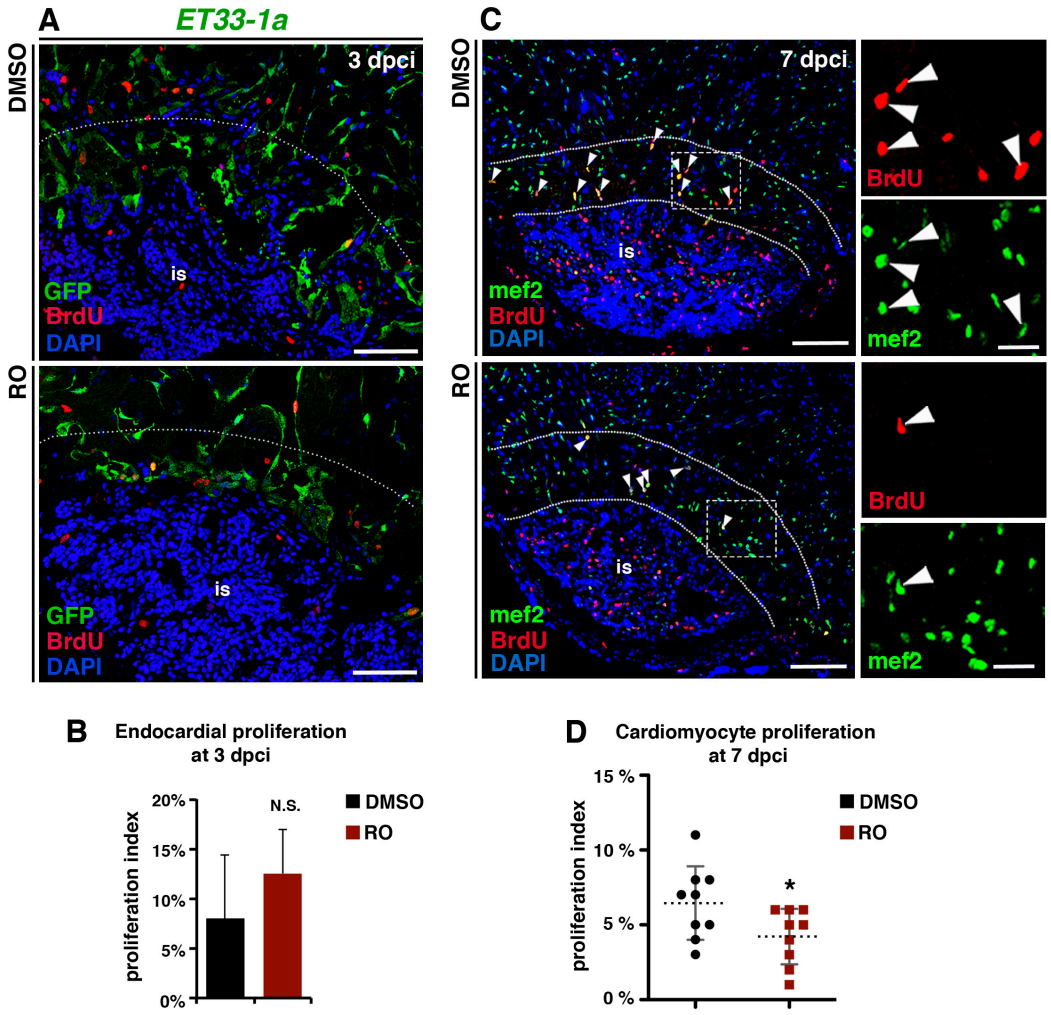

Figure 31: Notch signalling inhibition decreases proliferation in cardiomyocytes but not the endocardium
A: Immunohistochemistry against BrdU and GFP on heart sections of *ET33-1a* transgenic fish (3 dpci), showing BrdU incorporation by GFP^+ endocardial cells adjacent to the injury site (is). **B**: Quantification of $BrdU^+$:GFP^+ cell ratio in hearts of fish treated with DMSO (n= 4) or RO (n= 4), indicating no difference in endocardial cell proliferation between RO- and DMSO-treated hearts. **C**: Immunohistochemistry against BrdU and mef2 on heart sections (7 dpci), showing lower BrdU–incorporation in $mef2^+$ cells (white arrowheads) adjacent to the injury (between the dashed lines) after treatment with RO than after treatment with DMSO. **D**: Scatter plot showing quantification of $BrdU^+$ $mef2^+$ cells in DMSO- (n= 9) and RO-treated hearts (n= 9) (discontinuous line = mean; *P< 0.05, scale bar, 100 µm.)

However, fibrotic tissue abundance decreased in heat-shocked control fish until 90 dpci whereas *Tg(UAS:NICD)* transgenic hearts retained massive fibrotic tissue (Fig. 32E, F), confirming that long-term overactivation of the Notch pathway impairs heart regeneration. A more detailed

examination of the fibrotic tissue revealed that fibrin receded dramatically from 33 to 90 dpci in this region in WT hearts (Fig. 32G, H), whereas *Tg(UAS:NICD)* hearts maintained large amounts of fibrin at 90 dpci (Fig. 32G, H), suggesting that Notch overactivation impairs fibrin resorption.

Next we examined cell proliferation in our gain-of-function setting. Notch overactivation had no effect on endocardial cell proliferation at 3 dpci (Fig. 33A, B) but significantly increased the cell cycle entry of mef2^{+} injury-adjacent cardiomyocytes at 7 dpci (Fig. 33C, D). This result seemed to contrast to the previous observation that Notch signalling overactivation impairs regeneration. We then quantified mef2^{+} cells adjacent to the injury site and detected an increase in cardiomyocyte density in transgenic hearts comparing to control animals at 7 dpci (Fig. 34A, B). In line with this ISH for *heart- and neural crest derivatives-expressed protein 2* (*hand2*) and *homeobox protein NK-2 homolog E* (*nkx2.5*), two hallmark transcription factors of dedifferentiated cardiomyocytes (Lepilina et al., 2006), revealed an increase in dedifferentiated cardiomyocytes adjacent to the injury site in *Tg(UAS:NICD)* hearts (Fig. 34C, D).

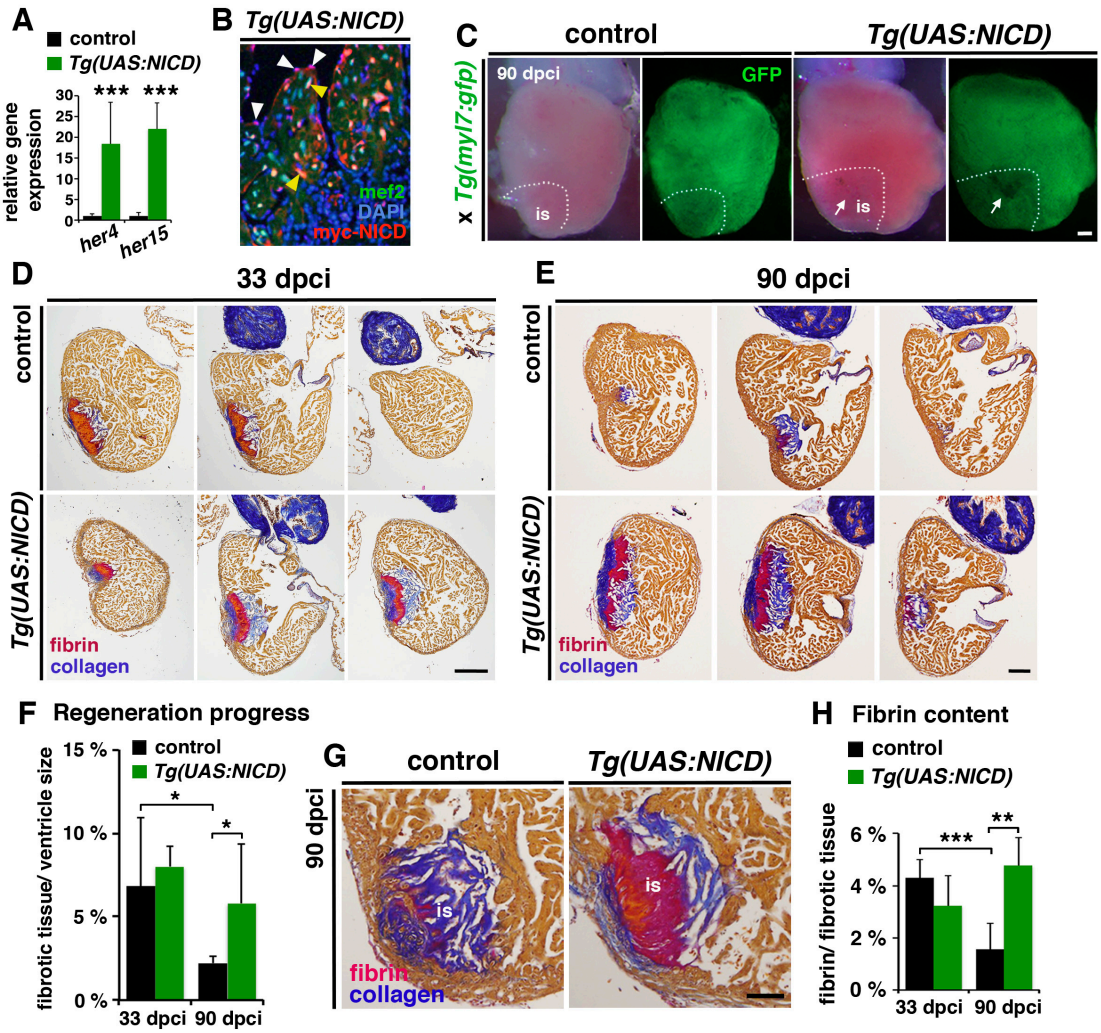

Figure 32: Notch signalling over activation impairs cardiac regeneration.
A: Relative gene expression (qRT-PCR) of *her4* and *her15*, showing increased expression in injured hearts of transgenic *Tg(UAS:NICD)* fish compared with the control at 3 dpci. **B**: Immunohistochemistry for mef2 and myc indicating myc-NICD expression in cardiomyocytes (yellow arrowhead) and endocardial cells (white arrowhead) in *Tg(UAS:NICD)* fish. **C**: Bright-field and green-filter views of whole-mount injured hearts (90 dpci) from crosses of *Tg(myl7:gfp)*-reporter fish with WT and *Tg(UAS:NICD)* fish. The injury site (is, dotted line) is smaller in control hearts and has stronger GFP expression, indicating more cardiomyocytes than in transgenic *Tg(UAS:NICD)* hearts. Arrows indicate the region devoid of GFP^+ cardiomyocytes. **D**: Three AFOG-stained sections of the same heart, either from control or *Tg(UAS:NICD)* fish, at 33 dpci do not show differences. **E**: Analysis of 3 AFOG–stained sections taken at different anatomical levels of the same control or *Tg(UAS:NICD)* heart at 90 dpci**,** showing the extent of fibrotic tissue. **F**: Quantification of the progress in regeneration at 33 dpci (control: n= 6; *Tg(UAS:NICD)*: n= 5) and 90 dpci (n= 5; n= 6). **G, H**: Analysis of fibrin content in the injury site (is). Magnified views of AFOG-stained heart sections of control and *Tg(UAS:NICD)* fish. Transgenic hearts show intense and extensive fibrin staining, contrasting with weak staining in control hearts. The bar chart shows fibrin content relative to the size of the IA at 33 (n=5; n=4) and 90 dpci (n=5; n=5). (Scale bars: C, D, E: 200 μm; G: 50 μm the dotted line defines the injury site; **P*<0.05; ***P*<0.01; ****P*<0.005).

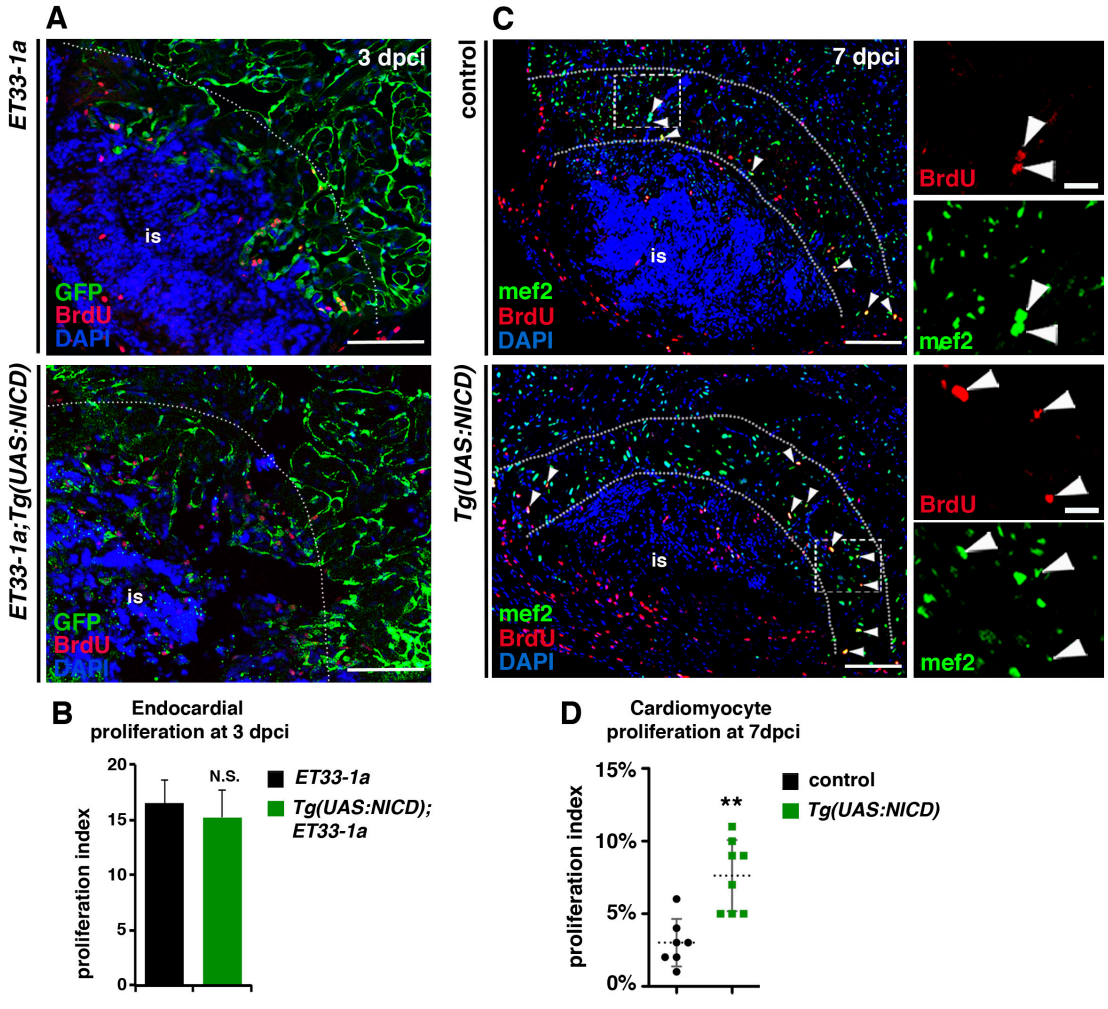

Figure 33: Notch signalling over activation increases proliferation in cardiomyocytes but not the endocardium.
A: Immunohistochemistry against BrdU and GFP on heart sections of *ET33-1a* transgenic fish alone or crossed with *Tg(UAS:NICD)* at 3 dpci showing BrdU incorporation by GFP^+ endocardial cells adjacent to the injury site (is). **B**: Quantification of $BrdU^+$:GFP^+ cell ratio in hearts in *ET33-1a* and *Tg(UAS:NICD); ET33-1a* transgenic fish, indicating no difference in endocardial cell proliferation. **C**: Immunohistochemistry against BrdU and mef2 on sections of control and *Tg(UAS:NICD)* transgenic hearts. White arrowheads indicate $mef2^+$/ $BrdU^+$ cardiomyocytes. **D**: The scatter plot in shows the higher percentage of $BrdU^+$ cardiomyocytes ($mef2^+$) at the injury border (between dotted lines) at 7 dpci in *Tg(UAS:NICD)* (n = 8) hearts than in control hearts (n= 7) (Scale bars: 100 μm; ***P*<0.01).

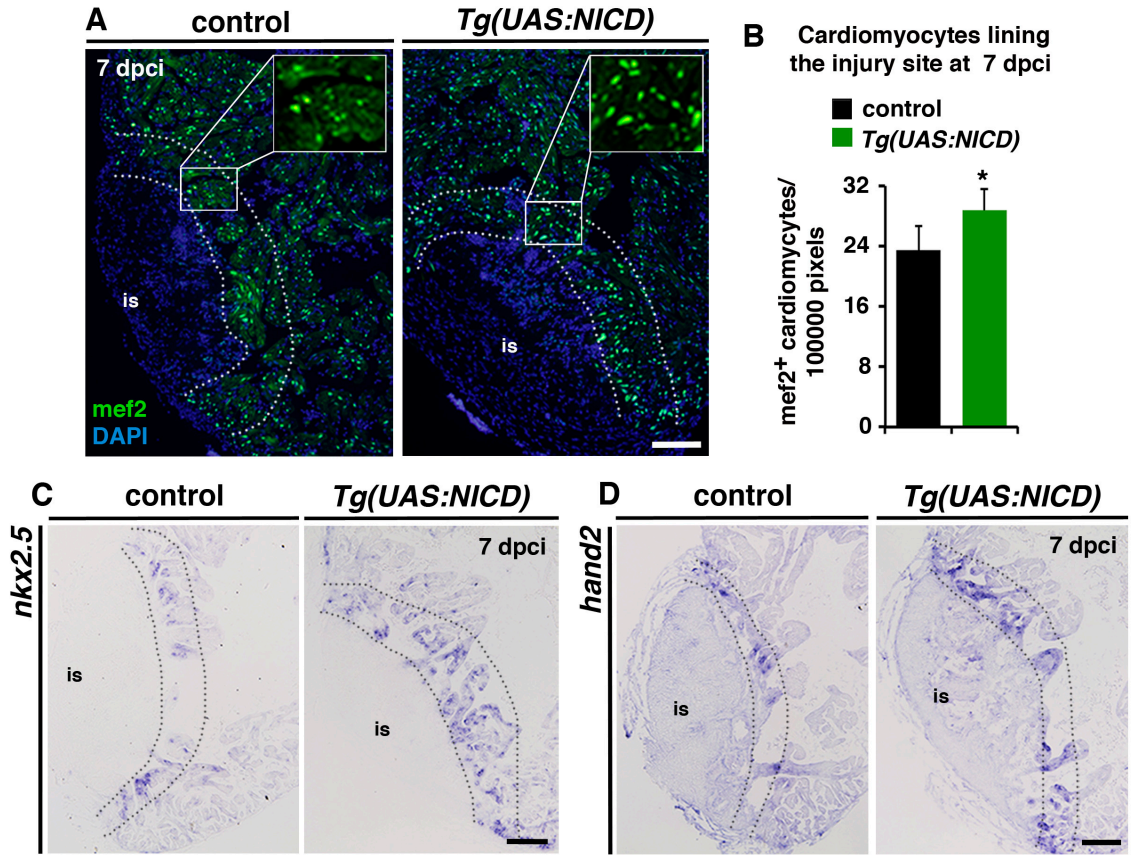

Figure 34: Notch signalling over activation results in cardiomyocyte accumulation adjacent to the injury.
A: Immunohistochemistry against mef2 on heart sections of control and *Tg(UAS:NICD)* fish at 7 dpci. **B**: Quantification of $mef2^+$ cardiomyocyte number relative to their area (between the dotted lines), indicating higher cardiomyocyte density at the injury border in *Tg(UAS:NICD)* hearts (n=5) than in the control hearts (n=4). **C, D**: ISH against *hand2* (n= 4) and *nkx2.5* (n= 3) at 7 dpci, showing higher numbers of cardiomyocytes expressing these genes at the injury border (between the dotted lines) in *Tg(UAS:NICD)* hearts than in the WT hearts. (Scale bars: 100 μm; **P<0.01).

2.3. Notch signalling inhibition interferes with endocardial organization

Although Notch signalling manipulation did not affect endocardial cell proliferation we sought to investigate on whether Notch signalling inhibition interferes with the expansion of the endocardium in the injury site. We quantified the relative volume of GFP^+ cells after RO or DMSO treatment for 5 dpci as described before (Fig. 7, 25). By using this method we did not detect significant differences on GFP^+ cell expansion in the injury site (Fig. 35A, B). However detailed morphological analysis revealed that endocardial cells are less organized in RO-treated comparing to control hearts at 5 dpci (Fig. 35C).

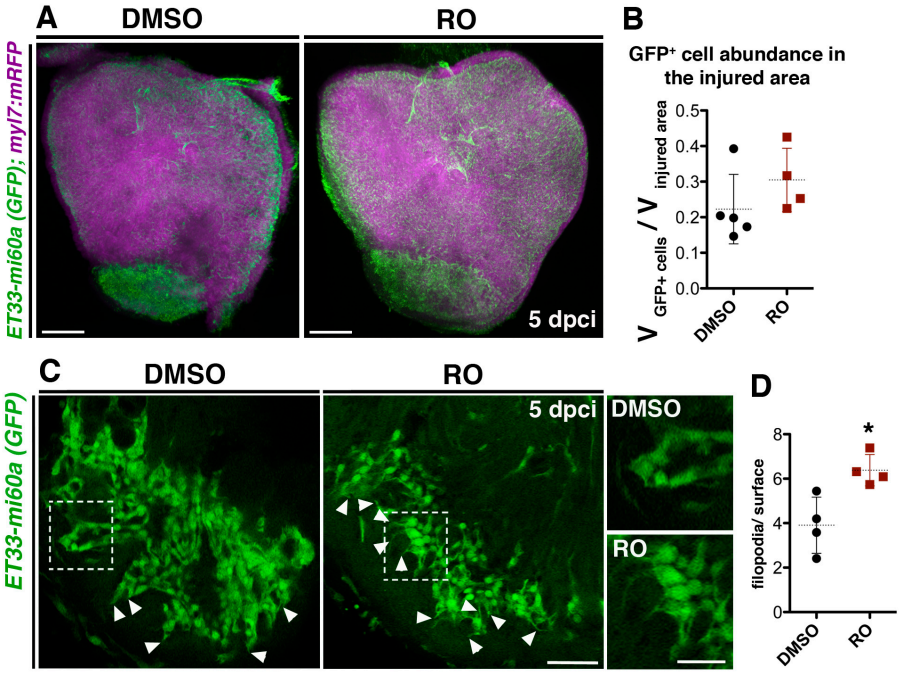

Figure 35: Endocardial organization requires Notch signalling activation.
A: Volume rendering of injured ventricles of *ET33mi-60A; myl7mRFP* hearts at 5 dpci, after DMSO or RO treatment for 4 dpci; endocardium in green and myocardium in magenta. **B**: Scatter plot presenting the relative volume of GFP^+ cells within the injury site in DMSO- and RO-treated fish. **C**: Optical sections of the injury site of DMSO- and RO-treated fish, showing impaired organization of endocardial cells and more filopodia-like protrusions (arrowheads) after RO-treatment. The boxed areas are magnified in the right hand panels. **D**: Scatter plot showing the number of filopodia-like protrusions on outer-front endocardial cells relative to the length of the front, which is increased after RO treatment. (Discontinuous line = mean, SD, $*P<0.05$; scale bars: A: 200 μm; C: 50 μm; magnified views: C: 25 μm).

One feature of poorly organized endocardial cells was the high abundance of cellular filopodia-like protrusions at the outer front of the endocardium (Fig. 27). We quantified those filopodia-like protrusions in hearts treated with RO and DMSO. In control, DMSO-treated hearts the number of filopodia was low at this stage (5 dpci, Fig. 35C, D). However we noticed a higher abundance of

filopodia in hearts with attenuated Notch signalling (Fig. 35C, D), suggesting that Notch is required for the organization of the endocardium.

3. Molecular changes in the regenerating heart upon Notch signalling inhibition

3.1. Decreased Notch signalling affects cardiovascular system and wound healing processes

To study the molecular changes resulting from Notch abrogation in the cryoinjured heart, we intraperitoneally injected RO into fish once a day for two days, and then dissected the ventricle adjacent to the injury site at 3 dpci (Fig. 36A) for RNA extraction and sequencing. RNA-seq analysis identified 347 genes differentially expressed between RO- and DMSO-treated fish, 196 of them upregulated and 151 downregulated (Fig. 36B, see Supplementary Table 1). An Ingenuity-based gene ontology (GO) classification revealed that Notch signalling inhibition affects genes involved in various endothelial cell related processes (Fig. 36C, D). This is not surprising, as Notch signalling is crucial for angiogenesis during development and in the adult (Herbert & Stainier, 2011). However, this also points to a function for Notch in endocardial cells, as they are specialized endothelial cells. Further, genes required in the cardiovascular system but also genes related to wound healing appeared deregulated (Fig. 36C, D). Altered cardiovascular system genes include genes involved in cardiovascular development and angiogenesis and genes implicated in heart disease and cardiac hypertrophy (Fig. 36C, D). The RNA-seq analysis also identified genes involved in the inflammatory response, fibrosis, and fibroblast proliferation (Fig. 36C, D). The GO assignments of differentially expressed genes to categories related to endothelial cells, the cardiovascular system or wound healing are indicated in Fig. 36D. The data obtained from our phenotypic analysis after Notch signalling manipulation let us focus on endothelial/ endocardial genes; genes related to inflammation, ECM remodelling and myocardial genes. We analysed temporal and spatial expression of a subset of these genes and examined the effect of Notch signalling manipulation at 3 or 7 dpci.

3.2. Notch signalling inhibition affects developmental and injury related endocardial/ endothelial gene expression

RNAseq analysis revealed that Notch inhibition affects the expression of multiple endothelial/endocardial genes (Fig. 36D, 37A). Compromised Notch signalling abrogates the expression of a subset of genes involved in the regulation of angiogenesis (*sprouty2*, *vgfc*, *id1*, *ephrinb2a*, *egr1*), endothelial integrity (*claudin5b*, *heg*) and endothelial cell differentiation (*klf2a*, *klf2b*) (Fig. 37A).

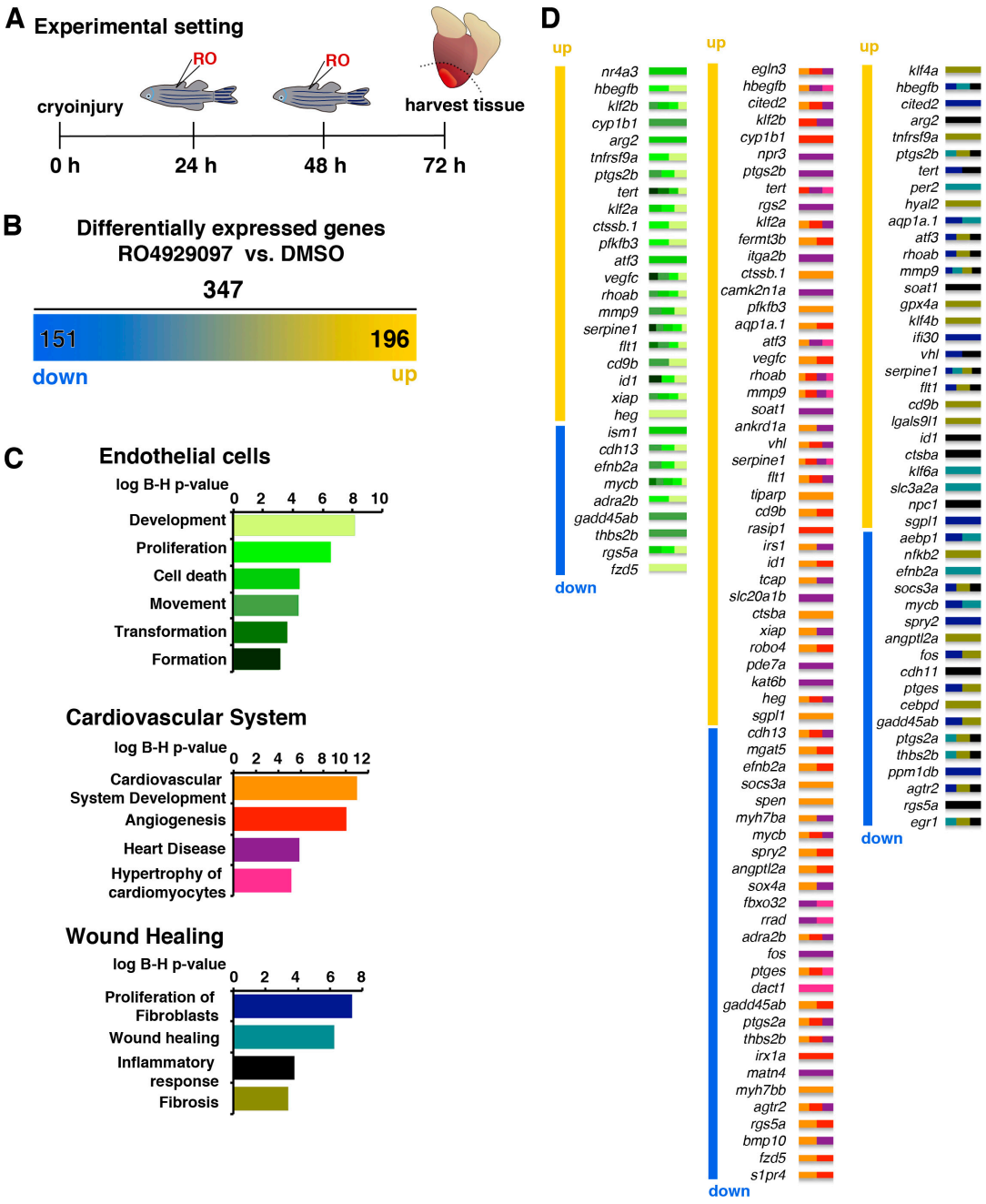

Figure 36: RNA-sequencing analysis

A: Experimental scheme for RO-injection and RNA-extraction. RNA was extracted from the ventricular apex (below the dotted line) at 72 hpci (3 dpci). **B**: RNA-sequencing results: 347 genes are differentially expressed in injured hearts after RO treatment (fold change > 0.5; $P<0.05$), with 196 upregulated (yellow) and 151 downregulated (blue). **C**: Ingenuity-based RNA-sequencing data analysis. The charts represent selected Ingenuity categories affected in our analysis. These are represented in three groups: Endothelial cells, Cardiovascular System, and Wound Healing. **D**: Genes assigned to the three categories in **C**. Genes are ordered according to their level of differential expression (upregulated upon RO-treatment, yellow; downregulated, blue). The colour of small bars indicates the assigned Ingenuity categories (presented in the chart in **C**).

Some of these genes are also implicated during heart development (*klf2a*, *ephrinb2a*, *egr1*, *spry2*, *heg*, *bmp10*) (Banjo, Grajcarek et al., 2013, Grego-Bessa et al., 2007, Mably, Mohideen et al., 2003, Vermot et al., 2009). *Ephrinb2a*, a known notch target in endothelial (Krebs, Xue et al., 2000) and endocardial cells (Grego-Bessa et al., 2007) is downregulated in the RNAseq (Fig. 37A) confirming the downregulation of the Notch pathway. ISH for *ephrinb2a* showed endocardial expression in the ventricle but not specifically at the injury site (Fig. 37B). *Bmp10* expression also decreased upon Notch signalling inhibition (Fig. 37A), consistent with its positive regulation by Notch during chamber development (Grego-Bessa et al., 2007). However, endocardial gene expression of *bmp10* in the zebrafish heart is not specific to the injury but also present throughout the whole ventricle and in the uninjured heart (Fig. 37C), indicating its implication during homeostatic growth of the heart. ISH localized *inhibitor of DNA binding 1* (*id1*), the *vascular endothelial growth factor c* (*vegfc*) and early *growth response factor 1* (*egr1*) to the inner injury border (Fig. 37 D, E, F) and cell morphology suggested that *id1* and *egr1* may be expressed in endocardial cells (Fig. 37D, F). The expression of *egr1* decreased upon Notch signalling inhibition (Fig. 37A). Egr1 is implicated in endothelial cells upon vascular injury, regulating pro-angiogenic genes (Fahmy, Dass et al., 2003, Khachigian, Lindner et al., 1996) but is also expressed in endocardial cells during zebrafish valve development (Banjo et al., 2013). mRNA levels of *krüppel-like transcription factor 6* (k*lf6*) were increased upon Notch signalling inhibition, revealed by RNAseq analysis (Fig. 37A). Klf6 is a key endothelial transcription factor during vascular injury and remodelling (Atkins & Jain, 2007, Garrido-Martin, Blanco et al., 2013). ISH for *klf6* combined with immunohistochemistry against GFP in *ET33-mi60a* transgenic fish indicated *klf6* expression by endocardial cells at the injury site, suggesting its implication in the injury response of the endocardium.

Three other endocardial genes, *heart of glass* (*heg)* and *krüppel like factor 2a and b* (*klf2a, klf2b*) and their target *aquaporin 1a.1* (*aqp1a.1*; (Dekker, van Soest et al., 2002)) were upregulated upon Notch signalling inhibition (Fig. 37A). *heg* is important for endothelial/endocardial integrity (Kleaveland, Zheng et al., 2009) and regulates the concentric growth of the zebrafish myocardium (Mably et al., 2003). *Klf2* expression is induced by shear forces in the endothelium and is related to a stretched, less migratory, differentiated phenotype in endothelial cells (Dekker, Boon et al., 2006, Dekker et al., 2002). *Heg* and *klf2a* are expressed in endocardial cells surrounding injury-adjacent cardiomyocytes (Fig. 38A) consistent with previous reports about *heg* expression in the resected heart (Kikuchi et al., 2011b). This pattern overlaps with *notch1b* expression adjacent to the injured tissue but not in rounded dense endocardial cells within the injury site (Fig. 38A), suggesting that *heg*- and *klf2a*- expression characterizes a different endocardial cell population adjacent to the injury. Analysis by qPCR confirmed that Notch signalling inhibition increases the expression of *klf2a* and *klf2b* (Fig. 38B).

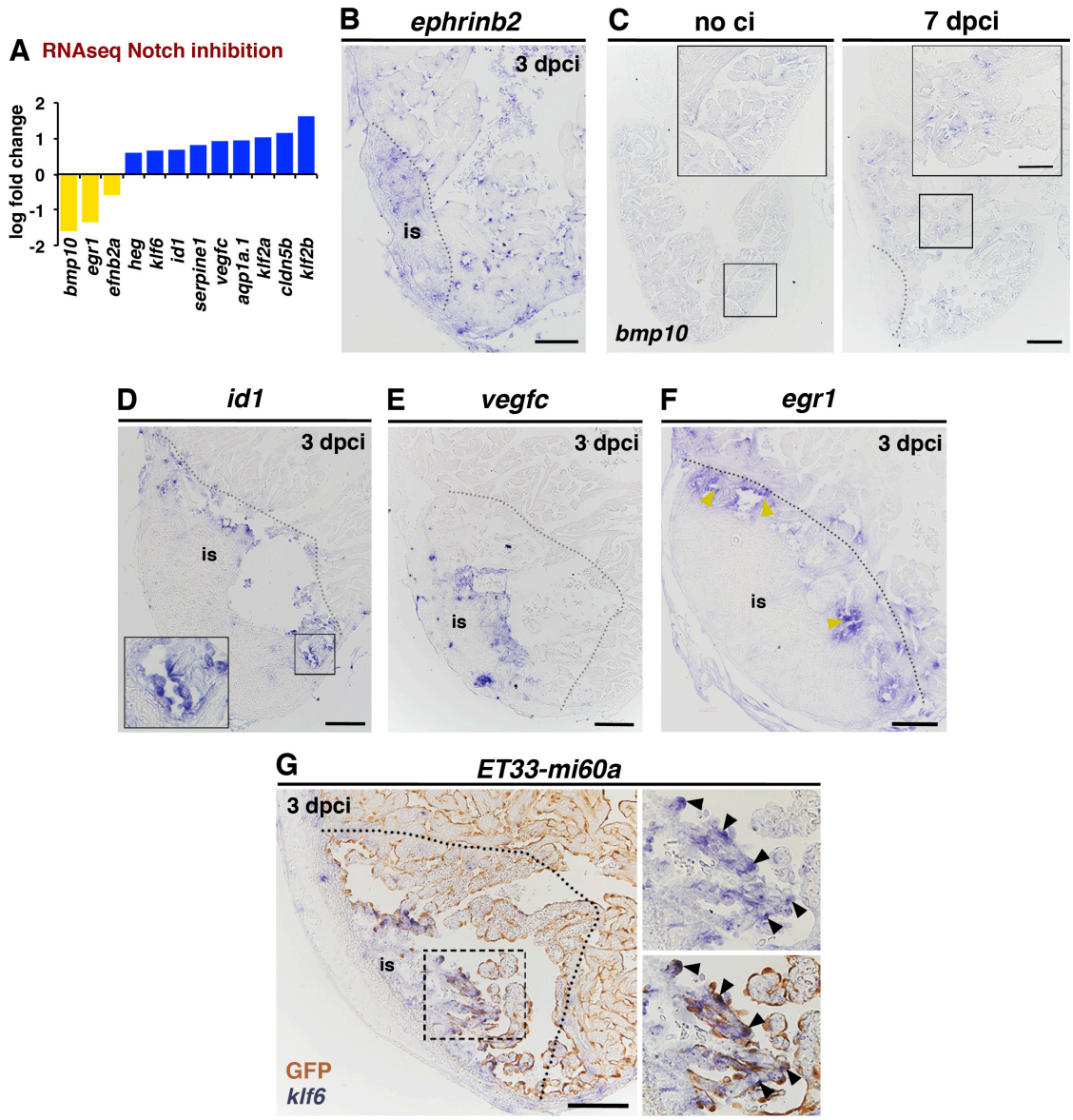

Figure 37: Differential regulation of endocardial genes by Notch signalling
A: RNA-seq analysis. Representation of differential cardiac expression of endothelial genes at 3 dpci between fish treated with RO or DMSO (experimental scheme in Fig 36A). **B**: ISH of *ephrinb2* in regenerating hearts. **C**: ISH of *bmp10* in a non injured and regenerating heart, showing expression throughout the ventricle (no ci, 7 dpci). **D**: ISH of *id1*, showing expression at the inner injury border at 3 dpci. **E**: ISH of *vegfc*, indicating gene expression at the inner injury border. **F**: ISH against *egr1*, showing expression in endocardial cells within the injury site (black arrowheads). **G**: ISH against *klf6* combined with immunohistochemistry against GFP in *ET33mi-60A* transgenic hearts. *klf6* coincides with GFP expression in endocardial cells (arrowheads) (Scale bars: G: 100 µm).

Moreover ISH for *klf2a* and *klf2b* in hearts following RO or DMSO treatment suggested that Notch signalling prevents the expansion of *klf2a* expression within the ventricle (Fig. 38C). However this effect was less pronounced on *klf2b*, whose expression is increased adjacent to the injury site upon

Notch inhibition (Fig. 38D). Temporal gene expression analysis in wild-type hearts by ISH indicated an early upregulation of *heg* in presumably endocardial cells adjacent to the injury site at 36 hpci (Fig. 38E).

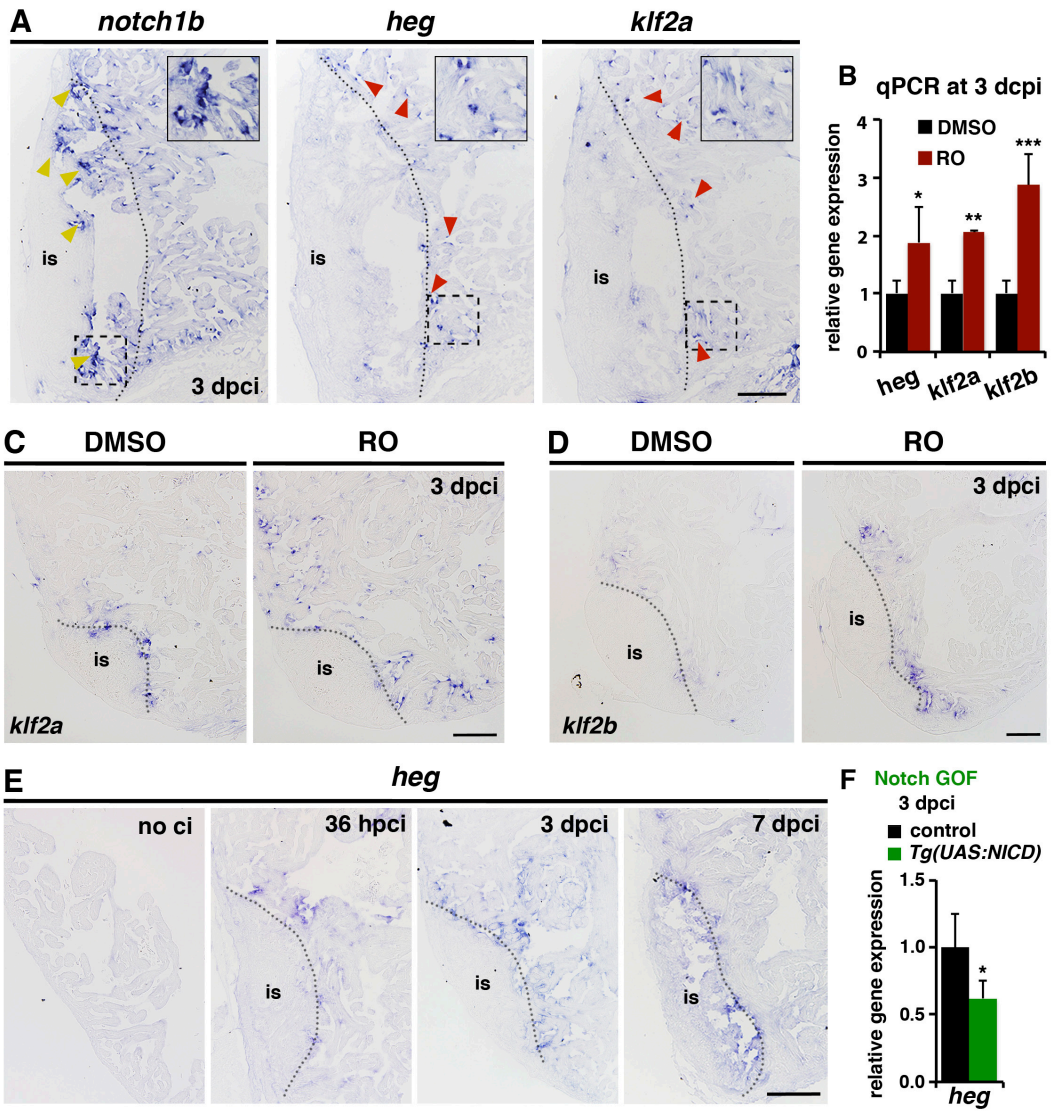

Figure 38: Notch inhibition affects *klf2a*, *klf2b* and *heg* expression.
A: ISH against *notch1b*, *heg* and *klf2a* on consecutive sections of the same heart. *Heg* and *klf2a* are expressed in endocardial cells surrounding cardiomyocytes in the healthy area adjacent to the injured tissue (red arrowheads), where *notch1b* expression is scattered. *Notch1b* expression is activated in more cells within the injury site (yellow arrowheads). Boxed areas are magnified in inserts. **B**: qRT-PCR analysis of *heg*, *klf2a* and *klf2b* expression in the injured heart at 3 dpci upon RO-treatment. **C:** ISH against *klf2a* shows more cells expressing *klf2a* after treatment with RO but not in DMSO-treated hearts. **D**: ISH against *klf2b* shows increased expression in RO- but not in DMSO-treated hearts. **E**: Time lapse of *heg* expression in the cryoinjured heart showing *heg* expression in endocardial cells lining injury adjacent cardiomyocytes from 36 hpci. **F**: qRT-PCR analysis of *heg* mRNA shows decreased expression upon Notch overactivation. (SD, * $P< 0.05$; ** $P<0.01$, ** $P<0.005$; scale bars: 100 μm).

Expression was sustained in this region as mentioned before at 3 dpci but less evident at 7 dpci (Fig. 38E). qPCR analysis confirmed the upregulation of *heg* mRNA levels upon Notch signalling inhibition (Fig. 38B) and the overactivation of the pathway could reduce *heg* expression at 3 dpci (Fig. 38F). This suggests that *heg* is expressed early after cryoinjury but may be restricted by Notch at later regeneration stages in endocardial cells adjacent to the injury site.

Another gene that was upregulated upon Notch signalling inhibition was the *plasminogen activator inhibitor-1* (*serpine1*) (Fig. 37A). It caught our attention because of its dual role in endothelial cells. Serpine1 promotes endothelial cell migration promoting angiogenesis (Isogai, Laug et al., 2001). In addition secreted Serpine1 is the main physiological inhibitor of urokinase plasminogen activator (uPA) and tissue plasminogen activator (tPA) and thus inhibits fibrinolysis (Declerck & Gils, 2013). To localize *serpine1* expression in the injured heart we performed ISH on *ET33-mi60A* heart sections combined with immunostaining for GFP. We found strong *serpine1* expression in GFP^+ endocardial cells in the injury site at 3 dpci (Fig. 39A). qPCR analysis revealed strong *serpine1*- expression levels at 36 hpci and 3 dpci, with expression declining at 7 dpci (Fig. 39B). This suggests that *serpine1* is an early injury responding gene and may initiate endocardial cell migration. ISH at later stages confirmed our qPCR results and showed reduced *serpine1* mRNA at 7 dpci and almost undetectable levels at 14 dpci (Fig. 39D). Comparing *notch1b* and *serpine1* expression pattern on transverse consecutive sections of injured hearts revealed that *serpine1* expressing cells are located presumably around dying cardiomyocytes (Fig. 39E) at the inner injury border at 3 dpci, in contrast to *notch1b* that showed strong expression in cells at the outer front of the endocardium facing the fibrotic tissue (Fig. 39E). qPCR gene expression analysis of *serpine1* revealed increased expression upon Notch signalling inhibition at 3 and 7 dpci, confirming the RNAseq results (Fig. 39C). Thus timely and local gene expression analysis let suggest that *serpine1* is activated early after cryoinjury in the endocardium, but may be restricted by Notch at later time points.

In summary, gene expression profiling after Notch inhibition revealed the expression of wound-related and endocardial/endothelial genes after cryoinjury. The spatial distribution of transcripts highlights the heterogeneity of endocardial cells in different regions surrounding and within the injury site. Loss-of-function gene expression analysis suggests that Notch negatively regulates genes involved in endocardial integrity (*heg*, *claudin5b*) and differentiation (*klf2a*, *klf2b*) and also restricts the expression of genes involved in endocardial migration (*serpine1*).

3.3. Notch signalling inhibition affects early-growth and sarcomere assembly genes

As Notch signalling manipulation affected cardiomyocyte proliferation we analysed myocardial genes that were differentially regulated in our RNA-seq analysis (Fig. 40A).

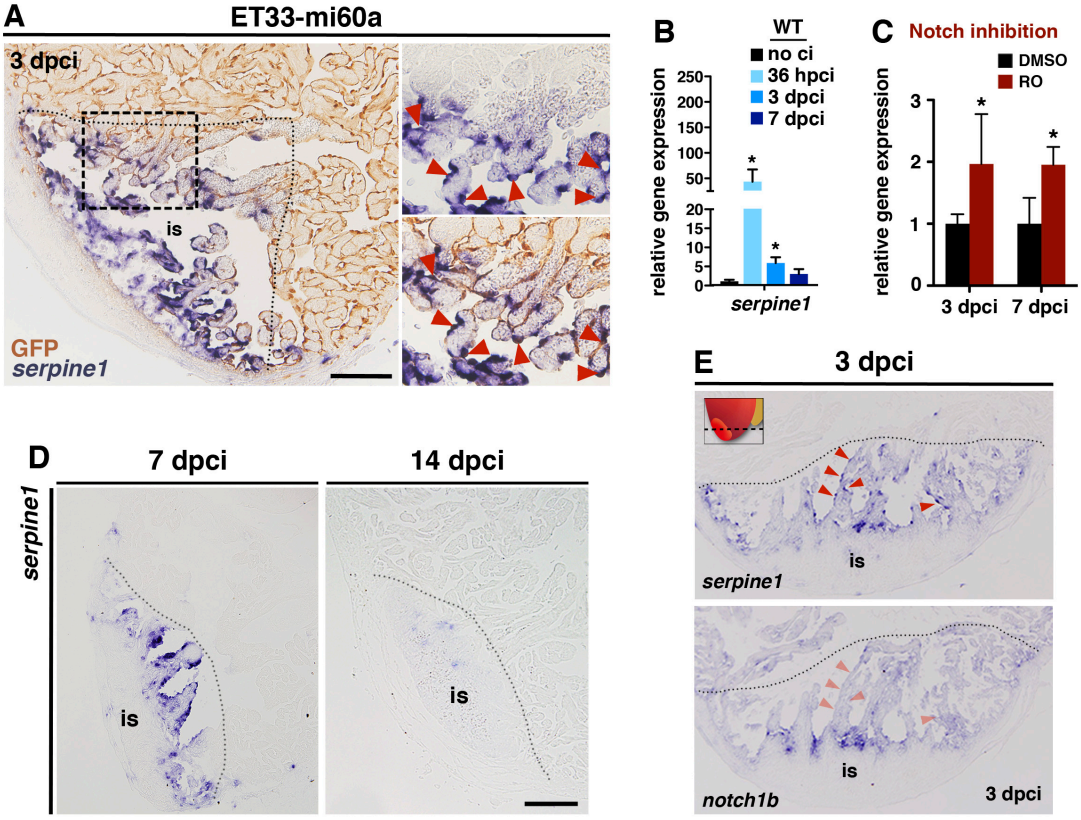

Figure 39: Notch inhibition affects *serpine1* expression
A: ISH against *serpine1* and immunohistochemistry against GFP in *ET33-mi60A* transgenic hearts, indicating *serpine1* expression in the endocardium (red arrowheads). Boxed areas are magnified in the right hand panels. **B**: qPCR analysis of *serpine1* in WT hearts with no cryoinjury (no ci), at 36 hpci and at 3 and 7 dpci (SD, * $P< 0.05$). **C**: qRT-PCR analysis showing increased *serpine1* mRNA levels in injured ventricles at 3 and 7 dpci after RO-treatment compared with DMSO-treated fish. **D**: ISH against *serpine1*, showing moderate expression at 7 dpci but almost no expression at 14 dpci. **E**: ISH against *serpine1* and *notch1b* on consecutive transversal sections. *Serpine1* is expressed in endocardial cells closer to the lumen of the heart (red arrowheads), whereas *notch1b* expression is higher in the endocardial front facing the fibrotic tissue. (*P< 0.05, dotted lines delineate the injury site = is, scale bars: 100 µm)

Myocardial proliferation has been related to dedifferentiation of cardiomyocytes indicated by embryonic transcription factor expression such as *gata4*, *nkx2.5* and *hand2* (Jopling et al., 2010, Kikuchi et al., 2010, Lepilina et al., 2006). Our RNA-seq data revealed differential gene expression of genes encoding different classes of proteins that characterize the cardiomyocyte differentiation state, including transcription factors, activating enzymes, and structural proteins (Fig. 40A). The identified genes included the immediate-early cardiac growth genes: *avian myelocytomatosis viral oncogene homolog b* (*myc-b*) and *activating transcription factor 3* (*atf3*) (Giraldo, Barrett et al., 2012, MacLellan & Schneider, 2000).

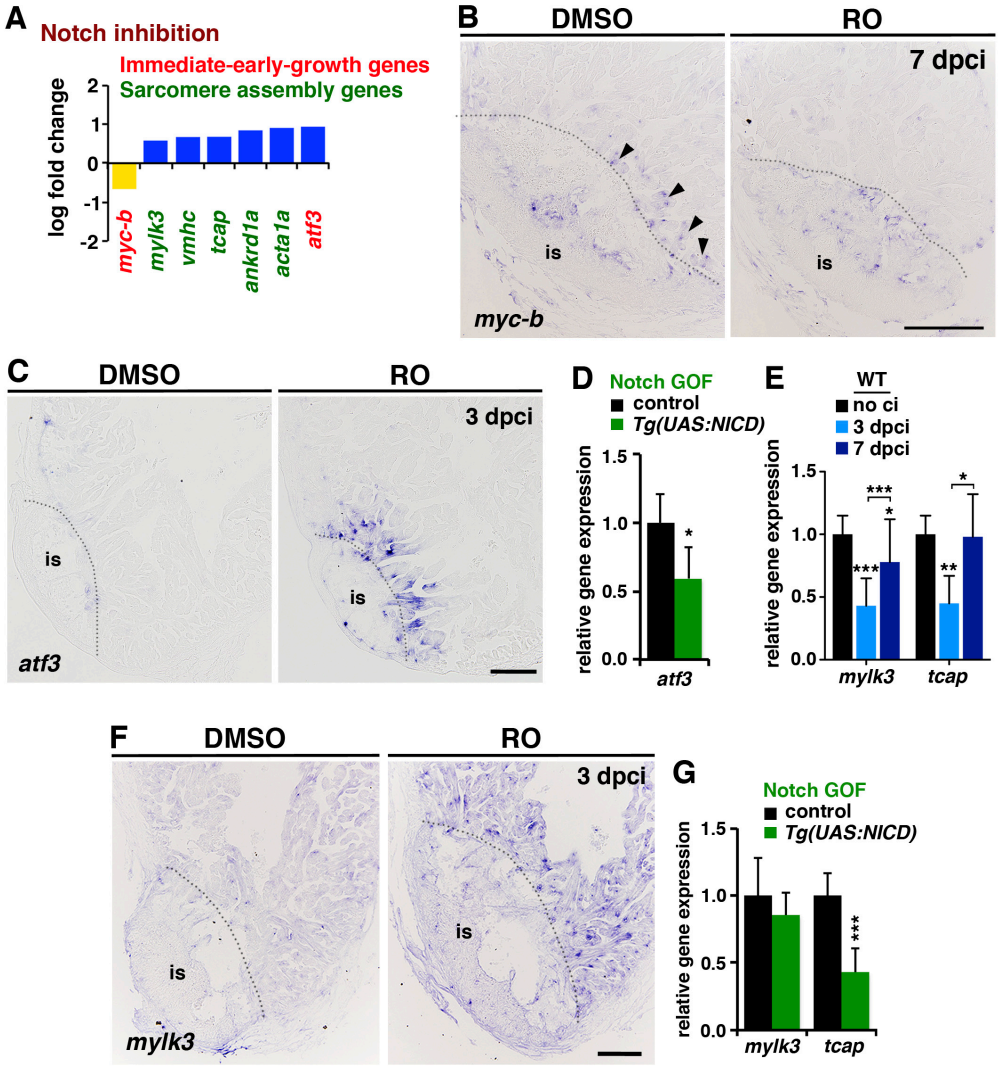

Figure 40: Notch signalling blockage affects immediate-early growth genes and sarcomere assembly genes.
A: RNA-seq analysis. Representation of the differential cardiac expression of genes related to cardiomyocyte differentiation between fish treated with RO or DMSO at 3 dpci. **B**: ISH against *myc-b* (3 dpci), showing expression in injury-adjacent cardiomyocytes (arrowheads) in DMSO- but not RO-treated hearts (asterisks). **C**: ISH against *atf3* (3 dpci), showing increased expression adjacent to the injury site in RO-treated hearts. **D**: Relative *atf3* gene expression (qPCR) in *Tg(UAS:NICD)* transgenic and control ventricles at 3 dpci. **E**: qPCR analysis of *mylk* and *tcap* genes in WT hearts with no cryoinjury (no ci) and at 3 and 7 dpci. **F**: ISH against *mylk3* (3 dpci), showing increased expression in cardiomyocytes in hearts treated with RO. **G**: Gene expression levels (qRT-PCR) of *mylk3* and *tcap* in control and *Tg(UAS:NICD)* ventricles at 3 dpci. (* $P< 0.05$; ** $P<0.01$, ** $P<0.005$*, dotted lines delineate the injury site = is, scale bars: 100 μm)

Recent findings demonstrate that dedifferentiated, proliferating cardiomyocytes express *myc-a* and *myc-b* (Aguirre, Montserrat et al., 2014). Notch signalling inhibition decreased the levels of *myc-b* in wound adjacent cardiomyocytes (Fig. 40B), indicated by ISH and confirming the RNA-seq data.

Changes in *myc-b* expression may be associated with the decrease in cardiomyocyte proliferation (Fig. 31C, D). In contrast *atf3* expression in injury adjacent cardiomyocytes was enhanced after RO-treatment (Fig. 40A, C) and concomitantly Notch signalling overactivation reduced *atf3* expression (Fig. 40D). The opposite regulation of this gene by Notch might be related to its role as a negative feedback regulator of other immediate-early cardiac growth genes (Giraldo et al., 2012). Moreover numerous genes, encoding proteins that contribute to sarcomere assembly and function were upregulated upon Notch signalling inhibition (Fig. 40A). They include: *cardiac specific myosin light chain kinase 3* (*mylk3*) (Seguchi, Takashima et al., 2007), *alpha skeletal actin* (*acta1a*), *ventricular myosin heavy chain* (*vmhc*), *tintin-cap* (*tcap*) (Gregorio, Trombitas et al., 1998) and the transcriptional regulator of sarcomeric proteins *ankyrin repeat domain 1a* (*ankrd1a*) (Chen, Zhong et al., 2012). Dedifferentiating cardiomyocytes need to disassemble the sarcomere in order for cell division to proceed (Jopling et al., 2010, Porrello et al., 2011), and high levels of sarcomeric proteins are characteristic of differentiated cardiomyocytes (O'Meara, Wamstad et al., 2015). Timely qPCR gene expression analysis revealed decreased levels of *mylk3* and *tcap* expression at 3 dpci, when cardiomyocyte proliferation initiates (Bednarek et al., 2015, Schnabel et al., 2011), comparing to non-injured hearts. However gene expression was restored at 7 dpci (Fig. 40E). ISH indicated weak myocardial expression of *mylk3* at 3 dpci but increased expression in RO-treated hearts (Fig. 40F), confirming the RNA-seq data. We also observed that *tcap* expression was decreased by Notch overactivation in *Tg(UAS:NICD)*-transgenic hearts (Fig. 40G).

Our results thus show that cryoinjury in zebrafish induces immediate-early growth genes and downregulates expression of sarcomere-assembly genes. These two features of cardiomyocyte dedifferentiation are required for cardiomyocyte proliferation and are perturbed upon Notch signalling inhibition.

3.4. Notch signalling impacts extracellular matrix gene expression

The impaired degradation of the fibrotic tissue upon long-term Notch pathway overactivation (Fig. 30, 32) prompted us to investigate the impact of Notch signalling inhibition on genes involved in extracellular matrix remodelling. We analysed their temporal and spatial expression as little is known about ECM gene activation upon cryoinjury. The RNA-seq data revealed that Notch inhibition leads to increased transcription of *hyaluronidase-2* (*hyal2*), the enzyme that degrades hyaluronan (Chowdhury, Hemming et al., 2013) and of *matrix-metalloprotease 9* (*mmp9*), which cleaves several collagens and gelatines and is linked to heart failure in mammals (Spinale, Coker et al., 2000) (Fig. 41A). Notch inhibition further increased expression of two cathepsins (*ctsba*, *ctssb.1*; Fig. 41A), proteases that degrade extracellular matrix molecules and are expressed after cardiac injury in mammals and fish (Shalia et al., 2012, Sleep et al., 2010). ISH localized *mmp9* and *ctssb.1* expression at the inner injury border at 36 hpci (Fig. 41B), a time point when *notch1b*

expression was still low (Fig. 41B). qPCR analysis confirmed maximal protease gene expression levels very early after cryoinjury in wild-type hearts (36 hpci), with levels declining thereafter (3 dpci) to reach near-baseline levels at 7 dpci (Fig. 41C).

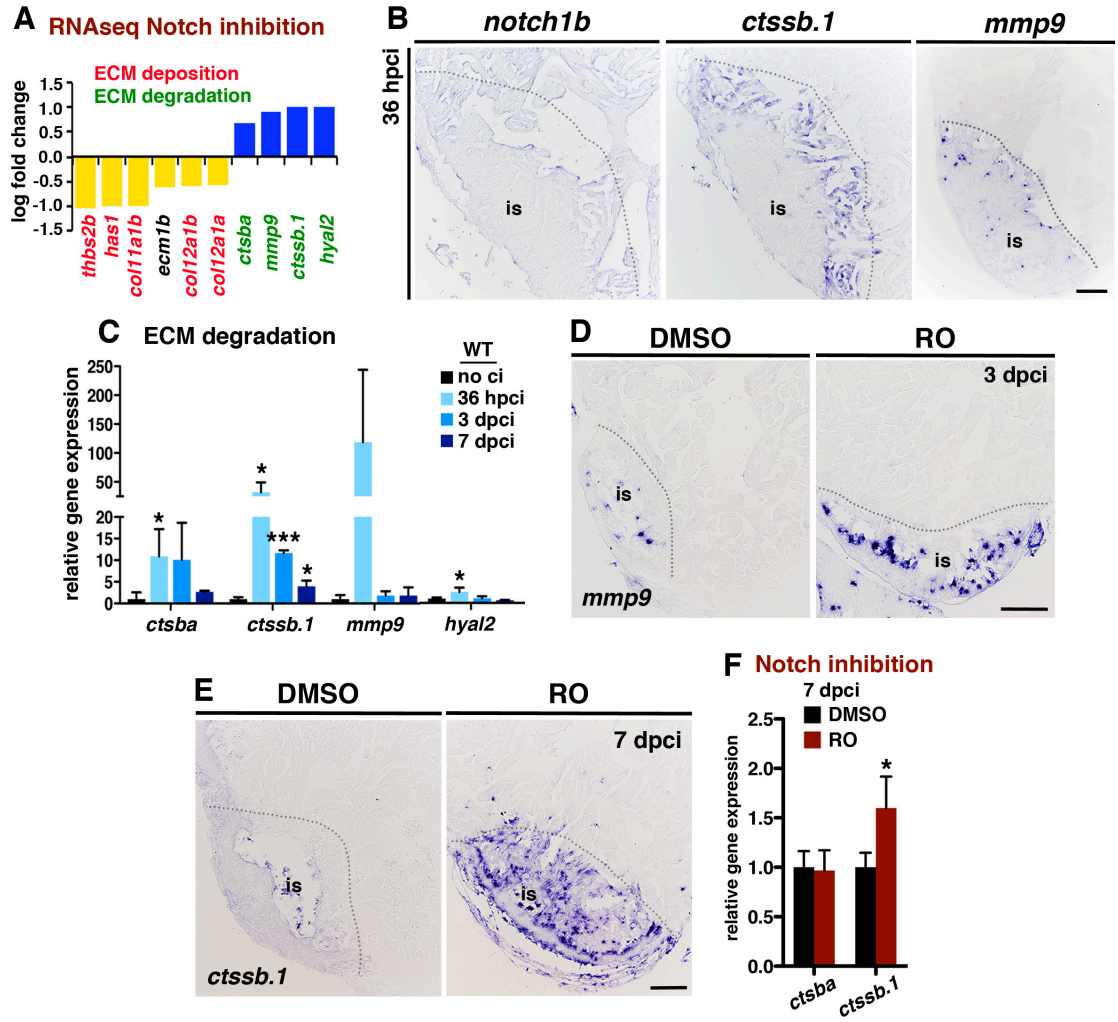

Figure 41: Notch signalling inhibition affects genes related to ECM remodelling and inflammation.
A: RNA-seq analysis. Differential cardiac expression of genes related to ECM-remodelling in fish treated with RO or DMSO at 3 dpci (experimental scheme in Fig 5A). **B**: ISH one heart sections showing strong *ctssb.1* and *mmp9* expression at the inner injury border at 36 hpci when *notch1b* expression is low. **C**: qPCR analysis of ECM-degradation genes in WT hearts with no cryoinjury (no ci) and at 3 and 7 dpci. **D**: ISH against *mmp9* (3 dpci), showing high numbers of positive cells within the injury site (is) of RO-treated hearts. **E**: ISH against *ctssb.1* (7 dpci), showing high numbers of positive cells within the injury site (is) of RO-treated hearts. **F**: qPCR analysis showing increased mRNA levels in injured ventricles after RO-treatment (SD **P*<0.05; ****P*<0.005; scale bars: 100 µm).

This finding is in line with observations in the mammalian heart, where proteases are activated shortly after injury to degrade the homeostatic cardiac matrix (Dobaczewski et al., 2010).

Consistent with the RNAseq data (Fig. 41A), by ISH and qPCR we observed an increased expression of *mmp9* (3 dpci) and *ctssb.1* (7 dpci) in regenerating hearts upon Notch signalling inhibition (Fig. 41D, E, F), indicating that endocardial Notch is implicated in the down regulation of injury induced protease expression at later regeneration stages.

RNA-seq analysis also identified genes encoding extracellular matrix molecules, including collagens (*col11a1b*, *col12a1a*, *col12a1b*), *thrombospondin 2b* (*thbs2b*) and the hyaluronan synthesizing enzyme *hyaluronan synthase 1* (*has1*) (Yoshida, Itano et al., 2000). Notch signalling inhibition with RO resulted in decreased cardiac expression of these genes at 3 dpci (Fig. 41A). RO-treatment also decreased transcript expression of *ECM protein 1b* (*ecm1b*), an inhibitor of *mmp9*-function (Fujimoto, Terlizzi et al., 2006) (Fig. 41A). Temporal analysis of gene activation in non-treated WT hearts detected expression of *col12a1a* and *has1* as early as 36 hpci (Fig. 42A), but transcript levels of *col11a1b*, *col12a1a* and *thbs2b* peaked at 3 dpci, with high levels sustained at 7 dpci (Fig. 42A), suggesting that ECM molecule encoding genes function later during heart regeneration.

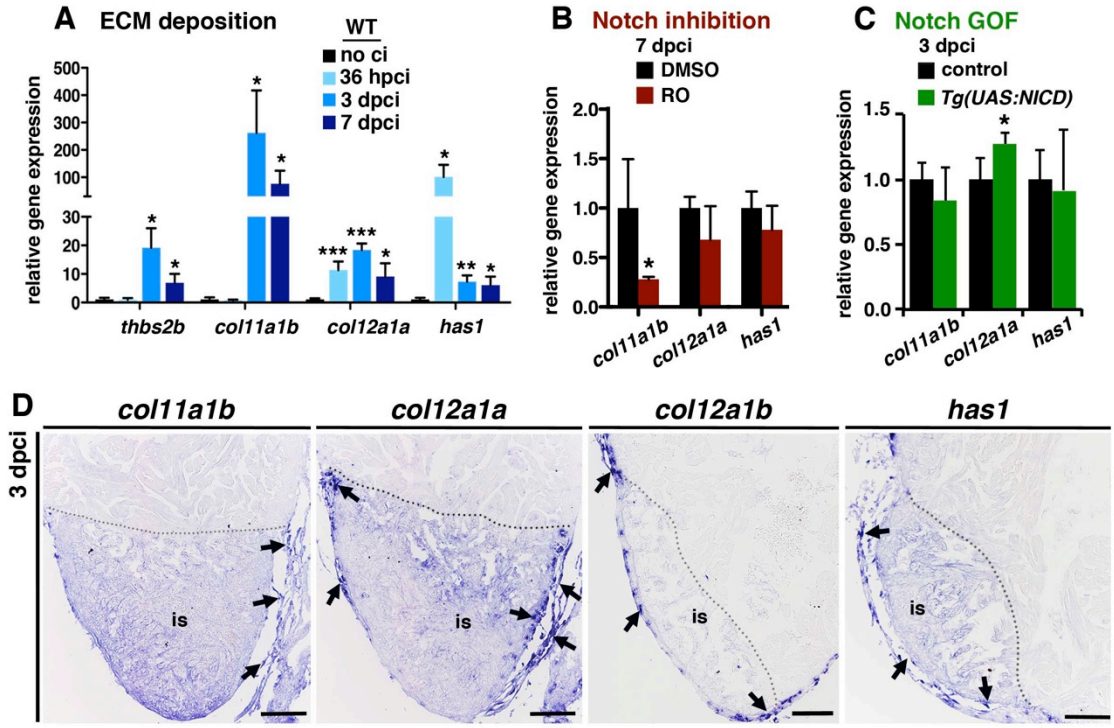

Figure 42: ECM molecule expression in the cryoinjured ventricle
A: qPCR analysis of ECM-deposition genes in WT hearts with no cryoinjury (no ci) and at 3 and 7 dpci. **B**: qPCR analysis showing decreased mRNA levels of *col11a1b* in injured ventricles after RO-treatment. **C**: qPCR analysis indicating increased expression levels of *col12a1a* in *Tg(UAS:NICD)* transgenic hearts comparing to the control. **D**: ISH for *col11a1b, col12a1a, col12a1b* and *has1* revealing strong expression in the epicardial region (arrowheads)(scale bars: 100 µm, SD, **P*<0.05; ***P*<0.01; ****P*<0.005).

RO-treatment decreased expression of *col11a1b* at 7 dpci comparing to DMSO treated hearts (Fig. 42B). Also *coll12a1a* and *has1* expression tended to be reduced after RO treatment, however not significantly. Moreover qPCR analysis of *Tg(UAS:NICD)*-transgenic and control hearts indicated that Notch overactivation is sufficient to slightly increase *col12a1a* but not *col11a1b* and *has1* expression at 3 dpci (Fig. 42C), suggesting that the affect of Notch signalling inhibition on these molecules may be indirect. ISH revealed *col11a1b, col12a1a*, *col12a1b* and *has1* expression in the outer epicardial region but not at the inner injury border (Fig. 42D). This indicates that these genes may depend on notch2 but not notch1b signalling, as *notch2* is also expressed in the epicardium (Zhao, Borikova et al., 2014).

Altogether in the WT cryoinjured heart, molecules involved in ECM degradation are strongly upregulated at 36 hpci and 3 dpci, but their expression then progressively declines. In contrast, genes that mediate ECM deposition were highly expressed at 3 dpci and 7 dpci. Notch inhibition results in reduced post-cryoinjury expression of ECM molecules but increased protease expression, indicating that Notch holds a profibrotic role in this context. Moreover the localization of ECM remodelling molecules suggests that different Notch receptors may be implicated in this transition from the inflammatory to the reparative phase in the regenerating cryoinjured heart.

3.5. Notch signalling attenuation extends the pro-inflammatory response during heart regeneration

RNAseq analysis further revealed an increased expression of inflammatory molecules (Fig. 43A). They include a characteristic gene for pro-inflammatory macrophages *phosphodiesterase 7a* (*pde7a*) (Smith, Brookes-Fazakerley et al., 2003), *sphingosine-1-phosphate lyase 1* (*sgpl1*), which degrades the anti-inflammatory molecule sphingosine 1-phosphate (S1P) (Peng, Hassoun et al., 2004) and the inflammatory marker *prostaglandin-endoperoxide synthase* 2b (*ptgs2b* (Ogryzko, Hoggett et al., 2014)) In addition we found two pro-inflammatory endothelial genes (Fig. 43A), *arginase2* (*arg2*) (Ryoo, Gupta et al., 2008) and the *tumor necrosis factor receptor superfamily member 9a* (*tnfrsf9a/* CD137) (Kwon, 2012), which are implicated in promoting atherosclerosis. This upregulation of inflammatory genes is accordance with augmented protease gene expression upon Notch signalling inhibition (Fig. 41A), considering the fact that low-molecular-weight fragments of ECM molecules, generated by proteases, induce pro-inflammatory signals and the recruitment of leukocytes (Dobaczewski et al., 2010).

We next analysed the temporal and local expression of selected genes after cryoinjury. The inflammatory genes *sgpl* and *tnfrsf9a* showed the highest expression levels at 36 hpci that declined progressively (Fig. 43B), concomitant with the high number of *l-plastin*- expressing cells at the inner injury border at this time point (Fig. 43C), indicating increased leukocyte infiltration shortly

after injury (36 hpci), when *notch1b* expression however is still low (Fig. 43C). *Tnfrsf9a* was expressed at the inner injury border (Fig. 43D) and, in line with the RNAseq data; qPCR analysis indicated that Notch inhibition augments *tnfrsf9a* mRNA levels even at later stages (7 dpci) (Fig. 43E). Also, the overactivation of the pathway could decrease *tnfrsf9a* expression in the injured heart (Fig. 43F), suggesting that Notch controls *tnfrsf9a* gene expression.

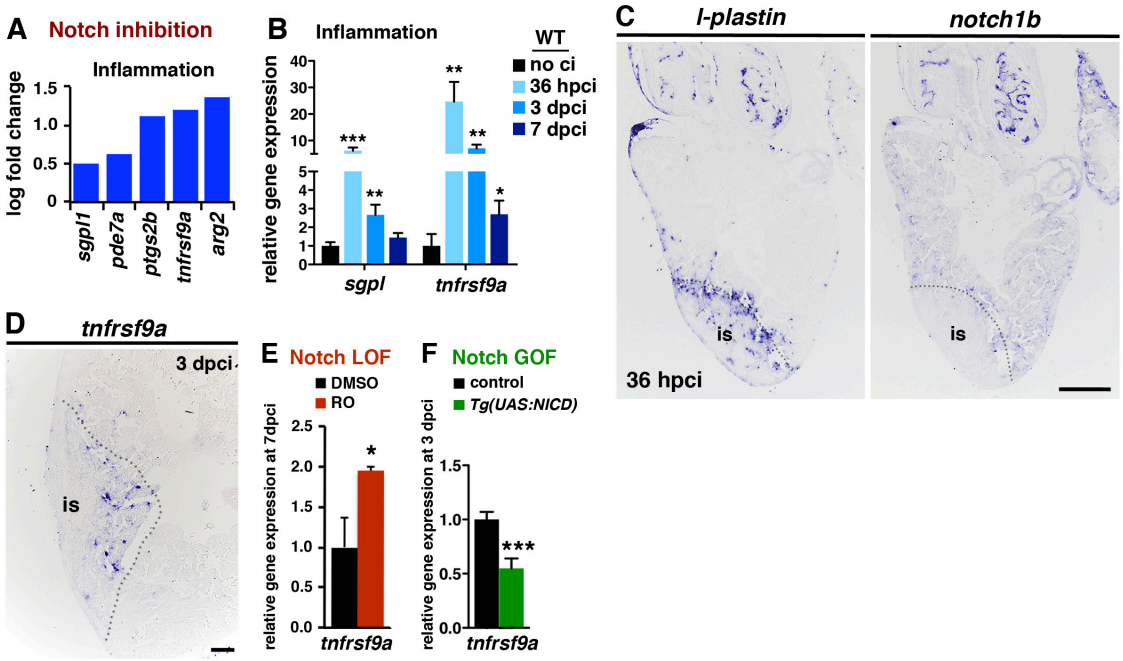

Figure 43: Notch signalling inhibition affects inflammatory genes.
A: RNA-seq analysis (3 dpci), showing upregulation of genes related to inflammation in hearts of RO-treated fish. **B**: Relative gene expression (qPCR) of *sgpl* and *tnfrsf9a* in WT hearts with no cryoinjury (no ci) and at 36 hpci, 3 and 7 dpci **C**: ISH on consecutive sections for *l-plastin* and *notch1b*, showing high *l-plastin* and low *notch1b* expression in the injury site at 36 hpci. **D**: ISH against *tnfrsf9a* on sections from an injured ventricle at 3 dpci, showing gene expression in cells with endocardial morphology within the injury site. **E**: Relative *tnfrsf9a* gene expression (qPCR) in ventricles at 7 dpci after treatment with RO or DMSO. **F**: Relative *tnfrsf9a* gene expression (qPCR) in ventricles of *Tg(UAS:NICD)* transgenic and WT ventricles at 3 dpci (scale bars: 100 μm, SD, **P*<0.05; ***P*<0.01; ****P*<0.005)

The increased expression of pro-inflammatory molecules upon Notch signalling inhibition prompted us to investigate whether also leukocyte infiltration is augmented. We examined the presence of *l-plastin*$^+$ macrophages upon Notch signalling inhibition, as an indication for the inflammatory response in the injury site. We noticed a higher abundance of *l-plastin*$^+$-macrophages in injured hearts after RO-treatment, especially at the inner the injury border at 7 dpci (Fig. 44A) but also later (30 dpci; Fig. 44B), suggesting that Notch inhibition caused a prolonged inflammatory response. To decipher if in turn Notch signalling overactivation can attenuate the inflammatory response at early stages we examined the presence of *l-plastin*$^+$ macrophages and

protease gene expression in control and *Tg(UAS:NICD)* transgenic hearts at 40 hpci. Macrophages were abundant at this time point in control but also *Tg(UAS:NICD)* transgenic injured hearts (Fig 44C). We further detected strong *ctssb.1* and *mmp9* expression in both control and *Tg(UAS:NICD)* transgenic hearts (Fig. 44D,E) suggesting that Notch signalling is not sufficient to reduce the inflammatory response early after cryoinjury.

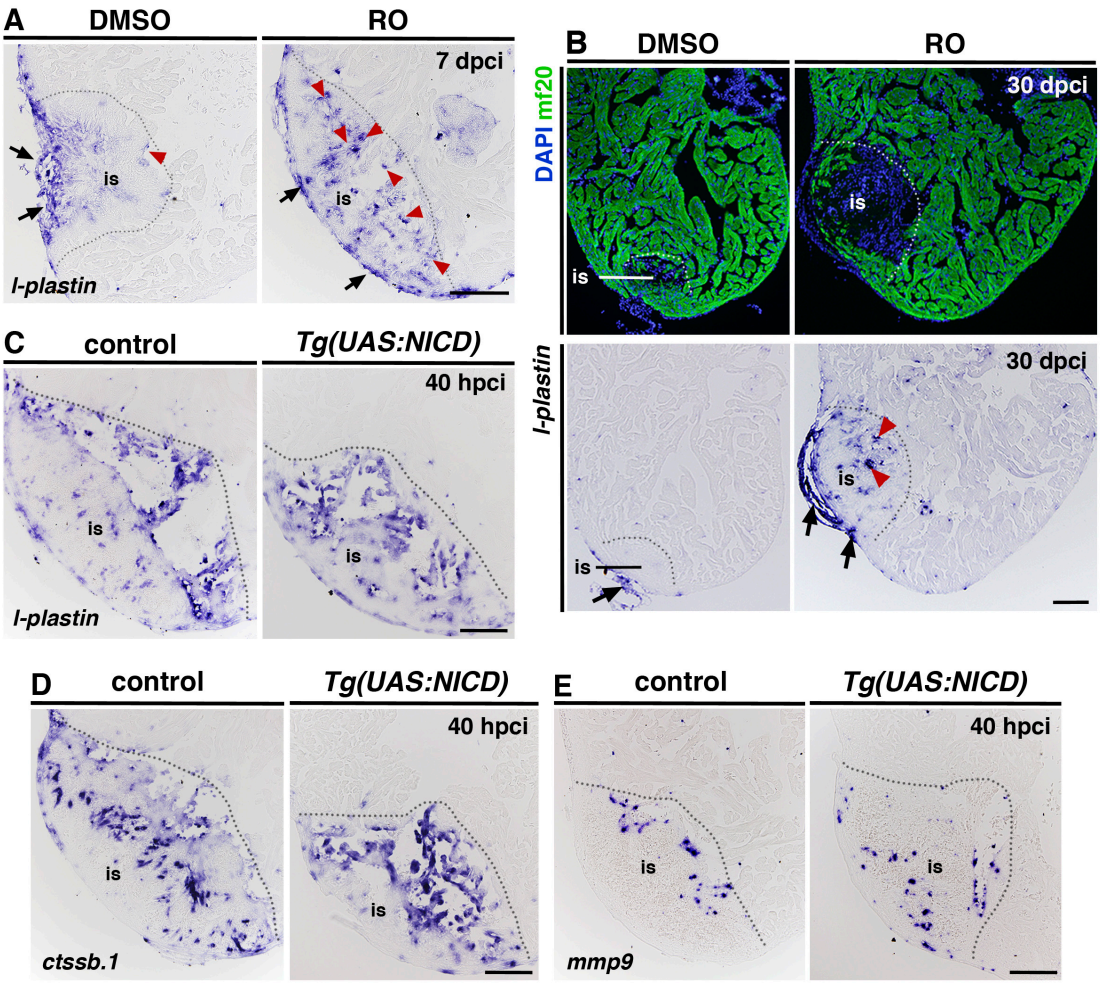

Figure 44: Notch signalling results in increased macrophage infiltration in the injury site. **A**: ISH against *l-plastin* (7 dpci), showing expression in the epicardial region (black arrows) in both conditions and higher numbers of *l-plastin*$^+$ macrophages within the injury site (red arrowheads) of RO-treated hearts. **B**: Immunohistochemistry against mf20 and ISH against *l-plastin* on consecutive heart sections of fish treated with RO or DMSO. RO treatment resulted in increased numbers of *l-plastin*$^+$ macrophages inside the injury site (is, black arrowheads), which is devoid of mf20$^+$ cardiomyocytes at 30 dpci. *l-plastin*$^+$ macrophages in the outer region of the injury can be found in both conditions (arrows) **C-E**: ISH for *l-plastin*, *ctssb.1* and *mmp9* revealed no difference in gene expression at 40 hpci. (Dotted lines delineate the injury site= is; Scale bars: 100 μm).

3.6. Notch regulates endocardial Tgfβ activation

Transforming growth factor beta (Tgfβ) signalling is strongly activated upon cryoinjury and is crucial for scar deposition and remodelling and for cardiomyocyte proliferation (Chablais & Jazwinska, 2012b). We sought to test if Notch signalling modulation affects Tgfβ signalling activation. Tgfβ signalling leads to the phosphorylation of the transcription factor Smad3, which is then translocated to the nucleus where it acts as a Tgfβ signalling effector in concert with Smad4 and other cofactors (Derynck, Muthusamy et al., 2014). Analysis of nuclear phospho-smad3 confirmed Tgfβ signalling activation in cardiomyocytes and cells in the epicardial region throughout the cryoinjured heart at 3 dpci (Fig. 45A). However, we also detected p-smad3 in the nuclei of GFP-expressing endocardial cells in *Tg(fli:GFP)* and *ET33-mi60a* transgenic fish (Fig. 45A, B), which was restricted to the injury site at 7 dpci (Fig. 45B).

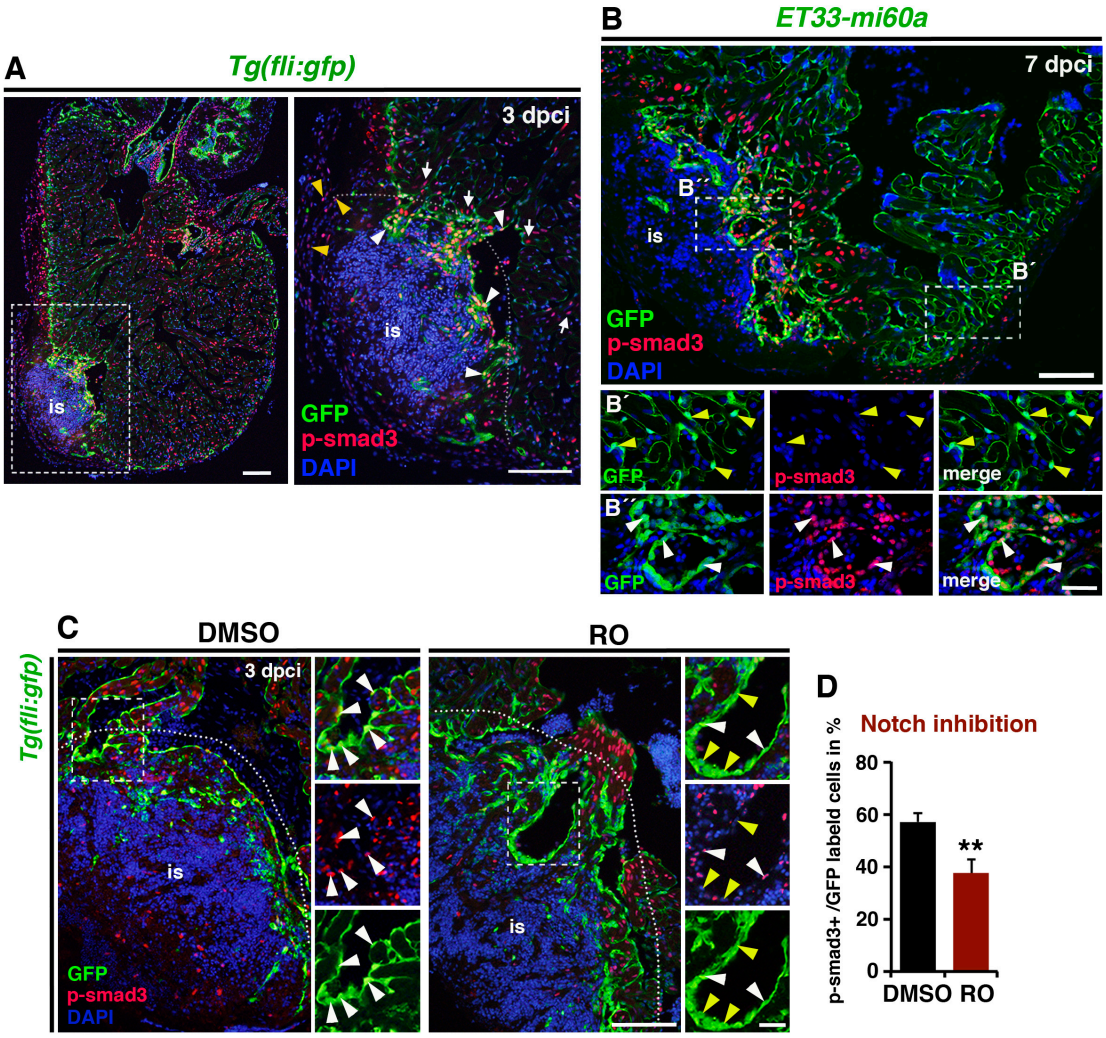

Figure 45: Notch signalling inhibition interferes with endocardial Tgfβ- signalling activation
A: Immunohistochemistry against p-smad3 and GFP on heart sections of the endocardial/endothelial reporter fish *Tg(fli:gfp)* at 3 dpci. The boxed area is shown in magnified view on the right. P-smad^{+} nuclei are present throughout the heart and in epicardial (yellow arrowheads), myocardial (white arrows) and GFP^{+} endocardial cells (white arrowheads), around and inside the injury site (is, defined by the dotted line). **B**: Immunohistochemistry against GFP and p-smad3 on heart sections (7 dpci), showing that GFP^{+} cells in the injury site (is) exhibit p-smad3 (B´´, white arrowheads), whereas in the periphery p-smad3 is missing in GFP^{+} cells (B´, yellow arrowheads). **C**: Immunohistochemistry against GFP and p-smad3 on heart sections of *Tg(fli:gfp)* endocardial/endothelial reporter fish (3 dpci). Compared with DMSO-treated hearts, the injury site in RO-treated hearts has fewer GFP^{+}/p-smad3^{+} cells (white arrowheads) but more GFP^{+}/ p-smad3^{-} cells (yellow arrowheads). **D**: Quantification of p-smad3^{+}/GFP^{+} cells at the inner injury border on sections of *Tg(fli:gfp)*- hearts (3 dpci) treated with RO (n= 4) or DMSO (n= 3). (Dotted lines delineate the injury site= is; scale bar, A: 200 µm; B, D: 100 µm. *P< 0.05.

We next analysed if Notch signalling inhibition affects endocardial Tgfβ signalling activation in *Tg(fli:GFP)*-fish. RO-treatment significantly decreased the number of fli:GFP^{+} endocardial cells containing nuclear p-smad3 (Fig. 45C, D), indicating that Notch signalling is required for endocardial Tgfβ signalling activation during heart regeneration.

Discussion

1. The role of Notch signalling during fin regeneration

1.1. Notch signalling maintains blastema cell dedifferentiation and proliferation

Fin regeneration proceeds through the dedifferentiation of cells that form a blastema distal to each fin ray (Nechiporuk & Keating, 2002, Santos-Ruiz et al., 2002). Our results show that Notch signalling is activated in blastema cells at 2 dpa just when the blastema has formed (Fig. 46A), suggesting a requirement for Notch from early stages of regeneration on. As regeneration proceeds, Notch activity is restricted to the distal region where undifferentiated proliferating progenitor cell populations are located (Nechiporuk & Keating, 2002, Santos-Ruiz et al., 2002). Indeed, our loss-of-function experiments indicate that Notch activation is not required for blastema formation but blastema cell proliferation (Fig. 46B). Constitutive Notch activation leads to an increased blastema indicated by the following observations: 1) the marked thickening of the blastema; 2) the disorganized appearance of blastema cells in the proximal region; 3) increased proliferation and 4) the expansion of blastema marker expression (Fig. 46C). These observations point to the role of Notch signalling in maintaining the dedifferentiated state of progenitor cells and in promoting cell proliferation. The function of Notch in stem/progenitor cell biology is crucial during developmental, homeostatic and regenerative processes but also context dependent. The consequences of its activation can vary from maintenance or expansion of stem cells to the promotion of stem cell differentiation (reviewed in (Koch, Lehal et al., 2013, Liu et al., 2010). Notch activation maintains progenitor cells in an undifferentiated state in the embryonic and adult nervous system (Chitnis, Henrique et al., 1995, de la Pompa, Wakeham et al., 1997, Henrique, Adam et al., 1995, Imayoshi, Sakamoto et al., 2010). In the skeletal muscle Notch mediates Pax7 expression and thus quiescence in satellite cells, however once they are activated Notch also sustains the self renewal capacity of these progenitor cells (Mourikis & Tajbakhsh, 2014).

An important question is what position Notch holds in the signalling network regulating fin regeneration. Retinoic acid (RA) controls blastema formation, proliferation and survival (Blum & Begemann, 2012) and regulates osteoblast differentiation (Blum & Begemann, 2015). Our findings suggest that Notch acts upstream of RA, since ectopic Notch activation increases *aldh1a2* expression. However *aldh1a2* is activated within the fin stump shortly upon amputation (Blum & Begemann, 2012), whereas Notch appears at later stages distal to the amputation plane, where it remains active. This suggests that blastema cell proliferation may be regulated by more than one mechanism. One possibility is that amputation triggers an initial RA signalling response that regulates early proliferation of dedifferentiated osteoblasts and fibroblasts within the stump to form the blastema. Later, in the regenerative outgrowth phase, the proliferation of blastema cells is regulated by Notch and RA signalling may be one of its effectors. Our data show that as

regeneration proceeds, a pool of fast-cycling cells persists at the distal tip of the fin, characterized by expression of *msxe* and *aldh1a2* and strong *msxb* expression. Constitutive Notch activation expands this *msxe*$^{+}$, *aldh1a2*$^{+}$ blastema, however transiently, as this phenotype is reversed when Notch induction is stopped. RA in this region maintains the blastema by enhancing expression of the pro-survival gene *bcl2* (Blum & Begemann, 2012), while msx-homologs are important regulators of dedifferentiation in several regenerating structures, such as the mouse digit tip (Han, Yang et al., 2003) and *Xenopus* and *Amphioxus* tails (Barker & Beck, 2009, Somorjai, Somorjai et al., 2012). This indicates that Notch maintains an undifferentiated, proliferative state of blastema cells by promoting *msxb, msxe* and *aldh1a2* expression.

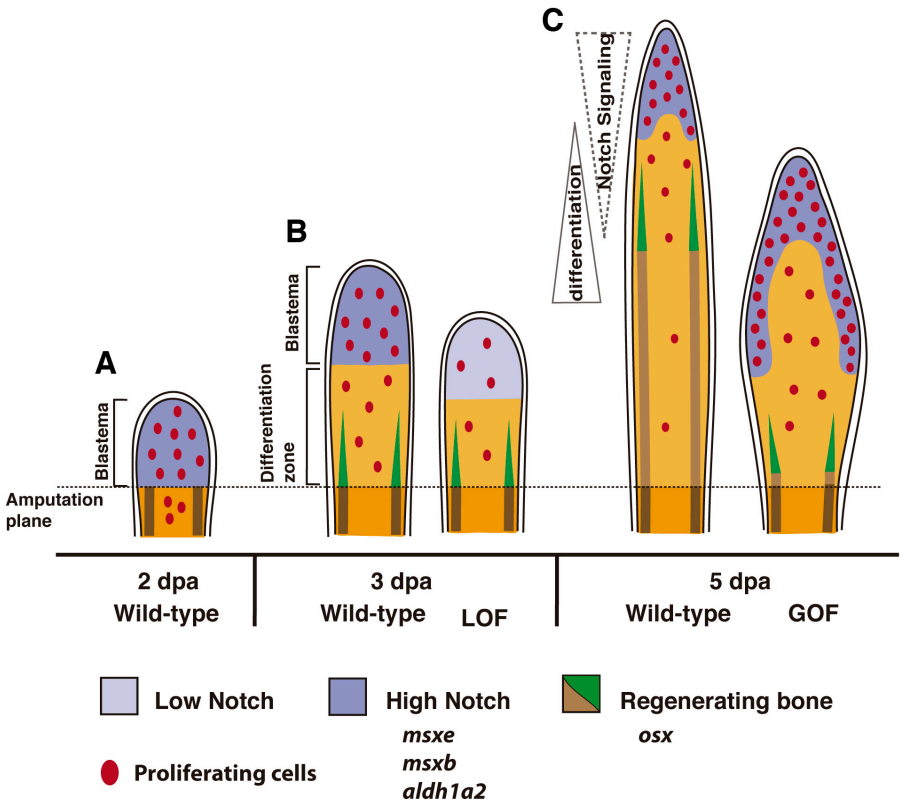

Figure 46. Model of Notch function during fin regeneration
The role of Notch in fin regeneration is to maintain blastema cells in a proliferative and undifferentiated state, so that the different cell lineages arise progressively. At 2 dpa, Notch is activated throughout the blastema (**A**) and remains restricted to the blastema at 3 dpa (**B**). In this region, *msxb*, *msxe* and *aldh1a2* are expressed and proliferation is higher. Notch loss-of-function (LOF) decreases blastemal proliferation. At 5 dpa (**C**), Notch activation persists in the blastema, while in the proximal region it is down-regulated and cells progressively differentiate to following their lineages, including the osteoblasts. Notch-GOF leads to an accumulation of proliferating, *msxb*-, *msxe*- and *aldh1a2*- expressing progenitor-like cells, and bone regeneration is inhibited.

1.2. Notch signalling prevents differentiation of osteoblasts

Various studies show that osteoblasts undergo dedifferentiation and proliferation during zebrafish fin regeneration (Knopf et al., 2011, Sousa et al., 2011). Osteoblasts migrate distally to the amputation plane and re-differentiate to rebuild the lost bone. Lineage restriction has been proposed to occur in all fin cell lineages (Tu & Johnson, 2011). Our data suggest that high Notch signalling prevents the progression of osteoblast differentiation, as indicated by the low number of osx-expressing cells in *Tg(hsp70l:Gal4); Tg(UAS:myc-notch1a-intra)* fins. In contrast, expression of *runx2* and *tcf7*, markers of the early stages of osteoblast differentiation (Knopf F, 2011, Li et al., 2009), is expanded throughout the blastema in transgenic fins. This goes in line with the the restricted expression of *bmp2b* to a more proximal region within the fin blastema as it promotes osteoblast differentiation (Quint et al., 2002, Smith et al., 2006). Recent findings demonstrate that RA restricts osteoblast differentiation in the distal regenerate via the inhibition of bmp2b-signalling (Blum & Begemann, 2015). This suggests that Notch-induced dedifferentiation of osteoblasts together with restricted *bmp2b*-expression result from increased *aldh1a2* levels throughout the blastema, seen upon sustained Notch overactivation. Also, *shh* gene expression is expanded proximally upon Notch overactivation, however its concrete position in the regulation of osteoblast differentiation is still under investigation (Wehner & Weidinger, 2015). Proximal *shh*-expression within the fin regenerate is restricted by wnt5b-mediated noncanonical Wnt signalling (Lee Y, 2009). As we observed a proximal expansion of *wnt5b* simultaneously to a restricted expression of *shh* we hypothesize an implication of Notch in a signalling network with the noncanonical Wnt and Hedgehog pathway. Rescue experiments modulating those pathways, would reveal the exact position of Notch signalling within this network.

These previously described changes in osteoblast gene expression are consistent with morphological differences that we observed upon Notch signalling over activation: impaired bone regeneration and regenerative outgrowth. GFP expression in the damaged bony fin ray in *ET33-mi60A* transgenic fish, also points to the implication of Notch in bone regeneration. A role for Notch in the regulation of osteoblast differentiation in the regenerating zebrafish fin is consistent with results from mice supporting the implication of Notch in bone homeostasis. Loss-of-function experiments in mice reveal that Notch maintains a pool of mesenchymal progenitor cells and suppresses osteoblast differentiation (Hilton, Tu et al., 2008) while gain-of-function experiments indicate that Notch stimulates the proliferation of immature osteoblasts (Engin, Yao et al., 2008).

Altogether we propose that in the wild-type regenerating fin Notch promotes cell proliferation and maintains the undifferentiated state of blastema cells. Notch activity is complementary to a proximal-distal gradient of cellular differentiation, so that the highest Notch activity occurs in the blastema, where dedifferentiated osteoblasts and fibroblasts are located (Fig. 46C). We have shown

that this model holds true for the osteoblast lineage, since early differentiation markers are expanded from the distal blastema to the differentiation zone in Notch gain-of-function experiments. Our findings contribute to a more detailed understanding of the molecular mechanisms underlying the development and maintenance of the regeneration blastema, a key process in epimorphic regeneration.

2. The role of Notch during heart regeneration

In this work we demonstrate the upregulation of Notch signalling components in the endocardium in the zebrafish injured heart. Recent reports have shown also *notch2* and *notch1a* receptor expression in the epicardium (Zhao et al., 2014). The endocardial localization is consistent with Notch signalling activation in the developing mammalian heart but not with reported Notch activation in cardiomyocytes in the neonate or adult injured (Collesi et al., 2008, Kratsios et al., 2010, Nemir et al., 2014, Urbanek et al., 2010) heart. As little was known about the function and behaviour of the endocardium in the context of cardiac injury we sought to investigate on this further as part of this thesis work.

2.1. Endocardial cell expansion and organization in the injury site

The analysis of histological tissue sections provides a limited view on tissue morphology. Cryoinjured tissue is heterogeneous, as the exogenously induced cryo-damage may not reach the same severity throughout the ventricle. During this work we set up a protocol that allows 3D imaging of the whole injured region of zebrafish cardiac ventricles by combining the CUBIC clearing method (Susaki et al., 2014) with confocal imaging analysis. Taking advantage of endogenous fluorescent proteins in transgenic cardiac reporter fish we visualized endocardium and myocardium at single cell level. The cryoinjury induces apoptosis in all cardiac tissues (Gonzalez-Rosa et al., 2011). Although we observed a great loss of endocardial and myocardial tissues within the injury site, we detected spared endocardial cells that persist after cryoinjury in a region where myocardial cells have completely disappeared. This might be explained by variances in apoptosis sensitivity of different cell types. Apoptosis sensitivity depends on various factors such as glutathione (Friesen, Kiess et al., 2004), proteins involved in glycolysis (Jeong, Kim et al., 2004) or the BCL-2/BAX complex (Konopleva, Contractor et al., 2006). In addition, the heterogeneous induction of a cold-induced damage does not produce a strict boundary between injured and healthy tissue, similar to the situation in mammalian myocardial infarction (Monceau, Belikova et al., 2006). Endocardial cells within and adjacent to the injury site become activated, round up and rapidly proliferate. This proceeds together with the upregulation of embryonic endocardial genes such as *cdh5*, *nfatc1* and notch pathway genes, suggesting that endocardial cells undergo

dedifferentiation. Also upon ventricular resection endocardial cells change their morphology and gene expression profile, indicated by the upregulation of *raldh1a2*, *hand2*, *gata5* and *flk1* (Kikuchi et al., 2011b).

A cryoinjury leaves behind a large portion of injured tissue, in contrast to ventricular resection, where tissue is removed. The injured tissue contains inflammatory and blood cells at early stages and fibrotic tissue later on (Chablais et al., 2011, Gonzalez-Rosa et al., 2011, Schnabel et al., 2011). Endocardial volume quantification revealed that the activated endocardium progressively expands within this injured region (Fig. 47A). This is achieved through massive endocardial cell proliferation but also presumably through the migration of endocardial cells. High magnification imaging analysis revealed a high abundance of filopodia-like protrusions, a feature of migratory cells (Ridley, 2011) at 3 dpci. This timely coincides with high proliferation of endocardial cells and the initiation of endocardial expansion. At later stages (9 dpci) filopodia-like protrusions are rare and the endocardium appears as a coherent single-layered finger-like structure. Cellular density of this structure however is still high and cells morphologically differ from endocardial cells in remote regions. Together, we demonstrate the dynamic behaviour of the endocardium after cardiac injury: Endocardial cells become activated, proliferate, organize and form a dense cellular network within the injured zebrafish heart (Fig. 47A). This observation opens a new field to study endocardial plasticity in zebrafish heart regeneration but also upon mammalian cardiac injury. Indeed, recent findings show the formation of endocardial flowers with angiogenic features, supporting vascularization in the injured heart (Miquerol, Thireau et al., 2015). Moreover that cellular plasticity needs to be controlled during regeneration was shown for the dystrophic skeletal muscle where various cells types adopt a fibrotic fate and thus increase muscle fibrosis (Pessina, Kharraz et al., 2015).

2.2. The activated endocardium separates injured and healthy tissue

Myocardial ischemia causes massive cell death accompanied by an intense inflammatory response in which leukocytes clear the tissue from dead cells. This inflammatory process occurs in various vertebrate cardiac injury models (Dobaczewski et al., 2010, Gonzalez-Rosa et al., 2011, Schnabel et al., 2011). Macrophages are crucial for wound healing and regenerative processes (Aurora, Porrello et al., 2014, Kyritsis, Kizil et al., 2012) but need to be controlled (Nathan, 2002). Leukocyte recruitment requires the active involvement of vascular endothelial cells, which produce signals mediating the adherence and passage of inflammatory cells to the injured tissue (Pober & Sessa, 2007). Our data provide evidence that after cryoinjury endocardial cells at the inner injury border plays this role. We observed a high abundance of *l-plastin*$^{+}$ macrophages at the inner injury border, suggesting that they arrived there with the blood stream. They may directly enter the damaged tissues with the blood, however also adhere and pass trough the endocardial layer. The

observation that *l-plastin*$^{+}$ cells adhere to the endocardium and endocardial cells enclose inflammatory aggregates, where leukocytes remove cellular debris, supports this assumption. Moreover we detected vcam-1, a cellular adhesion molecule involved in leukocyte recruitment (Wong & Dorovini-Zis, 1995), in endocardial cell. Inflammatory cell infiltration however needs to be tightly controlled (Nathan, 2002). Excessive inflammation can increase wound size and weaken the tissue due to an increased monocyte driven ECM remodelling (Frangogiannis, Smith et al., 2002).

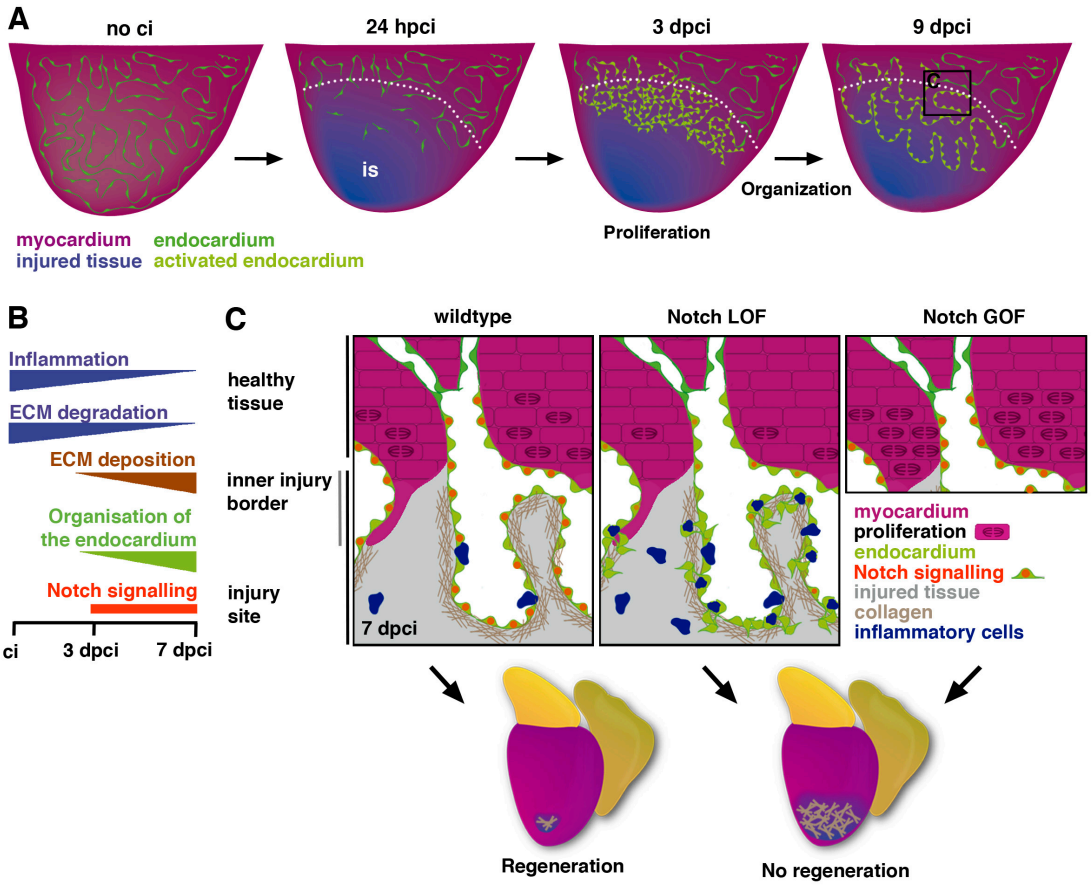

Figure 47: Endocardial dynamics upon cryoinjury
A: Scheme showing the dynamics of the injury-activated endocardium at different time points upon cryoinjury. At 24 hpci, spared endocardial cells reside at the injury site. Endocardial cells expand by proliferation and migration (3 dpci) and organize to from a coherent structure within the injury site (9 dpci). **B**: Progression of injury related processes (inflammation, ECM remodelling and ECM deposition) in relation to endocardium organization and Notch signalling activation. **C**: Tissue morphology at the inner injury border in wild-type and Notch loss- and gain-of-function conditions at 7 dpci. In the wild-type heart, activated dense endocardial cells surround injury-adjacent cardiomyocytes and form an organized structure in the injury site. This is associated with collagen deposition and inflammatory cell adhesion. Notch loss-of-function (LOF) results in reduced cardiomyocyte proliferation, a disorganized endocardial network, and increased inflammatory cell infiltration. Notch gain-of-function (GOF) increases cardiomyocyte proliferation. Regeneration fails upon Notch GOF and LOF.

We propose that the organized endocardial structure is implicated in controlling the infiltration of inflammatory cells into the injury site by two mechanisms: first as a physical barrier, as its forms an interface between healthy and damaged tissue, and second by controlling molecules that attract inflammatory cells and regulate their passage. Comparing gene expression analysis and endocardial morphology, we observed an inverse correlation: initially high inflammatory gene expression and leukocyte abundance reduce progressively (until 7 dpci) with increasing organization of the endocardium in the injury site (Fig. 47B). This suggests the organized endocardium being one requisite to control inflammatory cell infiltration into the injured tissue. Also, endothelial cells undergo specific changes and become activated in inflammatory conditions. This includes an increase in stickiness for inflammatory cells to adhere together with weakened cell junctions to allow cells to pass (Pober & Sessa, 2007). The organized endocardial structure may further prevent excessive reperfusion of the injured tissue. Myocardial-ischemia reperfusion is the return of blood supply after an ischemic injury, which can restrict cardiomyocyte death and prevent further damage. However, excessive reperfusion leads to increased inflammation and can itself induce cell death (Hausenloy & Yellon, 2013, Park & Lucchesi, 1999). We propose that the organized endocardial structure serves as a boundary to control the excessive inflow of blood and inflammatory cells in the injured tissue. We further suggest that the endocardium controls the oxygen supply to the injured tissue. Similarly to a mammalian cardiac injury, vascularization of injured tissue occurs (Gonzalez-Rosa et al., 2011, Lepilina et al., 2006), however is more evident in the outer region of the hearts. As trabeculated myocardium mainly receives oxygen by diffusion from the luminal blood through the endocardium (Hu et al., 2001), it is very likely that the endocardium controls oxygen transport to the injured tissue at the inner injury border. The observation that the endocardium in the injured tissue holds a finger-like morphology to increase its surface supports this assumption.

In conclusion, we propose that the activated endocardium in the zebrafish heart has several functions, which have been attributed to the endothelium after a myocardial infarction in mammals: controlling reperfusion and inflammatory cell infiltration and providing oxygen to the injured tissue. This is in accordance with the up-regulation of endothelial genes such as *cdh5*, *kdrl*, *id1*, *dll4*, *notch1b* and *notch2*.

2.3. The endocardium is involved in fibrotic tissue deposition

Ischemic cardiac injury results in massive tissue loss, which is compensated by the deposition of fibrous and collagen-rich tissue. This is crucial to prevent cardiac rupture and ensures proper cardiac pumping (Dobaczewski et al., 2010, Whittaker et al., 1991). Here, we report that the endocardium is associated to collagen deposition (Fig. 47C). The dense endocardial cellular network at the inner injury border may facilitate the rapid and organized formation of compact

collagen fibres. This may be achieved though the secretion of extracellular matrix molecules by endocardial cells itself and/or through a direct association of fibroblasts specifically to this endocardial structure. In fact *in vitro* experiments revealed that endocardial signals stimulate proliferation and collagen secretion of cardiac fibroblasts (Kuruvilla, Nair et al., 2007). Further activated endocardial cells may also transdifferentiate into fibroblasts. During mouse heart development and upon pressure overload in the heart a subset of cardiac fibroblasts have endocardial/ endothelial origin (Moore-Morris, Guimaraes-Camboa et al., 2014). Endocardial lineage tracing studies during cardiac regeneration in fish would give more insight into endocardium-fibroblast interactions or relations. Moreover a rapid and organized deposition of fibrotic tissue may facilitate its degradation, which is achieved in zebrafish (Chablais & Jazwinska, 2012a, Gonzalez-Rosa et al., 2011, Schnabel et al., 2011) but not in the mammalian heart (Bishop, Greenbaum et al., 1990).

2.4. The endocardium serves as a scaffold directing and facilitating cardiomyocyte migration towards the injured tissue

Cardiac injury induces the dedifferentiation and proliferation of existing cardiomyocytes, which peaks at 7 dpci (Bednarek et al., 2015, Jopling et al., 2010, Lepilina et al., 2006). Endocardial activation and proliferation starts earlier around 3 dpci. This proliferative endocardium progressively occupies the injured area, that lack cardiomyocytes. We suggest that the endocardium precedes the myocardium during regeneration, acting as a scaffold for cardiomyocytes that directs and facilitates its migration towards the injured tissue. Cardiomyocyte migration into the injury site is indicated by the presence of cellular protrusions in regenerating zebrafish (Schnabel et al., 2011) and mouse hearts (Morikawa, Zhang et al., 2015). We observed that the dense endocardial network surrounds thin clusters of protruding cardiomyocytes and that single myocardial cell protrusions were closely associated with the endocardium at the inner injury border (Fig. 47C). The endocardium thus creates a space in which the myocardium can enter the injury site. Collagen fibres that are deposited following the pattern of the endocardial structure provide mechanically support. Further the close association of the myocardium to the endocardium guarantees the oxygen supply.

During heart development endocardial-myocardial interaction is crucial during valve formation and for myocardial growth during chamber development (Tian & Morrisey, 2012). Trabeculation is initiated and guided by signals from the overlying endocardium (Tian & Morrisey, 2012). The zebrafish cloche mutant, that lack endocardial cells, fail to form trabecules (Stainier, Weinstein et al., 1995). Signalling from endocardium to myocardium maybe achieved through direct ligand-receptor signalling, through cytokine or growth factor secretion or the modulation of extracellular

matrix molecules. Myocardial ErBB2/ ErbBB4 activation by the endocardial growth factor Neuregulin1 is crucial, regulating trabecular growth during heart development (Gassmann, Casagranda et al., 1995, Lee, Simon et al., 1995, Meyer & Birchmeier, 1995). Also during mammalian heart regeneration the activation of this pathway induces cardiomyocyte dedifferentiation and proliferation (D'Uva, Aharonov et al., 2015). In injured adult fish hearts however *neuregulin* expression appears in perivascular cells in the cortical myocardial region but not in endocardial cells (Gemberling, Karra et al., 2015), suggesting that different stage- or species-specific endocardial signals maybe involved in endocardial-myocardial interaction. Further studies have to decipher the concrete mechanisms that allow endocardial- myocardial interaction in the context of heart regeneration.

2.5. The function of Notch signalling in the endocardium upon cryoinjury

Here we described the expression of *dll4*, *lunatic fringe* and the receptors *notch1b*, *notch2* and *notch3* in the endocardium adjacent and within the injured tissue. This is in line with data showing Notch activation after ventricular resection and during developmental cardiac regeneration (Zhang et al., 2013, Zhao et al., 2014). Although Zhao et al. reported notch receptor expression in the epicardium and we occasionally detected *notch2* in the epicardial region, we focused in this work on a possible function of Notch in the endocardium, by localizing gene expression to the inner injury border, where strong *notch1b* and dll4 expression was observed. Our study demonstrates that Notch signalling manipulation affects different cardiac tissues and processes and that both overactivation and inhibition of the pathway result in impaired regeneration after cryoinjury (Fig. 47C), indicating that precise levels of Notch signalling activation are crucial for cardiac regeneration.

Gene expression analysis revealed a number of endothelial/ endocardial genes that were deregulated upon Notch signalling inhibition. They include wound-related endothelial genes (*spry2*, *vgfc*, *id1*, *ephrinb2a*, *egr1*, *serpine1)*, genes implicated in endothelial integrity (*claudin5b*, *heg*) and endothelial cell differentiation (*klf2a*, *klf2b, aqp1*). We observed that Notch signalling inhibition results in decreased *egr1* expression. Egr1 is an important player in damaged endothelium, activating growth factors, cytokines and adhesion molecules, like Tgf-β, Tnf-α and ICAM-1 (Khachigian & Collins, 1997). Egr1 could act in a similar way in the endocardium, as we proposed that the endocardial structure in the injured heart holds endothelial functions. *Egr1* is also activated during valve formation in the zebrafish heart, similar to Notch signalling (Banjo et al., 2013), which suggests a signalling interaction also during heart development.

Another gene that changed upon Notch signalling inhibition was *serpine1*. Serpine1 is activated in various injured tissues coordinating proteolysis to allow the migration of different cell types

(Simone, Higgins et al., 2014). We observed strong *serpine1*-expression early on in endocardial cells within the injured tissue. Its expression progressively declines, revealing its importance early on in activated and less organized endocardial cells. We propose the implication of serpine1 in promoting endocardial cell migration by modulating the ECM in the injury site. Also, the fact that Notch inhibition results in increased abundance of filopodia-like protrusions and augmented *serpine1* expression could be related as Serpine1 causes increased filopodia formation in invasive breast cancer cells (Chazaud, Ricoux et al., 2002). A recent study showed that *Serpine1* is expressed in endocardial cells upon transmural cryoinjury (Darehzereshki, Rubin et al., 2015), which is reminiscent of the cryoinjury in the zebrafish heart as the infarcted region reaches the endocardium. Due to its inhibitory function on the fibrinolytic urokinase/tissue type plasminogen activator (uPA/tPA), Serpine1 is further implicated in the regulation of fibrotic tissue deposition in injury-related and pathogenic conditions in different organs (Ghosh & Vaughan, 2012). However the effect of Serpine1 on cardiac fibrosis is still unclear: elevated Serpine1 levels in cardiomyocytes increase cardiac fibrosis upon myocardial infarction (Takeshita, Hayashi et al., 2004) whereas Serpine1-deficiency leads to spontaneous cardiac fibrosis with age (Moriwaki, Stempien-Otero et al., 2004). Also in the skeletal muscle Serpine-1 needs to be well balanced to control disease related fibrosis (Ardite, Perdiguero et al., 2012, Suelves, Vidal et al., 2005). This points out that the regulation of Serpine1 expression levels is crucial for fibrotic tissues remodelling and cardiac regeneration. We propose that the increased *serpine1* expression upon Notch inhibition affects the activation and morphology of endocardial cells and/or the remodelling of the ECM within the injured tissue, as both may interfere with complete cardiac regeneration.

Notch signalling regulates cell fates in a homogeneous cell pool or layer (Lai, 2004, Li, Kapoor et al., 2012, Stanger, Datar et al., 2005). Morphological and gene expression analysis suggest that Notch blocks a migratory phenotype in endocardial cells within the injury site. This role of Notch in the endocardium after cryoinjury is reminiscent to its role during angiogenesis. There Dll4-Notch signalling blocks the migratory, tip cell fate of endothelial cells (Hellstrom, Phng et al., 2007, Lobov, Renard et al., 2007, Suchting, Freitas et al., 2007) and Notch inhibition interferes with blood vessel maturation (Ehling, Adams et al., 2013).

In summary our gene expression profiling revealed a high variety in endothelial /endocardial gene activation in the regenerating heart, which is in accordance with the highly dynamic endocardium at the injury site. Notch signalling affects endocardial/endothelial gene expression and is required for endocardial organization.

2.6. Notch signalling attenuates the inflammatory response

Our data provide evidence that at the inner injury border the endocardial structure may physically control the infiltration of blood and inflammatory cells into the injury site. We observed that Notch inhibition results in increased macrophage abundance at the inner injury border, indicating an increased inflammatory response (Fig. 47C). In addition, gene expression analysis suggests that there are more pro-inflammatory macrophages after Notch inhibition. We hypothesize that this results from a direct modulation of inflammatory signals by Notch in endocardial cells to attract inflammatory cells. We support this by the fact that two pro-inflammatory endothelial genes, *arg2* (Ryoo et al., 2008) and *tnfrsf9a* (Kwon, 2012) are upregulated upon Notch inhibition. Both genes are activated in endothelial cells in atherosclerosis and promote inflammation in this context (Olofsson, Soderstrom et al., 2008, Ryoo et al., 2008), suggesting their role in inflammatory cell recruitment to the injured tissue. Also the presence of low molecular weight ECM fragments, a possible consequence of the increased protease expression in Notch-supressed hearts, may enhance leukocyte recruitment indirectly. Timely gene expression analysis showed that inflammatory and ECM degradation gene activation inversely correlates with the organization of the endocardium (Fig. 47C). This suggests that the disorganized endocardial structure, observed upon Notch signalling inhibition, may prevent inflammatory and blood cell infiltration attenuation at later stages of regeneration. Indeed in a model of ischemic skeletal muscle injury, the inhibition of Dll4 similarly leads to uncontrolled sprouting of endothelial cells together with increased leukocyte infiltration (Al Haj Zen, Oikawa et al., 2010).

The attenuation of inflammatory cell infiltration is crucial for the transition from the inflammatory to the reparative phase after cryoinjury in zebrafish (Chablais & Jazwinska, 2012b). This could proceed through the regulation of TGF-β signalling in endocardial cells at the injury border. Chablais et al reported the implication of TGF-β signalling in fibrotic tissue deposition and remodelling, consistently with previous reports that delineate TGF-β as a crucial cytokine, repressing inflammatory signals and promoting extracellular matrix deposition mammals (Bujak & Frangogiannis, 2007, Chablais & Jazwinska, 2012b). Further studies have to determine, if Notch directly regulates genes, encoding for TGF-β pathway elements or if Notch indirectly modulates smad3 phosphorylation and the nuclear translocation cascade. The first one could be likely as Notch signalling induces Tgf-β2 expression in the endocardial cells in the developing valve in the mouse (Luna-Zurita et al., 2010).

2.7. Notch signalling regulates cardiomyocyte proliferation

Our loss-of-function studies show that Notch signalling is required for cardiomyocyte proliferation, which goes in line with previous reports (Zhang et al., 2013, Zhao et al., 2014).

Further we observed that Notch gain-of-function leads to augmented BrdU incorporation in cardiomyocytes adjacent to the injury (Fig. 47C). This seems to be in contrast to published results from Zhao et al as they showed decreased PCNA-labelled cardiomyocytes upon Notch signalling overactivation using the same transgenic model (*Tg(hsp70l:Gal4)*^{kca4}*;Tg(UAS:myc-Notch1a-intra)*^{kca3}). We examined BrdU incorporation to specifically detect DNA-synthesis, meaning cardiomyocyte cell cycle. We observed an increased number of cells entering the cell cycle during this time with Notch GOF. This conclusion cannot be reached by immunohistochemistry against PCNA, as this represents the state of the cells at only one time point (7 dpa or 14 dpa) and as PCNA can be detected throughout the whole cell cycle (Schonenberger, Deutzmann et al., 2015) and not only during DNA synthesis.

Gene expression profiling revealed that Notch signalling alterations affect the expression of immediate-early growth genes (*myc-b*, *atf3*). These are activated upon growth or stress stimuli and expressed in the zebrafish developing heart (Jia, King et al., 2007) but also in dedifferentiating, proliferating cardiomyocytes after heart injury (Aguirre et al., 2014). This suggests that the reduction of cardiomyocyte proliferation upon Notch signalling inhibition maybe related to decreased *myc-b* expression-levels and impaired dedifferentiation of cardiomyocytes. This is in line with the increased expression of sarcomeric genes caused by Notch signalling inhibition as cardiomyocyte dedifferentiation involves the down-regulation of sarcomeric genes and the sarcomere disassembly is needed for cardiomyocyte division in fish and neonatal mouse hearts (Jopling et al., 2010, Porrello et al., 2011). Consistent with reports about heart development we observed a non-cell autonomous role for endocardial Notch signalling to regulate cardiomyocyte proliferation. We searched our RNA seq data for secreted molecules that could be involved in mediating this effect, meaning cytokines, growth factors or extracellular matrix molecules. One candidate was the growth factor Bmp10, which is regulated by Notch during chamber development (Grego-Bessa et al., 2007). We show that in the adult fish heart *bmp10* is expressed in the endocardium and RNAseq analysis suggests its positive regulation by Notch. However as we found similar expression levels all over the heart both in injured and undamaged ventricles we propose that Notch and bmp10 interaction may not be regeneration specific in the adult heart.

RNAseq analysis also revealed increased expression of transmembrane protein *heg*, which is part of the cerebral cavernous malformation (CCM) complex (Gingras, Liu et al., 2012), *klf2a*, *klf2b* and its target *aqp1 (Dekker et al., 2006)* upon Notch signalling inhibition. We detected strong expression of *klf2a* and *heg*, in endocardial cells surrounding cardiomyocytes adjacent to the injury, the site of highest cardiomyocyte proliferation. Both genes are required in the endocardium during heart development (Mably et al., 2003, Vermot et al., 2009) but also in vascular endothelial cells (Kleaveland et al., 2009, Vermot et al., 2009), similar to Notch signalling (de la Pompa &

Epstein, 2012, Herbert & Stainier, 2011). *Notch1b* is also expressed within the same region and our results suggest that Notch negatively regulates these genes. Thus, Notch may control the levels of *klf2a* and *heg* expression in a subset of endocardial cells regulating the fate of a specific endocardial subtype. The increased expression of *klf2a*, *klf2b* and their target *aqp1* upon Notch signalling inhibition may be related to the decrease in cardiomyocyte cell cycle entry as augmented endocardial Klf2 levels interfere with cardiomyocyte proliferation through endocardial/ myocardial signalling during cardiac chamber development (Zhou, Rawnsley et al., 2015). The fact that in this context increased KLf2 expression resulted from a reduction of CCM complex members (Renz, Otten et al., 2015, Zhou et al., 2015), indicates that Notch may regulate *heg* and *klf2a* independently from each other. This new signalling interaction could have further implications in developmental and/or angiogenic processes that need to be addressed more in detail in the future.

Further, we observed that dedifferentiated cardiomyocytes accumulated at the inner injury border and fail to enter the injured area, explaining why regeneration is impaired upon Notch gain-of function. We propose two possible explanations for this. First, cardiomyocytes fail to enter the injury site, due to altered early ECM remodelling or affected endocardial organization within the injured tissue. Second, the dedifferentiated, proliferating state of cardiomyocytes prevents their migration. However, further experiments would be necessary to confirm either or the other hypothesis.

Altogether here we demonstrate the behaviour, morphology and function of the endocardium upon cryoinjury in zebrafish. We show its dynamic behaviour within and adjacent to the damaged tissue and propose its implication in orchestrating the inflammatory response and fibrotic tissue deposition. We show that Notch signalling is required for the organization of the endocardium and to control inflammatory cell infiltration. Our data also suggest that the endocardium promotes cardiac regeneration by providing Notch-dependent proliferative signals to cardiomyocytes and guides them within the damaged region of the heart. Our findings demonstrate the importance of a non-cardiomyocyte tissue, the endocardium, to regulate the injury response and regeneration upon a cardiac insult. Further studies have to determine more in detail specific signals coming from the endocardium that orchestrate inflammation, fibrotic tissues deposition and cardiomyocyte renewal.

3. Outlook

In this work we demonstrate that Notch signalling is required to maintain blastema cells in a dedifferentiated, proliferative state in the regenerating zebrafish fin. Defects on bone regeneration upon Notch overactivation suggest that Notch acts in dedifferentiated osteoblasts. However, to clarify this issue, tissue specific Notch signalling modulation would be necessary. This could be achieved by stage-specific expression of NICD (gain-of-function) or a dominant negative form of

the Notch co-activator mastermind like (*dnMAML*), in specific cells types within the regenerating fin. A transgenic line with osteoblast specific expression of the tamoxifen inducible Cre recombinase such as *osterix*:CreERT2-p2a-mCherry (Knopf et al., 2011) would serve to induce the recombination of a floxed stop codon flanking NICD or *dnMAML* alleles during fin regeneration. To complement this study, a Cre^{ERT2}, driven by gene regulatory sequences specific for fibroblasts, such as collagen-encoding genes could be used. Moreover, it would be interesting to combine gain- and loss-of-function approaches of signalling pathways involved in fin regeneration, to decipher for instance the specific position of Notch signalling in the previously described RA-Wnt-signalling network (Wehner et al., 2014).

Our functional and gene expression studies revealed the implication Notch in various processes during heart regeneration. However, we could not rule out unspecific effects, as transgenic NICD overexpression and chemical Notch inhibition occur throughout the zebrafish body and could affect heart regeneration. To better distinguish the individual effects of Notch signalling in specific subsets of cells in the heart, tissue specific Cre-lox technology would be required. Only a few studies have used so far the Cre-lox system for cardiac regenerations studies in zebrafish. Problems may arise due to the efficiency of promoter activity in the adult heart or due to inefficient induction of the Cre recombinase by tamoxifen at adult stage. Indeed, the mostly used Cre^{ER} transgenic line, *Tg(cmlc2:CreER)* (Fang et al., 2013, Gemberling et al., 2015, Jopling et al., 2010), functions with a very strong promoter of a gene encoding for the sarcomeric protein cardiac myosin light chain (cmlc2/ myl7), which is strongly activated and required in cardiomyocytes throughout ventricular development (Chen, Huang et al., 2008) and in the adult heart (Chen et al., 2008). A similarly strong promoter would be required to drive Cre^{ERT2} expression in the endocardium. One interesting candidate gene would be *cdh5* as we observed specifically strong *cdh5* expression in the endocardium in the injury site. Additional studies could be done also to trace the endocardium during regeneration. This can be achieved through the specific labelling of endocardial cells before cryoinjury by using either the Cre-lox system to induce the expression of a fluorescent protein or by photo conversion of a fluorescent protein as shown by Itou *et al*. for cardiomyocytes (Itou et al., 2012). To prove the functionality of the endocardium and its requirement for heart regeneration, a specific model for endocardial ablation would be appropriate. For this aim we propose a transgenic model consisting of an injury specific endocardial Cre^{ERT2} and the *bactin2:loxp-mCherry-STOP-loxp-DTA* construct, expressing diphtheria toxin A chain, which causes cell death (Wang et al., 2011) and thus endocardial cell ablation. In the future more efficient endocardial Cre^{ERT2} driver lines need to be generated to gain more detailed insight into endocardial function during heart regeneration.

4. Notch signalling – a key pathway for regeneration?

This work reports the implication of Notch signalling during the regeneration of two organs, the zebrafish fin and the heart. We show that both organs require the full activation of the Notch pathway and that in both settings Notch signalling activation needs to be tightly regulated. The zebrafish fin and the heart are complex but very different tissues. Whereas correct heart function is vital for the fish, an amputated or injured fin may not directly affect zebrafish survival. In terms of regeneration relatively similar mechanisms are required. These include the dedifferentiation of cells to replace lost tissue, which have been demonstrated for osteoblasts (Knopf et al., 2011, Sousa et al., 2011) and cardiomyocytes (Jopling et al., 2010, Kikuchi et al., 2010). Similarities also exist in injury-related processes such as cell death and leukocyte recruitment.. Although apoptosis is much more severe in the cryoinjured heart due to the massive amount of injured tissue (Gonzalez-Rosa et al., 2011, Schnabel et al., 2011), apoptosis also occurs after fin amputation and is essential for regeneration (Gauron, Rampon et al., 2013). Similarly, the inflammatory response is low in regenerating fins comparing to the injured heart. Recent findings however demonstrated that in both fin and heart regeneration (mouse neonate) the presence of macrophages is crucial for regeneration to proceed (Aurora et al., 2014, Petrie, Strand et al., 2014). Numerous studies have reported key signalling pathways during regeneration. Hippo signalling is for organ growth and thus must be precisely regulated during regenerative processes, as has been shown for heart (Tian et al., 2015) and fin regeneration (Mateus et al., 2015). The importance of Wnt signalling during organ regeneration however may result from the ability of the Wnt ligands, secreted from one tissue, to activate a reparative response in adjacent tissues. This holds true for fin (Stoick-Cooper et al., 2007), digit tip (Takeo, Chou et al., 2013) and planarian body regeneration. The Notch pathway is distinguished by allowing cell-to-cell communication, to induce a specific cellular outcome within a homogenous tissue. Notch signalling activation thus determines the fate of a cell, its differentiation state, whether a cell proliferates or whether it undergoes apoptosis. These cellular decisions are crucial in activated, dynamic tissues, such as during development, disease and tissue regeneration (de la Pompa & Epstein, 2012, Liu et al., 2010). Then it is not surprising that Notch signalling is implicated in many regenerative processes, independently of whether regeneration proceeds through resident stem cells or dedifferentiation, as cellular decisions made by Notch signalling are highly context- and tissue dependent. Here we demonstrate that in the regenerating fin Notch maintains blastema cells in a proliferative state and prevents their differentiation. In the regenerating zebrafish heart, Notch regulates endocardial gene expression and the organization of the activated endocardium, which has further consequences on the inflammatory response and cardiomyocyte proliferation. This work describes two very different roles of Notch signalling during the regeneration of two very different organs and adds new insights about the dynamic role of Notch signalling in mediating cellular decisions during regeneration and repair.

Conclusions

1. Notch signalling pathway elements are expressed as soon as the blastema is formed and remain expressed in the distal region of the fin regenerate during regenerative outgrowth.

2. Notch signalling regulates blastema cell proliferation and maintains blastema cells in an undifferentiated state.

3. Notch signalling prevents the redifferentiation of osteoblasts in the regenerating fin.

4. Notch signalling pathway genes are expressed in the endocardium upon cryoinjury in the zebrafish heart.

5. Upon cryoinjury spared endocardial cells within the injury site and adjacent to the injury become activated, indicated by embryonic gene expression and morphological changes.

6. Activated endocardial cells extensively proliferate (3 dpci), expand and organize (9 dpci) to form an endocardial structure within the injury site.

7. This injury-activated endocardium precedes the regenerating myocardium and is associated to collagen deposition and inflammatory cell adhesion.

8. Notch signalling modulates endocardial/ endothelial gene expression and is required for the organization of the injury-activated endocardium.

9. Notch signalling positively regulates cardiomyocyte proliferation.

10. Notch signalling is required for the attenuation of inflammatory and protease gene expression early after cryoinjury and the infiltration of inflammatory cells.

1. Varios elementos de la vía de señalización de Notch se expresan tras la formación del blastema y mantienen su expresión en la región distal de la zona en regeneración de la aleta durante el proceso.

2. La vía de señalización de Notch está implicada en la proliferación celular del blastema y mantiene sus células en un estado indiferenciado.

3. La vía de señalización de Notch regula la diferenciación temporal de los osteoblastos durante la regeneración de la aleta.

4. Tras una criolesión varios genes de la vía de señalización de Notch se expresan en el endocardio del corazón del pez cebra .

5. Tras una criolesión células endocárdicas en la lesión y adyacente a ésta se activan, como indican los cambios morfológicos y la expresión de genes embrionarios en estas células.

6. Las células endocárdicas activadas proliferan intensamente 3 dias después de la criolesíon (ddl), se expanden y se organizan (9 ddl) para formar una estructura endocardial dentro de la lesión.

7. La activación y expansión del endocardio tras la lesión precede a la regeneración del miocardio y está asociada a la deposición de colágeno y a la adhesión de las células inflamatorias.

8. La vía de señalización de Notch modula la expresión génica endocárdica y endotelial y es necesario para la organización del endocardio activado dentro de la lesión.

9. La vía de señalización de Notch está implicada en la regulación positiva de la proliferación de cardiomiocitos.

10. Se requiere la señalización de Notch para disminuir la expresión de genes inflamatorios y de las proteasas al comienzo del proceso, reduciendo también la infiltración de células inflamatorias.

References

Abou-Khalil R, Brack AS (2010) Muscle stem cells and reversible quiescence: the role of sprouty. Cell cycle (Georgetown, Tex) 9: 2575-80

Aguirre A, Montserrat N, Zacchigna S, Nivet E, Hishida T, Krause MN, Kurian L, Ocampo A, Vazquez-Ferrer E, Rodriguez-Esteban C, Kumar S, Moresco JJ, Yates JR, 3rd, Campistol JM, Sancho-Martinez I, Giacca M, Izpisua Belmonte JC (2014) In vivo activation of a conserved microRNA program induces mammalian heart regeneration. Cell stem cell 15: 589-604

Akimenko MA, Johnson SL, Westerfield M, Ekker M (1995) Differential induction of four msx homeobox genes during fin development and regeneration in zebrafish. Development 121: 347-57

Akimenko MA, Mari-Beffa M, Becerra J, Geraudie J (2003) Old questions, new tools, and some answers to the mystery of fin regeneration. Developmental dynamics : an official publication of the American Association of Anatomists 226: 190-201

Al Haj Zen A, Oikawa A, Bazan-Peregrino M, Meloni M, Emanueli C, Madeddu P (2010) Inhibition of delta-like-4-mediated signaling impairs reparative angiogenesis after ischemia. Circulation research 107: 283-93

Ardite E, Perdiguero E, Vidal B, Gutarra S, Serrano AL, Munoz-Canoves P (2012) PAI-1-regulated miR-21 defines a novel age-associated fibrogenic pathway in muscular dystrophy. The Journal of cell biology 196: 163-75

Artavanis-Tsakonas S, Rand MD, Lake RJ (1999) Notch signaling: cell fate control and signal integration in development. Science 284: 770-6

Atkins GB, Jain MK (2007) Role of Kruppel-like transcription factors in endothelial biology. Circulation research 100: 1686-95

Aurora AB, Porrello ER, Tan W, Mahmoud AI, Hill JA, Bassel-Duby R, Sadek HA, Olson EN (2014) Macrophages are required for neonatal heart regeneration. The Journal of clinical investigation 124: 1382-92

Banjo T, Grajcarek J, Yoshino D, Osada H, Miyasaka KY, Kida YS, Ueki Y, Nagayama K, Kawakami K, Matsumoto T, Sato M, Ogura T (2013) Haemodynamically dependent valvulogenesis of zebrafish heart is mediated by flow-dependent expression of miR-21. Nature communications 4: 1978

Barker DM, Beck CW (2009) Overexpression of the transcription factor Msx1 is insufficient to drive complete regeneration of refractory stage Xenopus laevis hindlimbs. Developmental dynamics : an official publication of the American Association of Anatomists 238: 1366-78

Beck CW, Christen B, Slack JM (2003) Molecular pathways needed for regeneration of spinal cord and muscle in a vertebrate. Developmental cell 5: 429-39

Bednarek D, Gonzalez-Rosa JM, Guzman-Martinez G, Gutierrez-Gutierrez O, Aguado T, Sanchez-Ferrer C, Marques IJ, Galardi-Castilla M, de Diego I, Gomez MJ, Cortes A, Zapata A, Jimenez-Borreguero LJ, Mercader N, Flores I (2015) Telomerase Is Essential for Zebrafish Heart Regeneration. Cell reports

Beis D, Bartman T, Jin SW, Scott IC, D'Amico LA, Ober EA, Verkade H, Frantsve J, Field HA, Wehman A, Baier H, Tallafuss A, Bally-Cuif L, Chen JN, Stainier DY, Jungblut B (2005) Genetic and cellular analyses of zebrafish atrioventricular cushion and valve development. Development 132: 4193-204

Bierkamp C, Campos-Ortega JA (1993) A zebrafish homologue of the Drosophila neurogenic gene Notch and its pattern of transcription during early embryogenesis. Mechanisms of development 43: 87-100

Bishop JE, Greenbaum R, Gibson DG, Yacoub M, Laurent GJ (1990) Enhanced deposition of predominantly type I collagen in myocardial disease. Journal of molecular and cellular cardiology 22: 1157-65

Blum N, Begemann G (2012) Retinoic acid signaling controls the formation, proliferation and survival of the blastema during adult zebrafish fin regeneration. Development 139: 107-16

Blum N, Begemann G (2015) Osteoblast de- and redifferentiation are controlled by a dynamic response to retinoic acid during zebrafish fin regeneration. Development 142: 2894-903

Blum N BG (2012) Retinoic acid signaling controls the formation, proliferation and survival of the blastema during adult zebrafish fin regeneration. Development 139(1):

Bode PM, Bode HR (1980) Formation of pattern in regenerating tissue pieces of hydra attenuata. I. Head-body proportion regulation. Developmental biology 78: 484-96

Bolos V, Grego-Bessa J, de la Pompa JL (2007) Notch signaling in development and cancer. Endocrine reviews 28: 339-63

Bosch TC (2007) Why polyps regenerate and we don't: towards a cellular and molecular framework for Hydra regeneration. Developmental biology 303: 421-33

Brockes JP, Kumar A (2005) Appendage regeneration in adult vertebrates and implications for regenerative medicine. Science 310: 1919-23

Bujak M, Frangogiannis NG (2007) The role of TGF-beta signaling in myocardial infarction and cardiac remodeling. Cardiovascular research 74: 184-95

Chablais F, Jazwinska A (2010) IGF signaling between blastema and wound epidermis is required for fin regeneration. Development 137: 871-9

Chablais F, Jazwinska A (2012a) Induction of myocardial infarction in adult zebrafish using cryoinjury. Journal of visualized experiments : JoVE

Chablais F, Jazwinska A (2012b) The regenerative capacity of the zebrafish heart is dependent on TGFbeta signaling. Development 139: 1921-30

Chablais F, Veit J, Rainer G, Jazwinska A (2011) The zebrafish heart regenerates after cryoinjury-induced myocardial infarction. BMC developmental biology 11: 21

Chazaud B, Ricoux R, Christov C, Plonquet A, Gherardi RK, Barlovatz-Meimon G (2002) Promigratory effect of plasminogen activator inhibitor-1 on invasive breast cancer cell populations. The American journal of pathology 160: 237-46

Chen B, Zhong L, Roush SF, Pentassuglia L, Peng X, Samaras S, Davidson JM, Sawyer DB, Lim CC (2012) Disruption of a GATA4/Ankrd1 signaling axis in cardiomyocytes leads to sarcomere disarray: implications for anthracycline cardiomyopathy. PloS one 7: e35743

Chen H, Wang J, Xiang MX, Lin Y, He A, Jin CN, Guan J, Sukhova GK, Libby P, Wang JA, Shi GP (2013) Cathepsin S-mediated fibroblast trans-differentiation contributes to left ventricular remodelling after myocardial infarction. Cardiovascular research 100: 84-94

Chen J, Huang C, Truong L, La Du J, Tilton SC, Waters KM, Lin K, Tanguay RL, Dong Q (2012) Early life stage trimethyltin exposure induces ADP-ribosylation factor expression and perturbs the vascular system in zebrafish. Toxicology 302: 129-39

Chen JN, Fishman MC (1996) Zebrafish tinman homolog demarcates the heart field and initiates myocardial differentiation. Development 122: 3809-16

Chen Z, Huang W, Dahme T, Rottbauer W, Ackerman MJ, Xu X (2008) Depletion of zebrafish essential and regulatory myosin light chains reduces cardiac function through distinct mechanisms. Cardiovascular research 79: 97-108

Cheng XW, Shi GP, Kuzuya M, Sasaki T, Okumura K, Murohara T (2012) Role for cysteine protease cathepsins in heart disease: focus on biology and mechanisms with clinical implication. Circulation 125: 1551-62

Chitnis A, Henrique D, Lewis J, Ish-Horowicz D, Kintner C (1995) Primary neurogenesis in Xenopus embryos regulated by a homologue of the Drosophila neurogenic gene Delta. Nature 375: 761-6

Chowdhury B, Hemming R, Hombach-Klonisch S, Flamion B, Triggs-Raine B (2013) Murine hyaluronidase 2 deficiency results in extracellular hyaluronan accumulation and severe cardiopulmonary dysfunction. The Journal of biological chemistry 288: 520-8

Collesi C, Zentilin L, Sinagra G, Giacca M (2008) Notch1 signaling stimulates proliferation of immature cardiomyocytes. The Journal of cell biology 183: 117-28

D'Uva G, Aharonov A, Lauriola M, Kain D, Yahalom-Ronen Y, Carvalho S, Weisinger K, Bassat E, Rajchman D, Yifa O, Lysenko M, Konfino T, Hegesh J, Brenner O, Neeman M, Yarden Y, Leor J, Sarig R, Harvey RP, Tzahor E (2015) ERBB2 triggers mammalian heart regeneration by promoting cardiomyocyte dedifferentiation and proliferation. Nature cell biology 17: 627-38

Darehzereshki A, Rubin N, Gamba L, Kim J, Fraser J, Huang Y, Billings J, Mohammadzadeh R, Wood J, Warburton D, Kaartinen V, Lien CL (2015) Differential regenerative capacity of neonatal mouse hearts after cryoinjury. Developmental biology 399: 91-9

de la Pompa JL, Epstein JA (2012) Coordinating tissue interactions: Notch signaling in cardiac development and disease. Developmental cell 22: 244-54

de la Pompa JL, Timmerman LA, Takimoto H, Yoshida H, Elia AJ, Samper E, Potter J, Wakeham A, Marengere L, Langille BL, Crabtree GR, Mak TW (1998) Role of the NF-ATc transcription factor in morphogenesis of cardiac valves and septum. Nature 392: 182-6

de la Pompa JL, Wakeham A, Correia KM, Samper E, Brown S, Aguilera RJ, Nakano T, Honjo T, Mak TW, Rossant J, Conlon RA (1997) Conservation of the Notch signalling pathway in mammalian neurogenesis. Development 124: 1139-48

de Oliveira-Carlos V, Ganz J, Hans S, Kaslin J, Brand M (2013) Notch receptor expression in neurogenic regions of the adult zebrafish brain. PloS one 8: e73384

Declerck PJ, Gils A (2013) Three decades of research on plasminogen activator inhibitor-1: a multifaceted serpin. Seminars in thrombosis and hemostasis 39: 356-64

Dekker RJ, Boon RA, Rondaij MG, Kragt A, Volger OL, Elderkamp YW, Meijers JC, Voorberg J, Pannekoek H, Horrevoets AJ (2006) KLF2 provokes a gene expression pattern that establishes functional quiescent differentiation of the endothelium. Blood 107: 4354-63

Dekker RJ, van Soest S, Fontijn RD, Salamanca S, de Groot PG, VanBavel E, Pannekoek H, Horrevoets AJ (2002) Prolonged fluid shear stress induces a distinct set of endothelial cell genes, most specifically lung Kruppel-like factor (KLF2). Blood 100: 1689-98

Del Monte G, Grego-Bessa J, Gonzalez-Rajal A, Bolos V, De La Pompa JL (2007) Monitoring Notch1 activity in development: evidence for a feedback regulatory loop. Developmental dynamics : an official publication of the American Association of Anatomists 236: 2594-614

Derynck R, Muthusamy BP, Saeteurn KY (2014) Signaling pathway cooperation in TGF-beta-induced epithelial-mesenchymal transition. Current opinion in cell biology 31: 56-66

Dias TB, Yang YJ, Ogai K, Becker T, Becker CG (2012) Notch signaling controls generation of motor neurons in the lesioned spinal cord of adult zebrafish. The Journal of neuroscience : the official journal of the Society for Neuroscience 32: 3245-52

Diep CQ, Ma D, Deo RC, Holm TM, Naylor RW, Arora N, Wingert RA, Bollig F, Djordjevic G, Lichman B, Zhu H, Ikenaga T, Ono F, Englert C, Cowan CA, Hukriede NA, Handin RI, Davidson AJ (2011) Identification of adult nephron progenitors capable of kidney regeneration in zebrafish. Nature 470: 95-100

Dobaczewski M, Gonzalez-Quesada C, Frangogiannis NG (2010) The extracellular matrix as a modulator of the inflammatory and reparative response following myocardial infarction. Journal of molecular and cellular cardiology 48: 504-11

Dornseifer P, Takke C, Campos-Ortega JA (1997) Overexpression of a zebrafish homologue of the Drosophila neurogenic gene Delta perturbs differentiation of primary neurons and somite development. Mechanisms of development 63: 159-71

Ehling M, Adams S, Benedito R, Adams RH (2013) Notch controls retinal blood vessel maturation and quiescence. Development 140: 3051-61

Engin F, Yao Z, Yang T, Zhou G, Bertin T, Jiang MM, Chen Y, Wang L, Zheng H, Sutton RE, Boyce BF, Lee B (2008) Dimorphic effects of Notch signaling in bone homeostasis. Nature medicine 14: 299-305

Fahmy RG, Dass CR, Sun LQ, Chesterman CN, Khachigian LM (2003) Transcription factor Egr-1 supports FGF-dependent angiogenesis during neovascularization and tumor growth. Nature medicine 9: 1026-32

Fang Y, Gupta V, Karra R, Holdway JE, Kikuchi K, Poss KD (2013) Translational profiling of cardiomyocytes identifies an early Jak1/Stat3 injury response required for zebrafish heart regeneration. Proceedings of the National Academy of Sciences of the United States of America 110: 13416-21

Fausett BV, Goldman D (2006) A role for alpha1 tubulin-expressing Muller glia in regeneration of the injured zebrafish retina. The Journal of neuroscience : the official journal of the Society for Neuroscience 26: 6303-13

Felician G, Collesi C, Lusic M, Martinelli V, Ferro MD, Zentilin L, Zacchigna S, Giacca M (2014) Epigenetic modification at Notch responsive promoters blunts efficacy of inducing notch pathway reactivation after myocardial infarction. Circulation research 115: 636-49

Frangogiannis NG (2008) The immune system and cardiac repair. Pharmacological research 58: 88-111

Frangogiannis NG, Smith CW, Entman ML (2002) The inflammatory response in myocardial infarction. Cardiovascular research 53: 31-47

Frey N, Olson EN (2003) Cardiac hypertrophy: the good, the bad, and the ugly. Annual review of physiology 65: 45-79

Friesen C, Kiess Y, Debatin KM (2004) A critical role of glutathione in determining apoptosis sensitivity and resistance in leukemia cells. Cell death and differentiation 11 Suppl 1: S73-85

Fujimoto N, Terlizzi J, Aho S, Brittingham R, Fertala A, Oyama N, McGrath JA, Uitto J (2006) Extracellular matrix protein 1 inhibits the activity of matrix metalloproteinase 9 through high-affinity protein/protein interactions. Experimental dermatology 15: 300-7

Garg V, Muth AN, Ransom JF, Schluterman MK, Barnes R, King IN, Grossfeld PD, Srivastava D (2005) Mutations in NOTCH1 cause aortic valve disease. Nature 437: 270-4

Garrido-Martin EM, Blanco FJ, Roque M, Novensa L, Tarocchi M, Lang UE, Suzuki T, Friedman SL, Botella LM, Bernabeu C (2013) Vascular injury triggers Kruppel-like factor 6 mobilization and cooperation with specificity protein 1 to promote endothelial activation through upregulation of the activin receptor-like kinase 1 gene. Circulation research 112: 113-27

Gassmann M, Casagranda F, Orioli D, Simon H, Lai C, Klein R, Lemke G (1995) Aberrant neural and cardiac development in mice lacking the ErbB4 neuregulin receptor. Nature 378: 390-4

Gauron C, Rampon C, Bouzaffour M, Ipendey E, Teillon J, Volovitch M, Vriz S (2013) Sustained production of ROS triggers compensatory proliferation and is required for regeneration to proceed. Scientific reports 3: 2084

Geling A, Steiner H, Willem M, Bally-Cuif L, Haass C (2002) A gamma-secretase inhibitor blocks Notch signaling in vivo and causes a severe neurogenic phenotype in zebrafish. EMBO Rep 3: 688-94

Gemberling M, Bailey TJ, Hyde DR, Poss KD (2013) The zebrafish as a model for complex tissue regeneration. Trends in genetics : TIG 29: 611-20

Gemberling M, Karra R, Dickson AL, Poss KD (2015) Nrg1 is an injury-induced cardiomyocyte mitogen for the endogenous heart regeneration program in zebrafish. eLife 4

Geurtzen K, Knopf F, Wehner D, Huitema LF, Schulte-Merker S, Weidinger G (2014) Mature osteoblasts dedifferentiate in response to traumatic bone injury in the zebrafish fin and skull. Development 141: 2225-34

Ghosh AK, Vaughan DE (2012) PAI-1 in tissue fibrosis. Journal of cellular physiology 227: 493-507

Gingras AR, Liu JJ, Ginsberg MH (2012) Structural basis of the junctional anchorage of the cerebral cavernous malformations complex. The Journal of cell biology 199: 39-48

Giraldo A, Barrett OP, Tindall MJ, Fuller SJ, Amirak E, Bhattacharya BS, Sugden PH, Clerk A (2012) Feedback regulation by Atf3 in the endothelin-1-responsive transcriptome of cardiomyocytes: Egr1 is a principal Atf3 target. The Biochemical journal 444: 343-55

Gonzalez-Rosa JM, Guzman-Martinez G, Marques IJ, Sanchez-Iranzo H, Jimenez-Borreguero LJ, Mercader N (2014) Use of echocardiography reveals reestablishment of ventricular pumping efficiency and partial ventricular wall motion recovery upon ventricular cryoinjury in the zebrafish. PloS one 9: e115604

Gonzalez-Rosa JM, Martin V, Peralta M, Torres M, Mercader N (2011) Extensive scar formation and regression during heart regeneration after cryoinjury in zebrafish. Development 138: 1663-74

Gonzalez-Rosa JM, Mercader N (2012) Cryoinjury as a myocardial infarction model for the study of cardiac regeneration in the zebrafish. Nature protocols 7: 782-8

Gonzalez-Rosa JM, Peralta M, Mercader N (2012) Pan-epicardial lineage tracing reveals that epicardium derived cells give rise to myofibroblasts and perivascular cells during zebrafish heart regeneration. Developmental biology 370: 173-86

Grandel H, Kaslin J, Ganz J, Wenzel I, Brand M (2006) Neural stem cells and neurogenesis in the adult zebrafish brain: origin, proliferation dynamics, migration and cell fate. Developmental biology 295: 263-77

Grandel H, Lun K, Rauch GJ, Rhinn M, Piotrowski T, Houart C, Sordino P, Kuchler AM, Schulte-Merker S, Geisler R, Holder N, Wilson SW, Brand M (2002) Retinoic acid signalling in the zebrafish embryo is necessary during pre-segmentation stages to pattern the anterior-posterior axis of the CNS and to induce a pectoral fin bud. Development 129: 2851-65

Grego-Bessa J, Luna-Zurita L, del Monte G, Bolos V, Melgar P, Arandilla A, Garratt AN, Zang H, Mukouyama YS, Chen H, Shou W, Ballestar E, Esteller M, Rojas A, Perez-Pomares JM, de la Pompa JL (2007) Notch signaling is essential for ventricular chamber development. Developmental cell 12: 415-29

Gregorio CC, Trombitas K, Centner T, Kolmerer B, Stier G, Kunke K, Suzuki K, Obermayr F, Herrmann B, Granzier H, Sorimachi H, Labeit S (1998) The NH2 terminus of titin spans the Z-disc: its interaction with a novel 19-kD ligand (T-cap) is required for sarcomeric integrity. The Journal of cell biology 143: 1013-27

Gude NA, Emmanuel G, Wu W, Cottage CT, Fischer K, Quijada P, Muraski JA, Alvarez R, Rubio M, Schaefer E, Sussman MA (2008) Activation of Notch-mediated protective signaling in the myocardium. Circulation research 102: 1025-35

Gupta V, Gemberling M, Karra R, Rosenfeld GE, Evans T, Poss KD (2013) An injury-responsive gata4 program shapes the zebrafish cardiac ventricle. Current biology : CB 23: 1221-7

Gupta V, Poss KD (2012) Clonally dominant cardiomyocytes direct heart morphogenesis. Nature 484: 479-84

Haddon C, Smithers L, Schneider-Maunoury S, Coche T, Henrique D, Lewis J (1998) Multiple delta genes and lateral inhibition in zebrafish primary neurogenesis. Development 125: 359-70

Halder G, Johnson RL (2011) Hippo signaling: growth control and beyond. Development 138: 9-22

Han M, Yang X, Farrington JE, Muneoka K (2003) Digit regeneration is regulated by Msx1 and BMP4 in fetal mice. Development 130: 5123-32

Hausenloy DJ, Yellon DM (2013) Myocardial ischemia-reperfusion injury: a neglected therapeutic target. The Journal of clinical investigation 123: 92-100

Hellstrom M, Phng LK, Hofmann JJ, Wallgard E, Coultas L, Lindblom P, Alva J, Nilsson AK, Karlsson L, Gaiano N, Yoon K, Rossant J, Iruela-Arispe ML, Kalen M, Gerhardt H, Betsholtz C (2007) Dll4 signalling through Notch1 regulates formation of tip cells during angiogenesis. Nature 445: 776-80

Henrique D, Adam J, Myat A, Chitnis A, Lewis J, Ish-Horowicz D (1995) Expression of a Delta homologue in prospective neurons in the chick. Nature 375: 787-90

Herbert SP, Stainier DY (2011) Molecular control of endothelial cell behaviour during blood vessel morphogenesis. Nature reviews Molecular cell biology 12: 551-64

Herbomel P, Thisse B, Thisse C (1999) Ontogeny and behaviour of early macrophages in the zebrafish embryo. Development 126: 3735-45

High FA, Jain R, Stoller JZ, Antonucci NB, Lu MM, Loomes KM, Kaestner KH, Pear WS, Epstein JA (2009) Murine Jagged1/Notch signaling in the second heart field orchestrates Fgf8 expression and tissue-tissue interactions during outflow tract development. The Journal of clinical investigation 119: 1986-96

Hilton MJ, Tu X, Wu X, Bai S, Zhao H, Kobayashi T, Kronenberg HM, Teitelbaum SL, Ross FP, Kopan R, Long F (2008) Notch signaling maintains bone marrow mesenchymal progenitors by suppressing osteoblast differentiation. Nature medicine 14: 306-14

Hu N, Yost HJ, Clark EB (2001) Cardiac morphology and blood pressure in the adult zebrafish. The Anatomical record 264: 1-12

Huynh C, Poliseno L, Segura MF, Medicherla R, Haimovic A, Menendez S, Shang S, Pavlick A, Shao Y, Darvishian F, Boylan JF, Osman I, Hernando E (2011) The novel gamma secretase inhibitor RO4929097 reduces the tumor initiating potential of melanoma. PloS one 6: e25264

Imayoshi I, Sakamoto M, Yamaguchi M, Mori K, Kageyama R (2010) Essential roles of Notch signaling in maintenance of neural stem cells in developing and adult brains. The Journal of neuroscience : the official journal of the Society for Neuroscience 30: 3489-98

Iso T, Kedes L, Hamamori Y (2003) HES and HERP families: multiple effectors of the Notch signaling pathway. Journal of cellular physiology 194: 237-55

Isogai C, Laug WE, Shimada H, Declerck PJ, Stins MF, Durden DL, Erdreich-Epstein A, DeClerck YA (2001) Plasminogen activator inhibitor-1 promotes angiogenesis by stimulating endothelial cell migration toward fibronectin. Cancer research 61: 5587-94

Itoh M, Kim CH, Palardy G, Oda T, Jiang YJ, Maust D, Yeo SY, Lorick K, Wright GJ, Ariza-McNaughton L, Weissman AM, Lewis J, Chandrasekharappa SC, Chitnis AB (2003) Mind bomb is a ubiquitin ligase that is essential for efficient activation of Notch signaling by Delta. Developmental cell 4: 67-82

Itou J, Oishi I, Kawakami H, Glass TJ, Richter J, Johnson A, Lund TC, Kawakami Y (2012) Migration of cardiomyocytes is essential for heart regeneration in zebrafish. Development 139: 4133-42

Jain R, Engleka KA, Rentschler SL, Manderfield LJ, Li L, Yuan L, Epstein JA (2011) Cardiac neural crest orchestrates remodeling and functional maturation of mouse semilunar valves. The Journal of clinical investigation 121: 422-30

Jarriault S, Brou C, Logeat F, Schroeter EH, Kopan R, Israel A (1995) Signalling downstream of activated mammalian Notch. Nature 377: 355-8

Jeong DW, Kim TS, Cho IT, Kim IY (2004) Modification of glycolysis affects cell sensitivity to apoptosis induced by oxidative stress and mediated by mitochondria. Biochemical and biophysical research communications 313: 984-91

Jia H, King IN, Chopra SS, Wan H, Ni TT, Jiang C, Guan X, Wells S, Srivastava D, Zhong TP (2007) Vertebrate heart growth is regulated by functional antagonism between Gridlock and Gata5. Proceedings of the National Academy of Sciences of the United States of America 104: 14008-13

Jopling C, Sleep E, Raya M, Marti M, Raya A, Izpisua Belmonte JC (2010) Zebrafish heart regeneration occurs by cardiomyocyte dedifferentiation and proliferation. Nature 464: 606-9

Kanzler B, Kuschert SJ, Liu YH, Mallo M (1998) Hoxa-2 restricts the chondrogenic domain and inhibits bone formation during development of the branchial area. Development 125: 2587-97

Khachigian LM, Collins T (1997) Inducible expression of Egr-1-dependent genes. A paradigm of transcriptional activation in vascular endothelium. Circulation research 81: 457-61

Khachigian LM, Lindner V, Williams AJ, Collins T (1996) Egr-1-induced endothelial gene expression: a common theme in vascular injury. Science 271: 1427-31

Kikuchi K, Gupta V, Wang J, Holdway JE, Wills AA, Fang Y, Poss KD (2011a) tcf21+ epicardial cells adopt non-myocardial fates during zebrafish heart development and regeneration. Development 138: 2895-902

Kikuchi K, Holdway JE, Major RJ, Blum N, Dahn RD, Begemann G, Poss KD (2011b) Retinoic acid production by endocardium and epicardium is an injury response essential for zebrafish heart regeneration. Developmental cell 20: 397-404

Kikuchi K, Holdway JE, Werdich AA, Anderson RM, Fang Y, Egnaczyk GF, Evans T, Macrae CA, Stainier DY, Poss KD (2010) Primary contribution to zebrafish heart regeneration by gata4(+) cardiomyocytes. Nature 464: 601-5

Kim J, Wu Q, Zhang Y, Wiens KM, Huang Y, Rubin N, Shimada H, Handin RI, Chao MY, Tuan TL, Starnes VA, Lien CL (2010) PDGF signaling is required for epicardial function and blood vessel formation in regenerating zebrafish hearts. Proceedings of the National Academy of Sciences of the United States of America 107: 17206-10

Kimmel CB, Ballard WW, Kimmel SR, Ullmann B, Schilling TF (1995) Stages of embryonic development of the zebrafish. Developmental dynamics : an official publication of the American Association of Anatomists 203: 253-310

Kirkham M, Hameed LS, Berg DA, Wang H, Simon A (2014) Progenitor cell dynamics in the Newt Telencephalon during homeostasis and neuronal regeneration. Stem cell reports 2: 507-19

Kleaveland B, Zheng X, Liu JJ, Blum Y, Tung JJ, Zou Z, Sweeney SM, Chen M, Guo L, Lu MM, Zhou D, Kitajewski J, Affolter M, Ginsberg MH, Kahn ML (2009) Regulation of cardiovascular development and integrity by the heart of glass-cerebral cavernous malformation protein pathway. Nature medicine 15: 169-76

Knopf F, Hammond C, Chekuru A, Kurth T, Hans S, Weber CW, Mahatma G, Fisher S, Brand M, Schulte-Merker S, Weidinger G (2011) Bone regenerates via dedifferentiation of osteoblasts in the zebrafish fin. Developmental cell 20: 713-24

Knopf F HC, Chekuru A, Kurth T, Hans S, Weber CW, Mahatma G, Fisher S, Brand M, Schulte-Merker S, Weidinger G. (2011) Bone regenerates via dedifferentiation of osteoblasts in the zebrafish fin. Dev Cell 20(5):

Koch U, Lehal R, Radtke F (2013) Stem cells living with a Notch. Development 140: 689-704

Konopleva M, Contractor R, Tsao T, Samudio I, Ruvolo PP, Kitada S, Deng X, Zhai D, Shi YX, Sneed T, Verhaegen M, Soengas M, Ruvolo VR, McQueen T, Schober WD, Watt JC, Jiffar T, Ling X, Marini FC, Harris D et al. (2006) Mechanisms of apoptosis sensitivity and resistance to the BH3 mimetic ABT-737 in acute myeloid leukemia. Cancer cell 10: 375-88

Kopan R, Ilagan MX (2009) The canonical Notch signaling pathway: unfolding the activation mechanism. Cell 137: 216-33

Kortschak RD, Tamme R, Lardelli M (2001) Evolutionary analysis of vertebrate Notch genes. Development genes and evolution 211: 350-4

Kratsios P, Catela C, Salimova E, Huth M, Berno V, Rosenthal N, Mourkioti F (2010) Distinct roles for cell-autonomous Notch signaling in cardiomyocytes of the embryonic and adult heart. Circulation research 106: 559-72

Krebs LT, Xue Y, Norton CR, Shutter JR, Maguire M, Sundberg JP, Gallahan D, Closson V, Kitajewski J, Callahan R, Smith GH, Stark KL, Gridley T (2000) Notch signaling is essential for vascular morphogenesis in mice. Genes & development 14: 1343-52

Kroehne V, Freudenreich D, Hans S, Kaslin J, Brand M (2011) Regeneration of the adult zebrafish brain from neurogenic radial glia-type progenitors. Development 138: 4831-41

Kujawski S, Lin W, Kitte F, Bormel M, Fuchs S, Arulmozhivarman G, Vogt S, Theil D, Zhang Y, Antos CL (2014) Calcineurin regulates coordinated outgrowth of zebrafish regenerating fins. Developmental cell 28: 573-87

Kulkarni GV, McCulloch CA (1994) Serum deprivation induces apoptotic cell death in a subset of Balb/c 3T3 fibroblasts. Journal of cell science 107 (Pt 5): 1169-79

Kuruvilla L, Nair RR, Umashankar PR, Lal AV, Kartha CC (2007) Endocardial endothelial cells stimulate proliferation and collagen synthesis of cardiac fibroblasts. Cell biochemistry and biophysics 47: 65-72

Kwon B (2012) Regulation of Inflammation by Bidirectional Signaling through CD137 and Its Ligand. Immune network 12: 176-80

Kyritsis N, Kizil C, Zocher S, Kroehne V, Kaslin J, Freudenreich D, Iltzsche A, Brand M (2012) Acute inflammation initiates the regenerative response in the adult zebrafish brain. Science 338: 1353-6

Lai EC (2004) Notch signaling: control of cell communication and cell fate. Development 131: 965-73

Lampugnani MG, Resnati M, Raiteri M, Pigott R, Pisacane A, Houen G, Ruco LP, Dejana E (1992) A novel endothelial-specific membrane protein is a marker of cell-cell contacts. The Journal of cell biology 118: 1511-22

Larson JD, Wadman SA, Chen E, Kerley L, Clark KJ, Eide M, Lippert S, Nasevicius A, Ekker SC, Hackett PB, Essner JJ (2004) Expression of VE-cadherin in zebrafish embryos: a new tool to evaluate vascular development. Developmental dynamics : an official publication of the American Association of Anatomists 231: 204-13

Laux DW, Young S, Donovan JP, Mansfield CJ, Upton PD, Roman BL (2013) Circulating Bmp10 acts through endothelial Alk1 to mediate flow-dependent arterial quiescence. Development 140: 3403-12

Lawson ND, Weinstein BM (2002) In vivo imaging of embryonic vascular development using transgenic zebrafish. Developmental biology 248: 307-18

Lee KF, Simon H, Chen H, Bates B, Hung MC, Hauser C (1995) Requirement for neuregulin receptor erbB2 in neural and cardiac development. Nature 378: 394-8

Lee Y HD, De Val S, Kagermeier-Schenk B, Wills AA, Black BL, Weidinger G, Poss KD. (2009) Maintenance of blastemal proliferation by functionally diverse epidermis in regenerating zebrafish fins. Dev Biol 331(2):

Lepilina A, Coon AN, Kikuchi K, Holdway JE, Roberts RW, Burns CG, Poss KD (2006) A dynamic epicardial injury response supports progenitor cell activity during zebrafish heart regeneration. Cell 127: 607-19

Lewis J, Hanisch A, Holder M (2009) Notch signaling, the segmentation clock, and the patterning of vertebrate somites. Journal of biology 8: 44

Li B, Dewey CN (2011) RSEM: accurate transcript quantification from RNA-Seq data with or without a reference genome. BMC Bioinformatics 12: 323

Li HJ, Kapoor A, Giel-Moloney M, Rindi G, Leiter AB (2012) Notch signaling differentially regulates the cell fate of early endocrine precursor cells and their maturing descendants in the mouse pancreas and intestine. Developmental biology 371: 156-69

Li N, Felber K, Elks P, Croucher P, Roehl HH (2009) Tracking gene expression during zebrafish osteoblast differentiation. Developmental dynamics : an official publication of the American Association of Anatomists 238: 459-66

Liu J, Sato C, Cerletti M, Wagers A (2010) Notch signaling in the regulation of stem cell self-renewal and differentiation. Current topics in developmental biology 92: 367-409

Lobov IB, Renard RA, Papadopoulos N, Gale NW, Thurston G, Yancopoulos GD, Wiegand SJ (2007) Delta-like ligand 4 (Dll4) is induced by VEGF as a negative regulator of angiogenic sprouting. Proceedings of the National Academy of Sciences of the United States of America 104: 3219-24

Logeat F, Bessia C, Brou C, LeBail O, Jarriault S, Seidah NG, Israel A (1998) The Notch1 receptor is cleaved constitutively by a furin-like convertase. Proceedings of the National Academy of Sciences of the United States of America 95: 8108-12

Lopez B, Gonzalez A, Hermida N, Valencia F, de Teresa E, Diez J (2010) Role of lysyl oxidase in myocardial fibrosis: from basic science to clinical aspects. American journal of physiology Heart and circulatory physiology 299: H1-9

Lorent K, Yeo SY, Oda T, Chandrasekharappa S, Chitnis A, Matthews RP, Pack M (2004) Inhibition of Jagged-mediated Notch signaling disrupts zebrafish biliary development and generates multi-organ defects compatible with an Alagille syndrome phenocopy. Development 131: 5753-66

Luistro L, He W, Smith M, Packman K, Vilenchik M, Carvajal D, Roberts J, Cai J, Berkofsky-Fessler W, Hilton H, Linn M, Flohr A, Jakob-Rotne R, Jacobsen H, Glenn K, Heimbrook D, Boylan JF (2009) Preclinical profile of a potent gamma-secretase inhibitor targeting notch signaling with in vivo efficacy and pharmacodynamic properties. Cancer research 69: 7672-80

Luna-Zurita L, Prados B, Grego-Bessa J, Luxan G, del Monte G, Benguria A, Adams RH, Perez-Pomares JM, de la Pompa JL (2010) Integration of a Notch-dependent mesenchymal gene program and Bmp2-driven cell invasiveness regulates murine cardiac valve formation. The Journal of clinical investigation 120: 3493-507

Lush ME, Piotrowski T (2014) Sensory hair cell regeneration in the zebrafish lateral line. Developmental dynamics : an official publication of the American Association of Anatomists 243: 1187-202

Luxan G, Casanova JC, Martinez-Poveda B, Prados B, D'Amato G, MacGrogan D, Gonzalez-Rajal A, Dobarro D, Torroja C, Martinez F, Izquierdo-Garcia JL, Fernandez-Friera L, Sabater-Molina M, Kong YY, Pizarro G, Ibanez B, Medrano C, Garcia-Pavia P, Gimeno JR, Monserrat L et al. (2013) Mutations in the NOTCH pathway regulator MIB1 cause left ventricular noncompaction cardiomyopathy. Nature medicine 19: 193-201

Ma EY, Rubel EW, Raible DW (2008) Notch signaling regulates the extent of hair cell regeneration in the zebrafish lateral line. The Journal of neuroscience : the official journal of the Society for Neuroscience 28: 2261-73

Mably JD, Mohideen MA, Burns CG, Chen JN, Fishman MC (2003) heart of glass regulates the concentric growth of the heart in zebrafish. Current biology : CB 13: 2138-47

MacLellan WR, Schneider MD (2000) Genetic dissection of cardiac growth control pathways. Annual review of physiology 62: 289-319

Mahmoud AI, O'Meara CC, Gemberling M, Zhao L, Bryant DM, Zheng R, Gannon JB, Cai L, Choi WY, Egnaczyk GF, Burns CE, Burns CG, MacRae CA, Poss KD, Lee RT (2015) Nerves Regulate Cardiomyocyte Proliferation and Heart Regeneration. Developmental cell 34: 387-99

Malliaras K, Zhang Y, Seinfeld J, Galang G, Tseliou E, Cheng K, Sun B, Aminzadeh M, Marban E (2013) Cardiomyocyte proliferation and progenitor cell recruitment underlie therapeutic regeneration after myocardial infarction in the adult mouse heart. EMBO molecular medicine 5: 191-209

Martin M (2011) Cutadapt removes adapter sequences from high-throughput sequencing reads. EMBnetjournal 17

Mateus R, Lourenco R, Fang Y, Brito G, Farinho A, Valerio F, Jacinto A (2015) Control of tissue growth by Yap relies on cell density and F-actin in zebrafish fin regeneration. Development 142: 2752-63

Mercer SE, Odelberg SJ, Simon HG (2013) A dynamic spatiotemporal extracellular matrix facilitates epicardial-mediated vertebrate heart regeneration. Developmental biology 382: 457-69

Meyer D, Birchmeier C (1995) Multiple essential functions of neuregulin in development. Nature 378: 386-90

Miquerol L, Thireau J, Bideaux P, Sturny R, Richard S, Kelly RG (2015) Endothelial plasticity drives arterial remodeling within the endocardium after myocardial infarction. Circulation research 116: 1765-71

Monceau V, Belikova Y, Kratassiouk G, Robidel E, Russo-Marie F, Charlemagne D (2006) Myocyte apoptosis during acute myocardial infarction in rats is related to early sarcolemmal translocation of annexin A5 in border zone. American journal of physiology Heart and circulatory physiology 291: H965-71

Moore-Morris T, Guimaraes-Camboa N, Banerjee I, Zambon AC, Kisseleva T, Velayoudon A, Stallcup WB, Gu Y, Dalton ND, Cedenilla M, Gomez-Amaro R, Zhou B, Brenner DA, Peterson KL, Chen J, Evans SM (2014) Resident fibroblast lineages mediate pressure overload-induced cardiac fibrosis. The Journal of clinical investigation 124: 2921-34

Morikawa Y, Zhang M, Heallen T, Leach J, Tao G, Xiao Y, Bai Y, Li W, Willerson JT, Martin JF (2015) Actin cytoskeletal remodeling with protrusion formation is essential for heart regeneration in Hippo-deficient mice. Science signaling 8: ra41

Moriwaki H, Stempien-Otero A, Kremen M, Cozen AE, Dichek DA (2004) Overexpression of urokinase by macrophages or deficiency of plasminogen activator inhibitor type 1 causes cardiac fibrosis in mice. Circulation research 95: 637-44

Moss JB, Koustubhan P, Greenman M, Parsons MJ, Walter I, Moss LG (2009) Regeneration of the pancreas in adult zebrafish. Diabetes 58: 1844-51

Mourikis P, Tajbakhsh S (2014) Distinct contextual roles for Notch signalling in skeletal muscle stem cells. BMC developmental biology 14: 2

Nathan C (2002) Points of control in inflammation. Nature 420: 846-52

Nechiporuk A, Keating MT (2002) A proliferation gradient between proximal and msxb-expressing distal blastema directs zebrafish fin regeneration. Development 129: 2607-17

Nemir M, Metrich M, Plaisance I, Lepore M, Cruchet S, Berthonneche C, Sarre A, Radtke F, Pedrazzini T (2014) The Notch pathway controls fibrotic and regenerative repair in the adult heart. European heart journal 35: 2174-85

Nicol RL, Frey N, Pearson G, Cobb M, Richardson J, Olson EN (2001) Activated MEK5 induces serial assembly of sarcomeres and eccentric cardiac hypertrophy. The EMBO journal 20: 2757-67

Ninov N, Hesselson D, Gut P, Zhou A, Fidelin K, Stainier DY (2013) Metabolic regulation of cellular plasticity in the pancreas. Current biology : CB 23: 1242-50

O'Meara CC, Wamstad JA, Gladstone RA, Fomovsky GM, Butty VL, Shrikumar A, Gannon JB, Boyer LA, Lee RT (2015) Transcriptional reversion of cardiac myocyte fate during Mammalian cardiac regeneration. Circulation research 116: 804-15

Ogryzko NV, Hoggett EE, Solaymani-Kohal S, Tazzyman S, Chico TJ, Renshaw SA, Wilson HL (2014) Zebrafish tissue injury causes upregulation of interleukin-1 and caspase-dependent amplification of the inflammatory response. Disease models & mechanisms 7: 259-64

Okochi M, Steiner H, Fukumori A, Tanii H, Tomita T, Tanaka T, Iwatsubo T, Kudo T, Takeda M, Haass C (2002) Presenilins mediate a dual intramembranous gamma-secretase cleavage of Notch-1. The EMBO journal 21: 5408-16

Olofsson PS, Soderstrom LA, Wagsater D, Sheikine Y, Ocaya P, Lang F, Rabu C, Chen L, Rudling M, Aukrust P, Hedin U, Paulsson-Berne G, Sirsjo A, Hansson GK (2008) CD137 is expressed in human atherosclerosis and promotes development of plaque inflammation in hypercholesterolemic mice. Circulation 117: 1292-301

Panin VM, Papayannopoulos V, Wilson R, Irvine KD (1997) Fringe modulates Notch-ligand interactions. Nature 387: 908-12

Park JL, Lucchesi BR (1999) Mechanisms of myocardial reperfusion injury. The Annals of thoracic surgery 68: 1905-12

Parks AL, Klueg KM, Stout JR, Muskavitch MA (2000) Ligand endocytosis drives receptor dissociation and activation in the Notch pathway. Development 127: 1373-85

Peng X, Hassoun PM, Sammani S, McVerry BJ, Burne MJ, Rabb H, Pearse D, Tuder RM, Garcia JG (2004) Protective effects of sphingosine 1-phosphate in murine endotoxin-induced inflammatory lung injury. American journal of respiratory and critical care medicine 169: 1245-51

Pessina P, Kharraz Y, Jardi M, Fukada S, Serrano AL, Perdiguero E, Munoz-Canoves P (2015) Fibrogenic Cell Plasticity Blunts Tissue Regeneration and Aggravates Muscular Dystrophy. Stem cell reports 4: 1046-60

Petrie TA, Strand NS, Yang CT, Rabinowitz JS, Moon RT (2014) Macrophages modulate adult zebrafish tail fin regeneration. Development 141: 2581-91

Pober JS, Sessa WC (2007) Evolving functions of endothelial cells in inflammation. Nature reviews Immunology 7: 803-15

Poleo G BC, Laforest L, Akimenko MA. (2001) Cell proliferation and movement during early fin regeneration in zebrafish. Dev Dyn 221(4)

Poon KL, Liebling M, Kondrychyn I, Garcia-Lecea M, Korzh V (2010) Zebrafish cardiac enhancer trap lines: new tools for in vivo studies of cardiovascular development and disease. Developmental dynamics : an official publication of the American Association of Anatomists 239: 914-26

Porrello ER, Mahmoud AI, Simpson E, Hill JA, Richardson JA, Olson EN, Sadek HA (2011) Transient regenerative potential of the neonatal mouse heart. Science 331: 1078-80

Porrello ER, Olson EN (2014) A neonatal blueprint for cardiac regeneration. Stem cell research 13: 556-70

Poss KD (2010) Advances in understanding tissue regenerative capacity and mechanisms in animals. Nature reviews Genetics 11: 710-22

Poss KD, Keating MT, Nechiporuk A (2003) Tales of regeneration in zebrafish. Developmental dynamics : an official publication of the American Association of Anatomists 226: 202-10

Poss KD, Shen J, Keating MT (2000) Induction of lef1 during zebrafish fin regeneration. Developmental dynamics : an official publication of the American Association of Anatomists 219: 282-6

Poss KD, Wilson LG, Keating MT (2002) Heart regeneration in zebrafish. Science 298: 2188-90

Prince VE, Holley SA, Bally-Cuif L, Prabhakaran B, Oates AC, Ho RK, Vogt TF (2001) Zebrafish lunatic fringe demarcates segmental boundaries. Mechanisms of development 105: 175-80

Quint E, Smith A, Avaron F, Laforest L, Miles J, Gaffield W, Akimenko MA (2002) Bone patterning is altered in the regenerating zebrafish caudal fin after ectopic expression of sonic hedgehog and bmp2b or exposure to cyclopamine. Proceedings of the National Academy of Sciences of the United States of America 99: 8713-8

Raya A, Koth CM, Buscher D, Kawakami Y, Itoh T, Raya RM, Sternik G, Tsai HJ, Rodriguez-Esteban C, Izpisua-Belmonte JC (2003) Activation of Notch signaling pathway precedes heart regeneration in zebrafish. Proceedings of the National Academy of Sciences of the United States of America 100 Suppl 1: 11889-95

Reddien PW (2013) Specialized progenitors and regeneration. Development 140: 951-7

Reddien PW, Oviedo NJ, Jennings JR, Jenkin JC, Sanchez Alvarado A (2005) SMEDWI-2 is a PIWI-like protein that regulates planarian stem cells. Science 310: 1327-30

Reddien PW, Sanchez Alvarado A (2004) Fundamentals of planarian regeneration. Annual review of cell and developmental biology 20: 725-57

Reimer MM, Sorensen I, Kuscha V, Frank RE, Liu C, Becker CG, Becker T (2008) Motor neuron regeneration in adult zebrafish. The Journal of neuroscience : the official journal of the Society for Neuroscience 28: 8510-6

Reinardy HC, Emerson CE, Manley JM, Bodnar AG (2015) Tissue Regeneration and Biomineralization in Sea Urchins: Role of Notch Signaling and Presence of Stem Cell Markers. PloS one 10: e0133860

Renz M, Otten C, Faurobert E, Rudolph F, Zhu Y, Boulday G, Duchene J, Mickoleit M, Dietrich AC, Ramspacher C, Steed E, Manet-Dupe S, Benz A, Hassel D, Vermot J, Huisken J, Tournier-Lasserve E, Felbor U, Sure U, Albiges-Rizo C et al. (2015) Regulation of beta1 integrin-Klf2-mediated angiogenesis by CCM proteins. Developmental cell 32: 181-90

Ridley AJ (2011) Life at the leading edge. Cell 145: 1012-22

Rohr S, Otten C, Abdelilah-Seyfried S (2008) Asymmetric involution of the myocardial field drives heart tube formation in zebrafish. Circulation research 102: e12-9

Roy S, Gatien S (2008) Regeneration in axolotls: a model to aim for! Experimental gerontology 43: 968-73

Ryoo S, Gupta G, Benjo A, Lim HK, Camara A, Sikka G, Lim HK, Sohi J, Santhanam L, Soucy K, Tuday E, Baraban E, Ilies M, Gerstenblith G, Nyhan D, Shoukas A, Christianson DW, Alp NJ, Champion HC, Huso D et al. (2008) Endothelial arginase II: a novel target for the treatment of atherosclerosis. Circulation research 102: 923-32

S.G. Lenhoff HML (1986) Hydra and the Birth of Experimental Biology, 1744: Abraham Trembley's Memoirs Concerning the Natural History of a Type of Freshwater Polyp with Arms Shaped like Horns. Boxwood Press, Pacific Grove, California

Sallin P, de Preux Charles AS, Duruz V, Pfefferli C, Jazwinska A (2014) A dual epimorphic and compensatory mode of heart regeneration in zebrafish. Developmental biology

Sandoval-Guzman T, Wang H, Khattak S, Schuez M, Roensch K, Nacu E, Tazaki A, Joven A, Tanaka EM, Simon A (2014) Fundamental differences in dedifferentiation and stem cell recruitment during skeletal muscle regeneration in two salamander species. Cell stem cell 14: 174-87

Santos-Ruiz L, Santamaria JA, Ruiz-Sanchez J, Becerra J (2002) Cell proliferation during blastema formation in the regenerating teleost fin. Developmental dynamics : an official publication of the American Association of Anatomists 223: 262-72

Schebesta M LC, Engel FB, Keating MT. (2006) Transcriptional profiling of caudal fin regeneration in zebrafish. ScientificWorldJournal Suppl 1

Scheer N, Groth A, Hans S, Campos-Ortega JA (2001) An instructive function for Notch in promoting gliogenesis in the zebrafish retina. Development 128: 1099-107

Schnabel K, Wu CC, Kurth T, Weidinger G (2011) Regeneration of cryoinjury induced necrotic heart lesions in zebrafish is associated with epicardial activation and cardiomyocyte proliferation. PloS one 6: e18503

Schonenberger F, Deutzmann A, Ferrando-May E, Merhof D (2015) Discrimination of cell cycle phases in PCNA-immunolabeled cells. BMC bioinformatics 16: 180

Sedmera D, Pexieder T, Vuillemin M, Thompson RP, Anderson RH (2000) Developmental patterning of the myocardium. The Anatomical record 258: 319-37

Seguchi O, Takashima S, Yamazaki S, Asakura M, Asano Y, Shintani Y, Wakeno M, Minamino T, Kondo H, Furukawa H, Nakamaru K, Naito A, Takahashi T, Ohtsuka T, Kawakami K, Isomura T, Kitamura S, Tomoike H, Mochizuki N, Kitakaze M (2007) A cardiac myosin light chain kinase regulates sarcomere assembly in the vertebrate heart. The Journal of clinical investigation 117: 2812-24

Senyo SE, Lee RT, Kuhn B (2014) Cardiac regeneration based on mechanisms of cardiomyocyte proliferation and differentiation. Stem cell research 13: 532-41

Shalia KK, Mashru MR, Shah VK, Soneji SL, Payannavar S (2012) Levels of cathepsins in acute myocardial infarction. Indian heart journal 64: 290-4

Shankaran SS, Sieger D, Schroter C, Czepe C, Pauly MC, Laplante MA, Becker TS, Oates AC, Gajewski M (2007) Completing the set of h/E(spl) cyclic genes in zebrafish: her12 and her15 reveal novel modes of expression and contribute to the segmentation clock. Developmental biology 304: 615-32

Shen CN, Burke ZD, Tosh D (2004) Transdifferentiation, metaplasia and tissue regeneration. Organogenesis 1: 36-44

Sieger D, Tautz D, Gajewski M (2003) The role of Suppressor of Hairless in Notch mediated signalling during zebrafish somitogenesis. Mechanisms of development 120: 1083-94

Simon A, Tanaka EM (2013) Limb regeneration. Wiley interdisciplinary reviews Developmental biology 2: 291-300

Simone TM, Higgins CE, Czekay RP, Law BK, Higgins SP, Archambeault J, Kutz SM, Higgins PJ (2014) SERPINE1: A Molecular Switch in the Proliferation-Migration Dichotomy in Wound-"Activated" Keratinocytes. Adv Wound Care (New Rochelle) 3: 281-290

Singh SP, Holdway JE, Poss KD (2012) Regeneration of amputated zebrafish fin rays from de novo osteoblasts. Developmental cell 22: 879-86

Sleep E, Boue S, Jopling C, Raya M, Raya A, Izpisua Belmonte JC (2010) Transcriptomics approach to investigate zebrafish heart regeneration. Journal of cardiovascular medicine 11: 369-80

Smith A, Avaron F, Guay D, Padhi BK, Akimenko MA (2006) Inhibition of BMP signaling during zebrafish fin regeneration disrupts fin growth and scleroblasts differentiation and function. Developmental biology 299: 438-54

Smith SJ, Brookes-Fazakerley S, Donnelly LE, Barnes PJ, Barnette MS, Giembycz MA (2003) Ubiquitous expression of phosphodiesterase 7A in human proinflammatory and immune cells. American journal of physiology Lung cellular and molecular physiology 284: L279-89

Somorjai IM, Somorjai RL, Garcia-Fernandez J, Escriva H (2012) Vertebrate-like regeneration in the invertebrate chordate amphioxus. Proceedings of the National Academy of Sciences of the United States of America 109: 517-22

Sousa S, Afonso N, Bensimon-Brito A, Fonseca M, Simoes M, Leon J, Roehl H, Cancela ML, Jacinto A (2011) Differentiated skeletal cells contribute to blastema formation during zebrafish fin regeneration. Development 138: 3897-905

Sousa S, Valerio F, Jacinto A (2012) A new zebrafish bone crush injury model. Biology open 1: 915-21

Spinale FG, Coker ML, Bond BR, Zellner JL (2000) Myocardial matrix degradation and metalloproteinase activation in the failing heart: a potential therapeutic target. Cardiovascular research 46: 225-38

Stainier DY, Weinstein BM, Detrich HW, 3rd, Zon LI, Fishman MC (1995) Cloche, an early acting zebrafish gene, is required by both the endothelial and hematopoietic lineages. Development 121: 3141-50

Stanger BZ, Datar R, Murtaugh LC, Melton DA (2005) Direct regulation of intestinal fate by Notch. Proceedings of the National Academy of Sciences of the United States of America 102: 12443-8

Stewart S, Gomez AW, Armstrong BE, Henner A, Stankunas K (2014) Sequential and opposing activities of Wnt and BMP coordinate zebrafish bone regeneration. Cell reports 6: 482-98

Stoick-Cooper CL, Weidinger G, Riehle KJ, Hubbert C, Major MB, Fausto N, Moon RT (2007) Distinct Wnt signaling pathways have opposing roles in appendage regeneration. Development 134: 479-89

Suchting S, Freitas C, le Noble F, Benedito R, Breant C, Duarte A, Eichmann A (2007) The Notch ligand Delta-like 4 negatively regulates endothelial tip cell formation and vessel branching. Proceedings of the National Academy of Sciences of the United States of America 104: 3225-30

Suelves M, Vidal B, Ruiz V, Baeza-Raja B, Diaz-Ramos A, Cuartas I, Lluis F, Parra M, Jardi M, Lopez-Alemany R, Serrano AL, Munoz-Canoves P (2005) The plasminogen activation system in skeletal muscle regeneration: antagonistic roles of urokinase-type plasminogen activator (uPA) and its inhibitor (PAI-1). Frontiers in bioscience : a journal and virtual library 10: 2978-85

Susaki EA, Tainaka K, Perrin D, Kishino F, Tawara T, Watanabe TM, Yokoyama C, Onoe H, Eguchi M, Yamaguchi S, Abe T, Kiyonari H, Shimizu Y, Miyawaki A, Yokota H, Ueda HR (2014) Whole-brain imaging with single-cell resolution using chemical cocktails and computational analysis. Cell 157: 726-39

Takeo M, Chou WC, Sun Q, Lee W, Rabbani P, Loomis C, Taketo MM, Ito M (2013) Wnt activation in nail epithelium couples nail growth to digit regeneration. Nature 499: 228-32

Takeshita K, Hayashi M, Iino S, Kondo T, Inden Y, Iwase M, Kojima T, Hirai M, Ito M, Loskutoff DJ, Saito H, Murohara T, Yamamoto K (2004) Increased expression of plasminogen activator inhibitor-1 in cardiomyocytes contributes to cardiac fibrosis after myocardial infarction. The American journal of pathology 164: 449-56

Tal TL FJ, Tanguay RL. (2010) Molecular signaling networks that choreograph epimorphic fin regeneration in zebrafish - a mini-review. Gerontology 56(2):

Thorel F, Nepote V, Avril I, Kohno K, Desgraz R, Chera S, Herrera PL (2010) Conversion of adult pancreatic alpha-cells to beta-cells after extreme beta-cell loss. Nature 464: 1149-54

Thummel R, Bai S, Sarras MP, Jr., Song P, McDermott J, Brewer J, Perry M, Zhang X, Hyde DR, Godwin AR (2006) Inhibition of zebrafish fin regeneration using in vivo electroporation of morpholinos against fgfr1 and msxb. Developmental dynamics : an official publication of the American Association of Anatomists 235: 336-46

Thummel R BS, Sarras MP Jr, Song P, McDermott J, Brewer J, Perry M, Zhang X, Hyde DR, Godwin AR. (2006) Inhibition of zebrafish fin regeneration using in vivo electroporation of morpholinos against fgfr1 and msxb. Dev Dyn 235(2):

Tian Y, Liu Y, Wang T, Zhou N, Kong J, Chen L, Snitow M, Morley M, Li D, Petrenko N, Zhou S, Lu M, Gao E, Koch WJ, Stewart KM, Morrisey EE (2015) A microRNA-Hippo pathway that promotes cardiomyocyte proliferation and cardiac regeneration in mice. Sci Transl Med 7: 279ra38

Tian Y, Morrisey EE (2012) Importance of myocyte-nonmyocyte interactions in cardiac development and disease. Circulation research 110: 1023-34

Timmerman LA, Grego-Bessa J, Raya A, Bertran E, Perez-Pomares JM, Diez J, Aranda S, Palomo S, McCormick F, Izpisua-Belmonte JC, de la Pompa JL (2004) Notch promotes epithelial-mesenchymal transition during cardiac development and oncogenic transformation. Genes & development 18: 99-115

Tu S, Johnson SL (2011) Fate restriction in the growing and regenerating zebrafish fin. Developmental cell 20: 725-32

Tu S JS (2011) Fate restriction in the growing and regenerating zebrafish fin. Dev Cell 20(5):

Urbanek K, Cabral-da-Silva MC, Ide-Iwata N, Maestroni S, Delucchi F, Zheng H, Ferreira-Martins J, Ogorek B, D'Amario D, Bauer M, Zerbini G, Rota M, Hosoda T, Liao R, Anversa P, Kajstura J, Leri A (2010) Inhibition of notch1-dependent cardiomyogenesis leads to a dilated myopathy in the neonatal heart. Circulation research 107: 429-41

Veldman MB, Bemben MA, Goldman D (2010) Tuba1a gene expression is regulated by KLF6/7 and is necessary for CNS development and regeneration in zebrafish. Molecular and cellular neurosciences 43: 370-83

Vermot J, Forouhar AS, Liebling M, Wu D, Plummer D, Gharib M, Fraser SE (2009) Reversing blood flows act through klf2a to ensure normal valvulogenesis in the developing heart. PLoS biology 7: e1000246

Wan J, Ramachandran R, Goldman D (2012) HB-EGF is necessary and sufficient for Muller glia dedifferentiation and retina regeneration. Developmental cell 22: 334-47

Wang J, Cao J, Dickson AL, Poss KD (2015) Epicardial regeneration is guided by cardiac outflow tract and Hedgehog signalling. Nature 522: 226-30

Wang J, Karra R, Dickson AL, Poss KD (2013) Fibronectin is deposited by injury-activated epicardial cells and is necessary for zebrafish heart regeneration. Developmental biology 382: 427-35

Wang J, Panakova D, Kikuchi K, Holdway JE, Gemberling M, Burris JS, Singh SP, Dickson AL, Lin YF, Sabeh MK, Werdich AA, Yelon D, Macrae CA, Poss KD (2011) The regenerative capacity of zebrafish reverses cardiac failure caused by genetic cardiomyocyte depletion. Development 138: 3421-30

Wehner D, Cizelsky W, Vasudevaro MD, Ozhan G, Haase C, Kagermeier-Schenk B, Roder A, Dorsky RI, Moro E, Argenton F, Kuhl M, Weidinger G (2014) Wnt/beta-catenin signaling defines organizing centers that orchestrate growth and differentiation of the regenerating zebrafish caudal fin. Cell reports 6: 467-81

Wehner D, Weidinger G (2015) Signaling networks organizing regenerative growth of the zebrafish fin. Trends in genetics : TIG 31: 336-43

Weissman IL, Anderson DJ, Gage F (2001) Stem and progenitor cells: origins, phenotypes, lineage commitments, and transdifferentiations. Annual review of cell and developmental biology 17: 387-403

Westin J, Lardelli M (1997) Three novel Notch genes in zebrafish: implications for vertebrate Notch gene evolution and function. Development genes and evolution 207: 51-63

Whitehead GG, Makino S, Lien CL, Keating MT (2005) fgf20 is essential for initiating zebrafish fin regeneration. Science 310: 1957-60

Whittaker P, Boughner DR, Kloner RA (1991) Role of collagen in acute myocardial infarct expansion. Circulation 84: 2123-34

Witman N, Heigwer J, Thaler B, Lui WO, Morrison JI (2013) miR-128 regulates non-myocyte hyperplasia, deposition of extracellular matrix and Islet1 expression during newt cardiac regeneration. Developmental biology 383: 253-63

Wong D, Dorovini-Zis K (1995) Expression of vascular cell adhesion molecule-1 (VCAM-1) by human brain microvessel endothelial cells in primary culture. Microvascular research 49: 325-39

Wong KS, Rehn K, Palencia-Desai S, Kohli V, Hunter W, Uhl JD, Rost MS, Sumanas S (2012) Hedgehog signaling is required for differentiation of endocardial progenitors in zebrafish. Developmental biology 361: 377-91

Yelon D, Ticho B, Halpern ME, Ruvinsky I, Ho RK, Silver LM, Stainier DY (2000) The bHLH transcription factor hand2 plays parallel roles in zebrafish heart and pectoral fin development. Development 127: 2573-82

Yoshida M, Itano N, Yamada Y, Kimata K (2000) In vitro synthesis of hyaluronan by a single protein derived from mouse HAS1 gene and characterization of amino acid residues essential for the activity. The Journal of biological chemistry 275: 497-506

Yoshinari N, Ishida T, Kudo A, Kawakami A (2009) Gene expression and functional analysis of zebrafish larval fin fold regeneration. Developmental biology 325: 71-81

Yu B, Song B (2014) Notch 1 signalling inhibits cardiomyocyte apoptosis in ischaemic postconditioning. Heart, lung & circulation 23: 152-8

Yurco P, Cameron DA (2007) Cellular correlates of proneural and Notch-delta gene expression in the regenerating zebrafish retina. Visual neuroscience 24: 437-43

Zhang C, Li Q, Lim CH, Qiu X, Jiang YJ (2007) The characterization of zebrafish antimorphic mib alleles reveals that Mib and Mind bomb-2 (Mib2) function redundantly. Developmental biology 305: 14-27

Zhang R, Han P, Yang H, Ouyang K, Lee D, Lin YF, Ocorr K, Kang G, Chen J, Stainier DY, Yelon D, Chi NC (2013) In vivo cardiac reprogramming contributes to zebrafish heart regeneration. Nature 498: 497-501

Zhao L, Borikova AL, Ben-Yair R, Guner-Ataman B, MacRae CA, Lee RT, Burns CG, Burns CE (2014) Notch signaling regulates cardiomyocyte proliferation during zebrafish heart regeneration. Proceedings of the National Academy of Sciences of the United States of America 111: 1403-8

Zhou Z, Rawnsley DR, Goddard LM, Pan W, Cao XJ, Jakus Z, Zheng H, Yang J, Arthur JS, Whitehead KJ, Li D, Zhou B, Garcia BA, Zheng X, Kahn ML (2015) The cerebral cavernous malformation pathway controls cardiac development via regulation of endocardial MEKK3 signaling and KLF expression. Developmental cell 32: 168-80

Zuniga E SF, Crump JG. (2010) Jagged-Notch signaling ensures dorsal skeletal identity in the vertebrate face. Development 137(11):

Appendix

Cover page: IMARIS volume rendering of a whole mount *ET33-mi60a* (green); *Tg(myl7:mdsred)* (magenta) cryoinjured transgenic heart at 9 dpci.

Back cover: Pseudo-coloured green fluorescence of a fin blastema at 4 dpa of *ET33-mi60a* fish.

The important thing is not to stop questioning.
Curiosity has its own reason for existing.

Albert Einstein

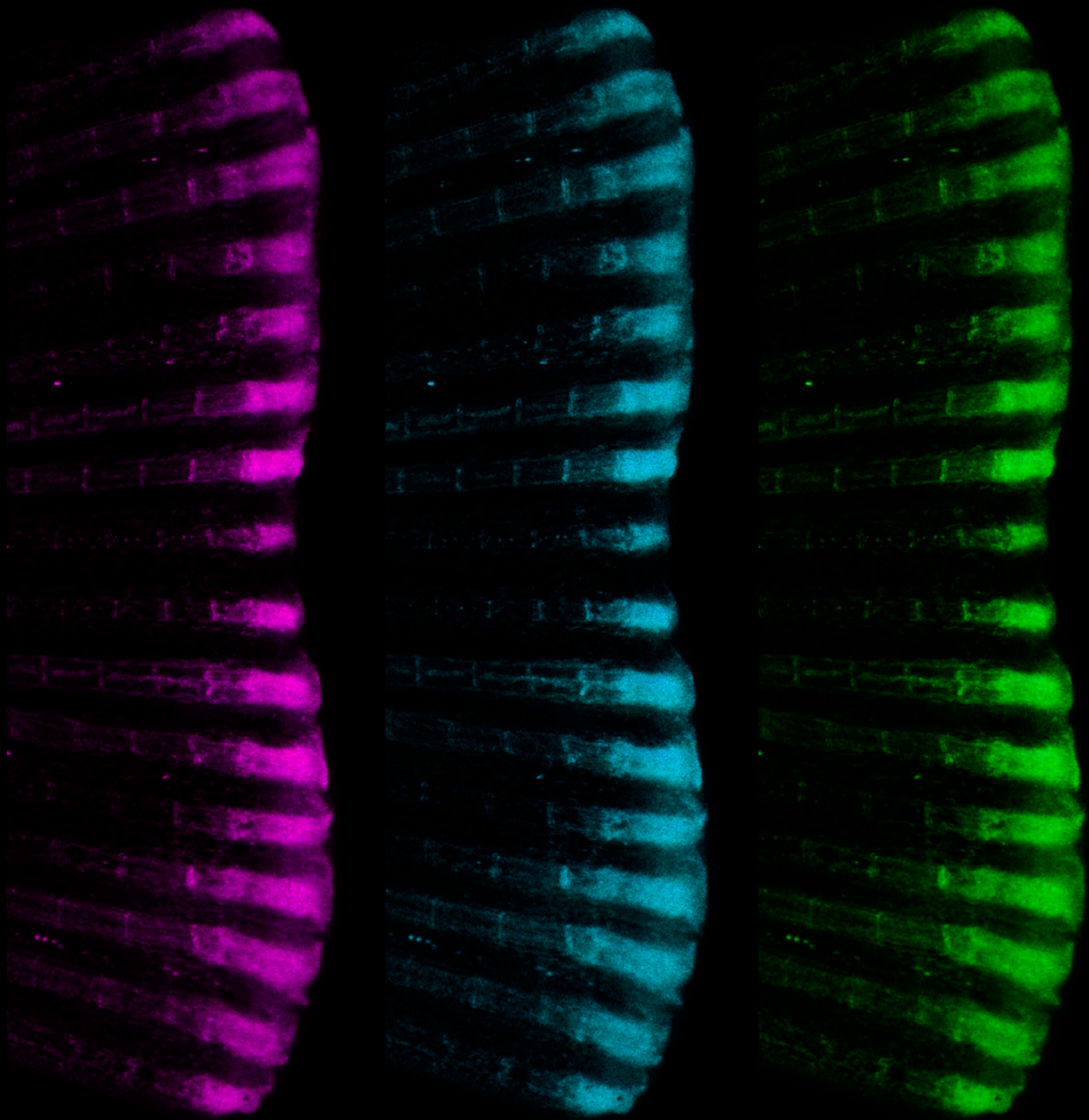

UAM
UNIVERSIDAD AUTONOMA
DE MADRID

cnic